

**BIOLOGICAL EQUIVALENCE
BETWEEN DIFFERENT RADIOTHERAPY SCHEDULES
STUDIED USING THE LINEAR QUADRATIC MODEL.**

Charles Deehan

Submitted to the University of Glasgow
for the degree of Doctor of Philosophy

West Glasgow Hospitals and University Trust
Department of Clinical Physics and Bio-Engineering

March, 1995

© C. Deehan, 1995

ProQuest Number: 13832520

All rights reserved

INFORMATION TO ALL USERS

The quality of this reproduction is dependent upon the quality of the copy submitted.

In the unlikely event that the author did not send a complete manuscript and there are missing pages, these will be noted. Also, if material had to be removed, a note will indicate the deletion.



ProQuest 13832520

Published by ProQuest LLC (2019). Copyright of the Dissertation is held by the Author.

All rights reserved.

This work is protected against unauthorized copying under Title 17, United States Code
Microform Edition © ProQuest LLC.

ProQuest LLC.
789 East Eisenhower Parkway
P.O. Box 1346
Ann Arbor, MI 48106 – 1346

Thesis
10060
Copy 1



ABSTRACT

The aim of this work was to investigate biological equivalence between different radiotherapy treatment schedules. The first three chapters form an introduction to radiobiological aspects of radiotherapy, these discuss radiation effects on cells and tissues, radiobiological models in radiotherapy and biological equivalence. In chapters 4, 5 and 6 conditions for general equivalence are derived for fractionated, continuous and combined treatments, based on biological effect calculations performed at specific points in a dose distribution. Chapters 7 and 8 introduce the subject of iso-effect surfaces and this concept is applied to both continuous and fractionated treatments. Finally results of this thesis are compared with clinical reports in chapter 9. The Linear Quadratic (LQ) iso-effect model is used in the derivation of general equivalence relationships and in iso-effect surface calculations.

To my Father and Mother
Charles and Elizabeth Deehan.

CONTENTS

	PAGE
Title page	1
Abstract	2
Dedication	3
Contents	4
Acknowledgements	11
Summary of thesis	12

Chapter 1: Radiation effects on cells and tissues.

1.1. Introduction	19
1.1.1. Radiotherapy and Radiobiology	19
1.1.2. Radiobiological equivalence in radiotherapy	19
1.1.3. Clinical radiobiology	21
1.2. The molecular basis of biological effects of ionising radiation	22
1.2.1. Damage to DNA	22
1.2.2. Linear energy transfer, LET	23
1.3. Radiobiology of normal tissues	26
1.3.1. Parenchymal cells and connective tissue	27
1.3.2. Hierarchical (H-type) tissues	27
1.3.3. Flexible (F-type) tissues	27
1.3.4. Acute and Late effect	28
1.3.5. Volume effects	29
1.4. Radiobiological factors governing cell survival	30

1.4.1.	Repair	30
1.4.2	Reassortment	31
1.4.3.	Repopulation	31
1.4.4.	Reoxygenation	31
1.4.5.	Radiosensitivity	32
1.5.	Radiotherapy	32
1.5.1.	Therapeutic ratio	33
1.5.2.	Tumour cure and normal tissue survival probability	33
1.5.3.	The effects of fractionation and dose rate	33
1.5.4.	Fractionated radiotherapy	34
1.5.5.	Brachytherapy treatments	37
1.5.6.	Dose rate effect	39
1.5.7.	Equivalence between different radiotherapy schedules	40
1.5.8.	Appendix 1. Manchester system of dosage used in intracavitary insertions in gynaecological oncology	41
	Chapter 1. Figures and tables	43
	Chapter 2: Radiobiological models in radiotherapy.	
2.1	Introduction	48
2.1.1.	Radiation damage to cells	48
2.1.2.	Sublethal damage	49
2.1.3.	Potentially lethal damage	49
2.2.	Survival curves and target theory	50
2.2.1.	Single-target single-hit	51
2.2.2.	Multi-target single-hit	51

2.2.3. Repair saturation models	53
2.2.4. Linear quadratic model	53
2.3. Early iso-effect models	55
2.4. The linear quadratic (LQ) model for normal tissue effects.	59
2.4.1. LQ model - Fractionated radiotherapy	59
2.4.2. LQ model - Continuous radiotherapy	63
2.5. Conclusions	66
Chapter 2. Figures and tables	68

Chapter 3: Biological equivalence using iso-effect models.

3.1. Introduction	73
3.1.1. Schedules and regimes	73
3.2. Biological equivalence	74
3.3. The use of iso-effect relationships	76
3.3.1. Fractionated radiotherapy	76
3.3.2. Continuous radiotherapy	82
3.3.3. Summary	87
Chapter 3. Tables	89

Chapter 4: Equivalence between fractionated radiotherapy schedules.

4.1. Introduction	90
4.2. Dissociation of biological effects	91
4.2.1. Implications of non-equivalence of treatment schedules in radiotherapy	91
4.3. General equivalence	92
4.3.1. General equivalence between single schedules	93

4.3.2.	General equivalence between schedules and regimes	94
4.3.3.	Application to Continuous Hyperfractionated Accelerated Radiotherapy Treatments (CHART)	99
4.4.	Conclusions	103
4.5.	Appendix 4.1 General equivalence with power law ("exponent of N") iso-effect models	105
	Chapter 4. Figures	113
	Chapter 5: Equivalence between continuous radiotherapy schedules.	
5.1.	Introduction	118
5.2.	General equivalence conditions for continuous schedules	119
5.2.1.	Single continuous treatments	120
5.2.2.	Sequences of continuous treatments	125
5.3.	Conclusions	131
5.4.	Appendix 5.1: Treatment times	135
5.5.	Worked examples	138
	Chapter 5. Figures and tables	143
	Chapter 6: Biological equivalence between fractionated and continuous radiotherapy treatments.	
6.1.	Introduction	147
6.2.	Equivalence conditions between fractionated and continuous schedules	148
6.2.1.	Fractionated and continuous schedules with fraction number equal to one	148
6.3.	Regimes of fractionated and continuous treatments	151

6.4.	Mixed schedules of fractionated and continuous treatments	156
	Chapter 6. Table 6.1	159
6.5.	Appendix 6.1: Worked examples	160

Chapter 7: Iso-effect surfaces in brachytherapy.

7.1.	Introduction	163
	7.1.1. Iso-dose or iso-dose-rate plots	164
	7.1.2. Iso-effect plots	164
7.2.	Changes in iso-effect distributions	165
7.3.	Method for calculating the magnitude and direction of iso-surface movement	168
	7.3.1. The relationship between distance and dose-rate	169
	7.3.2. Variation of ERD along the line PP' for different schedules	171
	7.3.4. Movement of iso-effect surfaces	175
7.4.	Liversage equation	177
7.5.	Conclusion	179
7.6.	Appendix 7.1: Matching of ERD plots for LDR and HDR where the total dose remains constant	181
	Chapter 7. Figures and tables	184

**Chapter 8: The movement of iso-effect surfaces in fractionated external beam
radiotherapy and changes in enclosed volume in intracavitary treatments.**

8.1.	Introduction	194
8.2.	Total dose and effect profiles in fractionated external beam radiotherapy	194
8.3.	Iso-effect surfaces	197

8.4.	General equivalence and iso-effect surface movement	200
8.5.	Volume effects	204
8.6.	Conclusions	207
	Chapter 8. Figures and tables	208
	Chapter 9: Analysis of clinical treatments.	
9.1.	Introduction	227
	9.1.1. Clinical results	227
	9.1.2. Brachytherapy	227
9.2.	Geometrical effects	231
	9.2.1. Position of sensitive organs	234
	9.2.2. Geometry versus radiobiology	234
9.3.	The Glasgow study	235
9.4.	Iso-effect analysis for the Glasgow study	238
	9.4.1. ERD calculation: single point	238
	9.4.2. General equivalence	239
	9.4.3. Movement of iso-effect surfaces	242
	9.4.4. Movement for complete matching of tumour or late effects	245
	9.4.5. Analysis for stages IIb, III and IVa of the Glasgow study	247
	9.4.6. Iso-effect surface movement with geometrical changes included	248
9.5.	The Manchester study	252
9.6.	Iso-effect analysis for the Manchester study	253
	9.6.1. ERD calculations: single point	253
	9.6.2. Movement of Iso-effect surfaces	253

9.7.	The Orton survey	255
9.8.	Iso-effect analysis for the Orton survey	256
9.8.1.	ERD calculations: single point	256
9.8.2.	General equivalence	257
9.8.3.	Movement of Iso-effect surfaces	258
9.9.	The Patel study	260
9.10.	Iso-effect analysis for the Patel study	261
9.10.1.	ERD calculations: single point	261
9.10.2.	Movement of Iso-effect surfaces	261
9.11.	Conclusions	262
9.12.	Appendix 9.1: Program for calculating the movement of iso-effect surfaces along PP'	264
9.13.	Appendix 9.2: Program for calculating the movement of iso-effect surfaces along B_{Man} B'	266
	Chapter 9. Figures and tables	268
	Chapter 10: Conclusions.	
10.1.	Advantages and limitations of general equivalence	288
10.2.	Iso-effect surfaces	290
10.3.	Future developments	292
	Chapter 10. Figure	297
	References	298

ACKNOWLEDGEMENTS

I would like to express my gratitude to the following people:

Dr Tom Wheldon and Professor Alex Elliott for reading the whole of this thesis and suggesting many improvements and for their constant encouragement and inspiration throughout the course of this work.

Dr Joe O'Donoghue for so many helpful discussions relating to all aspects of this work.

I am glad to acknowledge the generous support of the Department of Clinical Physics and Bio-Engineering without which this work would never have been possible. Also the support of the staff of the Beatson Oncology Centre, in particular Mr Bruce Barnett, business manager, who provided computing facilities which helped with many stages of this work.

Summary of thesis.

The work of this thesis was influenced by early experience in the use of the LQ model where advantage was taken of different tissue responses in order to devise alternative schedules which promised to give better tumour effects and at the same time lower levels of normal tissue damage (Withers, 1983). This thesis deals with the problem of equivalence between treatments, which can arise because of changes in scheduling in every-day treatments to answer the question of how an interrupted treatment should be continued in order to achieve a satisfactory result. The necessity to alter treatments can arise from breaks in treatment due to patient illness, machine breakdown or even errors in dose delivery. Another aspect of no less importance which can lead to alterations in scheduling is change in treatment dose-rate. Increasing dose-rate may have many practical advantages (e.g. shorter treatment times) but affects tissues and tumours in different ways which are as yet not clearly understood. With differential responses in mind this thesis asks firstly if general equivalence can be achieved between different treatments and secondly how can changing effect distributions be compared?

General equivalence.

Before this work the LQ model (and earlier power function models) were used in a way which assumed that the status quo with regard to all effects could not be restored following a schedule violation. This often led to a sub-optimal situation where alternative schedules were devised which matched for one specific effect and produced a mismatch for all others. However it is shown here that when the coefficients of the A and B type damage terms are equated for different treatments, conditions can sometimes

be found which lead to general equivalence, that is equivalence for all effects on all tissues. The conditions required for general equivalence in different situations are summarised below.

Fractionated radiotherapy.

Single schedules.

It was found that no two schedules were equivalent in their effects on tissues. This leads to the principle of non-equivalence between schedules (chapter 4, section 4.2.1.), a fact which has been assumed in radiotherapy but has not been formally proven until now.

Schedules and regimes

General equivalence is however possible between schedule $(N_r:d_r)$ and regime $(N_1:d_1 + N_2:d_2 + \dots + N_k:d_k)$ provided the following relationships are satisfied.

$$N_r d_r = \sum_{i=1}^{i=k} N_i d_i \text{ ----- 4.4}$$

and

$$N_r d_r^2 = \sum_{i=1}^{i=k} N_i d_i^2 \text{ ----- 4.5}$$

As demonstrated in chapter 4 these equations can yield results which are useful in every-day radiotherapy. The most basic application is where a number of schedules have been given; this approach then allows a single schedule to be derived which is generally

equivalent to that series (example 4.1). Alternatively if some treatment has already been given, it is possible to devise further treatment which when combined with the first will produce the same effects on all tissues as some reference schedule (example 4.2). The conditions under which the latter example produces valid results are laid out in section 4.3.2. and figures 4.1 and 4.2. General equivalence is also applied to schedule violations involving accelerated hyperfractionation (CHART) regimes. In this case interruptions to treatments in the CHART arm of the trial can require the patients to be moved to the conventional arm. Suitable schedules can be calculated using general equivalence theory which allow this transition to take place in such a way as to produce the same effects as if the patient had been treated on the conventional schedule from the start of the treatment. The limitation in this example is one of time scale, in that treatment interruptions which occur earlier in the hyperfractionated arm are easier to deal with than those occurring later. The conclusion of chapter 4, however was that in fractionated radiotherapy general equivalence was possible between schedules and regimes and that calculations could be performed which did not involve knowledge of the α/β ratio which was previously regarded as essential in deriving alternative schedules.

Continuous radiotherapy.

Using the same reasoning as for fractionated schedules, general equivalence conditions were derived between continuous schedules in chapter 5. Although it was possible to eliminate the α/β ratio from these equations μ , (the sublethal damage repair time constant) remains. This leads to relationships which are less straightforward than in the fractionated case and where true general equivalence in the strictest sense was not

possible. However, by considering different treatment times it was possible to identify regions where "near" general equivalence existed.

Single treatments.

General equivalence is only possible between single continuous treatments (i.e. fraction number, $N=1$) when the treatment time is less than 2.58min (see section 5.2.1(a)), a result which is in keeping with the conditions derived for fractionated radiotherapy. The condition which must be satisfied for this is the simple relationship given in the equation:

$$R_1 T_1 = R_2 T_2 \text{ ----- } 5.4$$

This trivial solution relates specifically to equivalence between single fractions of high dose-rate therapy (short delivery time). It makes it necessary to modify slightly the earlier statement that general equivalence is not possible between schedules of fractionated treatment. The solutions to equation 4.4 and 4.5 for general equivalence then are:

$$N_1 = N_2 \quad \text{and} \quad d_1 = d_2$$

But since $d_1 = R_1 T_1 = R_2 T_2 = d_2$ then in this special case general equivalence is possible between fractionated schedules if they are given on therapy machines with

different dose-rates, for example cobalt 60 and linear accelerator or ortho-voltage, where R and T ($< 2.58\text{min}$) can vary.

When the treatment time is greater than 2.58mins, general equivalence is not possible between different single continuous treatments. This result is proved in sections 5.2.1(b) and (c).

Schedules and regimes.

Equivalence between a schedule and a regime of continuous treatments was considered in section 5.2.2 where once more the α/β ratio could be eliminated from the derived relationships but μ could not. When treatment time was less than 2.58min conditions for general equivalence were obtained identical to those derived in chapter 4 for fractionated schedules (equations 5.10, 5.11, 4.4 and 4.5). This is an extension to fractionated radiotherapy where the dose per fraction, $d = R T$.

When T was greater than 8.5hr (see section 5.2.1(b)) "near" general equivalence was shown to exist between a continuous schedule and a regime (section 5.2.2(b)) but that if $2.58\text{min} < T < 8.5\text{hr}$ then even near general equivalence was not possible. Some examples of the use of the relationships derived are shown in appendix 5.2.

Combined fractionated and continuous treatments.

Using the method of chapters 4 and 5, equivalence between combinations of fractionated and continuous treatments were considered in chapter 6. Treatment time were chosen in the same way to simplify the expressions containing μ . A series of relationships was derived which shows that a fractionated schedule can be related to a combination of fractionated and continuous regimes and finally to a single continuous

treatment without the need to know the α/β ratio. Only knowledge of μ is necessary and this group of relationships reduces to the Liversage equation (see section 6.3) as a special case when $N=1$.

Chapters 7 and 8 introduce the concept of surfaces of equal effect or iso-effect surfaces. This representation is shown to be a useful way of describing the changes in effect distribution as treatment parameters are altered. Chapters 7 and 8 apply this concept to changing brachytherapy and external beam treatments respectively. It is shown that the movement of iso-effect surfaces can be plotted and that the magnitude and direction of movement can give a more global view of the changes in effect distribution than effect calculations performed at specific points.

By using the iso-effect representation it can be seen that going from low to high dose-rate treatments need not produce higher levels of late responding tissue damage for the same tumour effect. This result is in agreement with recently published clinical reports as shown in chapter 9 and seems to demonstrate that radiobiology theory is not in fact producing results which are at odds with clinical reports.

Chapter 1.

Radiation effects on cells and tissues

1.1. Introduction

1.1.1. Radiotherapy and Radiobiology

Radiation therapy has proved to be one of the most effective methods for the treatment of cancer. It is used for the long term treatment and control of many tumours: for example head and neck, prostate, cervix, bladder and skin and in addition has proved valuable in the treatment of Hodgkin's disease and other lymphomas. Radiotherapy also provides valuable palliation in many cases where the probability of cure is low, relieving distressing symptoms and improving the quality of life that remains (Paterson, 1963; De Vita, 1979; Steel, 1993). Over the years many advances have been made in the areas of dosimetry, dose delivery and radiobiology (del Regato, 1968, 1990; Horiot, 1991): this thesis will deal with the last of these. Radiobiology is the study of how cells, normal tissues and tumours behave when irradiated using ionising radiation, and allows us to compare the effects of different radiotherapy schedules. This chapter will provide an overview of radiobiology and its relationship to radiotherapy as both have developed over the last 50 years.

1.1.2. Radiobiological equivalence in radiotherapy.

The work for this thesis began in the mid nineteen eighties and it is important to set it in context with subsequent events. The effects on both normal tissue and tumour resulting from changes in radiotherapy treatment schedules have always been of great

interest to the radiotherapist. Interest in this area increased in the late seventies and early eighties when deliberate alterations of treatment resulting from developments such as the introduction of high dose-rate brachytherapy (Fowler, 1990; Mould, 1992, Joslin, 1993) and concepts such as hyperfractionation of treatment promised to bring many advantages (Thames et al, 1983; Dische & Saunders, 1990; Saunders et al, 1988, 1990).

At that time predicting the effects of treatment changes was difficult and was either based on limited clinical experience or early iso-effect models such as those of the NSD/CRE/TDF (Ellis, 1967, 1969, 1985; Kirk, 1971, 1972; Orton, 1973, 1990; Overgaard, 1993) type. Around that time however newer types of model were emerging for example the linear quadratic (LQ) model (Douglas & Fowler, 1976; Dale, 1985, 1986, 1990; Fowler, 1984, 1989, 1990; Orton, 1990; Warmelink, 1990; Joiner, 1993) which appeared to have advantages over the older models.

The purpose of this work is to investigate biological equivalence between different schedules using the LQ model. Some work had been published in the early eighties showing how this model could be used to devise alternative iso-effective schedules (Barendsen, 1982; Thames, 1982, 1983; Withers, 1982, 1983). Early iso-effect modelling was designed to exploit perceived differences in the response of normal tissues and tumours in an attempt to design new schedules which would prove more effective in treatment terms. Beginning with some reference schedule this approach often led to several options each matched for an effect on a specific tissue (Dale, 1985, 1986, 1990; Fowler, 1984, 1989). This was a specific equivalence and this thesis asks, for the first time, if the LQ model can be used to devise a schedule which is equivalent in all respects to a given reference schedule. This type of equivalence is defined here as general equivalence (Deehan & O'Donoghue, 1988). Later as the discussion develops it

will be seen that this led to a more general examination of equivalence and pointed the way to a method of studying the changes in effect distributions as treatment schedules were modified (Deehan & O'Donoghue, 1991, 1994). These topics will be discussed in chapters 4 to 8 of this thesis.

1.1.3. Clinical radiobiology.

Although absorbed radiation dose strongly correlates with damage to cells and tissues the detailed mechanisms are not well understood (Steel, 1994; Joiner, 1993; Overgaard, 1993). Pioneers in this field developed mathematical models which attempted to describe the responses of normal tissues and tumours to radiation. Early empirical attempts such as the NSD, TDF (Ellis, 1967, 1969, 1985; Orton, 1975; Overgaard, 1993) or CRE (Kirk, 1971, 1972; Overgaard, 1993) were based on specific end points in the radiation reaction eg. desquamation or erythema effects in the case of skin. It also became apparent that different tissues respond in different ways to radiotherapy schedules and the above models do not distinguish between different tissues. New and more sophisticated formulae have recently been developed and are currently being used to model the responses of different tissues. Aspects of modelling will be discussed in more detail in the next chapter. Accurate prediction of differential radiation response is especially important when a familiar schedule has to be replaced by an unfamiliar one. Changes of schedule can happen for a host of reasons such as changes in dose rate in the case of brachytherapy, the introduction of hyperfractionated treatment in external beam therapy or merely when treatment is interrupted because of illness or adverse reaction.

The following sections of this chapter will establish the basis for radiobiology in radiotherapy by reviewing the factors influencing the response of cells and tissues to ionising radiation which is delivered as treatment schedule.

1.2. The molecular basis of biological effects of ionising radiation.

1.2.1. Damage to DNA.

As high energy gamma rays and photons pass through normal tissue, ionisation takes place and energy is deposited in the tissue. This leads to cell sterilisation, that is the loss of reproductive integrity, due to radiation induced damage to the DNA in the cell nucleus (Hall, 1988; Thames & Hendry, 1987; Steel, 1993).

Damage to DNA is believed to be a critical factor in this process because:

a) Micro-irradiation studies show that to kill cells by irradiation only of the cytoplasm requires far higher radiation doses than irradiation of the nucleus.

b) Isotopes with short range emission (^3H , ^{125}I) when incorporated into DNA efficiently produce radiation cell killing and DNA damage but not when bound to cell membranes or extra-nuclear structures.

c) The incidence of chromosomal aberrations following irradiation is closely linked to cell sterilisation.

d) Thymidine analogues such as IUdR and BUdR when specifically incorporated into chromatin modify radiosensitivity.

1.2.2. Linear energy transfer, LET (Thames & Hendry, 1987; Hall, 1988; Joiner, 1993).

Radiation induced damage is of two types (see figure 1.1):

a) Direct action, where the ions interact directly with DNA causing strand breaks.

b) Indirect action, where toxic free radicals are produced in the vicinity of DNA and are able to diffuse far enough to reach and damage critical targets.

The relative contributions of these processes to cell sterilisation depends on the linear energy transfer (LET) characteristics of the radiation. LET is defined as:

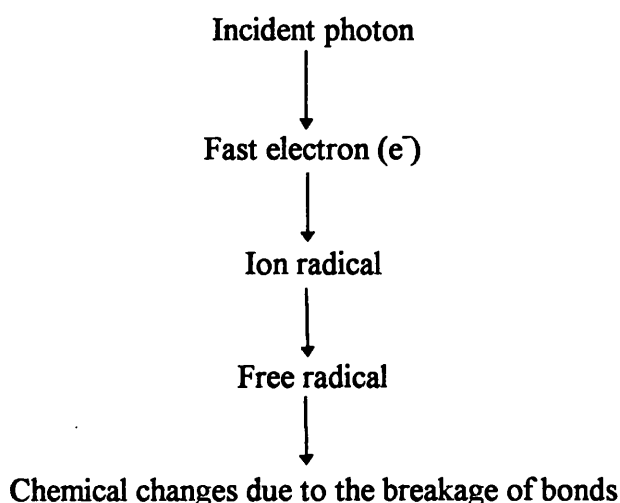
$$L_{\Delta} = \left(\frac{dE}{dl} \right)_{\Delta}$$

Where dE is the energy loss of charged particles along an incremental path of dl (Greening, 1985). The LET is often defined to only include energies below a certain threshold, Δ , thus excluding losses resulting from electrons (called δ rays) whose energy is not absorbed in the immediate vicinity of the main particle track. This is a more useful definition when deriving local energy deposition.

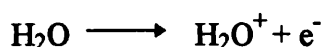
If the LET is high then the majority of the damage will be as a result of direct action and vice versa for low LET radiations. Gamma rays from cobalt 60 sources and

X-ray photons from linear accelerators are low LET radiations, they do not produce a high density of ionisation per unit length of track and so damage from these radiations arises mainly as a result of indirect action (Thames & Hendry, 1987; Hall, 1988; Joiner, 1993).

The sequence of events leading to indirect action can be summarised as follows:



If we consider the above process in water (about 80% of a cell is composed of water), then initially radiation with energy between 1 and 10 Mev produces ions mainly by Compton scattering (Greening, 1985):



H_2O^+ is an ion radical that is an atom which is electrically charged (ie an ion) which also contains an unpaired electron in the outer shell (ie a free radical) (Thames & Hendry, 1987; Hall, 1988; Steel, 1993). Because H_2O^+ is a free radical it is highly

chemically reactive. Ion radicals have a short lifetime (of the order of 10^{-10} sec and decay to produce free radicals, notably the hydroxyl radical (OH \cdot):



The OH \cdot free radical is a highly reactive entity and can diffuse a short distance, often reaching a critical target within a cell. It is believed that free radicals produced following ionization interactions with water molecules in tissue are of great importance in radiation induced cell damage process. The time scale of this process is of the order of 10^{-3} sec after exposure. During this time two main processes are at work, these are "scavenging reactions" that act in such a way as to neutralise the radicals and "fixation reactions" which lead to stable chemical changes within the DNA itself (Thames & Hendry, 1987; Hall, 1988; Steel, 1993). The latter of these processes is enhanced by the presence of oxygen and leads to cell damage. Radiation effects can manifest themselves over a period which varies from 10^{-18} sec to several years, some of these are shown in figure 1.2.

Three types of cell damage have been recognised these are: sublethal damage (SLD) (Elkind & Sutton, 1960; Elkind & Whitmore, 1967), potentially lethal damage (PLD) (Stapleton et al, 1953; Phillips & Tolmach, 1966; Belli & Shelton, 1969; Little, 1969; Hahn, 1975; Cornforth & Bedford, 1987) and lethal damage (LD) (Thames & Hendry, 1987; Hall, 1988). The last of these, LD, arises from lesions which are irreparable at the time of irradiation. The other two can lead to repair of damage and are described in chapter 2, sections 2.1.2. and 2.1.3.

1.3. Radiobiology of normal tissues.

The sterilisation of cells may occur immediately or may not occur until the cell has divided a number of times. An example of such an effect is the killing of stem cells and subsequent skin reactions referred to in figure 1.2. Reactions are often classified in terms of their time of onset following radiation for example acute or late reactions (see section 1.3.4.) (van der Kogel, 1993). Proliferation of normal cells can also take place soon after irradiation to compensate for cell damage (Steel, 1993). At intervals of perhaps months or even years after irradiation the effects of other processes are seen, these include fibrosis, telangiectasia of the skin, spinal cord and blood vessel damage and in some cases radiation induced cancers (Thames & Hendry, 1987; Hall, 1988; van der Kogel, 1993). The response of normal tissue to radiation is largely determined by three types of cells. These are stem cells, non-clonogenic proliferating cells and parenchymal or functional cells (see section 1.5.1.) (Thames & Hendry, 1987; Hall, 1988; van der Kogel, 1993). Tissues can be classified into two groups according to the cellular organisation within the proliferative and functional compartments (Michalowski, 1981). The first are Hierarchical (H-type) tissues, that have a clearly recognisable separation between stem cells, proliferative developing cells and mature parenchymal or functional cells. The second group are Flexible (F-type) tissues whose cells cannot be clearly separated into compartments and some of the functional cells at least can take part in cell renewal, see figure 1.3.

1.3.1. Parenchymal cells and connective tissue.

Parenchymal cells carry out the unique function of a particular tissue, but they are supported or held in position by connective tissue, and supplied with oxygen and nutrients by the blood vessels of the vascular system (Hall, 1988). Whether the parenchymal cells or the connective tissues and vascular system ultimately determine the level of tissue damage depends on the relative sensitivity of these tissue components. This will be described below (section 1.3.3.).

1.3.2. Hierarchical (H-type) tissues.

Skin, mucosae, intestinal epithelia and the haemopoietic system all have rapidly renewing parenchymal cell systems and are H-type tissue. The renewal process at work in the stem cells of this type contributes only a few percent to the total pool of proliferating cells while the bulk of these are involved in maturation into functional cells. In general radiation does not damage the mature cells in H-type tissues but instead affects the proliferative cells depriving them of their reproductive capacity (Hall, 1988; van der Kogel, 1993). The time lapse between irradiation and the onset of tissue response in this case is largely determined by the life span of the mature cells and is generally independent of the radiation dose. The time taken for these tissues to recover is however dose dependent and is related to the number of surviving stem cells (Steel, 1993).

1.3.3. Flexible (F-type) tissues.

These tend to have slowly renewing parenchymal cells eg. liver, kidney, lung and central nervous system. This type of tissue is not well characterised in terms of organisational compartments and factors such as vascular effects may contribute

significantly to the overall response. This is because parenchymal cells in these tissues require high doses of radiation in order to sustain significant damage. At these doses significant levels of damage may result to connective tissues and blood vessels and although the parenchymal cells may be able to repopulate in the short term delayed secondary damage such as the impairment of circulation or progressive breakdown of connective tissue may prevent recovery. Unlike the H-type tissues speed of response is dose dependent since mature cells which can take part in mitosis are sensitive to irradiation. Michalowski (1981) has proposed a model for the response of F-type tissues which predicts an avalanche effect. Here cells numbers reach a critical level and due to the homeostatic mechanism other irradiated cells are forced into mitosis which then also die.

1.3.4. Acute and Late effects.

Response can be broadly classified into acute responses, those occurring within a few days or weeks after irradiation, and late responses, those occurring after a few months or even over a period of years (Thames et al, 1989; Overgaard, 1993; van der Kogel, 1993).

Acute effects ordinarily appear in tissues with a rapid turnover of cells. Late reactions are associated with tissues which have a relatively slow turn over. Organs such as skin may exhibit both acute epidermal reactions and late responses such as fibrosis, atrophy and telangiectasia reflecting the diverse nature of different component tissues. This fact complicates the concept of tissue tolerance since different effects may be produced by different treatment regimes over different periods of time (Overgaard, 1993). The responses of tissue components of an organ can be unrelated as in the case of

epidermal and dermal reaction of the skin (Hopewell, 1991). Lung exhibits at least two types of injury, early pneumonitis, a "border line" acute reaction, and late fibrosis (van der Kogel, 1993). Split dose experiments showed (Down & Steel, 1983) that given the correct interval between treatments the pneumonitis could be made to subside but the late fibrosis remained. This indicated that the fibrosis was not a consequence of the pneumonitis but had a different origin. The central nervous system, also of interest in radiotherapy, has a number of responses associated with it, notably early white matter necrosis and late vascular damage. These reactions can again be separated out by split dose treatments with various intervals.

1.3.5. Volume effects.

One important aspect of radiation effect is the association with the volume of tissue irradiated which can have a marked influence on the tolerance dose levels (Overgaard, 1993; Steel, 1993). This tolerance level can be markedly different from that derived when tissue radiosensitivity is considered in isolation. This is not surprising bearing in mind that organs often possess considerable reserve capacity and only a fraction of their total volume may be required to sustain a high level of physiological function. Sensitivity therefore depends on how the tissue is divided into separate functional units and the volume irradiated coupled with the rate and the capacity of replacement cells to rapidly migrate in order to replace the losses in damaged areas.

Tissues whose cells have high migratory and reproductive capacity such as skin, mucosae and the intestine can tolerate relatively large doses to small volumes and still retain a high repair capacity. As the volume increases however and becomes large relative to the migration distance then repair is seriously effected and necrosis can result.

Tissues which are highly compartmentalised, for example lung and kidney, and which receive doses to large numbers of subunits (aveoli and nephrons in these cases) can obviously sustain irreparable damage easily because repopulation of cells from neighbouring subunits is unlikely. Organs may therefore be sensitive by virtue of the way they are organised as well as their own inherent sensitivity. Two types of organisation structures have been identified. Parallel organisation, for example kidney and lung where large numbers of cells can be irradiated without significant functional loss, and serial organisation such as spinal cord which is thought to consist of a series of subunits, the removal of any one of which may result in disastrous damage to the organ. Volume effects although by no means well understood, can lead to relatively insensitive organs being seriously damaged and relatively sensitive ones retaining adequate function depending on the type of organisation and the volume irradiated.

1.4. Radiobiological factors governing cell survival

Stem cells can in some cases be detected in assays by their ability to form colonies in vitro. Cells with this capacity are known as clonogenic cells (Steel, 1993; van der Kogel, 1993). The main factors which influence the response of clonogenic cells to radiotherapy can be summarised in the so called 4 "R's" (a fifth "R" was added by Steel (1989)) of Radiobiology which are:

1.4.1. Repair.

When cells are irradiated the majority of the damage is repaired in a way that allows cells to continue to function. Breaks in DNA strands can be seen to disappear in as little as a few hours following the irradiation. Repair refers to the process by which

the function of macromolecules is restored following irradiation (see sections 2.1.2. and 2.1.3).

1.4.2. Reassortment.

This process, otherwise known as "redistribution" refers to the progress of cells through less radiosensitive to more radiosensitive stages of the cell cycle, following preferential survival of cells in the more resistant phase. The cell cycle is divided into four stages (see figure 1.4.), these are mitosis (the cell division phase), the G1 phase, the S phase (DNA synthesis) and finally the G2 phase (figure 1.4(a)). The late part of the S phase is the most resistant with mitosis and the G1 phase being the most sensitive (figure 1.4(b)).

1.4.3. Repopulation.

This refers to the ability of the cells that survive irradiation to proliferate and this process can be stimulated by irradiation. Though beneficial for normal tissues it is obviously undesirable in tumours where effectively more cells have to be killed to produce a cure if repopulation begins during treatment.

1.4.4. Reoxygenation.

Tumour cells which are hypoxic (oxygen deficient) are less sensitive to radiation than aerobic (well oxygenated) cells. Aerobic cells may therefore be killed in the first dose of treatment so that those remaining will be nearly all hypoxic. However since they no longer compete with the cells already killed these cells become oxygenated over a period which may be as short as a few hours. As a result these cells are then more

sensitive to subsequent doses of radiation, so by fractionating the treatment resistant cells can be made sensitive to the radiation.

Steel (1989) suggested a fifth "R" associated with intrinsic radiosensitivity which has mostly been studied in cell cultures, this is:

1.4.5. Radiosensitivity.

Tissues as well as tumours differ greatly in their inherent sensitivity to radiation. The haemopoietic system for example is more sensitive than kidney.

1.5. Radiotherapy.

1.5.1. Therapeutic ratio.

Successful treatment in radiotherapy depends on maximising the destruction of tumour cells without exceeding the tolerance of critical normal tissues. An index of the effectiveness of treatment is the therapeutic ratio which can be expressed as:

$$\text{Therapeutic ratio} = \frac{\text{Effect on Tumour}}{\text{Effect on normal tissues}}$$

Expressing the therapeutic ratio in this way suggests that effects on tumour and normal tissue can be defined in the same numerical units. Later when mathematical models are discussed it will be shown that it is possible to derive units which represent effect. The success of radiotherapy depends on this ratio being favourable.

1.5.2. Tumour cure and normal tissue survival probability.

The probability of cure for tumour can be assessed against the dose delivered and this is often plotted in a sigmoid type graph, see figure 1.5(a). As the dose increases the cure probability rises sharply and proceeds asymptotically to a maximum value (100%) which is never attained by any dose however large. The probability of damage to normal tissues is related to the delivered dose in a similar way. Figure 1.5(b) shows two representative curves superimposed, if a high dose is delivered in an attempt to maximise tumour cure probability this can result in a very high risk of normal tissue damage. The relative slope of these curves and the gap between them ultimately determine the therapeutic ratio. A compromise is often necessary where less dose is given reducing the cure probability but at the same time reducing the probability of normal tissue damage or complication rate to an acceptable level. Typically the complication rate aimed for is no more than 5%.

1.5.3. The effects of fractionation and dose rate

External beam therapy given using linear accelerators or teletherapy units is fractionated, that is the total dose is not given all at once but is instead divided into short daily doses given over a minute or two. For standard treatment schedules the number of fractions and the total dose given has been determined by empirical means, nevertheless there are sound radiobiological reasons why these schedules produce good results. In the case of brachytherapy it is known that changing the dose-rate will effect the level of cell killing for both normal tissues and tumour. Traditionally brachytherapy was given at low dose-rate (eg 0.5Gy/hr) often over a period of a few days. Changing patterns of treatment either the time-dose-fractionation pattern in external beam or the dose rate in

brachytherapy, can have unforeseen consequences since different tissues and tumours react in different ways to these changes.

1.5.4. Fractionated radiotherapy.

Soon after the discovery of X-rays they were used to treat superficial skin lesions such as carcinomas of the lip. Some of these treatments produced excellent results and this was probably due to the fact that protracted fractions had to be used because of the extremely low dose-rates produced by the original X-ray generators. Following the first World War the situation had improved with the introduction of the cathode ray tube which not only allowed the production of higher dose-rates but resulted in greater penetration of the radiation into tissues (del Ragato 1990). These improvements made it possible for treatments times to vary and so many dose-time-fractionation patterns were possible. Methods varied from giving the largest permissible dose over the shortest time (Seitz & Wintz, 1920) to short intensive courses of two or more fractions (Holtzknecht, 1923) or doses which varied according to clinical experience without any real radiobiology rationale (Kingery, 1920; Freund, 1930). Claudius Regaud (1922), in Paris, was the first to demonstrate experimentally that a moderate total dose, fractionated over several days was more effective in terms of therapeutic ratio than a larger dose given all at once, and this was extended by Henri Coutard (1935) when he treated his patients twice daily for several weeks.

In 1920 - 1930 as commercial dosimeters became available radiobiologists and biophysicists sought to relate dose to biological effects such as skin reactions. However the threshold for reactions was difficult to define and to complicate matters it appeared that the same reactions could be obtained by using a number of different fractionation

schedules. Stenström (1926) was able to express this as a mathematical formula in which exponential recovery from radiation damage was assumed. Later Strandqvist (1944) plotted the total dose given against total time for treatments of the skin and lower lip on a log-log graph to find that successful treatments followed a straight line. Cases above the line resulted in necrosis while those below produced recurrences. This prompted radiobiologists to seek a mathematical expression which predicted the effects of radiotherapy on tissues. The most important of these models will be discussed in chapter 2, section 2.3.

Technical improvements in the way that doses were delivered, especially between 1950 - 1970, produced new radiotherapy therapy machines, leading in turn to new treatment techniques. Over this period efforts were concentrated on methods which would allow the tumour dose to be increased as much as possible and much of the radiobiology work was concerned with cellular and molecular aspects with less emphasis on tissue tolerance to radiotherapy regimes. External beam radiotherapy at this time was delivered 5 days per week with 1.7 to 2 Gy per fraction (ie. conventional fractionation). During the 1970s it became apparent that reducing the number of fractions and delivering a higher dose per fraction (hypofractionation) could not be used as a realistic option in radical treatments because of the increase in normal late responding tissue complications. (Horiot, 1991).

Awareness of the 4 "Rs" of radiobiology mentioned earlier led to laboratory and clinical experiments delivering more than one fraction per day. The underlying philosophy in this work was to take advantage of the supposedly superior capacity of late responding tissues to repair damage after small fractions (Horiot, 1991). Schedules such as these result in complex changes in cell kinetics (see table 1.1) for both normal

tissue and tumour cells. In view of these findings and acceptable clinical results, produced in many cases by conventional scheduling, it is easy to see why oncologists wisely exercised caution when considering changes in fractionation patterns.

However, in spite of this alterations have been made to the standard schedules, the most notable being:

a) Hyperfractionation treatments.

These are given with a higher number of smaller fractions but over the same time period as the standard treatment. The dose delivered each day is usually given in two fractions with an 6 hour interval between them to allow the recovery of normal tissues, a factor which essentially sets the late responding tissue tolerance. Table 1.2(a) shows two examples, one given in Europe (Horiot et al, 1988) and one from the USA (Parsons et al, 1988). Notice that with Horiot's schedule the total dose increases by 15%, an increase made possible by the relative gains in tolerance of late responding tissues. Parson's schedule adds 10% to the total dose and these two approaches should produce improvements of between 10% - 15% in local control with no increase in late response. This is in agreement with the reported clinical results and is also in keeping with the predictions of Thames et al, (1983) based on radiobiology theory.

b) Continuous Accelerated Hyperfractionated.

Where the overall time is reduced together with an increase in the number of fractions. This type of schedule was chosen for the CHART trial of Saunders et al (1988) details of which are given in table 1.2(b). This schedule is given over 12 days with no stoppages, even at weekends. Although the results of this trial are still being

evaluated preliminary reports show this type of scheduling has advantages in terms of tumour control over conventional schedules.

It is no accident that the results of alternative treatments of the type described above should coincide with the predications of current iso-effect models used in radiobiology. The use of models which reflect the basic radiobiological principles has assisted the process of change, this is particularly true of the Linear Quadratic (LQ) Model which is currently regarded as the modelling tool of choice (Fowler 1989; Brenner, 1991). The next chapter will review the LQ (Chapter 2, section 2.4.).

1.5.5. Brachytherapy treatments.

Instead of using external beam therapy, treatment may be given by placing radioactive sources on the surface of the skin (external mould), or implanting sources into tissues (interstitial treatment), (Paterson, 1963). The advantage of this approach is that the radioactive material is in close proximity to the treatment zone. Ideally, this means that the tumour should receive a much higher dose than surrounding normal tissues. In 1905, some 9 years after the discovery of radioactivity by Becquerel, radium was being used in Paris for the treatment of cancer (Mould, 1992). As with the development of fractionated treatments brachytherapy was initially limited by physical factors such as the low specific activity of sources and low dose rates. Although individual treatment techniques varied greatly, by the 1940s and 1950s successful techniques had been developed based on fixed geometrical arrangement of sources and known treatment times. Dose rates were around .5 Gy/hr and treatments often lasted a few days (Tod & Meridith, 1938; Paterson, 1963). One example of this method, which is

still in use today, is the Manchester System that uses calculated treatment application rules which can be applied to intracavitary, interstitial and external mould treatments. This system is described in appendix A1.

The introduction of sources with high specific activities and reliable rapid source carrier systems allowed remote controlled after loading techniques to develop which led to a number of benefits in the field of brachytherapy. The traditional Manchester approach required sources to be manipulated and loaded into the patient by hand. Even with remote handling tools, lead screening and carefully thought out procedures, this led to high exposure levels to theatre and ward staff (Joslin, 1990). The new method allowed the source carriers to be positioned empty and sources could be loaded and unloaded safely by remote control (Joslin, 1994). Traditional long treatment time also exposed ward staff and other patients to risk, whereas newer methods used higher dose rates resulting in shorter treatment times, and these could also be precisely programmed. Lastly, with Manchester type treatments the source were loaded into rubber containers which were prone to movement and distortion within the patient while rigid carrier systems achieved a more reproducible geometry.

The very real advantages achievable with remote after loading brought with them some doubts however which were associated with changes in the dose rate. It is well known that increasing the dose rate produces a higher level of damage not just to tumour but also to normal tissues (Steel et al, 1986; Dutreix, J. 1989; Hall, 1972, 1991; Fowler, 1990). In the chapters that follow the effects of varying dose rates will be discussed in relation to the predictions of iso-effect models. Much of the discussion will relate to intracavitary insertions but many of the result are equally applicable to interstitial and external mould treatments.

1.5.6. Dose rate effects.

In radiotherapy the useful range of dose rate lies between 0.1 Gy/hr and several Gy/min (Hall, 1991), see figure 1.6. Early intracavitary treatments used dose rates in the lower end of this region and a great deal of clinical experience was gained using these treatments over many years. Dose rates are often classified into three regions low (LDR), medium (MDR) and high (HDR) as in table 1.3 (Corbett, 1989). It has been shown by irradiating cells in vitro that increasing the dose rate increases the damage sustained per unit dose (Hall, 1991; Steel, 1993). In the same way as changing the dose per fraction in external beam therapy had different effects on different tissues, acute and late responding normal tissues and tumour respond in a different ways to changes in dose-rate.

The true "gold standard" for the treatment of cancer of the cervix is still the LDR Manchester type arrangements, this is because of the acceptable levels of local control and late normal tissue damage associated with LDR, although an increasing number of patients are treated with MDR and HDR insertions. Late responding tissues seem to be more sensitive to changes in dose rate than acute responding tissues. Many tumours are thought to respond in a way similar to that of acute responding tissues (Orton, 1990; Fowler, 1990). Differential responses may be offset by fractionation of the treatment especially at HDR (Fowler, 1990), with the result that HDR treatments are generally given in 3 or more fractions, when replacing 1 fraction at LDR. The tendency at MDR is to simply alter the treatment time in order to give a lower dose compared with LDR (Wilkinson et al, 1983; Symonds et al, 1989, Stout et al, 1989; Jones et al, 1990; Hunter, 1994).

Treatment times of the order of 72 hours are common at LDR. This time can be reduced to under 20 hours with MDR and HDR is often given over several fractions, each lasting a few minutes at most. The optimal dose per fraction and number of fractions required at MDR or HDR to produce the same result as LDR (ie biological equivalence) are difficult to determine and ultimately will depend on clinical comparisons. Randomised clinical trials are difficult to conduct and results are complicated by changes in the geometry of the insertions and the fact that external beam therapy is often used in conjunction with this type of brachytherapy.

1.5.7. Equivalence between different radiotherapy schedules.

This chapter has laid down the basis for radiobiology in radiotherapy and reviewed the contribution of radiobiologists have made in recent years. There is a clear need not only to devise new improved types of treatment (fractionated radiotherapy) but also to devise schedules which are biologically equivalent to existing schedules (brachytherapy) in relation to some biologically meaningful end point. This thesis deals with equivalence between radiotherapy schedules in the following chapters.

Appendix 1. Manchester system of dosage used in intracavitary insertions in gynaecological oncology (Paterson, 1963).

The dose distribution around an intracavitary insertion is far from homogeneous and falls off rapidly with distance from the centre of the insertion (see figure A1.1). It is necessary to find a representative point at which the dose can be specified. The point chosen in the Manchester system is known as the "A" point (see figure A1.2). This point is in the paracervical triangle and was believed to be an appropriate point for recording normal tissue and tumour doses while at the same time being reasonably comparable from case to case. The A point is defined as being 2 cm lateral to the central canal of the uterus and 2 cm up from the mucous membrane of the fornix in the axis of the uterus (Tod & Meridith, 1938; Paterson, 1963).

The lateral fornix is accepted as being at the level of the lower end of the central uterine tube containing the radio-active sources (see figure A1.2). This definition of the standard dose point is extremely useful except in cases where the position of the uterus is displaced or angulated. In these cases an inequality of A point dose can arise (between the left and right side) but it is found that in 90% of cases inequalities are less than 10%.

It can be seen therefore that the classification of the standard point is useful in comparing different intracavitary insertions.

Normally the dose must be considered at various tissues which are radio-sensitive for example the interior of the uterus, the vaginal mucosa, the recto-vaginal septum and the region around the A point. In two insertions the total dose levels which were determined on the basis of the original Manchester system are shown in table A1.1.

Table A1.1 Manchester dosage system	
Position	Dose (Gy)
at the A point	74
on the wall of uterus	over 27.75
on the vaginal mucosa (vault)	18.5 to 23.125
in the retro vaginal septum	62.44

These are the dose levels considered acceptable on the basis of dose-rates around 0.5 Gy/hr.

The main limitation to the total dose is set by normal tissue tolerances around the A points. The A point is regarded as important because evidence exists which suggests that high dose effects in the paracervical tissues in this region produce extrinsic rectal reactions. Although the A point is the main consideration it must be emphasised that tolerance levels in other normal tissues are also important, for example the bladder, and these can often limit the dose.

Table 1.1	Response of the 4 "Rs" in tissue and tumour to increases in fractionation number		
	Acute responding tissues	Late responding tissues	Tumours
Repopulation	E	V	E
Repair	V	E	V
Reoxygenation	U/M	U/M	E
Redistribution	E	V	E
Key: E = enhanced, U/M = unlikely to be modified, V = variable			

(from Horiot 1991)

Table 1.2 (a)	Hyperfractionation schedules Vs conventional control arm			
	Dose per fraction (Gy)	Number of fractions	Total dose (Gy)	Total Time (weeks)
Conventional arm	2.00	35	70	7
Horiot et al	1.15	70	80.5	7
Parsons et al	1.20	65	78	6.5

Table 1.2(b)	Accelerated hyperfractionation (CHART) versus conventional control arm			
	Dose per fraction (Gy)	Number of fractions	Total dose (Gy)	Total Time
Conventional control arm	2.0	30	60	6 weeks
CHART	1.50	36	54	12 days

Table 1.3	Dose-rate ranges in brachytherapy (Gy/hr)
Low dose-rate (LDR)	0.1 ----- 2.0
Medium dose-rate (MDR)	2.0 ----- 12
High dose-rate (HDR)	Above 12 Gy/hr but usually 150 Gy/hr

(from Corbett 1990)

Figure A1.1 Dose-distribution around an insertion (Gy).

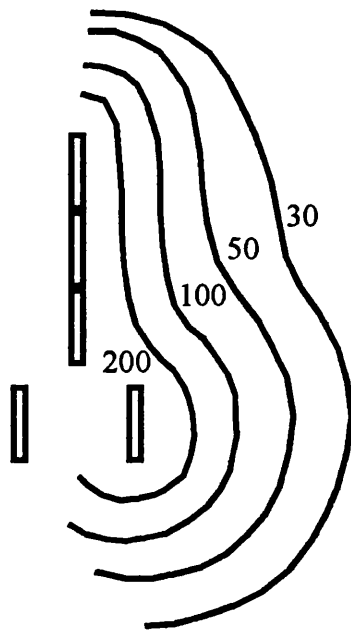


Figure A1.2 Position of the A point.

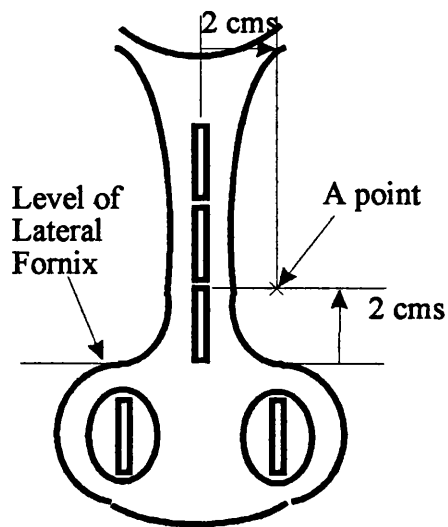


Figure 1.1 Interaction of radiation with cells.

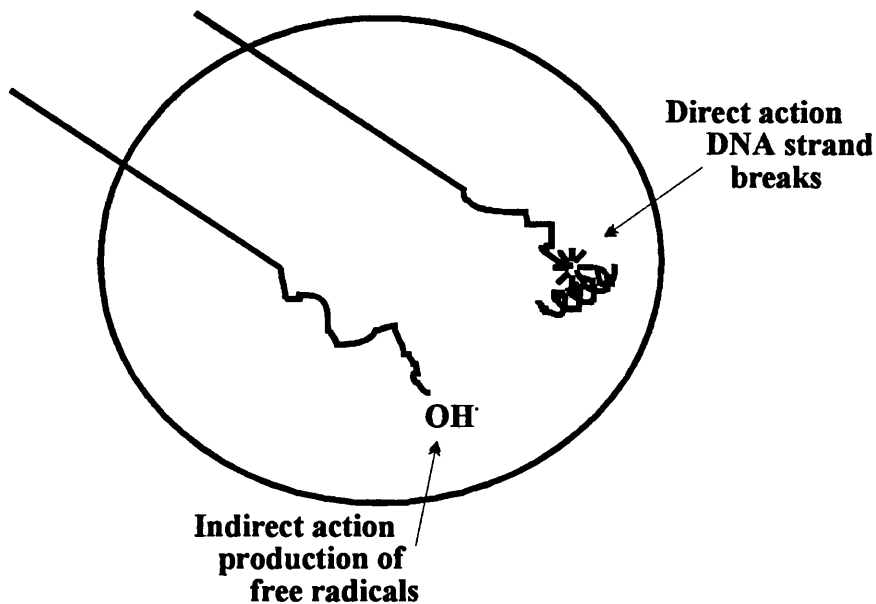


Figure 1.2 Timescale of radiation interactions and damage.

A C U T E		Excitation, ionisation	10 ⁻¹⁸ sec
	Free radical reactions	10 ⁻³ sec	
	Nausea (whole body)	hours	
E F F C T S	Gastro intestinal symptoms	1 day	
	Clinical signs of blood upset	1 week	
	Moist desquamation of skin	2 weeks	
	Effects on the vascular system	3 months	
L A T E			
E F F C T S			
	Leukaemogenesis induction of cancer		8 - 10 years

Figure 1.3 Hierarchical (H - type) tissues and Flexible (F - type) tissues

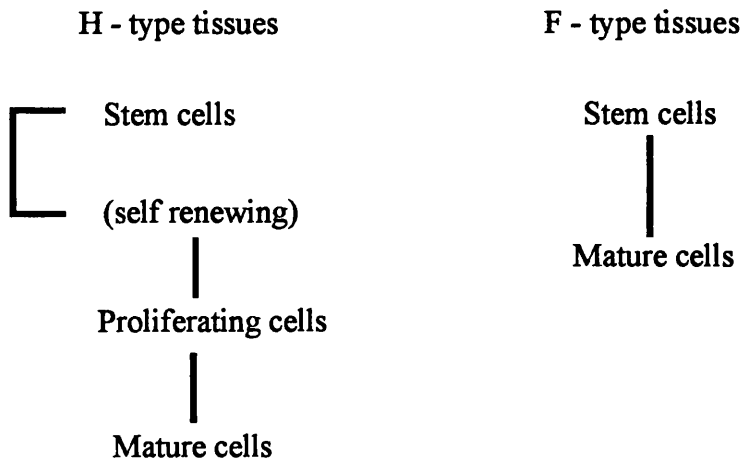


Figure 1.4 Cell cycle (a) and radiosensitivity (b).

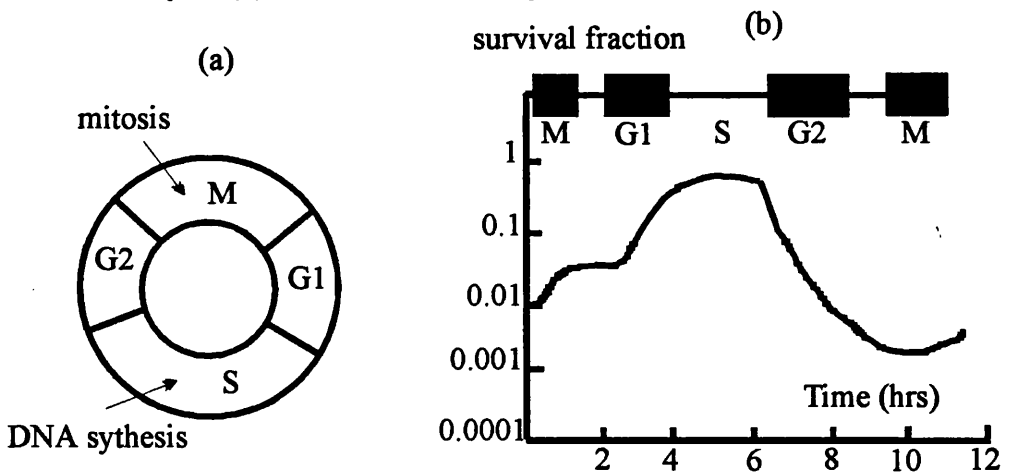


Figure 1.5 Cure probability for tumour (a) and damage probability for normal tissue (b).

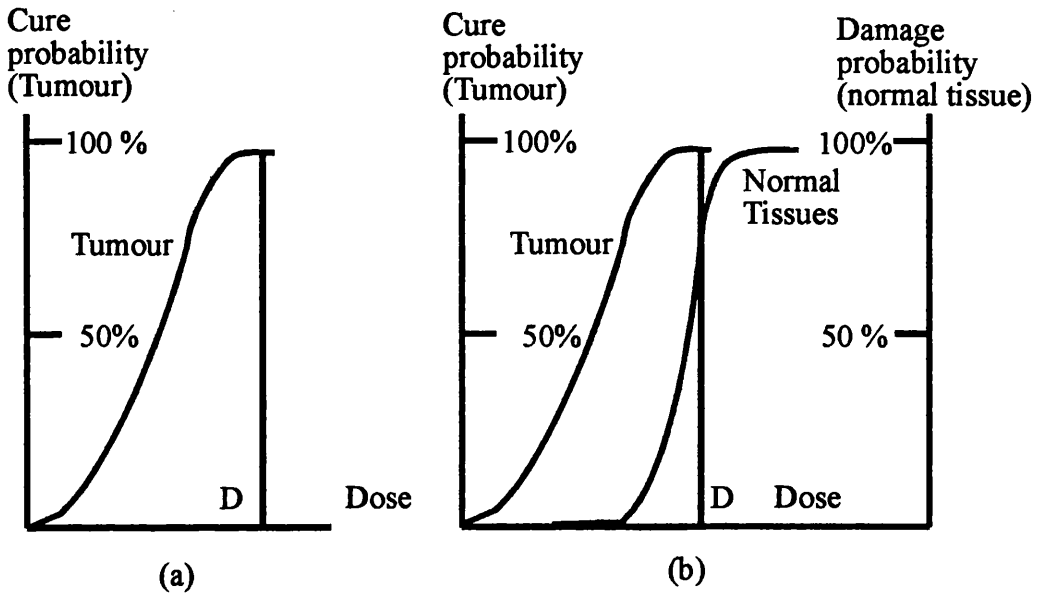
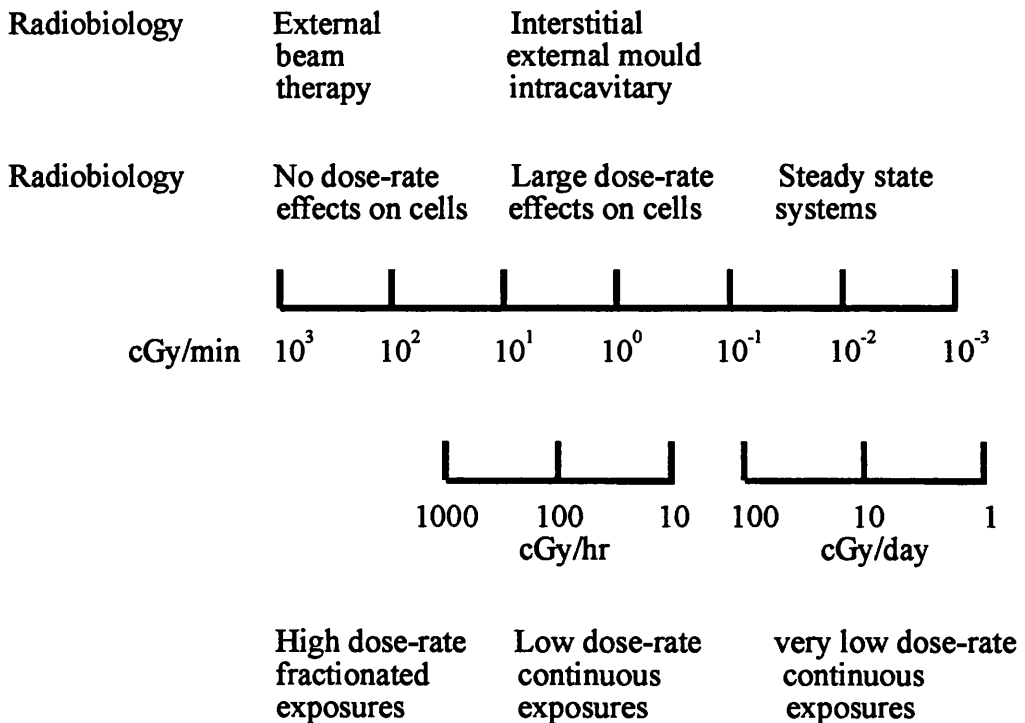


Figure 1.6 Dose-rate spectrum for radiotherapy and radiobiology.



Chapter 2

Radiobiological models in radiotherapy.

2.1. Introduction.

The relationship between absorbed dose and cell damage or cell death is a fundamental issue in radiobiology theory. Numerous attempts have been made to model this process which depends in a complex way on the level of dose, the type of radiation used and the way the dose is delivered, ie the dose-time-fractionation pattern (Stenström, 1926; Strandqvist, 1944; Oliver, 1962; Ellis, 1967, 1969; Kirk et al, 1971, 1972, 1976; Laurie et al, 1972; Chadwick & Leenhouts, 1973; Douglas & Fowler, 1976; Elkind, 1976; Gilbert et al, 1980; del Regato, 1990; Horiot, 1991). This chapter outlines the origin of these models and how well their predictions agree with experimental and clinical data. Early models are described and the progress of this work is discussed up to those formalisms currently in use such as the linear quadratic (LQ) model.

2.1.1. Radiation damage to cells.

Radiation kills cells by depriving them of their reproductive capacity (in radiobiology, cell killing usually means reproductive sterilisation, see chapter 1, section 1.2). Various types of DNA lesions are possible, the most important of which seems to be unrepaired double strand breaks. Just one residual double strand break in a vital section of DNA may be sufficient to produce a chromosome aberration and sterilise the cell (Bahari, 1990; Bedford, 1991). Damage to mammalian cells produced by ionising radiation can be divided into three categories which are: lethal damage (LD) which leads

irrevocably to cell death, sub-lethal damage (SLD) (Elkind & Sutton, 1960; Elkind & Whitmore, 1967) which may or may not be repaired between radiation doses and potentially lethal damage (PLD) (Stapleton et al, 1953; Phillips & Tolmach, 1966; Belli & Shelton, 1969; Little, 1969; Hahn, 1975; Cornforth & Bedford, 1987) which is influenced by post irradiation environmental conditions. The true nature of damage is still uncertain and these classifications are purely convenient ways of describing the process. A brief description of SLD and PLD is given below.

2.1.2. Sublethal damage.

This model of cell damage assumes the accumulation of lesions in some but not all of its critical targets, following irradiation. SLD damage at one site can interact with that at another to produce LD, or it may repair itself in the course of a few hour leaving clonogenicity intact. The time course and extent of SLD can be measured by split-dose recovery. This is done by delivering a test dose to a cell population at varying times after an initial dose and measuring the survival fraction of that population. Provided there is no progression through the cell cycle, then the survival fraction increases with increasing time interval to a plateau. This increase is believed to be due to the repair of sub-lethal damage (Thames & Hendry, 1987; Hall, 1988). For most cells half of the increase in survival is reached in about 1 hour (repair half-time) and in 2 to 4 hours the total increase is achieved (Thames & Hendry, 1987; Hall, 1988). At the end of this time the cells behave as though they had not been irradiated before.

2.1.3. Potentially lethal damage.

If after irradiation, cells are placed in growth medium which is suboptimal for growth, (for instance physiologically balanced salt solution), this often slows down the growth rate of the cells. Under these conditions cells can show less damage than those which are immediately returned to ordinary (optimal) conditions. The increased survival is enhanced by increasing the delay between irradiation and the return to optimal growth conditions. The mechanism thought to be responsible for this enhancement of survival is the repair of PLD. It is believed that this type of damage would be potentially lethal under conditions which are optimal for cell growth but PLD repair may lead to enhanced survival under suboptimal growth conditions, for example *in vivo* as compared to where cells are incubated in full growth medium.

2.2. Survival curves and target theory .

The survival characteristics of cells grown in tissue culture and then exposed to radiation can be used to deduce important information associated with cell killing. If the log of survival fraction is plotted against delivered dose for a given cell line then a characteristic curve is obtained (figure 2.1). Traditionally this has been regarded as having a curved or "shoulder region" followed by an approximated straight line region (Deacon et al, 1984; Thames & Hendry, 1987; Hall, 1988). It is possible to explain the shape of the survival curve on the basis that regions of DNA exist which are important to maintain the reproductive capacity of the cells. If these sensitive regions or targets are not hit during irradiation then the cells will survive the radiation exposure (Lea, 1947; Thames & Hendry, 1987; Hall, 1988). If on the other hand any of these targets are hit then cell sterilisation may occur. Two main theories exist regarding the statistics of this

process: these are the single-target single-hit and the multi-target single-hit theories (Chadwick & Leenhouts, 1973; Thames & Hendry, 1987; Hall, 1988).

2.2.1. Single-target single-hit.

In this theory a hit on a single target is all that is required to bring about cell death. In this case the plot of the survival fraction versus dose looks like that shown in figure 2.2. Notice in this case there is no shoulder region at low doses as occurs in figure 2.1.

Poisson statistics can be used to model this process and the probability (p) of survival can be shown to be:

$$p(s) = \exp(-D/D_0) \text{ ----- 2.1}$$

This is the probability that there will be no hits occurring within the target region of a given cell, where D is the given dose and D_0 is the dose that gives an average of one hit per cell. A dose of D_0 reduces the survival probability by a factor of $1/e$. Although this rather simplified approach cannot be used to predict all of the responses of cells to radiation, many simple organisms such as viruses and bacteria respond in this way and produce a straight line on a log-linear plot as shown in figure 2.2.

2.2.2. Multi-target single-hit.

This more general version of target theory begins with the proposition that cell death requires just one hit by radiation on each of n sensitive targets in the cell. From equation 2.1 the probability of survival is:

$$p(s) = \exp(-D/D_0)$$

for a specific target. If the probability that the target will be inactivated is $p(\text{in})$, then:

$$p(\text{in}) = 1 - p(\text{s})$$

$$p(\text{in}) = 1 - \exp(-D/D_0)$$

as there are n targets in the cells the probability that they are all irradiated is $p(\text{ir})_{\text{all}}$ then:

$$p(\text{ir})_{\text{all}} = (1 - \exp(-D/D_0))^n$$

or $p(\text{s})_{\text{all}}$ is the probability that all targets will not be irradiated:

$$p(\text{s})_{\text{all}} = 1 - (1 - \exp(-D/D_0))^n \text{ -----2.2}$$

This gives a shouldered survival curve of the type shown in figure 2.1. (Thames & Hendry 1987; Hall, 1988). The shoulder region can be classified in terms of:

D_q , the quasi-threshold dose which is the dose at which the extrapolated straight line portion of the dose-response curve cuts the dose axis.

n , the extrapolation number which corresponds to the point on the y axis which is cut by the back extrapolation line, and is a measure of the "width" of the initial shoulder region.

The relationship between n , D_0 and D_q is:

$$D_q = D_0(\ln(n))$$

At low doses, that is below 3Gy, in a region which corresponding to individual doses delivered in fractionated radiotherapy, the multi-target model predicts a response that is very flat, (figure 2.3), ie these low doses should produce very little cell killing. Most experimental results indicate that the dose-response relationship in this region is,

however, not flat. Various attempts have been made to resolve this discrepancy, for example the combination of multiple and single hit formalisms in one model. A better description of cell response in the low dose region is obtained using the linear quadratic (LQ) model, and is one of the reasons for this model being currently favoured (see section 2.4).

2.2.3. Repair saturation models.

Another way of explaining the shape of cell survival curves is to use repair saturation models. It is assumed that potentially lethal damage is repaired successfully or fixed (remains unrepaired or develops into lethal damage) as the cell goes through some critical stage in its cycle. The downward bending of the survival curves occurs because at low doses the system is unsaturated and the repair can cope with potentially lethal damage (ie. repair it). At higher doses too much damage is produced for the repair process to cope with and the system essentially "saturates". It is uncertain what mechanism is at the heart of the repair process in cells which have been irradiated and both sub-lethal and saturation repair models have their own way of explaining the phenomena of this process.

2.2.4. Linear quadratic model.

The arguments above rely on all targets being inactivated and although useful in describing the shape of the cell survival curves, equation 2.2 has not been derived from a biological basis. Even though rapid processes are at work to repair damage following cell irradiation, the presence of even one non repaired or misrepaired genetic lesion can cause cell death during mitosis. Incorporating this concept into the mathematical modelling of survival curves is more complicated than in the case of multi-target models.

This reasoning is based on the inactivation of target pairs by a single event or two interacting events leading to a break in the double stranded DNA. In this case the survival curve equation can be well approximated to:

$$SF = \text{EXP} (- \alpha d - \beta d^2) \text{-----} 2.3$$

The factors α and β are parameters which are specific to the type of cells irradiated and are described more fully in section 2.4. (Douglas & Fowler, 1976; Thames & Hendry, 1987). These parameters are more often expressed as the α/β ratio which has units of Gy. This model produces a curve which is continuously bending and whose curvature is characterised by the ratio α/β (Barendsen, 1982; Thames et al, 1982; Withers et al 1982(c)). The form of equation (2.3) is appropriate for radiation delivered in high dose rate fractions. The lower the value of the α/β ratio the more "curvy" or the steeper the slope of the survival curve. The linear quadratic (LQ) equation for cell survival comprises two terms:

i) A linear term where the number of lethal events is proportional to the dose, d , known as A-type damage.

ii) A quadratic term, βd^2 , representing the process where two sublesions (each produced in number proportional to dose) interact to produce a lethal event the production of which is proportional to dose, known as B-type damage.

The α/β ratio is the dose at which the quadratic component (βd^2) equals the linear component (αd) (at higher doses it exceeds it) see figure 2.4. (Thames & Hendry, 1987). The mean number of lethal events produced is therefore equal to $(\alpha d + \beta d^2)$ and the survival fraction is as shown in equation 2.3. From its origin in cell survival theory

the LQ model is now widely used in radiotherapy to model the response of tissues to different treatment schedules (Dale, 1985; Fowler, 1989, 1990; Orton, 1990). At present the LQ model seems to be the modelling tool of choice for many experimental and clinical applications (Brenner 1991). Its application to tissue and tumour responses is discussed in section 2.4.

2.3. Early iso-effect models.

Radiation effects on cells grown in tissue culture can be most important in understanding the damage process. For these findings to be of clinical use it is necessary to accurately predict the effects of radiation on normal tissues and tumours in vivo. The relationship between the overall treatment time, the total dose and the fraction size has been an issue of great interest since radiation was first used to treat malignant disease. Early in the history of radiotherapy it became evident that the biological effect of a dose given as a series of fractions was less than if that dose was given all at the same time (chapter 1., section 1.5.4.). This fact was investigated by Strandqvist (1944) in his study of lip and skin lesions. His aim was to establish an iso-effect plot which would allow the effects of changing dose patterns to be predicted, see figure 2.5. When the overall times were plotted on double logarithmic scales he found that recurrences lay below the line and complications above the line. In addition to which the response could apparently be modelled using the relationship (Strandqvist, 1944; Thames & Hendry, 1987):

$$D = kT^{0.22} \text{ ----- } 2.4$$

Where D = total dose, T = overall time and k is a constant.

Experiments performed by Fowler (1965) on pig skin showed that the fraction number, N, was a more important parameter than the overall time. These findings led Ellis (1969) to the realisation that the time factor was actually a composite effect of N and T. This fact is in keeping with current thinking in that modern formalism such as the LQ model stress the dose per fraction rather than the fraction number. Ellis (1969) suggested that the formula for tissue tolerance should be:

$$D = NSD.(N^{0.22}).(T^{0.11}) \text{ ----- 2.5}$$

with D = total dose, N = fraction number and T = total time. The term NSD is the nominal standard dose and is a constant expressed in units known as the ret (radiation - equivalent - therapy). It is important to note that this model expressed results in these units and not in units of absorbed dose (Gy), and later versions of this formula used a fraction number exponent of 0.24 instead of 0.22 (Ellis, 1985). The cumulative radiation effect (CRE) model was developed by Kirk et al (1971) from the NSD model of Ellis. Mathematically this could be described as a rearrangement of the terms of the NSD type expression but with the important difference that it incorporates the concept of iso-effect at sub-tolerance doses. A further development came when Orton and Ellis (1973) derived the time dose factor model (TDF) from the NSD model. This had the advantage that the TDF result was linearly proportional to N so that different parts of a radiotherapy course could be added together in a simple way (Orton & Ellis, 1973).

$$TDF_{(total)} = TDF_1 + TDF_2 + \dots + TDF_n$$

for n courses of treatment. The full TDF formula is:

$$TDF = 1.19N(d^{1.54})(T/N)^{-0.17} \text{ ----- 2.6}$$

for fractionated radiotherapy. Here the scaling factor of 1.19 is present in order to make TDF = 100 equal to tolerance. For continuous treatments the formula was:

$$TDF = 2.39TR^{1.35} \text{ ----- } 2.7$$

Where R = the dose-rate in Gy/hr and T is the treatment time in hours. Once again the factor 2.39 is added to scale TDF = 100 as tolerance. Since the TDF for continuous treatments is linearly proportional to time (T) then the TDF for subsequent treatments can be added, and since they are both normalised to the same tolerance then both fractionated and continuous can be simply added:

$$TDF_{(total)} = TDF_{(fract)} + TDF_{(cont)}$$

This simple process is not possible with the more general NSD formula so that the TDF derivation can be regarded as one which has been developed for computational convenience. Liversage (1971) reviewed the NSD type approach and pointed out some weaknesses in the rationale underlying this type of formalism. He begins with the general equation:

$$D_n = D_1 (N^A) (T^B) \text{ ----- } 2.8$$

In order for this equation to hold there are certain assumptions which have to be made these are:

- (i) That iso-effect curves may be described by this type of relationship (ie those of the type Strandqist plotted).
- (ii) A is a constant for all tissues and tumours.
- (iii) B is a constant for all normal tissues.
- (iv) B is zero for all tumours lacking homoeostatic control (ie no altered repopulation by tumours during therapy).

The first assumption implies that iso-effect curves obtained by plotting iso-effect dose against number of fractions will produce a straight line and that the slope will be equal to $(A+B)$. Such plots are however in practice slightly curved, the consequence of which is that no matter what values of A or B that are chosen the power law representation is never totally correct. The second assumption that A is a constant (0.24 in later NSD formula) for all tissues implies that the therapeutic ratio is independent of the number of fractions used in a given overall time. This assumption is certainly wrong and could be dangerous since it could lead to treatments being given in fewer fraction with larger doses per fraction. The temptation would exist therefore to reduce the number of fractions in a given treatment schedule for example from 30 in six weeks say to 6 over the same time period for social and treatment management reasons. The NSD, CRE and TDF formulae all imply that a total dose could be found which would cause an unorthodox schedule to have exactly the same effects as a conventional one. It has now been established as discussed in chapter 1, section 1.5.4., that converting to treatments of fewer, larger fractions can produce dramatic increases in radiation damage (when the total dose is too high) which are greater for some tissues than for others. In particular the NSD type approach under estimates the effect to late responding tissues if the dose per fraction is increased and the number of fractions reduced, because of the dissociation of both acute and late effects. Taken together the weakness of these first two of Ellis's assumptions is one of the reasons for the rise in popularity of the Linear Quadratic (LQ) model (section 2.4). Strictly speaking, even if different tissue parameters are used to account for different responses, the power law model would still not give correct predictions. If assumptions (ii) and (iv) are correct, then iso-effect curves for tumour having no homoeostatic control would have the same slope and this

would equal A. At the time of his article Liversage could refer to results which showed different slopes for different tumours (Pearlman & Freidman, 1968). If assumptions (ii) and (iii) were correct then iso-effect slopes for all normal tissues would have the same slope. This has been tested with many normal tissues and slopes are different for different tissues. Although there were little data available at the time Liversage concluded that the NSD formula may be generally valid for two particular tissues, these are skin and squamous cell carcinoma (Liversage 1969). Recently the most frequently used iso-effect model has been the LQ model which does not suffer from many of the shortcomings of the NSD type approach.

2.4. The linear quadratic (LQ) model for normal tissue effects.

In order to interpret the results of skin iso-effect doses for fractionated radiotherapy Douglas and Fowler (1976) used the LQ model because it allowed easier determination of parameters from iso-effect data than other models. Use of the early LQ models grew primarily because of the realisation that it was possible to specify tissue fractionation sensitivity with the ratio of the parameters α and β shown in equation 2.3. The LQ model is one of the most important recent developments in radiobiology and been used to describe the relationship between total iso-effective dose and dose per fraction in vivo in fractionated radiotherapy. It has also been extended by Dale (1985) for use in continuous or protracted treatments with the fractionated form of the LQ model emerging as a special case at high dose-rate.

2.4.1. LQ model - Fractionated radiotherapy.

If we recall the shape of the survival curves of the type shown in figure 2.1 then the shoulder region can be modelled by this type of relationship:

$$\text{Survival fraction for a dose } d, \text{ SF}(d) = \exp(-\alpha d - \beta d^2)$$

where d is the dose per fraction, and where α and β are constants required to model the slope of the survival curve for a particular cell line. If a series of fractions is given (N) then the survival fraction can be expressed as:

$$\text{SF}(Nd) = \exp(-\alpha d - \beta d^2)^N = (\text{SF}(d))^N$$

The effect is defined as: $E = -\ln(\text{SF}) = -N\ln(\text{SF}(d))$

$$E = N(\alpha d + \beta d^2)$$

$$\text{or } E = \alpha D + \beta Dd \text{ ----- 2.9}$$

Where $D = Nd = \text{total dose}$

This relationship is generally expressed as:

$$E/\alpha = Nd(1 + d/(\alpha/\beta)) \text{ ----- 2.10}$$

The basis for this type of model lies in the concept of the production of lethal and sub-lethal damage to cells by the irradiation process. When using the LQ model it is assumed that cells sustain lethal damage which kills directly or sub-lethal damage from which cells may recover or from which lethal damage may develop as a result of interaction with other damage sites (sublethal damage, SDL, section 2.1.2. and section 2.2.4.). In the form shown above it is essentially a complete repair model, in other words a sufficiently long time gap must exist between fractions to allow the repair of sublethal damage. This consideration does not generally limit the use of the LQ model clinically except when the interfraction time is short for example in the case of

accelerated hyperfractionated treatments of the type mentioned in chapter 1 (section 1.5.4.), where at least six to eight hours is left between fractions to allow for the repair of sub-lethal damage. There are however versions of this model which take account of incomplete repair (Thames et al, 1984; Thames, 1985), for fractionated radiotherapy and also for continuous radiotherapy (Dale, 1985; Brenner and Hall, 1990). Uncertainty exists as to the limits of dose per fraction which govern the use of iso-effect models. In continuous (or protracted) applications these limits are very difficult to determine, whereas in fractionated radiotherapy the upper limit is often taken as between 8 and 10 Gy (Fowler, 1989). Accurate values of the LQ parameters α and β used in this model are often difficult to obtain, so caution must also be exercised when interpreting results. Estimates of the α/β ratio can be obtained for specific end points or damage levels for not only cells in culture but tissues and tumours in vivo. If the value of α/β associated with a given level of functional damage to an organ is required then this can be found by rearranging equation 2.10, we obtain:

$$1/D = (\alpha/E) + (\beta/E)d \text{ ----- 2.11}$$

equation 2.11 is a linear relationship between dose per fraction and reciprocal total dose and can be used along with experimental data to obtain the α/β ratio as the following example shows.

Example 2.1

This example is taken from a report by Stewart et al (1984), where iso-effective functional damage to kidney was achieved using a number of fractionated schedules. The fraction number ranged from 1 to 64 and the results are shown in figure 2.6. As can be seen a series of sigmoid shaped curves are obtained for each of the seven

schedules. This figure illustrates the fact that the larger the fraction number used in a schedule the greater the total dose required to produce the same effect (chapter 1, section 1.5.4.). The sigmoid appearance also demonstrates the rapid increase in effect over a small range of total dose for each curve (chapter 1, section 1.5.2.). If a particular level of effect is chosen, for example that shown by the arrow in figure 2.6, then at this level on each plot a value of total dose, D can be obtained. Plotting the reciprocal of this against the corresponding value of dose per fraction produces a straight line, see figure 2.7. From this the value of the α/β ratio can be obtained from the negative dose per fraction intercept, in this case about 3 Gy. This can be seen by recalling equation 2.11. At the intercept $1/D = 0$ therefore $\alpha/E = (-\beta/E)d$, and therefore $\alpha/\beta = -d(\text{Gy})$. Individual contributions of α and β to the α/β ratio can be determined by comparing the reciprocal total dose intercept α/E and the slope of the line β/E . Values of the α/β ratio are different for different tissues and many estimates have been made for different tissue types in animals and man. Acute responding tissues (Chapter 1, section 1.3.4.) which manifest damage over a period of days or weeks after irradiation typically have α/β ratios in the range 7 - 20 Gy. Late responding tissues (Section 1.3.4.) which show damage after periods of months or years following irradiation have values in the range 0.5 - 6 Gy. The range of values emphasises the need to choose values of α/β which are representative of the tissues under consideration. Table 2.1 shows examples of acute and late α/β ratios for various tissue types. Tumours which are well oxygenated appear to respond to radiation in a way similar to that of acute responding tissues but have α/β ratios which are in general higher than these tissues. Examples of tumour α/β ratios are also shown in table 2.1 (Thames et al, 1989). Many α/β ratios have been derived

from animal studies. Human tissues and tumour values cannot be as precisely determined as those derived from animal work because the number of variations in schedules possible with animals is much greater than with humans.

2.4.2. LQ model - Continuous radiotherapy.

Continuous radiotherapy is of great importance in oncology and the LQ model has been extended for use in this area. This was done by Dale (1985) and led to the introduction of another tissue specific parameter being included in the effect relationship in order to account for the repair of sublethal damage during treatment. This parameter, the sub-lethal damage repair time constant, is generally given the symbol μ (hr^{-1}) (Dale, 1985; Fowler, 1990; Brenner, 1991). It is related to the half time of repair of sub-lethal damage ($T_{1/2}$) by the relationship:

$$\mu = (\ln 2)/(T_{1/2})$$

The section that follows describes Dale's derivation which begins with equation 2.10:

$$E/\alpha = Nd(1 + d/(\alpha/\beta)) \text{ ----- 2.10}$$

and proceeds by identifying two important factors. Firstly for fractionated treatments Nd is a constant and E/α depends on the chosen level of effect so that equation 2.10 indicates that the effectiveness of a treatment for a given value of α/β depends on the dose per fraction, d . The factor $(1 + d/(\alpha/\beta))$ is defined as the relative effectiveness per unit dose (RE).

$$RE = (1 + d/(\alpha/\beta)) \text{ ----- 2.12}$$

A second important quantity can also be identified, this is the extrapolated response dose (ERD) (Barendsen, 1982), sometimes called the extrapolated tolerance dose (ETD) or biological effective dose (BED) (Fowler, 1989, 1990). It is proportional to the amount of log cell kill ($-\log(SF)$) in a cell survival model and may be thought of, as the total dose required to produce a given effect if the treatment were given in an infinite number of very small doses. The ERD can be defined by the expression:

$$\text{Total dose, TD} = Nd = \text{ERD}/\text{RE}$$

$$\text{or} \quad \text{ERD} = (\text{TD})(\text{RE}) \text{-----} 2.13$$

When the dose per fraction becomes vanishingly small the RE approaches unity then the ERD corresponds to the dose given in a treatment for which the RE has its lowest value. A convenient way of thinking of radiation damage is to classify it as type A or type B. Type A is damage due to simultaneous hits on each of the two critical targets in one radiation event. Type B damage is a result of the lethal combination of sub-lethal damage inflicted at two separate sites.

From equation 2.10, the effect E of a single dose d (ie $N=1$) can be written as:

$$E = \alpha d + \beta d^2$$

In this equation type A damage is represented as αd and the type B as βd^2 . We may also define the RE as:

$$\text{RE} = 1 + \frac{\text{Total type B damage}}{\text{Total type A damage}}$$

$$\text{or} \quad \text{RE} = (1 + \beta d^2/\alpha d) = (1 + d/(\alpha/\beta))$$

Dale stresses two points, firstly that the ERD associated with a particular end point will be the same whether that end point was achieved using fractionated or

continuous irradiation. Secondly that the clinical problems are more easily analysed in terms of the RE concept so as a starting point it is important to derive an expression for this factor for continuous radiotherapy. If the dose rate is R and the irradiation time is T then the total type B damage can be expressed as:

$$\text{Type B damage} = n\epsilon p^2 \cdot R^2 \cdot T^2 \text{ ----- 2.14}$$

Where ϵ = the interaction probability between two sub lethal damage targets,

n = the number of target pairs and p is the probability per unit dose that only one target is hit. Now since $RT = D$ the total dose given:

$$\text{Type B damage} = \beta D^2$$

where $\beta = n\epsilon p^2$

the total type A damage = αRT (ie αD) since this is proportional to total dose. To derive the expression for RE it is necessary to assume that the sub-lethal damage repairs exponentially with a time constant μ . In his original derivation Dale uses one value of μ to derive the RE, and for the purposes of this chapter it will be assumed that this is the case, although recent work suggests that the repair may not be mono-exponential and that more than one value of μ may be involved (Brenner, 1992; Millar & Canney, 1993) (see chapter 3 section 3.3.2.). Dale showed that the probability that sub-lethal damage still existed at time t after it was produced is given by $2pR\exp(-\mu t)dt$. Based on this assumption it can be shown (Dale 1985) that the full expression for type B damage is given by:

$$\text{Type B damage} = (2R^2 (\beta/\mu))(T - (1/\mu)(1 - \exp(1 - \exp(-\mu T)))) \quad \text{and}$$

since Type A damage = αRT the full expression for RE can be written as:

$$RE_{(\text{protract})} = 1 + (2R/\mu(\alpha/\beta))(1 - (1/\mu T)(1 - \exp(-\mu T))) \quad \text{----- 2.15}$$

A number of interesting points emerge from this expression for RE one of which is the ERD equation for continuous irradiation:

$$\text{Since} \quad \text{ERD} = (\text{Total dose})(RE)$$

$$\text{Then} \quad \text{ERD} = RT(1 + (2R/\mu(\alpha/\beta))(1 - (1/\mu T)(1 - \exp(-\mu T)))) \quad \text{----- 2.16}$$

As shown earlier the ERD is an additive quantity and so for N protracted treatments:

$$\text{ERD} = NRT(1 + (2R/\mu(\alpha/\beta))(1 - (1/\mu T)(1 - \exp(-\mu T)))) \quad \text{----- 2.17}$$

When the treatment time is small ($T < 10\text{hrs}$) the expression

$$(1 - (1/\mu T)(1 - \exp(-\mu T)))$$

in equation 2.17 approximates to $\mu T/2$. Consequently when applied to high dose rate brachytherapy equation 2.17 approximates to:

$$\text{ERD} = NRT(1 + RT/(\alpha/\beta))$$

when T is small ($T < 10\text{ min}$), or since $RT = d$ the dose per fraction:

$$\text{ERD} = Nd(1 + d/(\alpha/\beta)) \quad \text{-----2.18}$$

2.5. Conclusions .

This chapter has reviewed some of the important developments which have taken place in the field of iso-effect modelling over the last decade or so, the main development being the introduction of a formalism which accounts for the different responses of tissues to radiotherapy schedules. The model used almost exclusively in

this thesis is the LQ model since it is the most widely used in the literature today. One reason for this must surely be its simplicity and convenience compared to other survival based models (Thames & Hendry, 1987). Another is its success in its agreement with experimental results, for example that of Douglas and Fowler (Hethcote et al 1976), in cases where the multi-target single-hit and power model are found to be inadequate. The LQ still lacks a time factor to account for the effects of cell repopulation and, in this thesis, time factors have to be accounted for by assuming that different schedules are given over the same time period.

Table 2.1 α/β values for tissues and tumours (Thames 1989)

Responses	α/β ratio	sources
Early reactions		
skin (erythema)	7.5 (5.4 - 10.9)	Turesson/ Thames (1989)
skin (desquamation) T < 29 days	11.2 (7.8 - 18.6)	“
T > 29 days	18.0 - 35.0	Cox (1987)
Late reactions		
supraglottic larynx (late sequalea)	3.8 (0.8 - 14.0)	Marczejewski (1986)
skin (telangiectasia)	3.9 (2.7 - 4.8)	Turesson/ Thames (1989)
spinal cord	< 3.3	Dische (1981)
Tumours		
vocal cord	> 9.9	Harrison (1988)
cervix	> 13.9	Watson (1978)
melanoma	0.6 (1.1 - 2.5)	Bentzen (1989)

Figure 2.1 Typical cell survival curve.

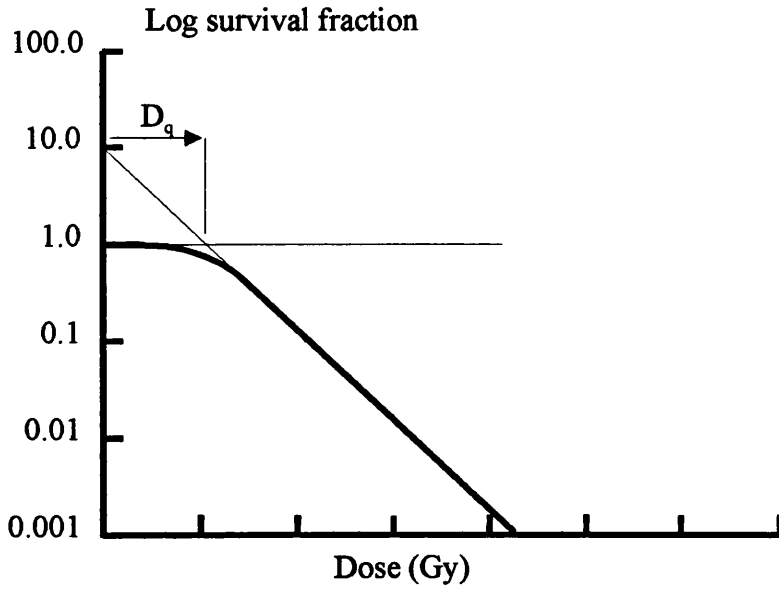


Figure 2.2 Single-target single hit survival curve.

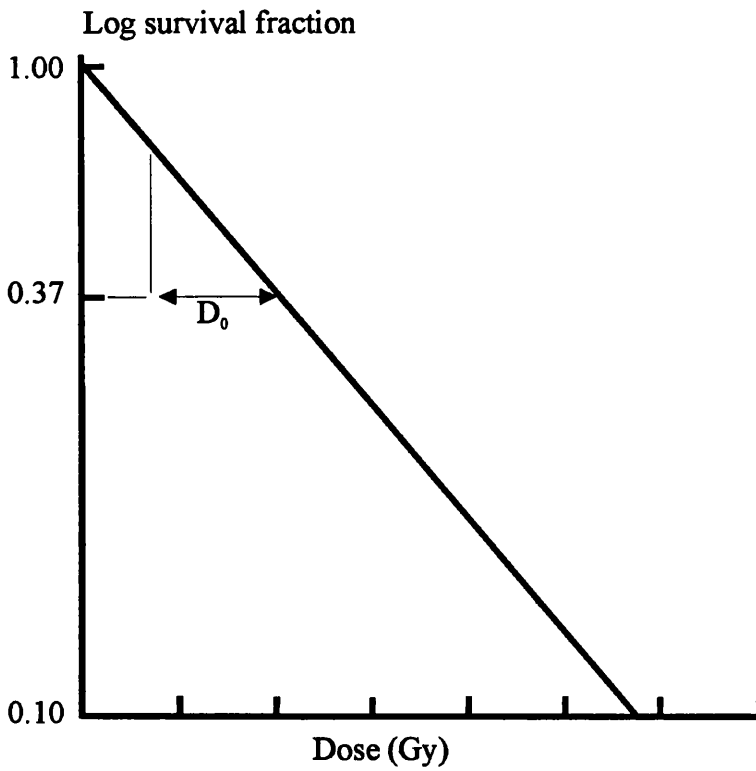


Figure 2.3 Initial slope multi-target model.

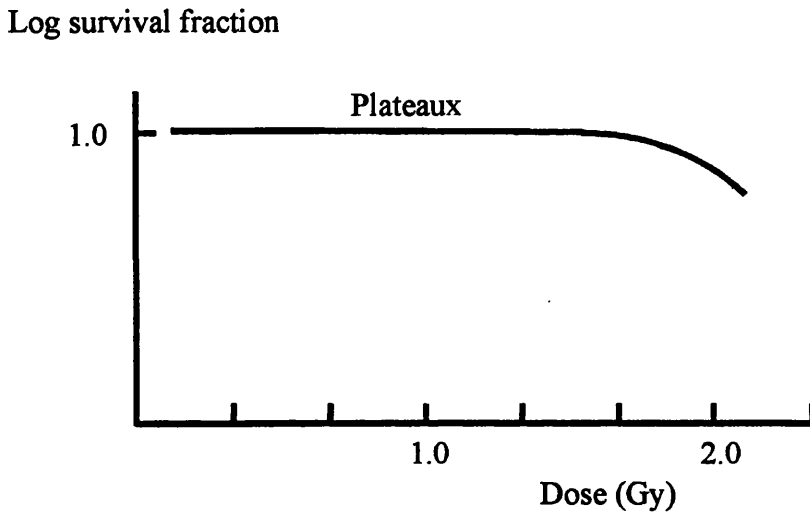


Figure 2.4 Linear quadratic (LQ) model - produces a continuous bending curve which models the region of the survival curve of interest in radiotherapy

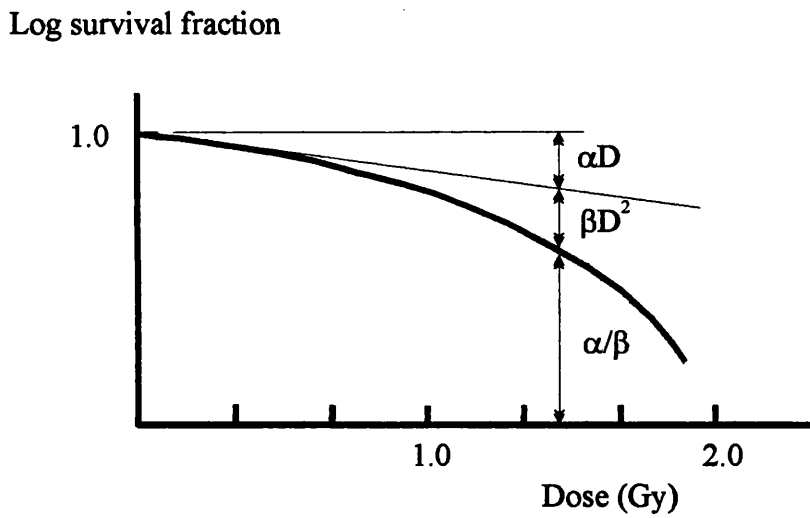


Figure 2.5 Strandqvist plot of iso-effect for skin and lip lesions.

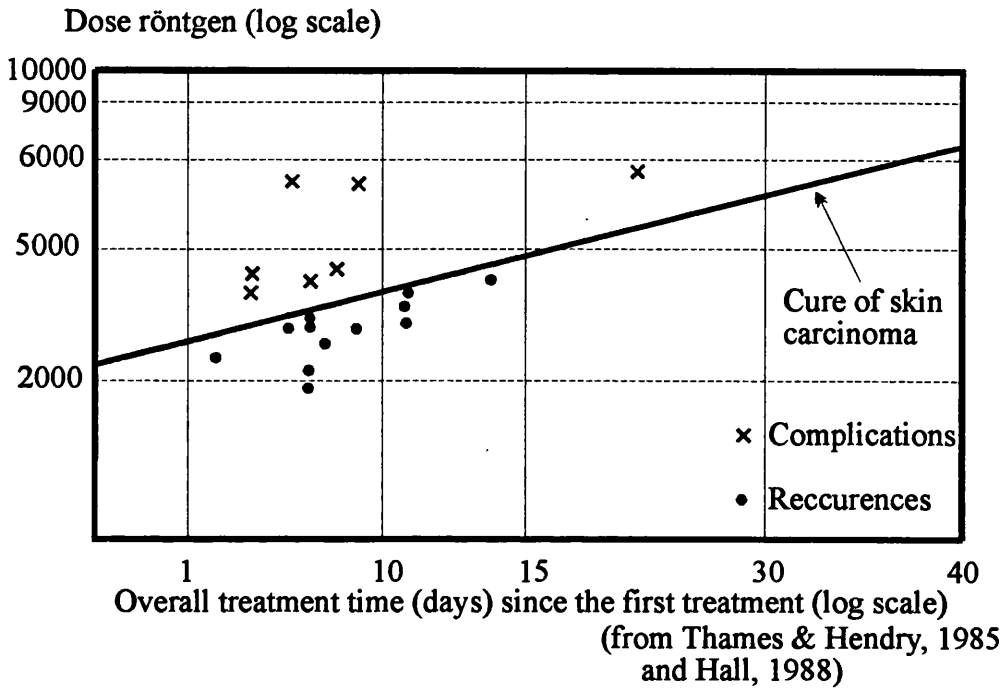


Figure 2.6 Damage versus total dose.

Residual blood activity after 1 hr following a single injection of ^{51}Cr EDTA. The higher the residual activity per ml of blood the poorer the clearance. (from Stewart et al, 1984)

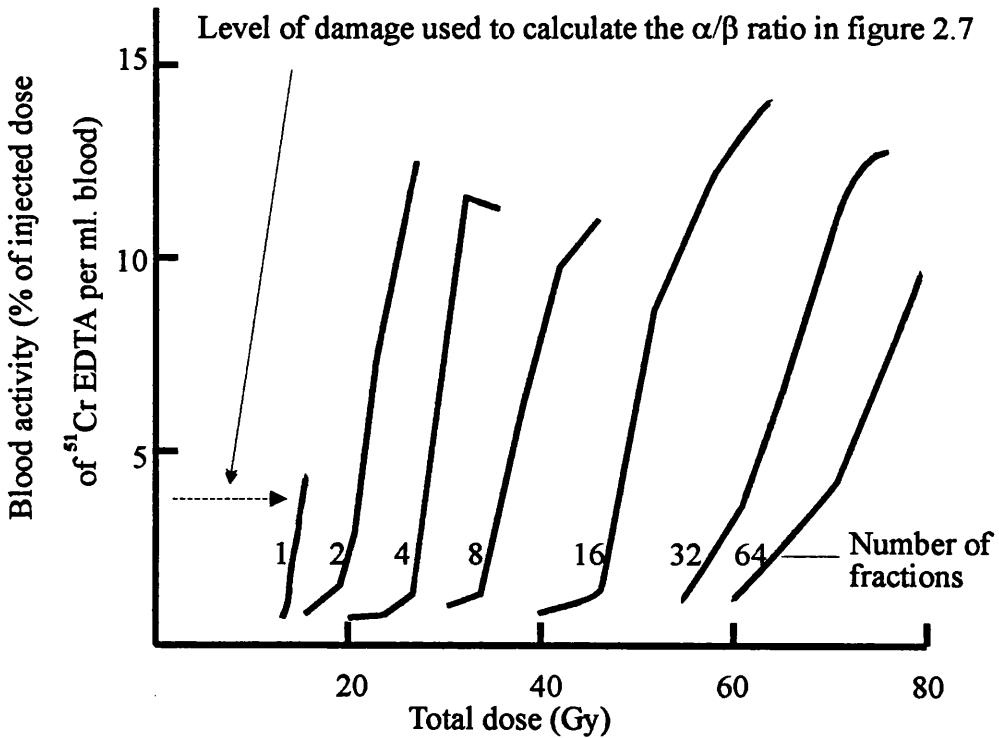
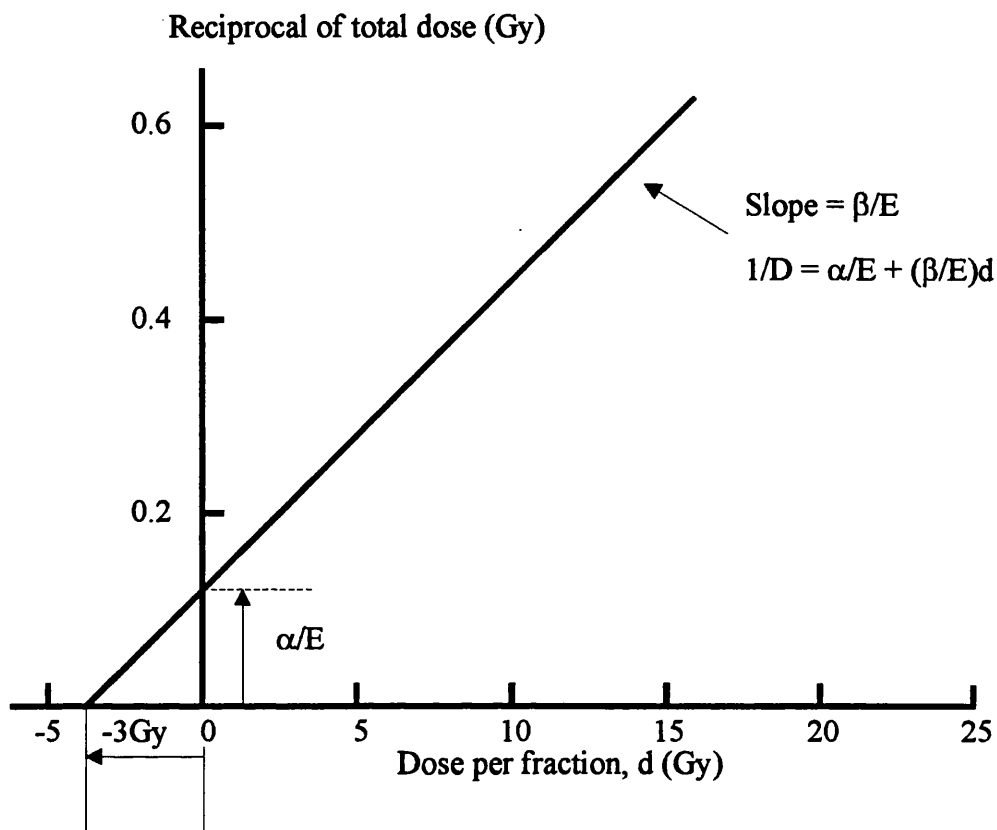


Figure 2.7 Reciprocal of total dose versus dose per fraction for level of damage at arrow (----->) in figure 2.6.



Chapter 3.

Biological equivalence using iso-effect models

3.1. Introduction.

Chapters 1 and 2 have given an overview of the relationship between radiotherapy and radiobiology as well as the origin of iso-effect models. This chapter will concentrate on the use of iso-effect models to compare the biological effects of different radiotherapy treatments. Iso-effect calculations have up to now been mainly confined to single point calculations of ERD, normally performed within a treatment volume or a radio-sensitive structure (Dale 1985, 1986, 1990, 1989; Fowler, 1989, 1990; Orton, 1988, 1990). Although this approach can provide valuable information, a point representation cannot give a good overall view of changing effects. The objective of this thesis was to examine the subject of equivalence between radiotherapy schedules and to see if the effects of treatments could be compared using a method other than that of single point calculations. This chapter considers biological equivalence in the two main areas of fractionated and continuous radiotherapy. The LQ model will be used to illustrate how iso-effect calculations are performed.

3.1.1. Schedules and regimes.

It is important to define the terms "schedule" and "regime"; in this thesis the following definitions will be used (Kirk et al, 1971):

a) A schedule of treatment is the repetitive application of fractions of equal dose at equal time intervals over a specified treatment time.

b) A regime of treatment is a systematic course of radiotherapy comprising one or more schedules.

For example a treatment of total dose 60 Gy given in 30 fractions each of 2 Gy over a period of 6 weeks (ie one fraction on each weekday with no treatments at weekends) will be considered a schedule. However if 6 fractions of 3.33 Gy were given over two weeks (ie 3.33 Gy in 3 fractions per week) followed by 20 fractions of 2 Gy for 4 weeks then this would be a regime consisting of two schedules (see table 3.1).

3.2. Biological equivalence.

Many treatments schedules and regimes used currently in radiotherapy have evolved empirically to produce an acceptable therapeutic effect and at the same time a tolerable level of normal tissue damage (Fowler, 1989). Treatment parameters must conform to the practical constraints set not only by the technical limitations of equipment but also by working practices. However there may be good reasons for changing these schedules, some of which arise from planned modification such as the introduction of new regimes that may bring a therapeutic advantage (Thames et al, 1983; Parsons et al, 1980,1988; Peters et al, 1988 (a) and (b), Saunders et al, 1988, 1990; Dische, 1990) . Other changes may result from unforeseen circumstances such as illness or treatment machine breakdown or even errors in treatment delivery. These factors may force the therapist to modify the treatment often at short notice when there may be little clinical precedent to indicate a clear course of action. In continuous radiotherapy, developments in remote controlled afterloading (see chapter 1, section 1.5.5.) have made it possible to achieve much higher treatment dose-rates. These can be as high as those encountered in external beam treatments, and these changes will affect

late responding tissues differently from tumours and acute responding tissues (Dale, 1985, 1990; Fowler, 1989, 1990) (see chapter 1, section 1.5.6.).

Besides being of direct clinical importance the question of equivalence is often vital when experimental and clinical data sets are to be analysed retrospectively or regimes and schedules from different institutions are being compared. Some of the reasons for considering biological equivalence between treatments are:

- i) Modification of treatment regimes or schedules (planned or unplanned).
- ii) Development of new treatment regimes.
- iii) Comparison of treatments intra- or inter-institutional.
- iv) Retrospective analysis of clinical data.

It is worthwhile at this point to define what is meant by equivalence (Deehan & O'Donoghue, 1988, 1991, 1994) in this thesis.

a) General equivalence: where different treatment regimes or schedules are absolutely equivalent in all respects, that is they produce the same effects on all tissues.

b) Specific equivalence:- where different treatment regimes or schedules are equivalent with respect to one specific type of effect. That is they produce the same biological end point with respect to effects on tumour for example, but may be mismatched for all other effects. Examples of iso-effect calculations performed using current methods are shown in section 3.3. below to demonstrate that they have been largely confined to deriving relationships for the second of these two, ie specific equivalence. Orton (1988) and Warmelink et al (1989), however, did show that it was possible to match for two effects simultaneously, but this must still be regarded as only an extension of specific equivalence (example 3.5, section 3.3.2.).

Chapters 4, 5 and 6 of this thesis will use the LQ model to derive conditions for general equivalence which represent a new aspect in the way that this model can be used.

3.3. The use of iso-effect relationships.

This section is intended to introduce the methodology for performing iso-effect calculations using the LQ model (Dale 1985, 1986; Fowler 1989, 1990).

3.3.1. Fractionated radiotherapy.

In chapter 2 it was shown that the biological effects of treatments can be expressed in terms of the total dose ($TD = Nd$), the extrapolated response dose (ERD) and the relative effectiveness per unit dose (RE) (Dale 1985). Recalling equation 2.13 these are related in the expression:

$$TD = ERD/RE$$

or
$$ERD = (TD)(RE) \text{ -----} 2.13$$

When the time interval between fractions is sufficient that sub-lethal damage can be completely repaired between fractions then the ERD can be written as:

$$ERD = Nd(1 + d/(\alpha/\beta)) \text{ -----} 2.18$$

Where the α/β ratio is a tissue specific parameter. If we consider the schedule $N_r:d_r$ (ie N_r fractions of d_r dose/fraction) then equation 2.18 can be expressed as:

$$ERD_r = N_r d_r (1 + d_r/(\alpha/\beta)) \text{ Note that the ERD value depends on}$$

the value of the α/β ratio, which will in general vary from one tissue to another. If we regard schedule $N_r:d_r$ as a reference, that is one whose effects on tumour and normal

tissues are known, then it is possible to devise other schedules which are iso-effective to $N_r:d_r$ with respect to effects on specific tissues. Suppose we wish to devise a new schedule $N_1:d_1$ which will produce the same specific end point as $N_r:d_r$ then:

$$N_1 d_1 (1 + d_1 / (\alpha / \beta \mu)) = ERD_1 = ERD_r \text{ ----- 3.1}$$

Two possible methods of solving the equation exist. Firstly we can select d_1 and then solve for N_1 to obtain the fraction number. So that:

$$N_1 = ERD_r / d_1 (1 + d_1 / (\alpha / \beta))$$

or
$$N_1 = N_r d_r (1 + d_r / (\alpha / \beta \mu)) / d_1 (1 + d_1 / (\alpha / \beta)) \text{ ----- 3.2}$$

Alternatively it is possible to choose the fraction number N_1 and solve for d_1 .

Then:

$$d_1 = \frac{\left[-N_1 + \left(N_1^2 + \frac{4N_1 ERD_1}{\alpha / \beta} \right)^{1/2} \right]}{\frac{2N_1}{\alpha / \beta}} \text{ ----- 3.3}$$

Two roots emerge from the solution of 3.1 when solving for d_1 but only the positive root is physically meaningful (Dale, 1986) as shown in equation 3.3. The first of these two methods is perhaps the least frequently used in practice and it is generally an equation of the type 3.3 which has to be solved. Solving for fraction number generally leads to a non integer solution for N and in practice the value has to be rounded up or down as required. This process, though sub-optimal, is generally acceptable. Solution of

equation 3.3 can be simplified by using a graphical technique (Dale, 1986) or by the use of a simple computer programme.

Typical examples of LQ calculations are shown below. In these it is of vital importance that representative values of the α/β ratio are used. In the examples that follow, which are typical of those presented in the literature, a ratio of 10 Gy will be used for acute responding normal tissues and tumour, and a value of 3 Gy for late responding normal tissues (Barendsen, 1982; Fertil et al, 1981; Deacon et al, 1984; Hendry & Moore, 1985; Williams et al 1985; Fowler, 1984, 1989; Thames et al, 1982, 1989; Dale, 1990; Brenner, 1992). These are only used as broad classifications to illustrate the process and should not be regarded as precise values (chapter 2, see table 2.1).

Example 3.1. A schedule of 60 Gy total dose is given in 30 fractions (ie over 6 weeks) with a dose per fraction of 2 Gy (ie the reference schedule). What dose per fraction would be required if the treatment were to be given in 20 fractions and matching is required for a) late and b) tumour effects?

a) Late effects $\alpha/\beta = 3$ Gy First of all it is necessary to calculate the ERD associated with late effects corresponding to the existing or reference schedule:

Using equation 2.18:

$$ERD = 30 \times 2 \times (1 + 2/3) = 100 \text{ Gy.}$$

Now using equation 3.3 a value of d the dose per fraction can be found for the new schedule which will give the same ERD for late effects:

$$d = ((3^2 + 4 \times 3 \times 100 / (20))^{1/2} - 3) / 2$$

$$d = 2.65 \text{ Gy}$$

A dose per fraction of 2.65 Gy would be required. This corresponds to a total dose of 53 Gy.

b) Tumour effects $\alpha/\beta = 10$ Gy

Once more the reference schedule gives:

$$\text{ERD} = 30 \times 2 \times (1 + 2/10) = 72 \text{ Gy}$$

and solving equation 3.3 for dose per fraction gives:

$$d = ((10^2 + 4 \times 10 \times 72/10)^{1/2} - 10)/2$$

$$d = 2.81 \text{ Gy}$$

This corresponds to a total dose of 56.2 Gy and is greater than that calculated for late effect equivalence. This illustrates one of the problems encountered in the search for equivalent schedules. If equivalence for one type of effect is achieved (ie specific equivalence) then it is not possible for other effects. Here it can be seen that if equivalence for tumour effects is achieved then late responding normal tissues would be overdosed. On the other hand, if we match for late effects then the tumour is underdosed. This result is in keeping with clinical findings (Coutard, 1932; Baclesse, 1958; Fowler, 1989; Horiot, 1991) in that reducing the number of fractions tends to raise the level of late responding normal tissue damage for the same level of tumour control. If on the other hand, the number of fractions is increased compared with that of the reference schedule and the above calculations repeated, the opposite is true ie less late damage for the same tumour control (see table 3.2). This forms the basis for hyperfractionation where a higher tumour dose can be given for the same effects on late responding normal tissues. With this example as with others calculated on the basis of

the LQ model it must be remembered that the effects of cell proliferation are not taken into account.

Example 3.2. If the same reference schedule is used as in example 1 but this time the dose per fraction is to be reduced to 1.75 Gy what number of fractions will be required to produce the same effects for a) late responding normal tissue and b) for tumour?

Using the same α/β ratios as in example 3.1 the ERD values associated with late and tumour effects have already been calculated. These were:

$$\text{ERD}_{(\text{late})} = 100 \text{ Gy} : \text{ERD}_{(\text{tumour})} = 72 \text{ Gy}$$

a) Late effects.

Using equation 3.2 the new fraction number can be calculated:

$$N_1 = 100/1.75 \times (1 + 1.75/3)$$

$$N_1 = 36.09 \sim 36 \text{ fractions.}$$

This would result in a total dose of 63 Gy.

b) Tumour effects.

This time
$$N_1 = 72/1.75 \times (1 + 1.75/10)$$

$$N_1 = 35 \text{ fractions ie a total dose of 61.3 Gy}$$

This example reinforces the result of example 3.1: by reducing the dose per fraction the total dose necessary to produce the same tumour effect increases but not by the same amount as that required to produce the same late effects (Dale, 1985; Fowler, 1990; Orton, 1990).

The following examples make use of the additive properties of the ERD (Dale 1986).

Example 3.3 If we consider the reference schedule in the previous two examples and assume that after 15 fractions the remainder of the treatment has to be given in only 7 fractions. What dose per fraction would have to be given in order to achieve this and keep late responding tissue reactions at the same level?

After 15 fractions the value of the ERD associated with late responding tissues would be 50 Gy (equation 2.18) for the reference schedule so that an ERD value of 50 Gy is still required. We know from the additive nature of the ERD that:

$$ERD_1 + ERD_2 = ERD_r$$

Where ERD_1 corresponds to that treatment already given, ERD_r to the complete reference schedule and ERD_2 to that value required to bring the late effects up to 100 Gy. Using equation 3.3:

$$d_2 = ((3^2 + 4 \times 3 \times 50/7)^{1/2} - 3)/2$$

$$d_2 = 3.37 \text{ Gy/fraction.}$$

So that 7 fractions of 3.37 Gy/fraction would be required if the expected level of late damage was to be maintained. For tumour effects this would mean:

$$ERD_2 = 7 \times 3.37 \times (1 + 3.37/10)$$

$$ERD_2 = 31.5 \text{ Gy}$$

The total ERD for tumours would then be:

$$ERD_{(\text{tumour})} = 36 + 31.5 = 67.5 \text{ Gy}$$

which is less than that based on the original reference schedule. Reducing the fraction number while restricting the treatment to normal tissue tolerance leads to an underdose in terms of tumour effects. The additive properties of the LQ model can simplify calculation and this will be used in the next section and later in the thesis when equivalence is considered in greater depth.

3.3.2. Continuous radiotherapy.

In continuous radiotherapy, remote afterloading has made it possible to achieve higher treatment dose-rates than those which were used in manual loading systems such as the Manchester approach (see chapter 1, appendix A1). Manchester dose-rates of around 0.5 Gy per hour to the "A" points have already been replaced by higher dose-rates in many centres. Dose-rates are often classified in three broad groups, LDR, MDR and HDR (Corbett, 1990) (see chapter 1. table 1.3). To complicate matters further, continuous treatments have rapidly changing dose distributions and are often given in conjunction with external beam radiotherapy (Warmelink et al, 1989; Orton, 1991; Stitt et al, 1992).

Equation 2.17 is the one used most often in the literature to perform iso-effect calculations (Dale, 1985) for continuous radiotherapy. For continuous treatments however, the expression for ERD includes a factor for the repair of sub-lethal damage during the time of irradiation. Recalling the ERD relationship from chapter 2, equation 2.17:

$$ERD = NRT(1 + 2R/(\mu(\alpha/\beta))(1 - (1/(\mu T))(1 - EXP(-\mu T)))) \quad \text{-----} \quad 2.17$$

Where N = the fraction number: R = dose-rate in Gy/hr, μ = the sublethal damage repair time constant (hr^{-1}) and the α/β ratio (Gy) is as defined previously.

Examples will be shown of how this relationship can be used to calculate isoeffective schedules in continuous radiotherapy. As in the case of fractionated treatments it will be assumed that the interval between treatments must be sufficient for the repair of sub-lethal damage. Normally, the starting point is some familiar or reference low dose-rate schedule and an alternative medium or high dose-rate alternative is calculated. The form of equation 2.17 is that for use with radioactive sources with long half lives (eg Caesium 137, half life 30 years). Dale (1985) however has derived corresponding expressions appropriate for materials with short half lives compared with treatment times.

In the examples values of the α/β ratio for tissues and tumour will be as before in section 3.3.1. on fractionated radiotherapy. Values for μ are not so readily available in the literature. Some authors use the same value of μ for all tissues and tumours (Fowler 1990) and others use two distinct values (Orton, 1988; Warmelink, 1989)(see also Brenner, 1992; Millar & Canney, 1993). For the examples that follow two values of μ will be used these are:

Late responding tissues: $\mu = 0.46 \text{ hr}^{-1}$ ($T_{1/2} = 1.51 \text{ hr}$)

Tumour: $\mu = 1.4 \text{ hr}^{-1}$ ($T_{1/2} = 0.49 \text{ hr}$)

($T_{1/2}$ is the half time for repair of sub lethal damage and is related to μ by the expression: $\mu = \ln 2/T_{1/2}$).

Example 3.4 A low dose-rate treatment of total dose 70 Gy is given at a dose-rate of 0.5 Gy/hr in one fraction. If a high dose-rate treatment with a point dose-rate of 150 Gy/hr is to be used instead then what total dose is required if the treatment is to be given in 8 fractions and is to give a) equal late effects or b) equal tumour effects at the "A" points?

a) Late effects The low dose-rate treatment time is $70/0.5$ Gy/hr ie 140 hrs. So that the ERD for late responding tissues is:

$$ERD_{(late)} = 119.9 \text{ Gy using equation 2.17.}$$

At short treatment times less than 10 mins then equation 2.17 reduces to 2.18:

$$ERD = Nd(1 + (2R/(\mu(\alpha/\beta)))(T\mu/2))$$

or
$$ERD = Nd(1 + d/(\alpha/\beta))$$

(*This is because the factor $(1 - 1/(\mu T)(1 - \text{EXP}(-\mu T)))$ in equation 2.17 reduces to $T\mu/2$ where T is less than 10 mins.).

If the dose per fraction at high dose-rate is d then:

$$8 \times d = 119.9 / (1 + d/3)$$

solving by the method of equation 3.3 gives:

$$d = 5.37 \text{ Gy}$$

(note that if $R = 150$ Gy/hr this leads to a treatment time of 0.0358 hr or 2.15 mins which satisfies the time constraint above *.).

$$\text{The total dose} = 8 \times 5.37$$

$$TD = 43 \text{ Gy}$$

b) Tumour effects.

Once again equation 2.17 can be used to calculate the tumour ERD for the low dose-rate reference schedule. ie $ERD_{(tumour)} = 75$ Gy using the same calculation as before but with tissue parameters for tumour.

Repeating the above process for matching of tumour effects leads to a dose per fraction of 5.89 Gy and a total dose of 47.1 Gy. This result shows that if a high dose-rate treatment is to replace a low dose-rate treatment and matching is achieved for tumour effects, then late responding tissues will sustain more damage.

The last example shows that equation 2.17 approximates to the fractionated form of the LQ model (equation 2.18) when treatment times are small, as expected. As in the case of fractionated treatments, iso-effect calculations performed using this method lead to solutions requiring a choice of which type of effect should be matched. Warmelink et al showed that it was possible to obtain solutions for fraction number and treatment time which satisfy two constraints simultaneously (ie matching can be achieved for both late response and tumour response at the same time) (Warmelink et al, 1989). In doing so they followed a method suggested by Orton (1987) which is shown in the next example.

Example 3.5. Using a reference schedule of 30 Gy given at 0.5 Gy/hr in 60 hrs, what dose per fraction and number of fractions would be required to produce the same level of late effects and tumour effects if the treatment is to be given at a dose-rate of 2.5 Gy/hr?

For the reference schedule the important values of ERD are those associated with late and tumour responses:

$$ERD_{(late)} = 50.95 \text{ Gy}$$

$$ERD_{(tumour)} = 32.12 \text{ Gy}$$

these are obtained using equation 2.17.

To find the new fraction number and the treatment time such that the new medium dose-rate treatment produces the same effects it is necessary to solve the following simultaneous equations which are derived from equation 2.17:

$$N_1 R_1 T_1 (1 + 2R_1 / (\mu_1 (\alpha/\beta)_l) (1 - (1/(\mu_1 T_1)) (1 - \text{EXP}(-\mu_1 T_1)))) = 50.95 \text{ Gy} \text{ ----- } 3.4$$

$$N_1 R_1 T_1 (1 + 2R_1 / (\mu_t (\alpha/\beta)_t) (1 - (1/(\mu_t T_1)) (1 - \text{EXP}(-\mu_t T_1)))) = 32.12 \text{ Gy} \text{ ----- } 3.5$$

Where N_1, R_1, T_1 are the fraction number, dose-rate ($= 2.5 \text{ Gy/hr}$) and treatment time for the new treatment schedule respectively. The factors $\mu_l, \mu_t, (\alpha/\beta)_l$ and $(\alpha/\beta)_t$ are the repair constants for late responding tissues and tumour, and the corresponding α/β ratios, respectively.

If equation 3.4 is divided by 3.5 then:

$$\frac{(1 + 2R_1 / (\mu_l (\alpha/\beta)_l) (1 - (1/(\mu_l T_1)) (1 - \text{EXP}(-\mu_l T_1))))}{(1 + 2R_1 / (\mu_t (\alpha/\beta)_t) (1 - (1/(\mu_t T_1)) (1 - \text{EXP}(-\mu_t T_1))))} = 1.586 \text{ ----- } 3.6$$

In equation 3.6, R_1 is known and a solution for T_1 can be found using an iterative method. In this case:

$$T_1 = 1.288 \text{ hr}$$

Substituting into either 3.4 or 3.5 gives:

$$N_1 = 8.37$$

Equation 2.17 can be used to check that these values of N and T produce the same ERDs for late responding tissues and tumours as the reference schedule. In the above example the matching of late and tumour responses is done at one point i.e. at the "A" point.

3.3.3. Summary.

Examples 3.1 to 3.4 show the method commonly used to devise alternative schedules which are iso-effective to some reference schedule, for both fractionated and continuous radiotherapy using the LQ model.

The approach adopted by most authors is to produce matching effects for only one type of tissue. Even though a method of matching for two different effects has been suggested (Warmelink 1990) the use of the LQ model seems to pre-suppose that general equivalence as defined in section 3.2. of this chapter is not possible.

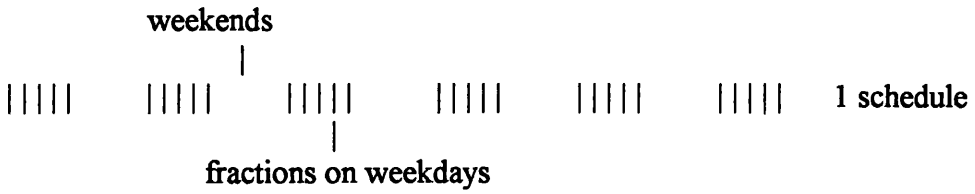
This thesis will show that the LQ model can be used to derive conditions for general equivalence. These were first reported for fractionated radiotherapy in 1988 (Deehan and O'Donoghue) and will be described in detail in chapter 4. In chapter 5 the corresponding relationships for continuous treatments will be derived and chapter 6 will show that this reasoning can be extended to combinations of both fractionated and continuous treatments.

The above examples involve calculations which are associated with single points in space. Though this is helpful it will be demonstrated in this thesis that this approach

is of limited value in assessing the overall changes in the effect distribution which result from alterations in treatment parameters. A more global view of these can be obtained by considering lines (in 2 dimensions) or surfaces (3 dimensions) of equal effect, called iso-effect surfaces (Deehan and O'Donoghue 1991, 1994). Chapters 7 and 8 discuss this subject in the context of both continuous and fractionated treatments. Finally chapter 9 relates the findings of this thesis to clinical results which have been reported in the literature.

Table 3.1 Schedules and regimes

a) 60 Gy in 30 fractions of 2 Gy/fraction in 6 weeks



b) 60 Gy in: (1) 6 fractions of 3.33 Gy/fraction in 2 weeks

(2) 20 fractions of 2 Gy/fraction in 4 weeks

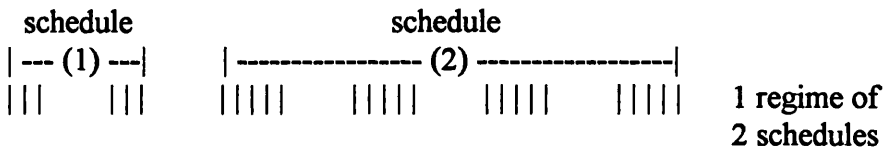


Table 3.2 Results from example 3.1

				ERD (Gy)	
	N	d (Gy)	TD (Gy)	Late	Tumour
Reference	30	2.00	60	100	72
Late match	20	2.65	52	100	67
Tumour match	20	2.81	56	109	72
Late match	40	1.62	65	100	75
Tumour match	40	1.56	62	95	72

Chapter 4.

Equivalence between fractionated radiotherapy schedules.

4.1. Introduction.

The primary aim of radiotherapy is to produce as much damage as possible to tumour cells without exceeding tolerable levels of damage to normal acute and late responding tissues. A variety of "standard" schedules are used in everyday radical treatments which have mainly evolved through clinical experience (Fowler, 1989). In this chapter the question addressed is: if we have a particular fractionated schedule in mind can an alternative fractionated schedule or regime be found which is equivalent for all biological end points?

Normal tissues differ in their response to changes in fractionation, therefore iso-effect relationships which attempt to predict the effects of schedule changes must take account of this. The linear quadratic (LQ) model does this by using tissue specific parameters (chapter 2, section 2.4.). For simplicity two categories of effect will be considered in the following discussion. These are tumour and normal late responding tissue effects. It will be shown here for the first time that in fractionated radiotherapy no two schedules can be generally equivalent (chapter 3, section 3.2.), that is equivalent for all effects on all tissues. Schedules can only be equivalent for a single value of α/β , that is they can only exhibit specific equivalence (section 3.2.). However when regimes (defined as two or more schedules in sequence, see chapter 3, section 3.1.1.) are considered then more complex possibilities emerge. Mathematical conditions can be derived for general equivalence of regimes which do not depend on the α/β ratio

(Deehan & O'Donoghue 1988). Although these conditions may not always be physically achievable, in many cases useful results can be obtained. It will emerge from the worked examples that the concept of general equivalence is a useful one with practical applications in clinical radiotherapy.

4.2. Dissociation of biological effects.

When seeking an alternative schedule to some reference using the method shown in example 3.1 the dissociation of biological effects becomes apparent. No single equivalent schedule can be found; instead a number of alternative schedules are possible, one for each tissue involved (ie each value of α/β) (Withers et al, 1983; Deehan & O'Donoghue, 1988; Fowler, 1989).

4.2.1. Implications of non-equivalence of treatment schedules in radiotherapy.

The above argument emphasises the non-equivalence of treatment schedules with respect to the dissociation of effects in normal tissues and tumours when the dose per fraction is altered, but the total time remains the same.

This result is an example of what can be called the "principle of non-equivalence" for radiotherapy schedules. It can be stated explicitly as follows: no two schedules differing in dose per fraction have identical biological effects on all tissues. If a total dose is chosen such that two schedules are "matched" for effects on a tissue characterised by a particular α/β ratio, the schedules will be "mismatched" for effects on any other tissues with a different value of α/β ratio (Deehan & O'Donoghue, 1988). Often, therapists will choose to match for late effects; the schedule will then be mismatched for acute effects and effects on typical tumours.

This reinforces the view that changes in the structure of fractionation of schedules should not be undertaken lightly (Withers et al, 1983). There is no way in which altered schedules can be made to produce the same effects on all tissues as the original. This seriously restricts the concept of so called radiobiological equivalence in clinical practice and so should be more widely considered. It will be seen that the principle of non-equivalence for single schedules emerges naturally from the reasoning as we proceed to derive the conditions for general equivalence.

4.3. General equivalence.

Consider a reference schedule of N_r fractions of d_r dose per fraction and also some other schedule $N_1:d_1$ with a different fraction number and dose per fraction. These two schedules will be iso-effective for one value of the α/β ratio if their ERDs are equal.

That is:

$$ERD_r = ERD_1$$

In this analysis we will suppose that the schedules are given in the same overall time or that time effects will be of negligible consequence for all tissues.

Equating the expressions for ERD (ie equation 2.18) gives:

$$N_r d_r (1 + d_r/\alpha/\beta) = N_1 d_1 (1 + d_1/\alpha/\beta)$$

$$N_r d_r + N_r d_r^2 (1/(\alpha/\beta)) = N_1 d_1 + N_1 d_1^2 (1/(\alpha/\beta)) \text{ ----- 4.1}$$

Previous examples (eg. example 3.1) have shown that if N_r and d_r are known and if N_1 is fixed at some suitable value then equation 4.1 can be solved for d_1 (equation 3.3), or for N_1 if d_1 is chosen (equation 3.2). Two schedules can therefore exhibit

specific equivalence ie they can be equivalent for one end point but non-equivalent for all others. Little consideration has been given to the possibility that there may be circumstances in which schedules may be generally equivalent, ie a total dose can be found for a schedule such that its effects on all tissues (regardless of α/β ratio) is identical to that of some other schedule. This possibility is considered below and the conditions derived which must apply for general equivalence to hold.

4.3.1. General equivalence between single schedules.

The conditions for general equivalence can be found from equation 4.1 by equating the coefficients of the terms associated with A and B type damage.

The conditions are:

$$\text{Total A type damage, } N_r d_r = N_1 d_1 \text{ ----- 4.2}$$

$$\text{Total B type damage, } N_r d_r^2 = N_1 d_1^2 \text{ ----- 4.3}$$

If these conditions are to be satisfied then: $N_r = N_1$ and $d_r = d_1$ ie the two schedules must be identical (equal numbers of equal sized fractions).

For any uniform schedule, therefore, no other non-identical schedule can be found which gives the equivalent effects for all values of α/β . Uniform schedules are unique in terms of their effects on different tissues and only specific equivalence is possible between them. This proves for the first time the principle of non-equivalence defined in section 4.2.1.

4.3.2 General equivalence between schedules and regimes.

If we now consider the uniform schedule $N_r:d_r$, can a sequence of schedules exist $N_1:d_1 + N_2:d_2 + \dots + N_k:d_k$ which is generally equivalent to this schedule, ie equivalent for all values of α/β ?

It has been shown that the ERD is an additive quantity (Dale, 1986). It therefore follows that for equivalence between the schedule and the sequence of schedules:

$$ERD_r = ERD_1 + ERD_2 + \dots + ERD_k$$

$$ERD_r = \sum_{i=1}^{i=k} ERD_i$$

$$N_r d_r (1 + d_r / (\alpha / \beta)) = \sum_{i=1}^{i=k} N_i d_i (1 + d_i / (\alpha / \beta))$$

$$N_r d_r + N_r d_r^2 / (\alpha / \beta) = \sum_{i=1}^{i=k} N_i d_i + \sum_{i=1}^{i=k} N_i d_i^2 / (\alpha / \beta)$$

Solutions exist if two conditions hold:

$$N_r d_r = \sum_{i=1}^{i=k} N_i d_i \text{ ----- 4.4}$$

and

$$N_r d_r^2 = \sum_{i=1}^{i=k} N_i d_i^2 \text{ ----- 4.5}$$

It can be seen that in equations 4.4 and 4.5, the α/β ratio does not appear. Therefore, if meaningful solutions to these equations can be found, the uniform schedule $N_r:d_r$ and the sequence $N_1:d_1 \dots N_k:d_k$ will be generally equivalent and independent of the α/β ratios (ie they will be equivalent for all values of α/β).

General equivalence may therefore be possible between a schedule and a regime. The parameters of the uniform schedule may be expressed in terms of those of the regime by first squaring equation 4.4, then dividing the resulting equation by equation 4.5, to obtain:

$$N_r = \frac{\left(\sum_{i=1}^{i=k} N_i d_i \right)^2}{\sum_{i=1}^{i=k} N_i d_i^2} \text{ ----- 4.6}$$

and dividing equation 4.5 by 4.4 to give:

$$d_r = \frac{\sum_{i=1}^{i=k} N_i d_i^2}{\sum_{i=1}^{i=k} N_i d_i} \text{ ----- 4.7}$$

The relationships 4.6 and 4.7 have been derived for general cases where k may be any integer value. However in many applications regimes considered only consist of two uniform schedules one of which is known. Then we have:

$$N_r = \frac{(N_1 d_1 + N_2 d_2)^2}{(N_1 d_1^2 + N_2 d_2^2)} \text{-----} 4.8$$

$$d_r = \frac{(N_1 d_1^2 + N_2 d_2^2)}{(N_1 d_1 + N_2 d_2)} \text{-----} 4.9$$

The following examples show how these relationships can be used when schedules have to be altered during treatment.

Example 4.1 A regime consisting of 10 fractions of 1.5 Gy followed by 5 fractions of 4 Gy is given in treatment. To what single schedule is this generally equivalent?

Using equations 4.8 and 4.9:

$$N_r = \frac{(10 \times 1.5 + 5 \times 4)^2}{(10 \times 1.5^2 + 5 \times 4^2)}$$

ie $N_r = 11.95$ fractions

$$d_r = \frac{(10 \times 1.5^2 + 5 \times 4^2)}{(10 \times 1.5 + 5 \times 4)}$$

ie $d_r = 2.93$ Gy

Neglecting the effects of time therefore, a schedule of 11.95 fractions of 2.93 Gy per fraction would be generally equivalent to the regime of 10 fractions of 1.5 Gy followed by 5 fractions of 4 Gy.

Example 4.2 A schedule consists of 15 fractions each of 1.36 Gy. What additional treatment must be given to make the effect on all tissues equivalent to a schedule of 25 fractions of 2.4 Gy?

Re-arranging equation 4.8 and 4.9 gives:

$$N_2 = \frac{(25 \times 2.4 - 15 \times 1.36)^2}{(25 \times 2.4^2 - 15 \times 1.36^2)}$$

ie $N_2 = 13.49$ fractions

$$d_2 = \frac{(25 \times 2.4^2 - 15 \times 1.36^2)}{(25 \times 2.4 - 15 \times 1.36)}$$

ie $d_2 = 2.94$ Gy

Therefore a further 13.49 fractions of 2.94Gy should produce the same effects on all tissues as the reference schedule.

It is obviously not possible to give a non-integer number of fractions, so that if 14 fractions of 2.83 Gy (this has the same total dose as 13.49 fraction of 2.94Gy) were given the difference in result can be assessed using the method in example 4.1.

$$N_r = \frac{(15 \times 1.36 + 14 \times 2.83)^2}{(15 \times 1.36^2 + 14 \times 2.83^2)}$$

$$N_r = 25.75 \text{ fractions}$$

$$d_r = \frac{(15 \times 1.36^2 + 14 \times 2.83^2)}{(15 \times 1.36 + 14 \times 2.83)}$$

$$d_r = 2.33 \text{ Gy per fraction.}$$

This result differs from the intended schedule but the difference in total dose (equivalent to A type damage) is less than -0.01% and the difference in the B type damage components is -2.92%. It is difficult to define difference levels which would be significant but it is generally accepted that clinical differences of ~ 3.0% to ~ 5.0% in

total dose can be detected clinically. This solution is well within $\sim 3.0\%$ in terms of total dose difference, and just within $\sim 3.0\%$ in terms of the B type term.

The foregoing discussion and examples demonstrate that although only a tissue specific equivalence is possible between uniform schedules, general equivalence can exist between schedules and regimes.

Although the conditions for general equivalence were derived using the LQ model, a similar result can be shown with other models (see appendix 4.1). The phenomenon of general equivalence is represented diagrammatically in figure 4.1. This shows a plot of the relationship between the ERD and total dose for a reference schedule $N_r:d_r$ (full lines).

Although a number of end points for this schedule can be identified only late $L(r)$ and tumour effects $T(r)$ are shown. The straight lines represent the effect of the schedule as it proceeds. The gradient associated with each end point for the schedule is $(1 + d/(\alpha/\beta))$ (ie dependent on the fraction size and the α/β ratio). Dotted lines represent the course of schedules $N_1:d_1$ and $N_2:d_2$. These can combine to form a regime which will be generally equivalent to the reference schedule if the end points match at each value of α/β . Note that if the conditions for general equivalence hold between a schedule and a regime then the order in which the schedules in the regime are given is not important.

If however the first part of the regime $N_1:d_1$ has exceeded the late end point for the reference schedule, for example, then general equivalence cannot be achieved; this is shown in figure 4.2.

4.3.3. Application to Continuous Hyperfractionated Accelerated Radiotherapy Treatments (CHART).

Comparison of conventional and CHART schedules are underway in some centres (Saunders et al, 1988). These trials involve two arms: a CHART arm given as 3 fractions per day over 12 days with a six hour gap between fractions, and a conventional arm given as 1 fraction per day over 6 weeks. Both the CHART and conventional arms are divided into two parts treating volumes of different sizes. Figure 4.3 shows the number of fractions in each part. CHART patients are often treated in a batch over the 12 day period and if a patient's treatment is interrupted, even for one day, this may eliminate them from this arm of the trial. The problem then is how to continue the patient's treatment using a treatment schedule with a more conventional structure. Although further treatment can be given based on clinical judgement, it is also possible to use the principle of general equivalence to indicate a salvage strategy as the following example demonstrates. Using the general equivalence approach has the advantage that no assumptions need be made about the values of the α/β ratio and that the results obtained are therefore independent of this ratio.

In practice the number of patients who have to be removed from the CHART arm is at present very small (only two in the Glasgow trial). This is because of the careful monitoring process designed to select only those patients who can tolerate the more disciplined daily routine of CHART. Part of the reason that this process is necessary is because little clinical experience exists which would allow straightforward switching of patients between schedules that are so different. The following example demonstrates for the first time a method based on the use of the LQ model which suggests a transfer strategy. This will prove helpful even though the numbers transferring are at present still small, and even more helpful if CHART is to be adopted as standard treatment

method in the future since this will mean that greater numbers of patients will undergo CHART type treatments and so the need to transfer will increase.

Example 4.3 Suppose that after 3 fractions of part 1 of a CHART schedule the patient's treatment is interrupted in such a way as to result in removal from the CHART arm. What further treatment would be required so that transfer to the conventional arm would result in the same general effects (on all tissues) as if treatment had been on that arm from the outset.

In this case $N_1:d_1 = 3:1.5$

$$N_r:d_r = 22:2$$

$$N_2 = \frac{(N_r d_r - N_1 d_1)^2}{(N_r d_r^2 - N_1 d_1^2)}$$

$$N_2 = 19.2 \text{ fractions}$$

$$d_2 = \frac{(N_r d_r^2 - N_1 d_1^2)}{(N_r d_r - N_1 d_1)}$$

$$d_2 = 2.06 \text{ Gy}$$

It is obviously impossible to give a non integer number of fractions and so 19 fractions of 2.08 Gy per fractions could be given (keeping the total dose the same as

19.2:2.06) Using the relationship previously derived in 4.8 and 4.9 it is possible to calculate the equivalent reference schedule parameters:

$$N_r = \frac{(3 \times 1.5 + 19 \times 2.08)^2}{(3 \times 1.5^2 + 19 \times 2.08^2)}$$

$$N_r = 21.78 \text{ fractions}$$

$$d_2 = \frac{(3 \times 1.5^2 + 19 \times 2.08^2)}{(3 \times 1.5 + 19 \times 2.08)}$$

$$d_2 = 2.02 \text{ Gy per fraction} \quad (\text{TD} = 44 \text{ Gy as with conventional arm 1}).$$

The problem in example 4.3 is illustrated in figure 4.4. Here the ERD is plotted for the reference schedule $N_r \cdot d_r$ (ie part 1 of the conventional control arm) against various values of the α/β ratio (full line). Also shown is the corresponding plot for that part of the CHART arm already given 3:1.5 (lower broken line). When general equivalence is applied it has the effect of increasing the ERD of each point on the CHART curve so that it matches the corresponding point on the conventional curve. It is also possible to plot for part 1 of CHART a graph showing the number of fractions required to transfer a patient to the conventional arm as a function of fractions already received on the CHART arm. This is shown in figure 4.5(a). From these graphs it can be seen that interruptions early on in the CHART schedule, for example before 10 fractions have been given, result in required fraction numbers of greater than 12 and doses of around 2 Gy per fraction to be given for transfer to the conventional arm. Above this point the

dose per fraction begins to rise more rapidly going from around 2Gy to about 5 Gy: at the same time the number of fractions continues to drop. The plots corresponding to part two are shown in figure 4.5(b) and these show a similar pattern. It is obvious however that the general equivalence method of dealing with interruptions in CHART is probably only valuable at the beginning of parts 1 or 2. This is because of the difference in time scales of the two arms and the restriction that the new regime (ie the schedule from part 1 plus the new general equivalent schedule) should be given in roughly the same time as the conventional arm of part 1; the same is true of part 2. To see this more clearly we can recall example 4.3 where the required schedule to achieve iso-effectiveness with the conventional schedule was 19 fractions of 2 Gy which could be given on a daily basis over 29 days (as opposed to a schedule of 22 fractions over a period of 30 days for the conventional arm). However if the interruption to CHART occurs later, for example after 15 fractions of part 1 (see figure 4.4 upper broken line), then 8.5 fractions of 2.5 Gy per fraction would be required for general equivalence. In this case the CHART schedule has run for 5 days which means the remaining schedule of 8.5 fractions would have to be spread over 21 days (the remainder of the conventional schedule). This limitation of the technique results from the accelerated nature of the CHART scheme and so the use of the general equivalence would be limited in this case to interruptions occurring near the beginning of parts 1 and 2 of CHART. Breaks in treatment at other times would require different strategies.

4.4. Conclusions

In fractionated radiotherapy the use of the LQ model to obtain alternative iso-effective schedules has pre-supposed a choice between different solutions, one for each

value of the α/β ratio. The method discussed in this chapter (section 4.3.) demonstrated for the first time that the LQ relationship could be used to derive conditions under which regimes are generally equivalent, ie independent of the value of the α/β ratio (Deehan & O'Donoghue 1988). This reasoning also yields the result that no two schedules can be generally equivalent (the principle of non-equivalence) a result which has not previously been demonstrated rigorously . The examples in this chapter have also shown that it is possible to use the principle of general equivalence to solve practical re-scheduling problems that can arise in everyday fractionated radiotherapy. In the following chapters the general equivalence concept is extended to continuous radiotherapy and also combined fractionated and continuous treatments. The reasoning applied here is confined to point calculations and the implications of general equivalence for volumes is discussed later. The appendix to this chapter derives the equivalence conditions using NSD, CRE and TDF type relationships. The conditions for equivalence produced from these models are not as universal as the general equivalence of the linear quadratic model, but they do show that general equivalence is not merely a peculiarity of the LQ formalism but is, to some extent, implicit in the clinical and experimental isoeffect data.

4.5. Appendix 4.1 General equivalence with power law ("exponent of N") iso-effect models.

Models of the NSD, CRE and TDF (Ellis, 1967, 1969, 1985; Kirk, 1971, 1972; Orton, 1973, 1990) type can be modified to describe tissue specific effects by incorporating tissue specific parameters. Unlike the LQ model, these models attempt to make allowance for changes in overall time. However, it is unlikely that the time structure of the power law models is clinically reliable (Liversage, 1971; Fowler 1989; Dale, 1990).

The calculations and examples given here are included to show how the general equivalence analysis may be applied to iso-effect models having a radically different structure from the LQ model. It must also be stressed that the analysis in this appendix should not be taken as an endorsement of the use of power law models in practice.

These models are of the form:

$$E = D N^a T^b \text{ ----- 4A.1}$$

where:

E is some quantitative measure of radiation damage,

D is the total dose,

N is the number of fractions,

and T is the duration of the schedule.

For example the CRE can be written as:

$$E = D N^{-0.24} T^{-0.11} \text{ ----- 4A.2}$$

Alternatively for models of this sort we may write:

$$E = d N^m T^b \text{ ----- 4A.3}$$

where $m = 1 + a$ and d is the dose per fraction.

To assess the combined effect of two schedules given in sequence the equivalence conditions at the junction between schedules must be considered.

Two schedules 1 and 2 are given separately in order to achieve a certain level of effect, E , then ϕ_1 fractions in time γ_1 , and ϕ_2 fractions in time γ_2 would be required respectively i.e.

$$E = d_1 \phi_1^m \gamma_1^b = d_2 \phi_2^m \gamma_2^b \text{ ----- 4A.4}$$

For intermediate effect, E^i , achieved by lesser numbers of fractions, n_1 and n_2 in times t_1 and t_2 we have similarly:

$$E^i = d_1 n_1^m t_1^b = d_2 n_2^m t_2^b \text{ ----- 4A.5}$$

The increment of radiation damage required to make up the difference is:

$$E - E^i = d_1(\phi_1^m \gamma_1^b - n_1^m t_1^b) = d_2(\phi_2^m \gamma_2^b - n_2^m t_2^b)$$

i.e. we need to give $(\phi_1 - n_1)$ additional fractions in the additional time of $(\gamma_1 - t_1)$ on schedule 1 and $(\phi_2 - n_2)$ additional fractions in an additional time of $(\gamma_2 - t_2)$ on schedule 2. If schedule 1 were given to achieve the intermediate effect E^i and the treatment was then continued to on schedule 2 to the effect level E we would require:

$$E = d_1 n_1^m t_1^b + d_2 (\phi_2^m \gamma_2^b - n_2^m t_2^b) \text{ ----- 4A.6}$$

ϕ_2 is the total number of fractions which would have to be given as schedule 2 to achieve the effect E in the absence of any other treatment i.e.

$$\phi_2 = (N_2 + n_2) \text{ ----- 4A.7}$$

Where N_2 is the actual number of fractions in schedule 2 and n_2 , as has been seen, is the number of fractions which would have to be given as schedule 2 to achieve the intermediate effect E^i i.e. identical to the effect produced in schedule 1. From equations (4A.6) and (4A.7) we have:

$$E = d_1 n_1^m t_1^b + d_2 [(N_2 + n_2)^m (T_2 + t_2)^b - n_2^m t_2^b] \text{-----4A.8}$$

which, from equation 4A.4 is

$$E = d_2 (N_2 + n_2)^m (T_2 + t_2)^b \text{----- 4A.9}$$

Equation 4A.5 permits us to write:

$$n_2 = \frac{(d_1 t_1^b)^{1/m}}{(d_2 t_2^b)^{1/m}} n_1 \text{----- 4A.10}$$

and, let $n_1 = N_1$, the total number of fractions in schedule 1

$$E = d_2 \left[N_2 + \left(\frac{d_1 t_1^b}{d_2 t_2^b} \right)^{1/m} N_1 \right]^m (T_2 + t_2)^b \text{----- 4A.11}$$

This effect can be produced by a uniform schedule, number 3, if:

$$d_3 N_3^m T_3^b = d_2 \left[N_2 + \left(\frac{d_1 t_1^b}{d_2 t_2^b} \right)^{1/m} N_1 \right]^m (T_2 + t_2) \text{----- 4A.12}$$

If now we make the assumption that isoeffective schedules are given in the same overall time i.e.

$$t_1 = t_2 \quad \text{and} \quad T_3 = T_2 = T_1$$

then

$$d_3 N_3^m = d_2 \left[N_2 + \left(\frac{d_1}{d_2} \right)^{1/m} N_1 \right]^m \text{----- 4A.13}$$

i.e. $d_3 N_3^m = (N_2 d_2^{1/m} + N_1 d_1^{1/m})^m \text{----- 4A.14}$

This assumption is also implicit in the linear quadratic formulation. In order to establish a condition for multi-tissue equivalence equation 4A.14 must hold for more than one value of the exponent, e.g. we require:

$$d_3 N_3^{m_1} = (N_2 d_2^{1/m_1} + N_1 d_1^{1/m_1})^{m_1} \text{----- 4A.15}$$

$$d_3 N_3^{m_2} = (N_2 d_2^{1/m_2} + N_1 d_1^{1/m_2})^{m_2} \text{----- 4A.16}$$

From 4A.16

$$N_3 = \left[\frac{(N_2 d_2^{1/m_2} + N_1 d_1^{1/m_2})}{d_3^{1/m_2}} \right] \text{----- 4A.17}$$

Substituting into 4A.15

$$\left[d_3 \frac{(N_2 d_2^{1/m_2} + N_1 d_1^{1/m_2})^{m_1}}{d_3^{m_1}} \right] = (N_2 d_2^{1/m_1} + N_1 d_1^{1/m_1})^{m_1} \quad \text{-----} \quad 4A.18$$

$$d_3 = \left[\frac{(N_2 d_2^{1/m_1} + N_1 d_1^{1/m_1})^{m_1 m_2}}{(N_2 d_2^{1/m_2} + N_1 d_1^{1/m_2})^{m_1}} \right]^{\frac{m_1 m_2}{m_2 - m_1}} \quad \text{-----} \quad 4A.19$$

from 4A.16

$$d_3 = \frac{(N_2 d_2^{1/m_2} + N_1 d_1^{1/m_2})^{m_2}}{N_3^{m_2}}$$

substituting into 4A.15

$$\frac{N_3^{m_1}}{N_3^{m_2}} (N_2 d_2^{1/m_2} + N_1 d_1^{1/m_2})^{m_2} = (N_2 d_2^{1/m_1} + N_1 d_1^{1/m_1})^{m_1}$$

$$\text{i.e. } N_3 = \left[\frac{\left(N_2 d_2^{1/m_1} + N_1 d_1^{1/m_1} \right)^{m_1}}{\left(N_2 d_2^{1/m_2} + N_1 d_1^{1/m_2} \right)^{m_2}} \right]^{\frac{1}{m_1 - m_2}} \text{----- 4A.20}$$

Equation 4A.19 and 4A.20 therefore provide the conditions for multi-tissue equivalence or, to be more specific, dual-tissue equivalence. Two of the following examples that follow are the same as those appearing earlier in the chapter. This time the appendix equations are used instead of those derived from linear quadratic model. For acute effects the CRE formula is used:

$$E = D N^{-0.24} T^{-0.11} = d N^{0.76} T^{-0.11}$$

Where m is therefore 0.76.

For late effects a modified NSD-type formula, originally determined for CNS is used:

$$E = D N^{-0.45} T^{-0.03} = d N^{0.55} T^{-0.03}$$

Where m is therefore 0.55.

Example 4A.1. A regime consisting of 10 fractions of 1.5Gy followed by 5 fractions of 4Gy is given in treatment. What single schedule is this generally equivalent to? Using equations (4A.19) and (4A.20):

$$d = 2.97\text{Gy} : N = 11.4$$

Example 4A.2. A schedule has been given of 15 fractions each of 1.36Gy. What additional treatment must be given to make the total effects equivalent to a schedule of 25 fractions of 2.4Gy?

re-arranging (4A.19) and (4A.20) gives:

$$d = 2.89\text{Gy} : n = 14.0$$

It can be seen that the results in the examples above are similar to those produced by the linear quadratic model in examples 4.1 and 4.2 earlier in this chapter.

Example 4A.3. It is intended to give a schedule of 30 fractions of 2Gy in a course of treatment. However after 11 fractions the dose per fraction was increased 3Gy for a remainder of 13 fractions. What schedule is generally equivalent to this regime?

Again from equations (4A.19 and 4A.20):

$$d = 2.64\text{Gy} : N = 22.9$$

Limitations of dual tissue equivalence.

In the appendix above, it was necessary to make the assumption that the overall times were the same as for the iso-effective schedules. In practice for brain and other late responding tissues (e.g. lung, kidney) the overall time is not critical and time variations between schedules can largely be ignored (Fowler 1989). For acute responding tissues, while temporal factors are important it is almost certainly the case that the T^b formulation in the isoeffect is wrong (Liversage 1971; Fowler, 1989). However there is, as yet, no better description. This is an unsatisfactory position and questions on variations in the temporal parameters for acute responding tissues remain unanswered. Therefore it must be concluded that time factors incorporated in the power law models are probably not reliable. It is difficult to specify how large time differences have to be before they become clinically significant and this even now is largely a matter of clinical judgement.

It should also be noted that the LQ model in its original form does not incorporate a time factor. When it is used to devise schedules which are iso-effective with respect to a given reference schedule it is almost always assumed that all of the schedules considered are of roughly the same time scale.

Figure 4.1 General equivalence.

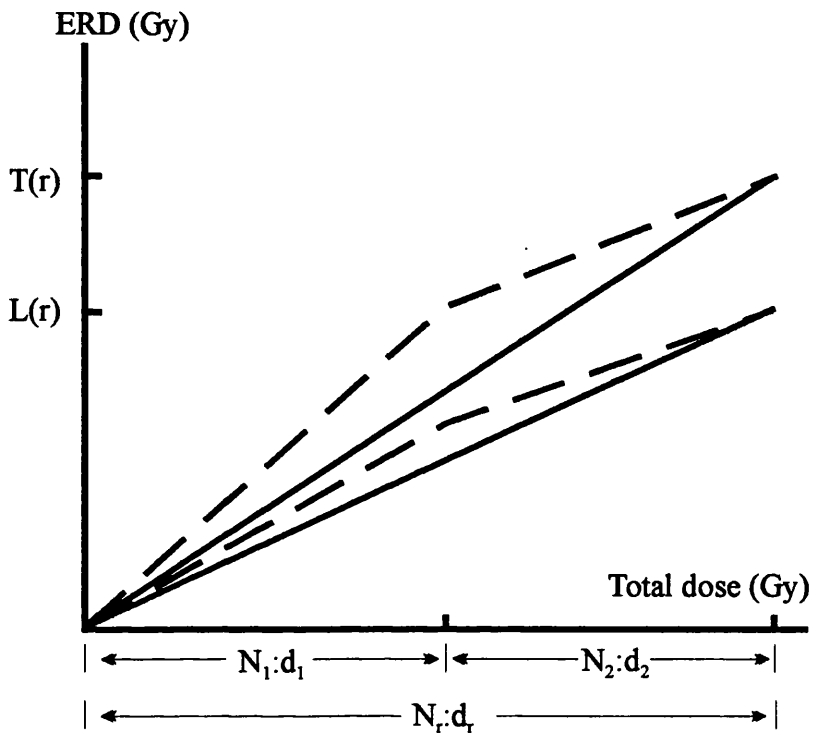


Figure 4.2 General equivalence — Threshold for general equivalence exceeded

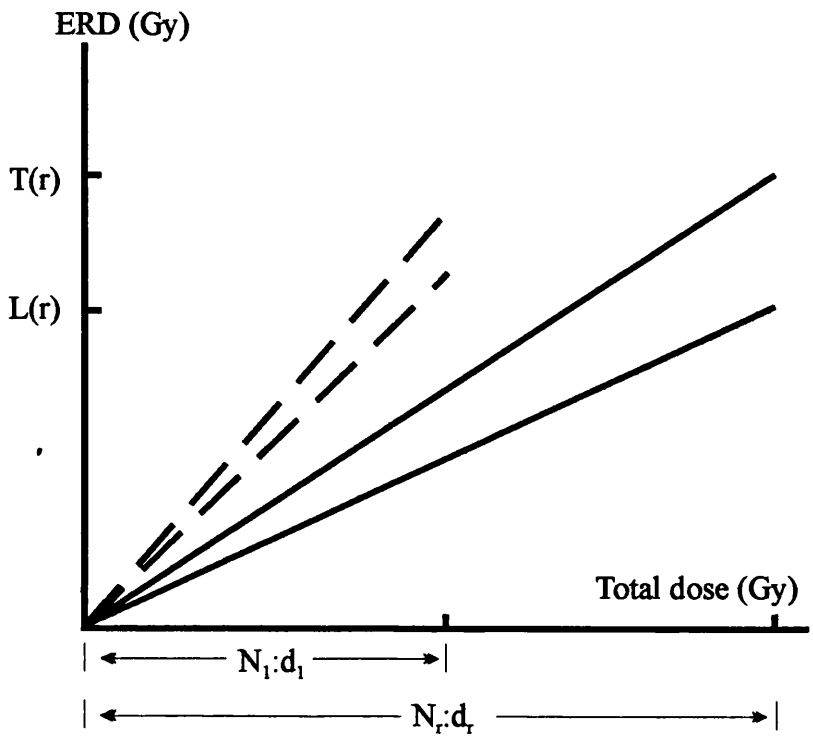


Figure 4.3 CHART arm and conventional control arm.

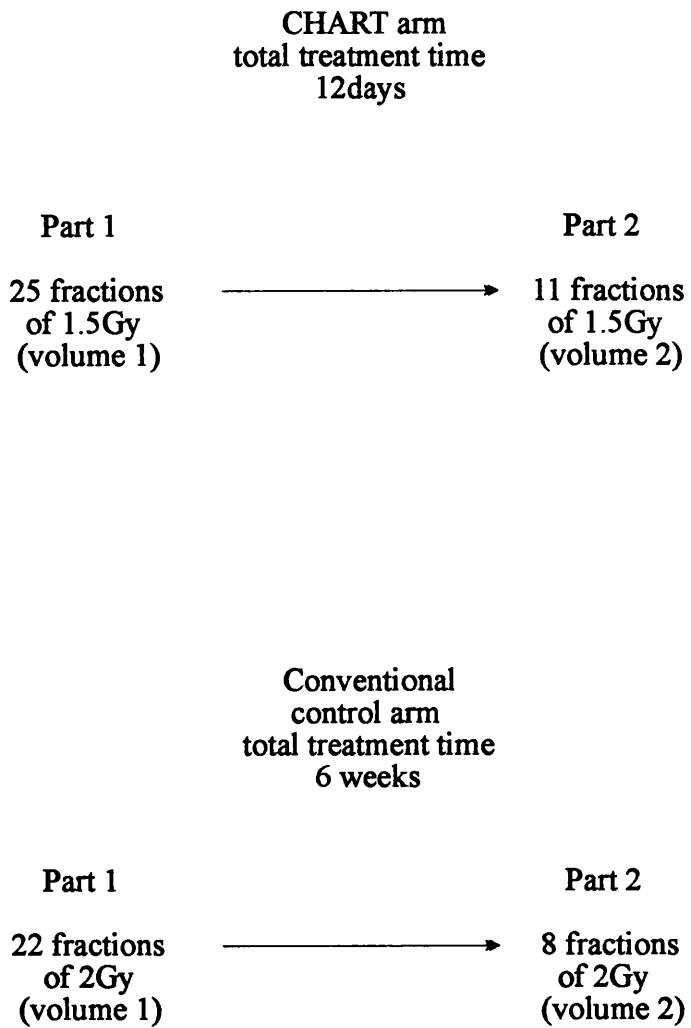


Figure 4.4 Conversion from CHART to conventional treatment.

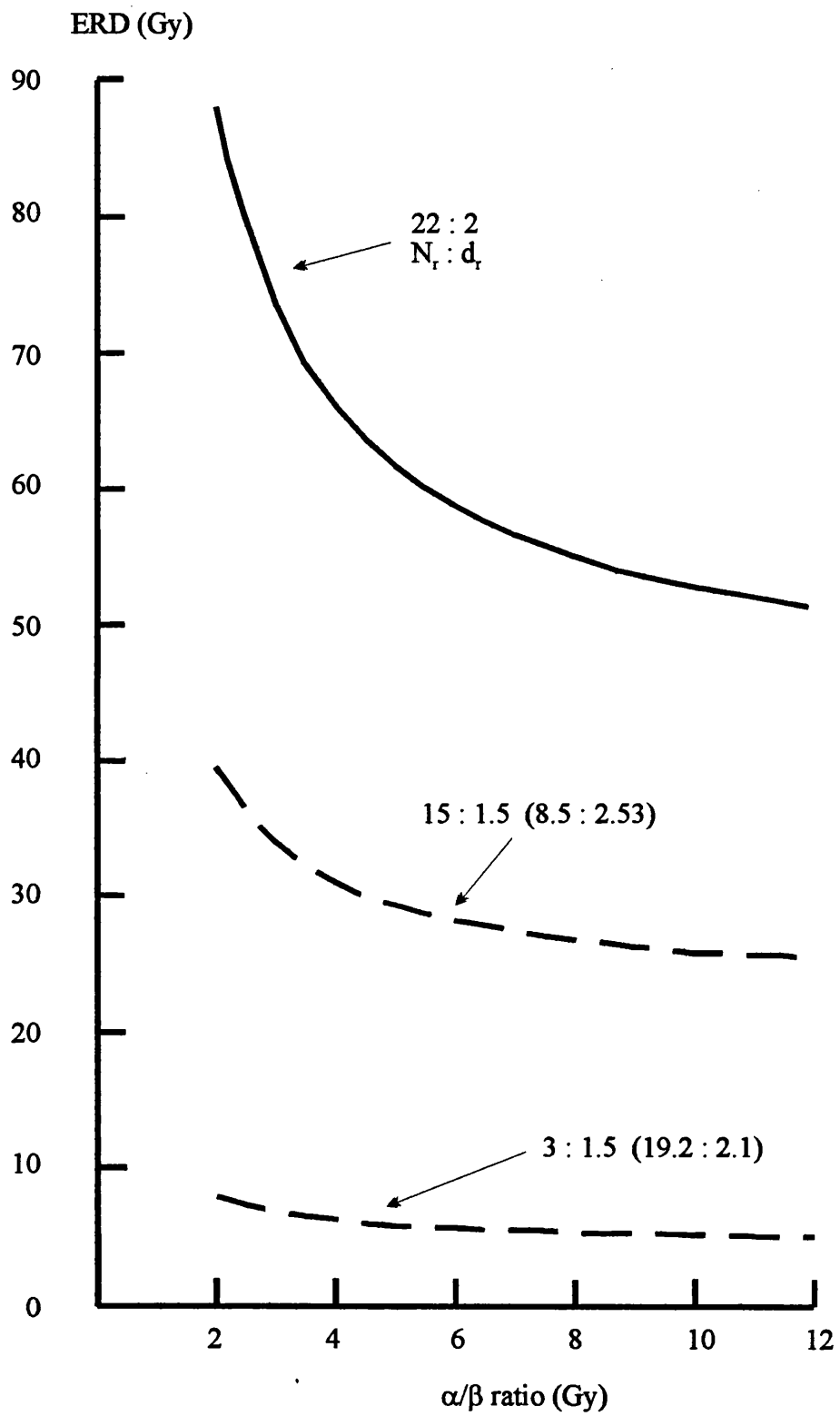
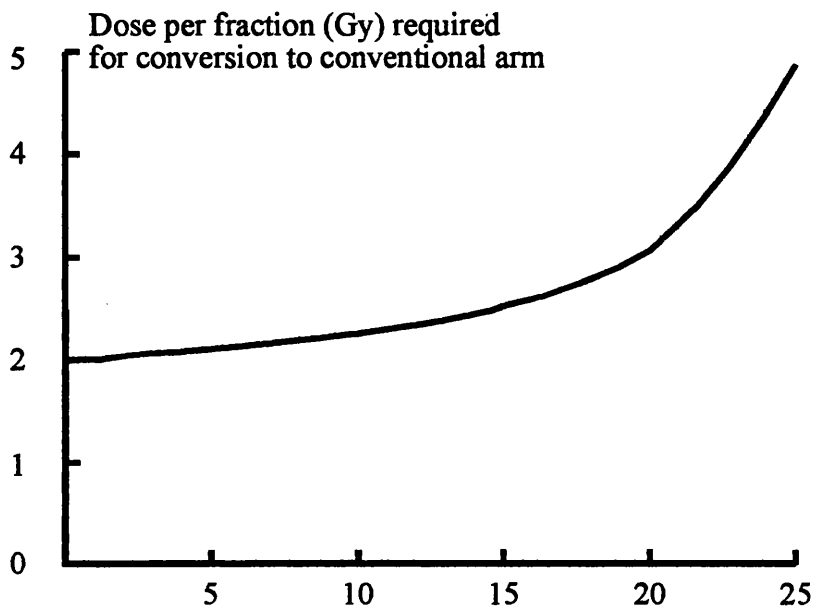
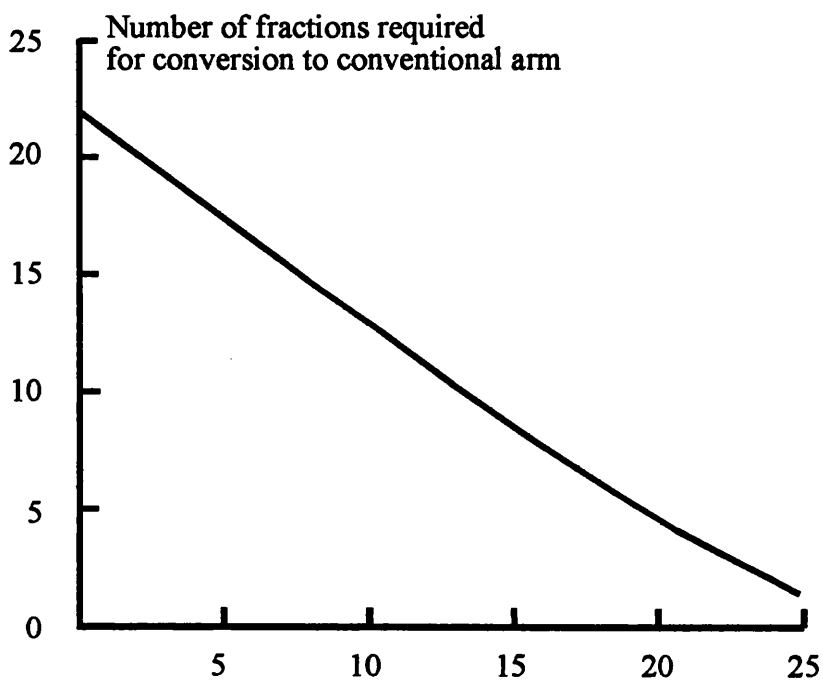


Figure 4.5 (a) Number of fractions and dose per fraction required to convert from CHART part 1 to the conventional arm.

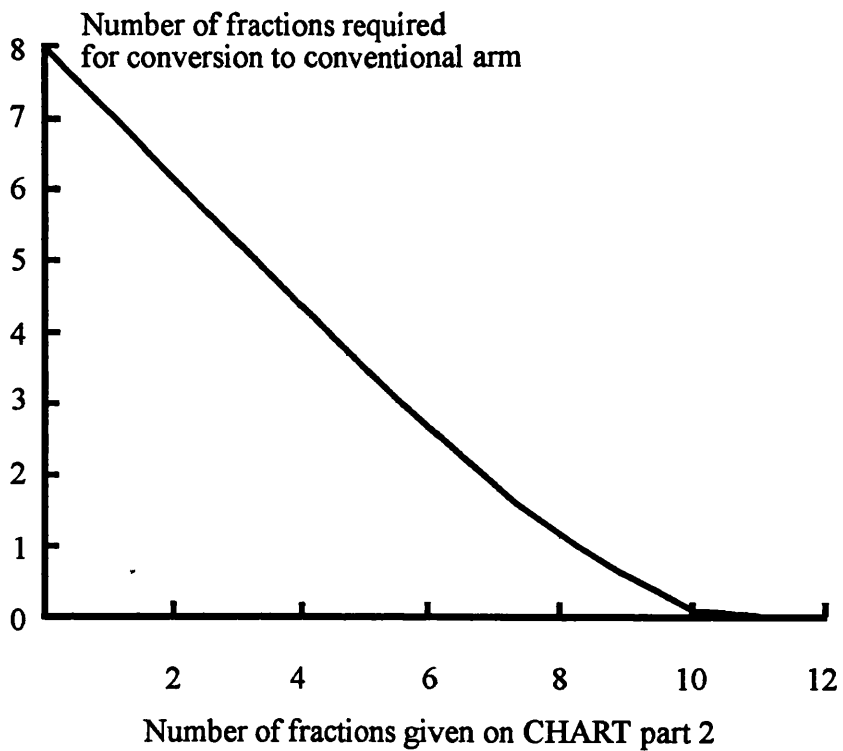
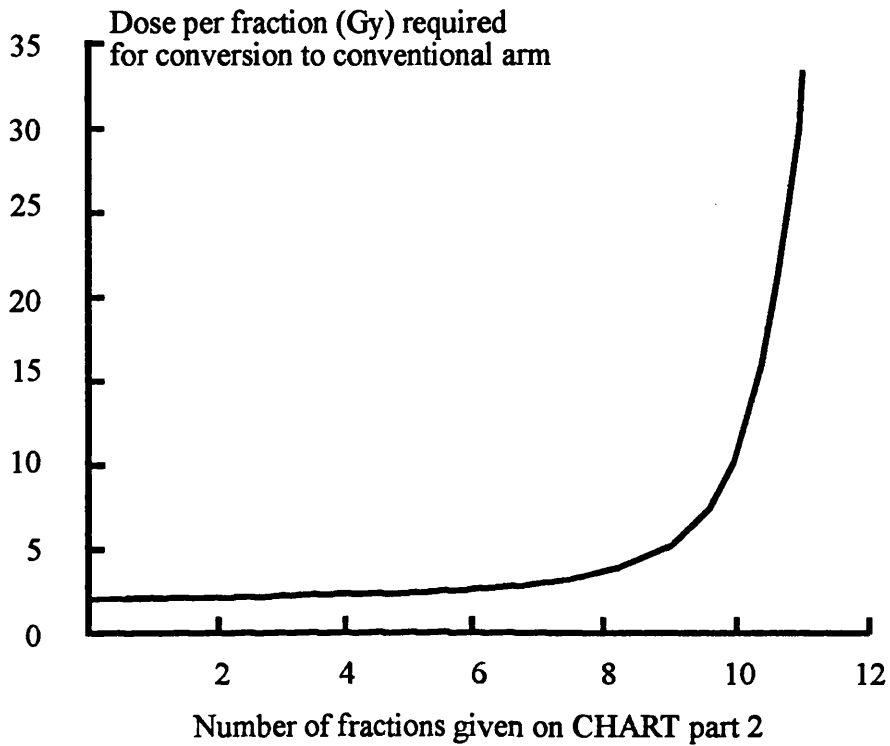


Number of fractions that have been given on CHART part 1.



Number of fractions that have been given on CHART part 1.

Figure 4.5 (b) Number of fractions and dose per fraction required to convert from CHART part 2 to the conventional arm.



Chapter 5

Equivalence between continuous radiotherapy schedules

5.1. Introduction.

In the previous chapter, conditions for general equivalence between fractionated schedules were derived. In this chapter general equivalence between continuous treatments is considered using the same technique as for fractionated treatments. The treatments considered are those where a distribution of radioactive sources is used to produce irradiation at constant dose-rates and is applied to the treatment area for a fixed time and then removed (permanent implants and radioactive decay are not considered here). Sources may be implanted into cavities, for example in the case of intracavitary brachytherapy (Tod & Meredith, 1938; Wilkinson, 1982; Wilkinson et al, 1983; Fleishman, 1983; Sherrah-Davies, 1985; Joslin, 1972, 1990, 1994) or as in the case interstitial brachytherapy, directly into tissues (Paine, 1972; DeBlasio et al, 1988; Paine & Ash, 1988). Although the equivalence argument for continuous treatments is developed in this thesis with reference to intracavitary insertions, the results are just as applicable to interstitial work. At this point it is worth noting that with continuous treatments the term treatment time is used in a slightly different sense than with fractionated treatments. In fractionated radiotherapy this term is often used to refer to the entire course of the treatment, that is the number of days or weeks over which the patient attends the radiotherapy centre. Whereas in continuous therapy treatment time is regarded as the actual time during which the irradiation is applied.

In a new analysis, it will be shown that although equivalence relationships can be derived between some continuous schedules which are independent of the α/β ratio, in many cases the sublethal damage repair time constant, μ , cannot be eliminated. When this occurs, general equivalence between continuous schedules is not possible if different tissues have different values of μ . In spite of this fact, some clinically useful results can still be obtained by means of approximations. The form of the LQ model used here will be that originally described in chapter 2, equation 2.17 (Dale, 1985), for schedules which involve continuous irradiation at a constant dose-rate over a finite time period.

5.2. General equivalence conditions for continuous schedules.

As with fractionated schedules, equivalence conditions will be considered between single continuous treatments and then between sequences containing more than one continuous treatment. The starting point will be Dale's expression for the Extrapolated Response Dose, ERD, which is:

$$ERD = NRT(1+(2R/(\alpha/\beta)\mu)(1-(1/\mu T))(1-EXP(-\mu T)))) \text{ ----- } 2.17$$

where N, R and T are the fraction number, dose rate and treatment time respectively and α/β and μ (the sublethal damage repair time constant) are tissue parameters (Dale, 1985; Warmelink, 1989; Fowler, 1990; Orton 1990). Using the properties of the ERD we can derive general equivalence conditions for continuous radiotherapy.

5.2.1 Single continuous treatments (ie fraction number N = 1).

If we consider two different continuous treatments R_1, T_1 and R_2, T_2 these will be equivalent if their ERDs are equal. ie:

$$ERD_1 = ERD_2$$

$$R_1 T_1 (1+(2R_1 /((\alpha/\beta)(\mu)))(1-(1/\mu T_1)(1-EXP(-\mu T_1)))) \\ = R_2 T_2 (1+(2R_2 /((\alpha/\beta)(\mu)))(1-(1/\mu T_2)(1-EXP(-\mu T_2))))$$

$$R_1 T_1 + (2R_1^2 T_1 /((\alpha/\beta)(\mu)))(1-(1/\mu T_1)(1-EXP(-\mu T_1))) \\ = R_2 T_2 + (2R_2^2 T_2 /((\alpha/\beta)(\mu)))(1-(1/\mu T_2)(1-EXP(-\mu T_2)))$$

Equivalence conditions which are independent of the α/β ratio can be found for these two treatments by equating the total dose coefficients and that of the $1/(\alpha/\beta)$ term, ie the coefficients for A and B type damage. These conditions are:

$$R_1 T_1 = R_2 T_2 \text{ -----(5.1)}$$

and

$$R_1^2 T_1 (1-(1/((\mu)T_1))(1-EXP(-\mu T_1))) \\ = R_2^2 T_2 (1-(1/((\mu)T_2))(1-EXP(-\mu T_2))) \text{ -----(5.2)}$$

These are not of course general equivalence conditions because μ is still present and this may be a tissue specific parameter. Therefore, an exact general equivalence does not seem possible. However, some useful approximations may be made associated with three different treatment time regions (values of T). A full discussion of these is contained in appendix 5.1. These time intervals are:

5.2.1(a) Treatment time $T < 0.043$ hr (ie $T < 2.58$ min).

In this region the term $(1-1/(\mu T))(1-EXP(-\mu T))$ approaches $\mu T/2$ (see figure 5.1(a)).

This time threshold results in a difference in the term $(1-1/(\mu T))(1-EXP(-\mu T))$ and the term $\mu T/2$ of less than -2%. Using the values of μ stated earlier in chapter 3, section 3.3.2 (see also examples 3.4 and 3.5) (Warmelink, 1989; Fowler 1990; Orton, 1988; Brenner, 1992; Millar & Canney, 1993), the actual differences are:

Tumour ($\mu = 1.4 \text{ hr}^{-1}$) ----- difference = -1.98%

Late responding tissue ($\mu = 0.46 \text{ hr}^{-1}$) -----difference = -0.66%).

This threshold is chosen because the approximation leads to a variation in the ERD of $\approx 0.5\%$ or less. This approximation should therefore be acceptable since it is generally accepted that variation in effect of $\approx 3.0\%$ to $\approx 5.0\%$ are considered to be clinically detectable.

Equation (5.2) becomes:

$$R_1^2 T_1^2 = R_2^2 T_2^2 \text{ -----(5.3)}$$

solving (5.1) and (5.3) gives the result that:

$$R_1 T_1 = R_2 T_2 \text{ -----(5.4)}$$

The time taken for the delivery of a single fraction of treatment on a linear accelerator falls into this region (typical outputs are between 2.5Gy/min and 3.5Gy/min from modern accelerators and $RT=d$, the dose per fraction) as do some high dose-rate brachytherapy treatments.

Provided the dose is equal then the two single fractions are generally equivalent as long as the treatment time, T is in each case less than about 2.58 minutes. Notice also in equation 5.4 that the dose rate and the time can vary as long as the product (total dose) is unchanged. This result is consistent with the equivalence conditions derived for fractionated radiotherapy in chapter 4 (Deehan and O'Donoghue, 1988)

In a strict mathematical sense this is not general equivalence because an approximation has been made for the expression $(1-(1/\mu T)(1-EXP(-\mu T)))$. Therefore this is approximately general equivalence.

5.2.1(b) Treatment time $T > 8.5$ hr.

In this region the term $(1-\text{EXP}(-\mu T))$ approximates to unity with a maximum deviation of 2% (see figure 5.1(b)). Equation (5.2) becomes:

$$R_1^2 T_1 - R_1^2 / \mu = R_2^2 T_2 - R_2^2 / \mu$$

Equating coefficients gives two more conditions:

$$R_1^2 T_1 = R_2^2 T_2 \text{ -----(5.5)}$$

$$R_1^2 = R_2^2 \text{ -----(5.6)}$$

In this treatment time region we have three conditions for approximate general equivalence governed by equations (5.1), (5.5) and (5.6). The only solutions are that:

$$R_1 = R_2 \qquad \text{and} \qquad T_1 = T_2$$

More rigorous conditions apply in this region than in 5.2.1 (a) above. The dose rates must be equal and also the treatment times, not just their products. Even approximate general equivalence is not possible between different single treatments when the treatment time is greater than 8.5 hr.

5.2.1(c) Treatment time $0.043 \text{ hr} < T < 8.5 \text{ hr}$.

We must look at equations (5.1) and (5.2) in this time region. Here μ cannot be eliminated thus making general equivalence impossible even though the α/β ratio has been removed, unless the μ values for different tissues involved are sufficiently similar.

From equation (5.1):

$$R_2 = (R_1 T_1 / T_2)$$

Substituting into (5.2) gives:

$$T_1 (1 - (1/(\mu T_1))(1 - \text{EXP}(-\mu T_1))) = T_2 (1 - (1/(\mu T_2))(1 - \text{EXP}(-\mu T_2)))$$

For any value of μ the only possible solution is that $T_1 = T_2$. Substituting this result into equation 5.1 above gives the result that $R_1 = R_2$. So that for general equivalence between single continuous treatments:

$$R_1 = R_2 \quad \text{and} \quad T_1 = T_2$$

The result over the three time periods is that for any single continuous treatment no other single continuous treatment exists which gives equivalent effects for all tissues. General equivalence is not possible between different single continuous treatments, and only in one special case, where treatment time is less than 2.58 min, is general equivalence approached. This special case is referred to later in the conclusions.

5.2.2. Sequences of continuous treatments.

Until now a distinction has been made between fractionated and continuous treatments. Fractionated treatments are those which involve treatment times which are short enough for no repair of sub-lethal damage to take place. In practice the treatment times for each fraction of a typical fractionated treatments is about 45 seconds. However a number of continuous schedules can be given in sequence to form a fractionated schedule or a regime. In this case the treatment times may vary from a few minutes in the case of high dose-rate treatments to over one hundred hours in the case of a very low dose-rate treatment. Equivalence between sequences of continuous schedules is now considered in this chapter (in chapter 6 equivalence between sequences of both fractionated and continuous treatments is considered). It should be stressed once more that all treatment schedules referred to in this thesis are assumed to be given in such a manner as to allow full repair of sub-lethal damage to take place between individual fractions. This is true regardless of whether a fractionated external beam treatment is considered or a continuous brachytherapy treatment is given in a series of fractions.

With the above in mind we consider the question: can general equivalence exist between two series of continuous treatments?

Let series a consist of r fractions:

$$\text{ie. } R_1^a:T_1^a + R_2^a:T_2^a + R_3^a:T_3^a + \dots + R_r^a:T_r^a$$

Let series b consist of k fractions:

$$\text{ie. } R_1^b:T_1^b + R_2^b:T_2^b + R_3^b:T_3^b + \dots + R_k^b:T_k^b$$

Using the additive property of the ERD (Dale 1986) it follows that for equivalence between these two series.

$$\sum_{n=1}^{n=f} \text{ERD}_n^a = \sum_{p=1}^{p=k} \text{ERD}_p^b$$

$$\sum_{n=1}^{n=f} \left[R_n^a T_n^a + R_n^{a^2} T_n^a (2 / (\alpha / \beta)(\mu)) (1 - (1 / (\mu T_n^a)) (1 - \text{EXP}(-\mu T_n^a))) \right]$$

$$= \sum_{p=1}^{p=k} \left[R_p^b T_p^b + R_p^{b^2} T_p^b (2 / (\alpha / \beta)(\mu)) (1 - (1 / (\mu T_p^b)) (1 - \text{EXP}(-\mu T_p^b))) \right]$$

Re-arranging the above equation slightly gives:

$$\sum_{n=1}^{n=f} \left[R_n^a T_n^a \right] + (1 / (\alpha / \beta)) \sum_{n=1}^{n=f} \left[R_n^{a^2} T_n^a (2 / (\mu)) (1 - (1 / (\mu T_n^a)) (1 - \text{EXP}(-\mu T_n^a))) \right]$$

$$= \sum_{p=1}^{p=k} \left[R_p^b T_p^b \right] + (1 / (\alpha / \beta)) \sum_{p=1}^{p=k} \left[R_p^{b^2} T_p^b (2 / (\mu)) (1 - (1 / (\mu T_p^b)) (1 - \text{EXP}(-\mu T_p^b))) \right]$$

Equivalence conditions which are independent of the α/β ratio can be found for these two series by equating the total dose and the coefficients of the $1/(\alpha/\beta)$ terms.

These conditions are:

$$\sum_{n=1}^{n=r} [R_n^a T_n^a] = \sum_{p=1}^{p=k} [R_p^b T_p^b]$$

and

$$\sum_{n=1}^{n=r} \left[R_n^a T_n^a \left(1 - \frac{1}{(\mu T_n^a)} (1 - \text{EXP}(-\mu T_n^a)) \right) \right] = \sum_{p=1}^{p=k} \left[R_p^b T_p^b \left(1 - \frac{1}{(\mu T_p^b)} (1 - \text{EXP}(-\mu T_p^b)) \right) \right]$$

In common with the case of two single treatments, true general equivalence is not possible because, although the α/β ratio has been eliminated from the conditions, μ remains. However "near" general equivalence situations can be identified. Although many situations could be considered, for simplicity, the following discussion only considers the case where one of the regimes is a schedule. If therefore series number one is a schedule (ie each part of the treatment is identical) with treatment time T_1^a and dose-rate R_1^a then:

$$rR_1^a T_1^a = \sum_{p=1}^{p=k} [R_p^b T_p^b] \text{-----}(5.7)$$

and

$$rR_1^a T_1^a (1 - (1/(\mu T_1^a))(1 - \text{EXP}(-\mu T_1^a))) \\ = \sum_{p=1}^{p=k} \left[R_p^b T_p^b (1 - (1/(\mu T_p^b))(1 - \text{EXP}(-\mu T_p^b))) \right] \text{-----}(5.8)$$

5.2.2(a) Treatment time $T < 0.043$ hr (ie $T < 2.58$ min). This threshold is chosen for the same reasons as in 5.2.1(a) where the term $(1 - (1/\mu T)(1 - \text{EXP}(-\mu T)))$ tends towards $(\mu T)/2$ (see figure 5(a)). Equation (5.8) reduces to :

$$rR_1^a T_1^a = \sum_{p=1}^{p=k} R_p^b T_p^b \text{-----}(5.9)$$

If $k=1$ the solutions of equation (5.7) and (5.9) give the conditions for near equivalence in this case.

$$r = k \quad \text{and} \quad R_1^a T_1^a = R_1^b T_1^b$$

The number of fractions and the dose per fraction have to be equal across the two schedules. As in case 5.2.2(a) for single continuous treatments the only variations possible are those of actual dose rate and treatment time but keeping the total dose per fraction constant.

If $R_p^b T_p^b$ is heterogeneous then:

$$R_1^a T_1^a = \frac{\sum_{p=1}^{p=k} R_p^{b^2} T_p^{b^2}}{\sum_{p=1}^{p=k} R_p^b T_p^b} \text{-----(5.10)}$$

$$r = \frac{\left(\sum_{p=1}^{p=k} R_p^b T_p^b \right)^2}{\sum_{p=1}^{p=k} R_p^{b^2} T_p^{b^2}} \text{-----(5.11)}$$

This is exactly what would be expected from the general equivalence conditions for fractionated radiotherapy in the case of a series of different single fractions ($RT = d$, the dose per fraction).

5.2.2(b) Treatment time $T > 8.5$ hr. Here the term $(1-\text{EXP}(-\mu T))$ in equation (5.8) approaches unity (see section 5.2.1(b) and figure 5(b)). Equation (5.8) reduces to:

$$\begin{aligned} r R_1^{a^2} T_1^a (1 - (1/(\mu T_1^a))) \\ = \sum_{p=1}^{p=k} \left[R_p^{b^2} T_p^b (1 - (1/(\mu T_p^b))) \right] \text{-----(5.12)} \end{aligned}$$

Near equivalence is possible if equation (5.7) holds and also if :

$$rR_1^{a^2} T_1^a = \sum_{p=1}^{p=k} R_p^{b^2} T_p^b \text{ ----- (5.13)}$$

and

$$rR_1^{a^2} = \sum_{p=1}^{p=k} R_p^{b^2} \text{ -----(5.14)}$$

Equations (5.7), (5.13) and (5.14) give the conditions for near equivalence when the treatment times are greater than 8.5hr. The α/β ratio and μ have been eliminated.

These equations can be solved:

Dividing 5.13 by 5.7 gives:

$$R_1^a = \left(\frac{\sum_{p=1}^{p=k} R_p^{b^2} T_p^b}{\sum_{p=1}^{p=k} R_p^b T_p^b} \right) \text{ -----(5.15)}$$

Dividing 5.13 by 5.14 gives:

$$T_1^a = \left(\frac{\sum_{p=1}^{p=k} R_p^{b^2} T_p^b}{\sum_{p=1}^{p=k} R_p^{b^2}} \right) \text{ -----(5.16)}$$

Substituting 5.15 into 5.14 gives:

$$r = \left(\sum_{p=1}^{p=k} R_p^{b^2} \frac{\sum_{p=1}^{p=k} R_p^b T_p^b}{\sum_{p=1}^{p=k} R_p^{b^2} T_p^b} \right)^2 \text{----- (5.17)}$$

5.2.2(c) Treatment time $0.043\text{hr} < T < 8.5\text{hr}$. As with the case of single continuous treatments the only solution for general equivalence in this region is that:

$$R_r^a = R_p^b \quad \text{and} \quad T_r^a = T_p^b$$

This can be seen by using similar reasoning as in 5.1.3 applied to equations 5.7 and 5.8.

Examples of the use of the relationships derived in section (5.2) are shown in appendix 5.2.

Conclusion.

This chapter has presented a new development of the linear quadratic model which allows study of general equivalence between continuous treatments. From this analysis it would seem that general equivalence is not achievable in a rigorous mathematical sense.

Although the α/β ratio can be eliminated from the general equivalence equations the sublethal damage repair time constant μ remains in all but a number of trivial cases.

Initially single continuous treatments were considered from which it was concluded that no two single continuous treatments $R_1 : T_1$ and $R_2 : T_2$ could be generally equivalent. Only when the treatment time was less than about 2.58 minutes could conditions be found which produced "near" general equivalence. The condition for equivalence was that:

$$R_1 T_1 = R_2 T_2 \text{ ----- (5.4)}$$

That is, the product of dose-rate and treatment time for both should be equal. Treatment times of the order of 45 seconds fall into the category of high dose rate fractionated therapy normally associated with external beam treatments delivered from a modern linear accelerator (see appendix 5.1). At first this result seems to conflict with that already derived in chapter 4 for single fractionated schedules where general equivalence was shown to be impossible. However since:

$$R_1 T_1 = d = R_2 T_2$$

where d is the dose per fraction and the fraction numbers are also equal:

$$N_1 = N_2 = 1.$$

This reveals the special (trivial) case where general equivalence is possible between single fractionated schedules and single continuous schedules if the treatment times is

less than 2.58 minutes (see appendix 5.1). More rigorous conditions apply when the treatment time is greater, that is:

$$R_1 = R_2 \quad \text{and} \quad T_1 = T_2$$

(sections 5.2.1(b) and 5.2.1(c))

In section 5.2.2 general equivalence is considered between a schedule and a regime both consisting of a number of continuous treatments (ie a number of continuous treatments given in sequence) and it was shown that in the region $0.043\text{hr} < \text{Treatment time, } T < 8.5\text{hr}$ that once more conditions obtained in sections 5.2.1(b) and 5.2.1(c) were required for general equivalence (section 5.2). That is the schedule and the regime had to be identical.

However when $8.5\text{hr} < T < 0.043\text{hr}$ then terms involving T in the mathematical relationships yielded approximations which led to a "near" general equivalence (sections 5.2.2(a) and 5.2.2(b))

The usefulness of these findings can be judged better by referring to figure 5.2. In 5.2.(a). the three treatment time regions mentioned above are shown. Below, in 5.2.(b), these times are linked to nominal dose-rates (assuming the typical dose per fractions shown) and in turn to the treatment dose-rate regions of HDR, MDR and LDR in 5.2.(c) (Corbett, 1990) (see also table 1.3). Near equivalence transitions are therefore possible within region A and C and also between regions A and C.

For transitions within region B schedules have to be identical to achieve equivalence and transitions between B and either A or C cannot be equivalent. The findings of general equivalence therefore favour transitions between LDR treatments and HDR treatments above 150 Gy/hr as well as a small region of the MDR range below

about 5.3 Gy/hr. Since a great deal of interest is now being shown in converting from LDR to HDR (Dale, 1985; Steel, 1986; Dutriex, 1989; Hall, 1972, 1991; Orton 1991; Joslin, 1972, 1994,) a general equivalence analysis may be useful to those considering such a change. It has to be mentioned, however that a general equivalence approach can predict fraction numbers which are too large to be of practical use and this is discussed later in connection with the distribution of biological effects.

In chapter 6 general equivalence is investigated for regimes containing both high dose rate fractionated and continuous low dose-rate fractionated treatments.

5.4. Appendix 5.1 Treatment times.

Treatment time regions have been identified in this chapter which allow approximations to be made in order to simplify mathematical expressions. This appendix is intended to discuss treatment times in more detail and point out some areas where the above approximations need to be applied with care. Although this chapter deals with continuous treatments the following section has a bearing on both fractionated and continuous treatments.

High dose-rate fractionated external beam treatments -- Linear accelerators.

The output dose-rates at 100cm focus to skin distance for modern linear accelerators range from about 2.5Gy/min to 3.5Gy/min. Assuming a standard treatment dose per fraction of 2Gy this would give a total treatment time per fraction in the range 0.8min (48sec) to 0.57min (34.2sec). Within this region the reasoning applied in 5.1.1 holds but it is clear that the total treatment time per fraction will be longer in practice. This is because the 2Gy dose is rarely given in one single exposure but instead is delivered as smaller fractions. The reason for this is of course the practical limitations of patient set up and the fact that for radical treatments a number of beams are almost always used. Each field will deliver its own contribution to the 2Gy dose (eg approximately 0.5Gy per field for a symmetrical four field treatment where the fields are of equal weighting). Between the treatments of individual fields there will be a period where radiographers have to physically set up the next field and this can take 2 or 3 minutes or more in difficult cases. If we assume 3 minutes between fields for set up, then a four field treatment fraction which delivers 2Gy will last between 9.8min ($3 \times 3\text{min} + .8\text{min}$) to 9.57min ($3 \times 3\text{min} + .57\text{min}$). Earlier in this chapter the set up time is not taken

into account in the treatment time per fraction (only the time for which the machine is delivering dose is considered that is the treatment time). Repair will continue while the beam is off and this "off time" should be included. Currently the LQ model does not attempt to take these effects into account (Warmelink, 1989; Fowler, 1989, 1990; Orton, 1990) and provided the set up time is comparable between two different treatments then "off time" can probably be ignored.

Cobalt 60 treatments.

Depending on the strength of the source, the typical output dose-rate variation for a 10x10 plain field is about 2.4Gy/min at 80cm source to skin distance for a 8k Ci source (at the time of installation). This drops to a value of about 1Gy/min when a new source is required (after about 5 years) so the delivery time for a 2Gy fraction is between 0.83min (50sec) and 2min over the lifetime of a source. If the set up times between beams are ignored as in the case of linear accelerators then we can use these times to look at the degree to which the $(1-(1/\mu T)(1-EXP(-\mu T)))$ term approximates to the expression $\mu T/2$. Table 5A1.1 shows the results and it can be seen that for treatment times of about 50sec the errors are small, less than 0.7% for both tumour and late responding tissues. For treatment times of the order of 2min the errors are greater especially for tumour, assumed to have acute responding characteristics (Thames, 1989), but these are still less than 2%. As expected the approximation made for "near" general equivalence at short treatment times is therefore better for linear accelerators than for Cobalt 60 treatments with the latter approximation increasing as the Cobalt 60 source decays. The point at which the approximation becomes too great is perhaps debatable but a value of 2% is used here (see section 5.2.1(a)).

Special types of external beam treatments.

There exist a few therapy techniques which have extended treatment times. This occurs particularly when the treatment distance is longer than usual, for example mantle and whole body treatments. These would have to be considered individually and once more a value of 2% error for the short treatment time is recommended. Orthovoltage and superficial treatments can also result in lengthened treatment times compared to linear accelerators or cobalt 60 treatments.

Brachytherapy treatments.

The use of remote after loading is increasing rapidly in modern brachytherapy treatments. This allows the treatment time to vary over a much wider range than that associated with external beam radiotherapy. This fact alone has produced a renewed interest in dose-rate effects over the last decade as discussed earlier in this thesis. Treatment dose-rates are often classified into three groups: these are shown in table 1.3, chapter 1, as low, medium and high dose-rate, (LDR, MDR and HDR respectively). LDR and MDR treatments are usually given in one or two fractions while HDR treatments are often spread over a number of fractions. If a standard 30Gy dose is to be given then this would result in a treatment time of between 300 and 15hr if given in one fraction at LDR and between 15 and 2.5hr if given in the same way at MDR. At HDR if the fraction size is 6Gy the treatment time would be around 2.4min (144sec). These treatment time ranges can be identified on the graphs in figure 5.1. The LDR and HDR treatments fall in regions where approximations can be made.

5.5. Appendix 5.2 Worked examples.

Examples of the use of the above relationships are shown below and can be divided into two categories. One is where the α/β ratio and μ (by virtue of the treatment time) can be eliminated (examples 5A.1 and 5A.2). The second is where the α/β ratio is eliminated but μ cannot be (examples 5A.3 and 5A.4).

Example 5A.1

A treatment regime consists of two continuous schedules one of 40.54hr with dose rate of .74 Gy/hr, and the other of 62.5hr with a dose rate of .48 Gy/hr (TD=30 Gy for both). Does a uniform schedule exist (ie one with a uniform dose rate and time given over a number of fractions) which is equivalent to these two schedules given in series?

i) Dose Rate: using equation (5.15)

$$R = (0.74^2 \times 40.54 + 0.48^2 \times 62.5) / (0.74 \times 40.54 + 0.48 \times 62.5) = 0.61 \text{ Gy/hr}$$

ii) Time: using equation (5.16)

$$T = (0.74^2 \times 40.54 + 0.48^2 \times 62.5) / (0.74^2 + 0.48^2) = 47.04 \text{ hr}$$

iii) Number of fractions: using equation (5.17)

$$N = (0.74^2 + 0.48^2) \left[\frac{(0.74 \times 40.54 + 0.48 \times 62.5)}{(0.74^2 \times 40.54 + 0.48^2 \times 62.5)} \right]^2$$

$$= 2.1 \text{ fractions}$$

A "near" generally equivalent schedule does exist which consists of 2.1 fractions each of 47.04 hr at a dose-rate of 0.61 Gy/hr.

Example 5A.2

A standard treatment schedule consists of two continuous schedules in series, each of dose rate 0.6 Gy/hr and a time of 50 hr to give 60 Gy, however the first schedule was given with a dose rate of 0.7 Gy/hr given in 40 hr. What further treatment is necessary to bring the total treatment back to the effects of the original schedule?

Rearranging equations (5.15)-(5.17):

$$R = (2 \times 0.6^2 \times 50 - 0.7^2 \times 40) / (2 \times 0.6 \times 50 - 0.7 \times 40)$$

$$= 0.513 \text{ Gy/hr}$$

$$T = (2 \times 0.6^2 \times 50 - 0.7^2 \times 40) / (2 \times 0.6^2 - 0.7^2)$$

$$= 71.39 \text{ hr}$$

$$N = (2 \times 0.6^2 - 0.7^2) \left[\frac{(2 \times 0.6 \times 50 - 0.7 \times 40)}{(2 \times 0.6^2 \times 50 - 0.7^2 \times 40)} \right]^2$$

$$= 0.87 \text{ fractions}$$

The further treatment required is therefore 0.87 fractions of dose-rate 0.513Gy/hr given over 71.39hr. We cannot of course have a non integer number of fractions. What if one fraction of 62.11 hr was given as a compromise? Then:

$$R = (0.7^2 \times 40 + 0.513^2 \times 62.11) / (0.7 \times 40 + 0.513 \times 62.11)$$

$$= 0.6 \text{ Gy/hr}$$

$$T = (0.7^2 \times 40 + 0.513^2 \times 62.11) / (0.7^2 + 0.513^2)$$

$$= 47.73 \text{ hr}$$

$$N = (0.7^2 + 0.513^2) \left[\frac{(0.7 \times 40 - 0.513 \times 62.11)}{(0.7^2 \times 40 + 0.513^2 \times 62.11)} \right]^2$$

$$= 2.08 \text{ fractions}$$

A single fraction of .513Gy/hr given in 62.11hr when given after 1 fraction of 0.7Gy/hr given in 40hr results in a "near" equivalence to 2 fractions each of 0.6Gy/hr and 50hr. We have seen that the α/β ratio can be eliminated from the general equivalence so that one can talk of results which are independent of this ratio and only dependent on μ . This means that if changes in treatment schedules (eg dose rate, treatment time or fraction number) are required then alternative schedules with

equivalent effects on specific tissues can be found and the process involved only requires knowledge of the sublethal damage repair time constant, μ and no knowledge of the α/β ratio is required. Hypothetical examples of this are given shown below.

Example 5A.3

A treatment is to be given with a dose rate of 1.75 Gy/hr: what treatment time and number of fractions are required to produce the same late effect as a continuous schedule with a dose rate of .5 Gy/hr given over 60 hrs ?

Late effects: assume a value of $\mu = .459$ /hr

Beginning with equations (5.7) and (5.8):

i) Continuous schedule $r = 1$: $R_1 = .5$ Gy/hr : $T_1 = 60$ hr

Assume that the new schedule will be homogeneous with fraction number k : $R_2 = 1.75$ Gy/hr

equation (5.7) gives $kR_2 = rR_1T_1 / T_2$ ----- (5.18)

substitution in (5.8) gives

$$\left(\frac{R_1}{R_2} \right) = \left(\frac{(1 - (1 / (\mu T_2))(1 - \text{EXP}(-\mu T_2)))}{(1 - (1 / (\mu T_1))(1 - \text{EXP}(-\mu T_1)))} \right) \text{----- (5.19)}$$

solving for T gives 1.488 hrs and k can be found by substitution in equation 5.18, $k = 11.52$ fractions. This result can be checked by calculating the ERD for each of these schedules for late effects (using equation 2.17) and notice that any value of the α/β ratio can be used provided $\mu = .46(\text{hr}^{-1})$.

Example 5A.4

For the same standard schedule as in example 5A.3 above, a treatment has to be devised to give the same late effects with a treatment time of 2 hrs. What dose rate and number of fractions is required for matching of late effects ?

solving (5.19) gives $R = 1.394 \text{ Gy/hr}$

substituting in (5.18) gives $k = 10.74$ fractions.

This result can be checked by calculating the ERD for both schedules (equation 2.17).

Table 5A1.1. Percentage difference between $(1-1/(\mu T))(1-EXP(-\mu T))$ and $\mu T/2$ for Tumour and Late responding tissues corresponding to Cobalt 60 treatments. Dose given = 2Gy						
Treatment time	Tumour $\mu = 1.4 \text{ hr}^{-1}$			Late $\mu = .46 \text{ hr}^{-1}$		
	$\mu T/2$ A	$(1-1/(\mu T))(1-EXP(-\mu T))$ B	$100-(A/B) \times 100$ (% Diff)	$\mu T/2$ A	$(1-1/(\mu T))(1-EXP(-\mu T))$ B	$100-(A/B) \times 100$ (% Diff)
50 sec	9.722	9.659	0.652	3.194	3.188	0.188
2 min	23.333	22.974	1.562	7.667	7.638	0.380

Figure 5.1(a) Plot of $(1 - (1/(\mu T))(1 - \text{EXP}(-\mu T))) \times 10^3$ versus treatment time (sec).

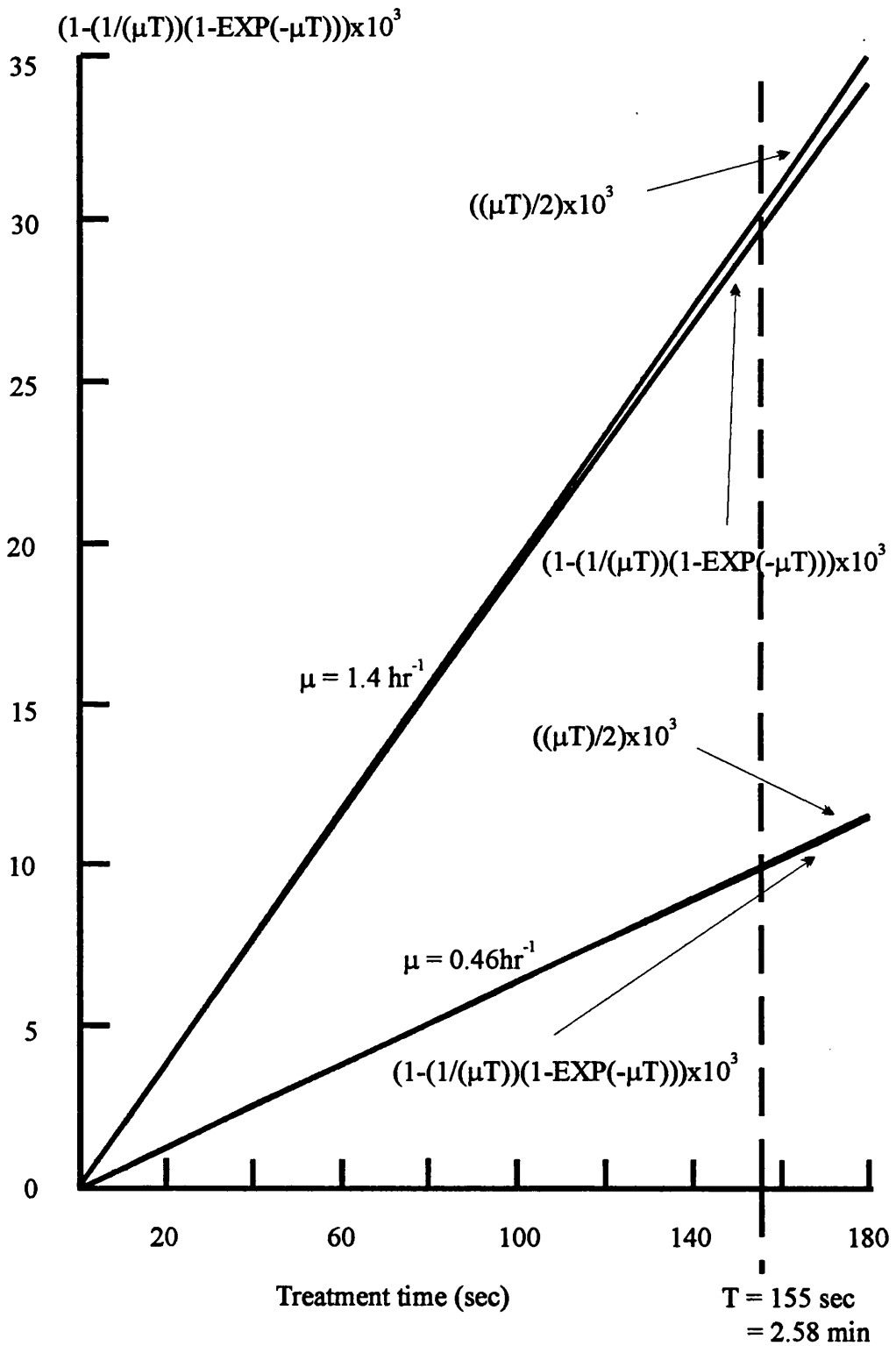


Figure 5.1(b) Plot of $(1-\text{EXP}(-\mu T))$ versus treatment time (hr).

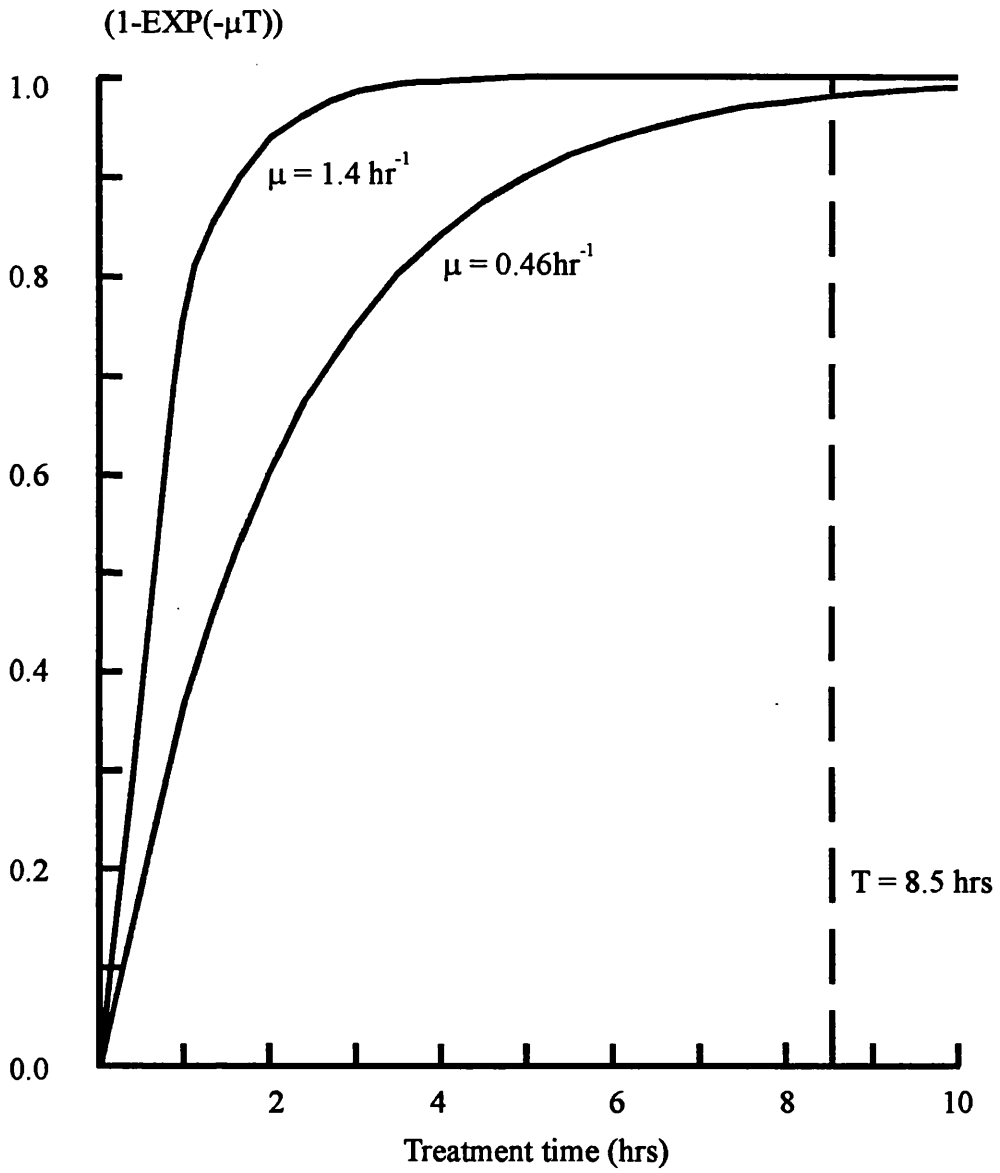
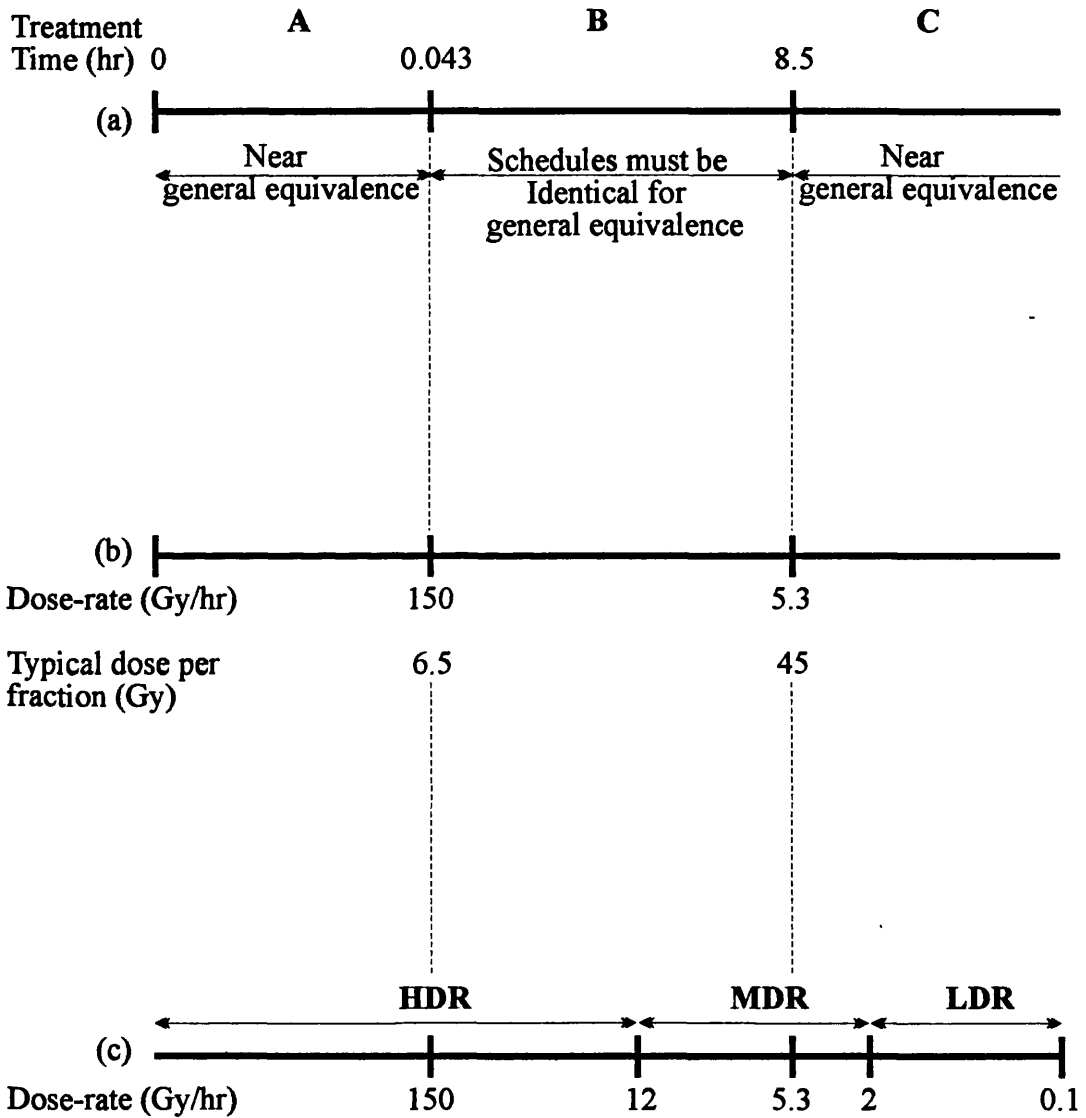


Figure 5.2 Treatment time ranges for equivalence between continuous schedules.



Chapter 6

Biological equivalence between fractionated and continuous radiotherapy treatments

6.1. Introduction.

The concept of general equivalence between fractionated treatment schedules and also between continuous schedules has been discussed in chapters 4 and 5 (Deehan & O'Donoghue, 1988, 1991). Although absolute general equivalence conditions can be derived for fractionated treatments which could be used in many practical cases, the same is not true for continuous treatments. In the latter case although the α/β ratio could be eliminated from calculations, the sublethal damage repair time constant, μ , remained. "Near" equivalence was possible in some limited cases when treatment times were less than 2.58 minutes or more than 8.5 hours (limited by the values of μ chosen for tumour and late responding tissues respectively, see figure 5.1(a) and (b) and sections 5.2.1(a) and (b)).

The purpose of this chapter is to discuss general equivalence between fractionated and continuous treatments. It will be shown that once again true general equivalence is not possible but that "near" general equivalence can be achieved assuming the treatment time restrictions indicated above. These results are also placed in context with the two earlier chapters on this subject to produce for the first time an overall picture of equivalence between radiotherapy treatment schedules from which the Liversage relationship (Liversage, 1969(a); Dale, 1985) emerges as a special case.

6.2. Equivalence conditions between fractionated and continuous schedule.

Beginning with the ERD relationships for fractionated and continuous treatments:

Fractionated (from equation (2.18))

$$ERD = Nd(1+d/(\alpha/\beta))$$

Where N is the fraction number and d is the dose per fraction.

Continuous (from equation (2.17))

$$ERD = NRT(1+(2R/(\alpha/\beta)\mu)(1-(1/\mu T))(1-EXP(-\mu T))))$$

Where N, R and T are the fraction number, the dose rate and treatment time respectively.

In these factors α/β and μ (the sublethal damage repair time constant) are tissue parameters (Dale, 1985) which have been defined in earlier chapters (see chapter 2, section 2.4.1. and section 2.4.2.). Using the properties of the ERD we can investigate the equivalence conditions between fractionated and continuous radiotherapy treatments in a way similar to that in which the subject of equivalence was addressed in the two previous chapters.

6.2.1. Fractionated and continuous schedules with fraction number equal to one.

If we consider a fraction of high dose rate treatment of dose d and a continuous treatment with dose rate R and treatment time T these will be equivalent if their ERDs are equal.

ie
$$ERD_{(fract)} = ERD_{(cont)}$$

$$d(1+d/(\alpha/\beta)) = RT(1+(2R/(\alpha/\beta)\mu)(1-(1/\mu T)(1-EXP(-\mu T))))$$

Expanding this gives:

$$d + d^2/(\alpha/\beta) = RT + (1/(\alpha/\beta))(2R^2 T/\mu)(1-(1/\mu T)(1-EXP(-\mu T))))$$

Equivalence conditions which are independent of the α/β ratio can be found for these two treatments by equating the coefficients for the total dose and $1/(\alpha/\beta)$ terms, that is the A and B type damage terms.

These conditions are:

$$d = RT \text{ -----(6.1)}$$

and
$$d^2 = (2R^2 T/\mu)(1-(1/\mu T)(1-EXP(-\mu T)))) \text{ -----(6.2)}$$

substituting (6.1) into (6.2) gives:

$$d = (2R/\mu)(1-(1/\mu T)(1-EXP(-\mu T)))) \text{ -----(6.3)}$$

This is not of course a general equivalence relationship because μ is still present in equation (6.3) and this is a tissue specific parameter so only specific equivalence is possible. To proceed further three different treatment time regions (values of T) must be considered. It will be assumed that the treatment times for the fractionated schedules in this chapter are of the order of 45 seconds (see appendix 5A) and that treatment time thresholds therefore refer to the continuous treatment times only. These are chosen

using the same reasoning as in chapter 5 (sections 5.2.1(a),(b) and (c)) where they have been identified as regions of interest in radiotherapy treatments.

6.2.1(a). Treatment time $T < 0.043$ hr (ie $T < 2.58$ mins).

In this region $(1 - (1/\mu T)(1 - \text{EXP}(-\mu T)))$ approaches $\mu T/2$ to within 2% (see section 5.2.1(a) and figure 5.1(a)). Equation (6.3) becomes:

$$d = R T$$

Provided the dose is equal then the two single fractions are equivalent as long as the treatment time for continuous exposure, T is less than about 2.58min. This result is consistent with the equivalence conditions derived for fractionated and continuous radiotherapy in chapters 4 and 5 (Deehan & O'Donoghue, 1988, 1991).

6.2.1(b) Treatment time $T > 8.5$ hr.

In this case the term $(1 - \text{EXP}(-\mu T))$ approximates to unity to within 2% (see section 5.2.1(b) and figure 5.1(b)). Equation (6.3) becomes:

$$d = 2R(1 - 1/\mu T)/\mu$$

No single high dose rate fraction can be equivalent in all tissue effects to a continuous treatment with $T > 8.5$ hrs.

6.2.1(c) Treatment time 0.043 hr $< T < 8.5$ hr.

In this case μ cannot be eliminated from equation 6.3 making general equivalence impossible even though the α/β ratio has been removed.

Therefore for any single fractionated treatment, no single continuous treatment exists which gives equivalent effects for all tissues. General equivalence is not possible between single fractionated and continuous treatments (ie when both fraction numbers equal 1), and only in one special case where treatment time is less than about 2.58 minutes is "near" equivalence possible.

6.3. Regimes of fractionated and continuous treatments.

Can general equivalence exist between regimes of fractionated and continuous treatments ?

Let a fractionated treatment consist of r fractions:

$$d_1 + d_2 + d_3 + \dots + d_r = \sum_{i=1}^{i=r} d_i$$

Let a continuous schedule consist of k treatments:

$$R_1 \cdot T_1 + R_2 \cdot T_2 + R_3 \cdot T_3 + \dots + R_k \cdot T_k = \sum_{i=1}^{i=k} R_i \cdot T_i$$

As in chapters 4 and 5 using the additive property of the ERD (Dale 1986) it follows that for equivalence between these two sequences.

$$\sum_{i=1}^{i=r} ERD_{(fract)i} = \sum_{p=1}^{p=k} ERD_{(cont)p}$$

$$\sum_{i=1}^{i=r} d_i (1 + d_i / (\alpha / \beta))$$

$$= \sum_{p=1}^{p=k} R_p T_p (1 + (2R_p / (\alpha / \beta) \mu) (1 - (1 / \mu T_p) (1 - \text{EXP}(-\mu T_p))))$$

General equivalence is possible between these treatments if the coefficients for A and B type damage terms are equal. The conditions for these are:

$$\sum_{i=1}^{i=r} d_i = \sum_{p=1}^{p=k} R_p T_p$$

and

$$\sum_{i=1}^{i=r} d_i^2 = \sum_{p=1}^{p=k} 2R_p^2 T_p (1 / (\mu)) (1 - (1 / \mu T_p) (1 - \text{EXP}(-\mu T_p)))$$

In common with the case of single treatments true general equivalence is not possible because although the α/β ratio has been eliminated from the conditions μ remains. However once more "near" equivalence situations can be identified.

If the fractionated schedule has fraction number N and dose per fraction d (ie we assume the fractionated schedule to be homogeneous , $d_1 = d_2 = d_3 = \dots \dots \dots d_r$) then:

$$Nd = \sum_{p=1}^{p=k} R_p T_p \text{-----}(6.4)$$

and

$$Nd^2 = \sum_{p=1}^{p=k} 2R_p^2 T_p (1/(\mu))(1 - (1/\mu T_p)(1 - \text{EXP}(-\mu T_p))) \text{ -----(6.5)}$$

dividing (6.5) by (6.4) we obtain:

$$d = \frac{\sum_{p=1}^{p=k} 2R_p^2 T_p (1/(\mu))(1 - (1/\mu T_p)(1 - \text{EXP}(-\mu T_p)))}{\sum_{p=1}^{p=k} R_p T_p} \text{ -----(6.6)}$$

Substituting 6.6 into 6.5 gives:

$$N = \frac{\left(\sum_{p=1}^{p=k} R_p T_p \right)^2}{\sum_{p=1}^{p=k} 2R_p^2 T_p (1/(\mu))(1 - (1/\mu T_p)(1 - \text{EXP}(-\mu T_p)))} \text{ -----(6.7)}$$

Equation (6.7) is a general expression which can be used to derive equivalence relationships between fractionated high dose-rate treatments and continuous treatments and from which the Liversage equation (Liversage, 1969(a)) emerges as a special case when $k=1$ (Deehan & O'Donoghue, 1991).

ie:

$$N = \mu T / (2(1 - (1/\mu T)(1 - \text{EXP}(-\mu T))))$$

(Liversage 1969, Dale 1985)

Equation (6.6) is the corresponding expression for dose per fraction (Table 6.1 (Fract. plus cont. schedules) contains an even more generalised form of equation 6.7 of which the Liversage equation is again a special case).

6.3.1(a) For $T < 2.58$ min the term $(1 - (1/\mu T)(1 - \text{EXP}(-\mu T)))$ tends towards $(\mu T)/2$ to within 2% (section 5.2.1(a)). Equations (6.6) and (6.7) reduce to:

$$d = \frac{\sum_{p=1}^{p=k} R_p^2 T_p^2}{\sum_{p=1}^{p=k} R_p T_p} \text{-----(6.8)}$$

$$N = \frac{\left(\sum_{p=1}^{p=k} R_p T_p \right)^2}{\sum_{p=1}^{p=k} R_p^2 T_p^2} \text{----(6.9)}$$

If $R_p:T_p$ is homogeneous (ie $R_1 = R_p$ and $T_1 = T_p$) then the only solutions of (6.8) and (6.9) are:

$$d = R_p T_p \quad \text{and} \quad N = k$$

That is the number of fractions and the dose per fraction have to be equal. As in 6.2.1(a) for single treatments, the only variations possible are those of actual dose rate and treatment time but keeping the total dose per fraction constant.

6.3.1(b) For $T > 8.5\text{hr}$ the term $(1-\text{EXP}(-\mu T))$ in equations (6.6) and (6.7) approaches unity to within 2% (see section 5.2.1(b)) and the solutions are:

$$d = \frac{\sum_{p=1}^{p=k} 2R_p^2 T_p (1/(\mu))(1-(1/\mu T_p))}{\sum_{p=1}^{p=k} R_p T_p} \text{-----(6.10)}$$

$$N = \frac{\left(\sum_{p=1}^{p=k} R_p T_p \right)^2}{\sum_{p=1}^{p=k} 2R_p^2 T_p (1/(\mu))(1-(1/\mu T_p))} \text{-----(6.11)}$$

Even near equivalence is impossible since μ is still in the equations.

6.4. Mixed Schedules of Fractionated and Continuous Treatments.

Equations (6.6) and (6.7) can be rewritten as :

$$d = \frac{\sum_{p=1}^{p=k} 2R_p T_p S_p (1/(\mu))}{\sum_{p=1}^{p=k} R_p T_p} \text{-----(6.12)}$$

$$N = \frac{\left(\sum_{p=1}^{p=k} R_p T_p \right)^2}{\sum_{p=1}^{p=k} 2R_p^2 T_p S_p (1/(\mu))} \text{-----(6.13)}$$

Where $S_p = (1 - (1/\mu T_p)(1 - \text{EXP}(-\mu T_p)))$

Now $\sum_{p=1}^{p=k} 2R_p^2 T_p S_p (1/(\mu))$ can be expressed as:

$$\sum_{p=1}^{p=a} 2R_p^2 T_p S_p (1/(\mu)) + \sum_{p=(a+1)}^{p=b} 2R_p^2 T_p S_p (1/(\mu))$$

Where $a + b = k$

$$\sum_{p=1}^{p=a} 2R_p^2 T_p S_p (1/\mu) + \sum_{f=1}^{f=g} N_f d_f^2 \quad (\text{using equation (6.5)})$$

and similarly with $\sum_{p=1}^{p=k} R_p T_p$

$$\sum_{p=1}^{p=a} R_p T_p + \sum_{f=1}^{f=g} N_f d_f$$

(using equation (6.11)) Then equations (6.12) and (6.13) can be used to combine fractionated and continuous schedules as follows:

$$d = \frac{\sum_{f=1}^{f=g} N_f d_f^2 + \sum_{p=1}^{p=a} 2R_p^2 T_p S_p (1/\mu)}{\sum_{f=1}^{f=g} N_f d_f + \sum_{p=1}^{p=a} R_p T_p} \quad \text{-----(6.14)}$$

$$N = \frac{\left(\sum_{f=1}^{f=g} N_f d_f + \sum_{p=1}^{p=a} R_p T_p \right)^2}{\sum_{f=1}^{f=g} N_f d_f^2 + \sum_{p=1}^{p=a} 2R_p^2 T_p S_p (1/\mu)} \quad \text{-----(6.15)}$$

This gives the equivalent high dose rate dose per fraction and the number of fractions for a combination of fractionated and continuous schedules. Equation (6.15) is the Liversage equation once again extended to include both fractionated high dose rate and continuous treatments. Table 6.1 shows the relationships which have been established in this chapter. Notice that these do not rely at all on the α/β ratio but can be calculated with only the value of μ the sublethal damage repair time constant. Examples of the use of these relationships are given in the appendix.

Equivalent Dose per Fraction (Gy)	Fractionated schedules	Fractionated plus continuous schedule	Continuous schedule	Single continuous schedule
d	$\frac{\sum_{f=1}^{f=g} N_f d_f^2}{\sum_{f=1}^{f=g} N_f d_f}$	$= \frac{\sum_{f=1}^{f=g} N_f d_f^2 + \sum_{p=1}^{p=a} 2R_p^2 T_p S_p (1/(\mu))}{\sum_{f=1}^{f=g} N_f d_f + \sum_{p=1}^{p=a} R_p T_p}$	$= \frac{\sum_{p=1}^{p=a} 2R_p^2 T_p S_p (1/(\mu))}{\sum_{p=1}^{p=a} R_p T_p}$	$= 2RS(1/(\mu))$
Equivalent Fraction Number	$= \frac{\left(\sum_{f=1}^{f=g} N_f d_f \right)^2}{\sum_{f=1}^{f=g} N_f d_f^2}$	$= \frac{\left(\sum_{f=1}^{f=g} N_f d_f + \sum_{p=1}^{p=a} R_p T_p \right)^2}{\sum_{f=1}^{f=g} N_f d_f^2 + \sum_{p=1}^{p=a} 2R_p^2 T_p S_p (1/(\mu))}$	$= \frac{\left(\sum_{p=1}^{p=a} R_p T_p \right)^2}{\sum_{p=1}^{p=a} 2R_p^2 T_p S_p (1/(\mu))}$	$= \frac{\mu T}{2S}$

Where $S_p = (1 - (1/\mu T_p)(1 - \text{EXP}(-\mu T_p)))$

Table 6.1 Equivalence relationships

6.5. Appendix 6.1 Worked examples.

Example 1. In the course of two continuous radiotherapy treatments a point in tissue receives:

1) 40 Gy from a treatment using a dose rate of .5 Gy/hr with a treatment time of 80 hours.

2) 20 Gy from a treatment using a dose rate of 1 Gy/hr with a treatment time of 11.43 hours.

What high dose rate fractionated schedules are equivalent to these two treatments combined, for acute effects ($\mu = 1.54 \text{ hr}^{-1}$) and for late effects ($\mu = .46 \text{ hr}^{-1}$) ?

Using equations (6.12) and (6.13) $k = 2$

Acute effects

$$d = .77 \text{ Gy}$$

$$N = 66.5$$

Late effects

$$d = 2.4 \text{ Gy}$$

$$N = 21.1$$

Example 2. A treatment consists of two high dose rate fractionated schedules:

20 fractions of 1.6 Gy per fraction followed by 15 fractions of 2.4 Gy per fraction.

What single fractionated schedule are these equivalent to for acute and late effects?

From table 6.1 (fractionated schedules):

$$d = 2.03 \text{ Gy}$$

$$N = 33.6$$

Note that, in this example as for all high dose rate schedules, there is no need to know the values of the α/β ratio or μ ; the schedule above is equivalent for effects on all tissues to the two schedules above.

Chapter 7

Iso-effect surfaces in brachytherapy

The concept of iso-effect surfaces is introduced in the next two chapters. These are three dimensional surfaces of equal biological effect around a distribution of radioactive sources (chapters 7 and 8), or associated with an external beam treatment (chapter 8). More accurately, these are surfaces of potential biological effect as their expression is dependent on the presence of appropriate tissue. (Joslin, 1972; Kirk et al, 1973; Godden, 1988; Deehan & O'Donoghue, 1991,1994). Just as the use of iso-dose-rate or iso-dose surfaces or lines produce a more complete display of absorbed dose than point calculations, so iso-effect surfaces display effects more clearly by making the same transition.

These chapters present for the first time a rigorous and comprehensive analysis of the iso-effect surface methodology in appraising the radiobiological consequences of alterations in treatment parameters (ie dose-rate, fraction number or dose per fraction). One important conclusion which emerges is in the field of brachytherapy where it is seen that increases in dose-rate need not automatically lead to increases in morbidity in late responding tissues (chapter 7). This seems at first to contradict the predictions of others (Steel et al, 1986; Fowler, 1990) but this is only because previous work has almost exclusively been confined to effect calculations performed at single points. Iso-effect surfaces can also be used to prove that if general equivalence holds at a single point in fractionated radiotherapy then it holds at all points in the treatment zone (chapter 8).

7.1 Introduction

General equivalence has been considered in chapters 4, 5 and 6 with regard to point calculations where biological effects were compared at specific points within a dose distribution (ie in the tumour volume) produced by externally applied beams or around a distribution of radioactive sources (ie at the A point) as in brachytherapy. Although this gives an indication of how the treatments are matched at specific points, it does not give an impression of how biological effects are matched at points elsewhere. In order to obtain a more global view of the changes in biological effect as the treatment parameters are altered, it is necessary to go from a one dimensional point representation to a two or three dimensional representation.

A method is proposed here for such a representation based on surfaces (three dimensions) or lines (two dimensions) of equal effect called iso-effect surfaces. Iso-surfaces or lines have been used by others to form an overall picture of the effect map associated with a specific treatment (Kirk et al, 1973). This chapter presents for the first time a systematic application of this concept to intracavitary brachytherapy. It will be shown that treatments of different dose-rates can be compared by considering the changes that take place in the position of these iso-surfaces or lines.

7.1.1. Iso-dose or iso-dose-rate plots.

In radiation physics, the iso-dose concept is well established. By this means absorbed dose distribution around an intracavitary insertion can be clearly visualised by plotting, in two dimensions, lines of equal dose (or equal dose-rate) and these are now in routine use in many treatment planning systems (figure 7.1). Viewing the insertion in planes, for example in the anterior/posterior or lateral directions can then give valuable information about how much area is treated and the amount of sensitive tissues enclosed by high dose regions. Features of the new generation of planning computers make it possible to display three dimensional iso-dose surfaces. Regions of interest can be merged with this information and the user can then rotate the reconstruction in an interactive manner (Chaney & Pizer, 1992; Lichter et al, 1992; Hilaris et al, 1994). Just as point representation has given way to iso-dose lines or surfaces to provide a comprehensive picture of the absorbed dose distribution, it will be shown in this chapter that the transition from point effects to iso-effect surfaces proves invaluable when considering changes in effect distributions.

7.1.2. Iso-effect plots.

If iso-dose levels can be plotted around a distribution of radio-active sources, then iso-effect levels can also be plotted. A specific iso-dose plot can be taken to represent a specific level of effect by calculating the associated value of ERD, using values α/β and μ . This type of representation has been suggested in the past for external beam (Joslin, 1972; Kirk, 1973) and intracavitary insertions (Joslin, 1972; Godden, 1988) using the CRE model. However the strategy is independent of the iso-effect model used and figure 7.2 shows how this is done using the LQ approach.

This section of the thesis begins at the point where the work of Kirk (1972) and Godden (1988) ends and asks: what changes take place in the shape and position of the iso-effect surfaces when treatment parameters change? It will be shown that this knowledge is vital in predicting the outcome for example when dose-rates are altered in radiotherapy. It will be demonstrated that the study of iso-effect distributions provides a means of comparing different treatments in a way that was not previously possible (Deehan & O'Donoghue, 1991).

7.2. Changes in iso-effect distributions.

To understand why and how iso-effect distributions change, it is useful to consider a standard intracavitary insertion. Figure 7.3 shows the diagram of an insertion consisting of caesium sources which give a dose-rate of R_1 (Gy/hr) at the standard Manchester "A" point with an insertion time of T_1 (hr) given in N_1 fractions (ie a total dose of $T_1 \times R_1 \times N_1$ Gy to the "A" point). If we look at the iso-dose line which corresponds to the total dose $T_1 \times R_1 \times N_1$ then this can represent many levels of iso-effect (ie many values of the ERD) depending on the values of α/β and μ used in the calculation of the ERD. For the purposes of this argument, it is simpler initially to consider just one value of these parameters and these are shown in figure 7.3 along with the corresponding value of the ERD.

If the treatment dose-rate at point "A" changes to R_2 for example as a result of more powerful sources being used and the new treatment time T_2 is used, then the ERD value for the new schedule ($N_2:R_2:T_2$) at the "A" can be calculated using equation 2.17:

$$\begin{aligned} & \text{ERD}(A_1, N_1:R_1:T_1) \\ & = N_2 R_2 T_2 \left[1 + \left(\frac{2R_2}{(\alpha/\beta)\mu} \right) \left(1 - \frac{1}{\mu T_2} \left(1 - \text{EXP} \left(-\frac{1}{\mu T_2} \right) \right) \right) \right] \text{----- 2.17} \end{aligned}$$

(Dale 1985) and will in general be different from that calculated for the initial schedule ($N_1:R_1:T_1$) (unless a deliberate attempt is made to achieve an exact match by careful choice of the treatment parameters ($N_2:R_2:T_2$)). This does not tell us very much about the overall change in ERD and although it is possible to perform the calculation at many points, it would be of interest to devise some method of determining the new position of the ERD surface that previously passed through point A for the initial insertion ($N_1:R_1:T_1$). This would reveal how much more or less effective or how much more or less damaging the new schedule is relative to the initial schedule. Since the initial ERD value now corresponds to a different dose-rate value then the position of this new iso dose-rate corresponds to the new position of the initial ERD surface. The new dose-rate value can be determined as follows:

The ERD value at point A produced by the initial schedule is:

$$\begin{aligned} & \text{ERD}(A_1, N_1:R_1:T_1) \\ & = N_1 R_1 T_1 \left[1 + \left(\frac{2R_1}{(\alpha/\beta)\mu} \right) \left(1 - \frac{1}{\mu T_1} \left(1 - \text{EXP} \left(-\frac{1}{\mu T_1} \right) \right) \right) \right] \end{aligned}$$

For the new schedule there will be a dose-rate R_N , occurring at P_N which will correspond to the same ERD value. We can write:

$$\begin{aligned} \text{ERD}(P_N, N_2:R_N:T_2) &= \text{ERD}(A_1, N_1:R_1:T_1) \\ &= N_2 R_2 T_2 \left[1 + \left(\frac{2R_2}{(\alpha/\beta)\mu} \right) \left(1 - \frac{1}{\mu T_2} \left(1 - \text{EXP} \left(-\frac{1}{\mu T_2} \right) \right) \right) \right] \end{aligned} \quad \text{----- 7.1}$$

From equation 7.1

$$\left[\left(\frac{2S_2}{(\alpha/\beta)\mu} R_N \right)^2 \right] + R_N - \left[\left(\frac{\text{ERD}(A_1, N_1:R_1:T_1)}{N_2 T_2} \right) \right] = 0 \quad \text{----- 7.2}$$

where $S_2 = (1 - 1/((\mu)T_2)(1 - \text{EXP}(-\mu T_2)))$

Equation 7.2 is a quadratic equation in R_N whose solution is:

$$R_N = \left[\frac{-1 + \left(1 + \frac{(4S_2 \text{ERD}(A_1, N_1:R_1:T_1))^{1/2}}{(\alpha/\beta)\mu N_2 T_2} \right)}{\left(\frac{4S_2}{(\alpha/\beta)\mu} \right)} \right] \quad \text{----- 7.3}$$

(the negative root being rejected). If the location of all points (P_N) where the dose-rate equals R_N can be determined then the position of the new iso-effect surface in space

is also known. The position will in general be different from that corresponding to the initial schedule.

In the next section a method is described which can be used to determine the direction and magnitude of the spatial displacement of surfaces. It will be seen that this approach is useful in indicating changes in effect distributions as the treatment dose-rate is altered in brachytherapy. This method will be checked against the theoretical predictions of the Liversage equation (Liversage, 1969(a); Dale, 1985).

7.3. Method for calculating the magnitude and direction of iso-effect surface movement.

In the argument that follows two aspects have to be distinguished clearly when insertions are compared in this way. These are:

a) Radiobiological factors which arise solely as a result of variations in dose rate caused by changes in the activity of the radioactive sources.

b) Geometrical factors related to the differences in source position between insertions which in any practical situation must always be considered when such comparisons are made.

In order to develop the idea of iso-effect surfaces, it is helpful initially to exclude difference caused by geometrical factors above and concentrate on the changes associated with biological factors alone. As will be discussed later in this chapter, changes in geometry can easily be included in practical situations.

To calculate the magnitude and direction of iso-effect surface movement it is necessary to derive an expression which relates displacement along a line extending outwards from an insertion to dose-rate. This is because a specific iso-effect surface (value of ERD) can be associated with a single value of dose-rate and this in turn with a

specific position in space. If the position where specific values of dose-rate occur can be calculated, then the initial and final positions of the ERD surface can be found giving the magnitude and direction of the movement of the iso-effect surface. It is therefore necessary to derive a relationship between distance and dose-rate and this is done in the following section.

7.3.1. The relationship between distance and dose-rate.

If we return to the example of an insertion shown in figure 7.3 then it is possible to plot for given source activities the dose-rate along a line PP' running from the "P" point out through the "A" point as defined in the Manchester system. Because insertions are so often compared with the Manchester low dose-rate standard a useful starting point is to suppose that the source activities result in a dose-rate of 0.5 Gy/hr at point "A". From these data points it is possible to express distance (X) as a function of dose-rate (R) using an exponential function of the form:

$$X = f_n(R) = 8.5 \times \text{EXP}(-17R) + 6.3 \times \text{EXP}(-4.2R) + 2 \times \text{EXP}(-0.64R) \text{ ----- } 7.4$$

The above function was chosen to be used in this thesis because it achieved the best fit to actual calculated data at distances of 2cm or greater from point P, along the line PP'. Calculated data were obtained using standard insertion geometry and source strengths, generated from an IGE Data General planning computer. Figure 7.4 shows a plot of the computer calculated data compared with that obtained using equation 7.4; the agreement is excellent and the data points in each case fall on the same line.

Equation 7.4 therefore allows the position associated with a specific dose-rate value to be obtained along the line PP'.

If the source activities are now altered so that the dose-rate at the "A" point changes from 0.5Gy/hr to R₂ while keeping the same source geometry, then the ratio of the old and new dose-rates at point "A" will be (0.5/R₂). This scale factor may be used in equation 7.4 applied to an insertion with different source strength, provided the dose-rate at the "A" point (R₂) is known and the insertion geometry is identical. It is now possible to rewrite equation 7.4 as:

$$\begin{aligned}
 X = & 8.5 \times \text{EXP}(-17(0.5/R_2)R_N) + 6.3 \times \text{EXP}(-4.2(0.5/R_2)R_N) \\
 & + 2 \times \text{EXP}(-0.64(0.5/R_2)R_N) \text{ ----- } 7.5
 \end{aligned}$$

Where R_N is the dose-rate at some point along the line PP' corresponding to an insertion which has a dose-rate of R₂ at the A point.

Equation 7.5 can now be used to determine the position of R_N (calculated from equation 7.3.) the dose-rate associated with the new position of ERD((A₁),N₁:R₁:T₁). Using equations 2.17 and 7.3 -- 7.5 the magnitude and direction of iso-surface movement can be determined.

7.3.2. Variation of ERD along the line PP' for different schedules.

To understand how iso-effect surfaces move when treatment parameters change, it is useful to consider how the ERD changes with distance in a particular direction around a distribution of radio-active sources (Deehan & O'Donoghue, 1994). If the variation in total dose is known along a line, for example PP' then using the LQ model the corresponding variation in ERD along that line can be plotted. This has been done in figures 7.5 and 7.6 for various HDR schedules and a reference LDR schedule of 1 fraction of 30Gy (to point A) given at a dose-rate of 0.5Gy/hr ($T = 60$ hr).

Figure 7.5 shows ERD plots corresponding to tumour responses. In this figure it is assumed that the HDR dose-rate at point A is 150Gy/hr and that the total dose delivered to point A is the same for both HDR and LDR, so that no dose correction factor is applied when going from LDR to HDR in this case. As the fraction number is increased the plots move towards the LDR plot but even with a fraction number of 6 the HDR plot still has a steeper gradient than the LDR plot. In addition to which the HDR schedules have a greater ERD value and at every point along PP'. A similar trend is seen with late responses shown in figure 7.6 for the same schedules. If the total dose is kept constant, then the only time the HDR and LDR plots coincide is when the fraction number at HDR equals that set by the Liversage equation (1969(a)) (see section 7.4) for equivalence (see appendix 7.1). HDR fraction numbers less than this will always lead to a greater ERD value than at LDR for the same total dose.

However as we will see later in this chapter the fraction numbers predicted by the Liversage relationship for matching of tumour or late effects are so large as to be well outside of the range that would be regarded as practical. Centres which have changed successfully from LDR to HDR use fairly modest fraction numbers of between 4 and 6

(Fowler, 1990; Joslin, 1990, Orton, 1991; Stitt et al, 1992, Patel, 1994) as well as a reduction in total dose of typically between 20% to 30%. This reduction of total dose has the effect of moving the HDR plot downwards towards the distance axis and at the same time producing little change in the overall shape of the plot. This is easy to show by plotting HDR curves corresponding to different values of total dose reduction which will begin to cross the LDR plot at some point. This is shown for tumour in figure 7.7. The greater the dose reduction the sooner the cross over or, match point, occurs along the line PP' as can be seen from figure 7.7. This is because the HDR plots drop down towards the distance axis and because the gradient of the HDR plot is still greater than that of the LDR reference plot. At the match point the ERD values for LDR and HDR must be equal. Representative plots for late effects are shown in figure 7.8.

In practice dose reductions appear to be chosen in a fairly arbitrary way although early figures seem to be derived from power function iso-effect models such as the CRE or TDF (Joslin, 1990). Figures 7.7 and 7.8 are representative of the situation which arises in clinical practice (Fowler, 1990; Joslin, 1990; Orton, 1991; Patel, 1994), that is a total dose reduction at HDR which leads to the HDR and LDR plots crossing within at most a few centimetres of the P point. The rest of this chapter will therefore be devoted to examining the consequences of this situation. Although the argument will be developed with reference to the transition between LDR and HDR schedules the reasoning and conclusions are just as applicable to the transition between LDR and MDR schedules.

Figure 7.9 shows plots of ERD versus distance for an LDR and an HDR insertion along the same line as in figures 7.5 to 7.8. Here the results are shown in a diagrammatic representation and differences have been somewhat enlarged to illustrate the argument.

Displaying the effect curves in this way shows some typical features, these are:

1) The two curves cross at some point "M", where the effects are matched. The justification for this statement lies in the fact that frequently when an alternative to a known schedule is chosen it is done in such a way as to deliberately produce a matching of effects at some point of interest. Alternatively it is common to find that ERD plots of schedules of different dose-rates which are reported in the literature as being similar in their effects do in fact cross at some point (often within centimetre or two of the "A" point). This last finding, shown later in chapter 9 where actual examples are described, is perhaps not surprising, since schedules producing similar clinical effects would be expected to show some degree of matching.

2) At distances smaller than "M" a level of effect expected at "a" for LDR would now appear at a greater distance "b" for HDR. The iso-effect surface which included point "a" at LDR has now moved outwards to include point "b" at HDR.

3) At distances greater than "M" a level of effect expected at "c" for LDR would now be expected at the shorter distance of "d" for HDR. The iso-effect surface which included point "c" at LDR has now moved inwards to include point "d" at HDR.

Iso-effect surfaces occurring before the match point move outwards when going to HDR and those occurring beyond the match point move inwards. This arises because of the relative steepness of the ERD plots and the fact that they cross at some point. When plots are repeated using different values of the α/β ratio and μ a similar pattern emerges with the match point in a different position. Similar findings have been reported by Dale and also Brenner and Hall for late tissue complications (Dale, 1990; Brenner & Hall, 1991).

Figure 7.10 illustrates the effect of varying the fraction number of the HDR schedule on the movement of iso-effect surfaces. Shown here are a number of HDR effect plots corresponding to schedules with different values of fraction number, N . As the fraction number increases, the HDR curves move towards the LDR plot resulting in a smaller movement of iso-effect surface in each case. Notice that in this diagram all curves are for convenience matched at the same point "M"; in practice this can be achieved by choosing a suitable value of the dose per fraction in each case. Figures 7.9 and 7.10 display in a qualitative way the direction of movement of iso-effect surfaces. To find out exactly how much movement is involved, it is necessary to solve equations 7.3 and 7.5 for a specific example with representative values of the α/β ratio and μ .

When comparisons of intracavitary insertions are made, the two tissues of interest are usually tumour and late responding normal tissue such as rectum, bladder and bowel (Symonds, 1989; Joslin, 1990; Fowler, 1989,1990,1991; Orton, 1990,1991). In order that the radiobiological effects can be properly assessed, appropriate values of the α/β ratio and μ must be determined. Workers differ in their opinions (Fowler, 1989,1990; Dale, 1990; Orton 1990) as to the values which should be used. Values of the α/β ratio for normal late responding tissue are generally around 3Gy while for tumour a value of around 10Gy is often quoted (Fowler 1989,1990; Orton, 1990,1991). Representative values of μ are not as easy to establish from the literature and on some occasions the same value is used for tumour as late responding tissue, that is around 0.46 hr^{-1} (Fowler 1990). Some authors distinguish between tumour and late responding tissue in terms of the μ value using a value of 0.46 hr^{-1} for late responders and a value of 1.4 hr^{-1} for tumour (Dale 1990, Orton 1990, Brenner 1992). In this thesis, a distinction is made for

μ values for late responding tissue and tumour (see chapter 3, section 3.3.2) (Warmelink, 1989; Fowler, 1990; Orton, 1988, 1990, 1994; Brenner, 1992; Millar & Canney, 1993). Values used are shown in table 7.1.

7.3.4. Movement of iso-effect surfaces.

This section uses two typical treatments in order to illustrate the movement of iso-effect surfaces. A reference schedule can be defined as:

$$\text{LDR } N_1=1 : R_1 = 0.5\text{Gy/hr} : T_1 = 60\text{hr.}$$

The effect of changing to an HDR schedule can be assessed by calculating the movement of the iso-effect surfaces. A number of alternative HDR schedules are considered below, each with a dose-rate of 150Gy/hr at the "A" point but with a different fraction number and dose per fraction. Movement of iso-effect surfaces were calculated along the line PP' defined earlier.

The method used to calculate movement was as follows:

Tumour effects.

1) The dose-rate at specific points along PP' for the LDR schedule were obtained from the IGE planning computer.

2) The ERDs associated with these dose-rates were then determined using equation 2.17:

$$\text{ERD}(R_X) = N_1 R_X T_1 \left[1 + \left(\frac{2R_X}{(\alpha/\beta)\mu} \right) \left(1 - \frac{1}{\mu T_1} \left(1 - \text{EXP} \left(-\frac{1}{\mu T_1} \right) \right) \right) \right]$$

Where R_X is the dose-rate at position X.

3) At HDR and for a fraction number $N=1$, a dose per fraction was chosen to give matched tumour effects at the "A" point.

4) With the HDR schedule now defined, equation 7.3 was used to calculate the value of dose-rate (at HDR) which corresponds to each value of ERD obtained at low dose-rate.

5) Using equation 7.5 the position at which that dose-rate occurs was calculated.

6) This is the new position of the iso-effect surface and can be compared with that of the original point at LDR to obtain the magnitude and direction of the movement.

7) The process was repeated for fraction numbers of 2,4 and 6 at HDR and the results plotted in figure 7.11. The process was repeated for late effects and the results are shown in figure 7.12.

In figures 7.11 and 7.12 movement of iso-effect surface is plotted against distance along PP' . Outward movement is positive and inward movement is negative. The trends established in figure 7.9 are seen, that is, outward movement at distances shorter than the match point and inward movement at greater distances. Both sets of data show a similar pattern, that is if the fraction number increases then the movement decreases. In general tumour and late response iso-effect surfaces are displaced by different amounts at a given distance. This means that tumour and late iso-surfaces separate in going from LDR to HDR (Deehan & O'Donoghue, 1991). For tumour, figure 7.11, the movement varies between +2.5 mm at 1 cm distance and -21 mm at 8 cm if the HDR treatment is

given in 1 fraction. As the fraction number increases to 6, these movements drop to +1.3mm and -8.8 mm respectively assuming that the match point occurs in the same place. Similar displacements can be seen for late iso-effect surfaces in figure 7.12.

7.4. Liversage equation.

The results of this method can be compared with the predictions of the Liversage equation (Liversage, 1969(a)) which gives the number of fractions (and hence the dose per fraction) at HDR which would give an exact match of LDR effects for a specific value of μ . The form of the equation is:

$$N = \mu T / 2(1 - (1/\mu T))(1 - \text{EXP}(-\mu T))$$

Where N = fraction number at HDR

T = the treatment time at LDR

If the dose-rate at HDR is known, then the dose per fraction can be obtained at HDR since the total dose at LDR and HDR has to be equal in both cases. Results obtained using the Liversage relationship are summarised in table 7.2. The HDR dose-rate is taken to be 150Gy/hr and the LDR reference schedule as ($N_1=1:R_1=0.5\text{Gy/hr}:T_1=60\text{hr}$). Using the treatment parameters derived from the Liversage equation for tumour matching in the procedure for calculating the movement derived earlier should produce zero movement of the tumour iso-effect surface at all points along PP'. The same should hold for late responses if the corresponding Liversage results are used.

Iso-effect surface movement resulting from the use of treatment parameters obtained from the Liversage equation are shown in figures 7.13 for tumour effects ($\mu=1.4 \text{ hr}^{-1}$) and 7.14 for late effects ($\mu=0.46 \text{ hr}^{-1}$). These show a change to the pattern seen previously in figures 7.11 and 7.12, since the familiar cross-over point is now absent from the plots. Figure 7.13 shows the HDR schedule matched for tumour effects and as can be seen the plot of displacement runs along the zero displacement position (apart from minor fluctuations caused by rounding errors in the calculation). The plot of late response displacement shows that this is all in a negative direction.

The HDR schedule in figure 7.13 should therefore produce identical tumour effects as the LDR reference and this is indeed what the Liversage result predicts. However because of the iso-effect surface movement, we are now able to see in addition that there ought to be a lower frequency of late effects. This is because the effect surfaces have moved inwards, enclosing less tissue than at LDR. At every point the ERD levels corresponding to late responses have been reduced relative to LDR. The fraction number however falls far outside the range which could be used in practice.

Figure 7.14 shows the case where late effects are matched and this time the plot of late effect movement lies along the zero displacement line. Surfaces corresponding to tumour are all displaced in an outward direction. This would suggest a treatment with better tumour control and identical late effects as the LDR reference. Once again the fraction number is probably too high for practical use, but figures 7.13 and 7.14 serve to illustrate that results obtained by using the method in section 7.3.4. to calculate the movement of iso-effect surfaces agree with the predictions of the Liversage equation.

7.5. Conclusion.

The concept of iso-effect surfaces has been introduced in this chapter. These are surfaces of equal biological effect which can be plotted around a configuration of radioactive sources, for example an intracavitary insertion. Although iso-effect surfaces have been used in the past to plot lines of equal effect, they have been used for the first time here to study the change in effect distributions which takes place as treatment parameters change. LDR and HDR intracavitary brachytherapy insertions were used to show that the iso-effect surfaces move as the treatment dose-rate changed.

A method has been described in this chapter which allows this movement to be calculated. Plotting the movement of surfaces against distance shows how the effect distribution changes with the schedule parameters. Therefore, studying the movements of surfaces, rather than simply comparing the calculated ERD at single points, gives a clearer view of how well effects are matched in going from one insertion to another. Smaller surface movements mean better matching. The direction of the movement also reveals how more or less effective one insertion is compared to another. In this chapter movement has been plotted against distance along a line, PP', running out from the insertion from the "P" point and passing through the "A" point as defined in the Manchester system (see appendix 1A). Results obtained using this method agree with the predictions of the Liversage equation.

Although only two dimensional plots of movement are shown here, this type of analysis could be incorporated into a treatment planning computer. Three dimensional plots of iso-dose surfaces surrounding distributions of radioactive sources are now routinely available in computerised planning systems. These could be easily converted into iso-effect surfaces for one treatment dose-rate and then their new positions

displayed at another. Planning computers already exist which have the facility to merge anatomical structures such as the rectum or bladder with a 3 dimensional reconstruction of the insertion and iso-dose plots (Chaney & Pizer, 1992; Hilaris et al, 1994; Joslin, 1994; Lichter et al, 1992).

Converting the iso-dose plots to iso-effect plots is not difficult and such a display would allow direct comparison of 3 dimensional radiobiological effects at different dose-rates since iso-effect surfaces could also be superimposed onto the insertion and anatomy. It must be emphasised that the results obtained here using the LQ model are only as good as our knowledge of the tissue parameters α/β and μ . However if the values in table 7.1 are representative of tumour and late responding tissue, then the results in this chapter indicate the trends in biological effects which are involved in going from LDR to HDR.

It is not possible at present to say how far the iso-effect surfaces have to move before any significant clinical difference can be expected. This knowledge would be useful in determining optimum parameters when treatment dose-rates change. It has also been pointed out that movement of iso-effect will be affected by differences in physical geometry of insertions. As the new fraction number at HDR increases, a point may be reached where the iso-effect movement resulting from radiobiology considerations becomes small compared to that caused by changes in geometry. At this point continuing to increase the fraction number in an effort to achieve better matching may not result in significant improvement.

7.6. Appendix 7.1. Matching of ERD plots for LDR and HDR where the total dose remains constant.

Consider two schedules, one a low dose-rate reference, $N_1:R_1:T_1$ (schedule 1), and another at higher dose-rate, $N_2:R_2:T_2$, (schedule 2). If schedule 1 is replaced by schedule 2, and at the same time the total dose is kept constant, under what conditions are the ERDs equal ?

These will be equal when:

$$N_1 R_1 T_1 \left[1 + \left(\frac{2R_1}{(\alpha/\beta)\mu} \right) \left(1 - \frac{1}{\mu T_1} \left(1 - \text{EXP} \left(-\frac{1}{\mu T_1} \right) \right) \right) \right]$$

$$= N_2 R_2 T_2 \left[1 + \left(\frac{2R_2}{(\alpha/\beta)\mu} \right) \left(1 - \frac{1}{\mu T_2} \left(1 - \text{EXP} \left(-\frac{1}{\mu T_2} \right) \right) \right) \right]$$

(using equation 2.17)

Since $N_1 R_1 T_1 = \text{Total dose} = N_2 R_2 T_2$ this reduces to:

$$R_1 \left(1 - \frac{1}{\mu T_1} \left(1 - \text{EXP} \left(-\frac{1}{\mu T_1} \right) \right) \right) = R_2 \left(1 - \frac{1}{\mu T_2} \left(1 - \text{EXP} \left(-\frac{1}{\mu T_2} \right) \right) \right)$$

$$\text{or } \frac{R_2}{R_1} = \frac{\left(1 - \frac{1}{\mu T_1} \left(1 - \text{EXP}\left(-\frac{1}{\mu T_1}\right)\right)\right)}{\left(1 - \frac{1}{\mu T_2} \left(1 - \text{EXP}\left(-\frac{1}{\mu T_2}\right)\right)\right)} \text{----- 7A.1}$$

If schedule 2 is HDR then:

$$\left(1 - \frac{1}{\mu T_2} \left(1 - \text{EXP}\left(-\frac{1}{\mu T_2}\right)\right)\right) \approx \frac{\mu T_2}{2}$$

and
$$T_2 = \frac{N_1 R_1 T_1}{N_2 R_2}$$

Substituting these into 7A.1 gives:

$$N_2 = \frac{N_1 \mu T_1}{2 \left(1 - \frac{1}{\mu T_1} \left(1 - \text{EXP}\left(-\frac{1}{\mu T_1}\right)\right)\right)}$$

this is the Liversage equation.

The only time that the ERDs are equal is when the fraction number equals that given by the Liversage equation. If the total dose is to be kept constant for both schedules then the ERD plots do not cross but do coincide when the Liversage equation is satisfied. That is the ERDs are equal not just at one point as in the case where the total dose is

reduced (see figures 7.7 and 7.8) but at all points around the insertion (for a particular value of μ).

Table 7.1 Tissue parameter values		
	Tumour	Late responses
α/β (Gy)	3	10
μ (hr^{-1})	1.40	.46

Table 7.2 ERD (Gy) values at LDR and HDR from schedules obtained using the Liversage relationship			
Manchester "A" point	LDR N=1: R=0.5Gy/hr T=60hr	HDR (tumour match) N=42.5 D=0.71Gy/fraction	HDR (late match) N=14.3 D=2.09Gy/fraction
Tumour	32	32	36
Late	51	37	51
N=fraction number: R=dose-rate: T=treatment time (hr): D=dose per fraction (Gy)			

Figure 7.1 Iso-dose rate plot around radio-active sources in an intracavitary insertion.

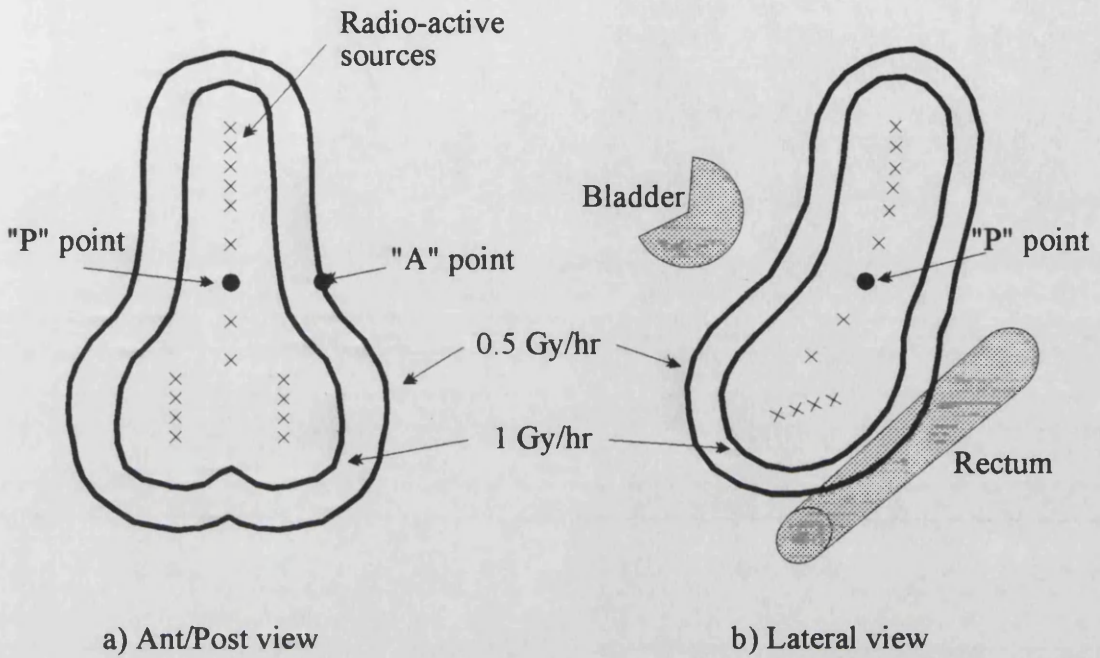


Figure 7.2 Transformation between Iso-dose distributions and Iso-effect distributions.

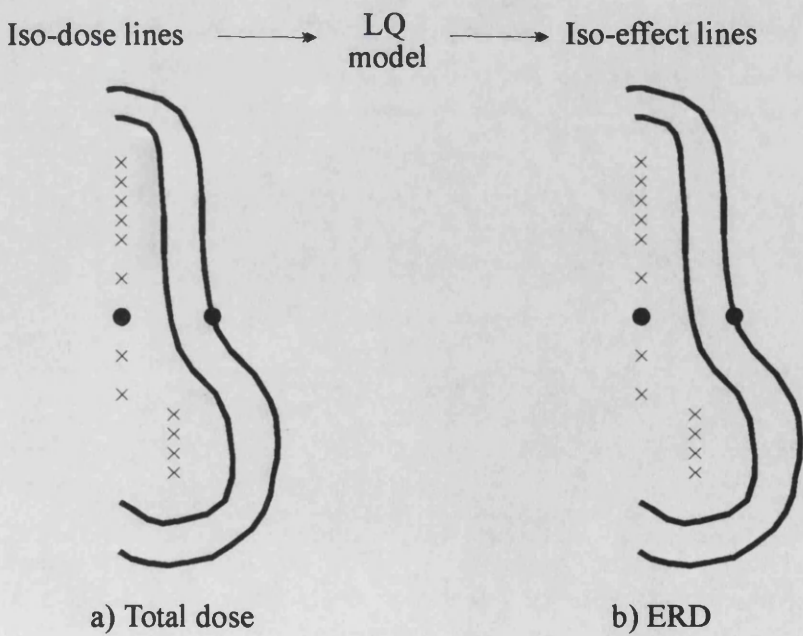
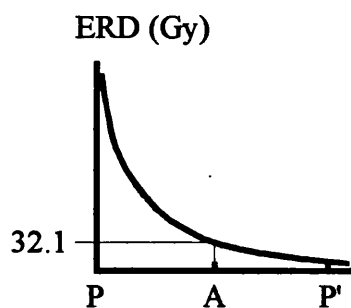
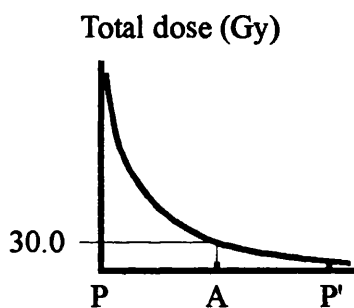
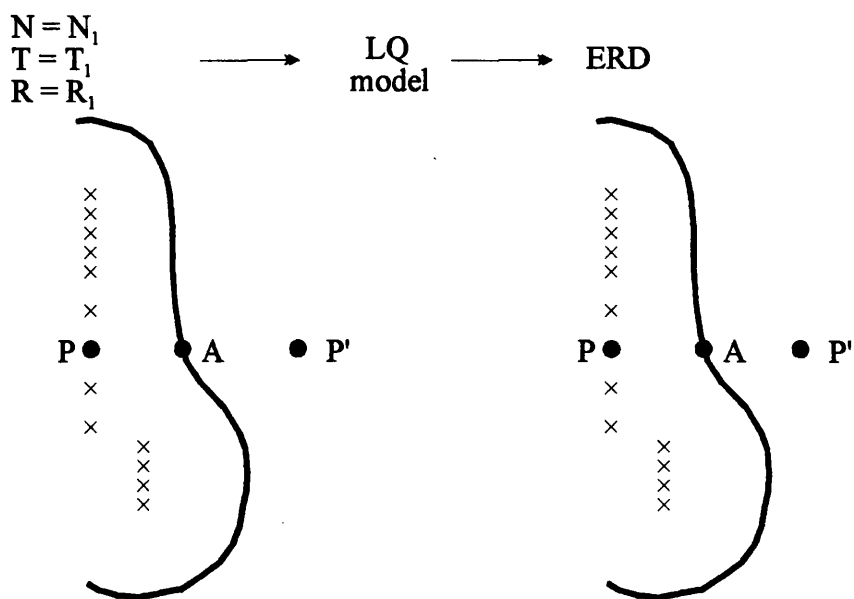


Figure 7.3



$N_1 = 1 : R_1 = 0.5 \text{Gy/hr} : T = 60 \text{ hrs}$

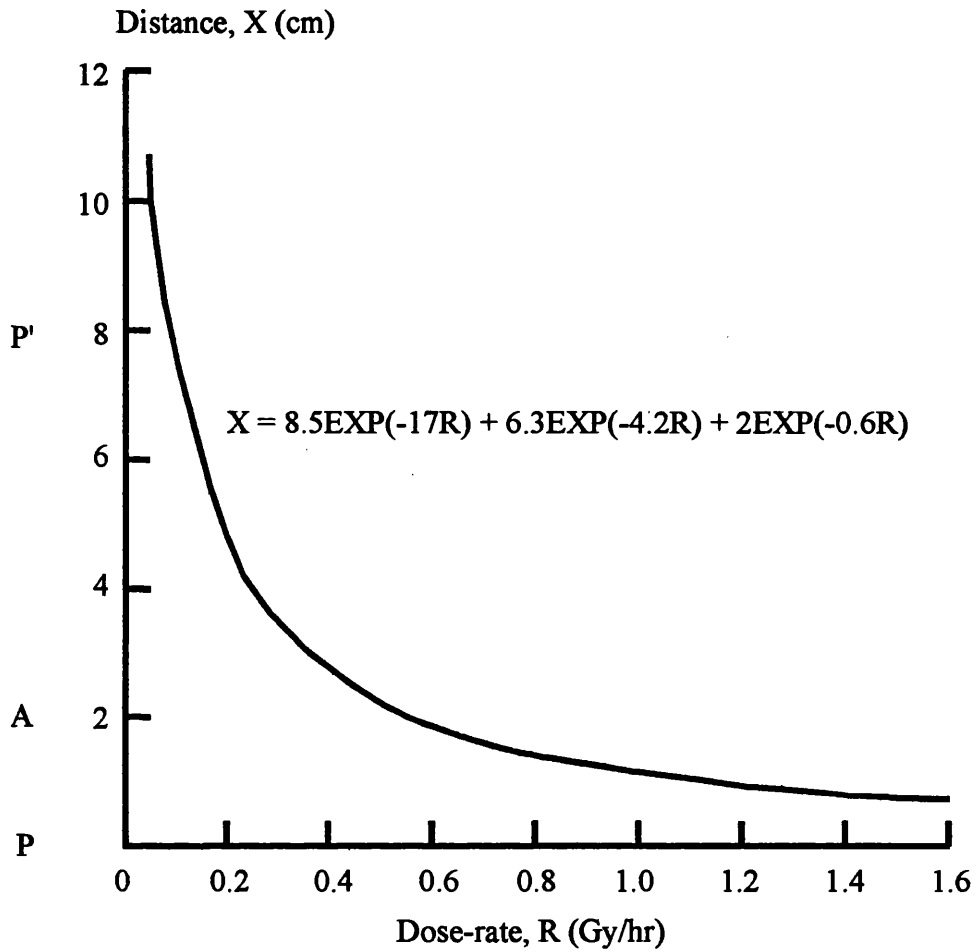
a) Total dose

b) ERD

LQ model

$30.0 \text{Gy} \longrightarrow \alpha/\beta = 10 \text{Gy} \longrightarrow 32.1 \text{Gy}$
 $\mu = 1.4 \text{hr}^{-1}$

Figure 7.4 Variation of dose-rate with distance along the line PP'. Plotted using function derived from computer generated data.



Dose-rate (Gy/hr)	Computer generated Distance (cm)	Function generated Distance (cm)
0.05	10.60	10.67
0.20	4.75	4.76
0.40	2.73	2.73
0.60	1.85	1.87
0.80	1.40	1.42
1.00	1.13	1.15
1.20	0.95	0.97
1.40	0.83	0.83
1.60	0.71	0.72

Figure 7.5 Plot of tumour ERDs for LDR and HDR schedules with the same total dose

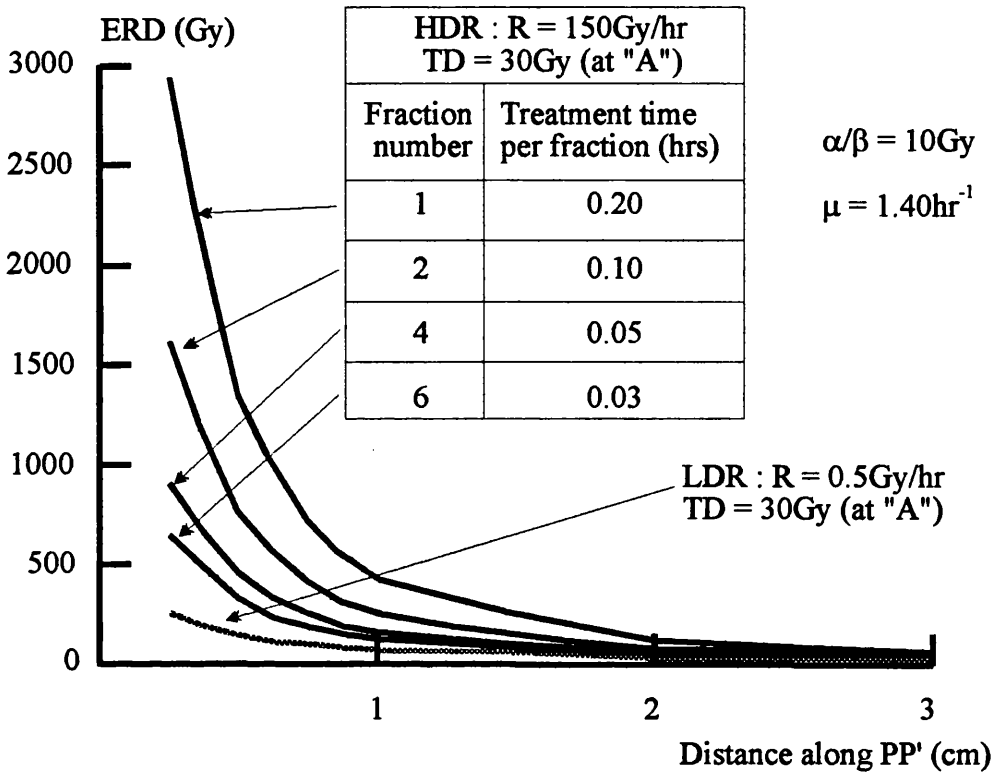


Figure 7.6 Plot of late ERDs for LDR and HDR schedules with the same total dose

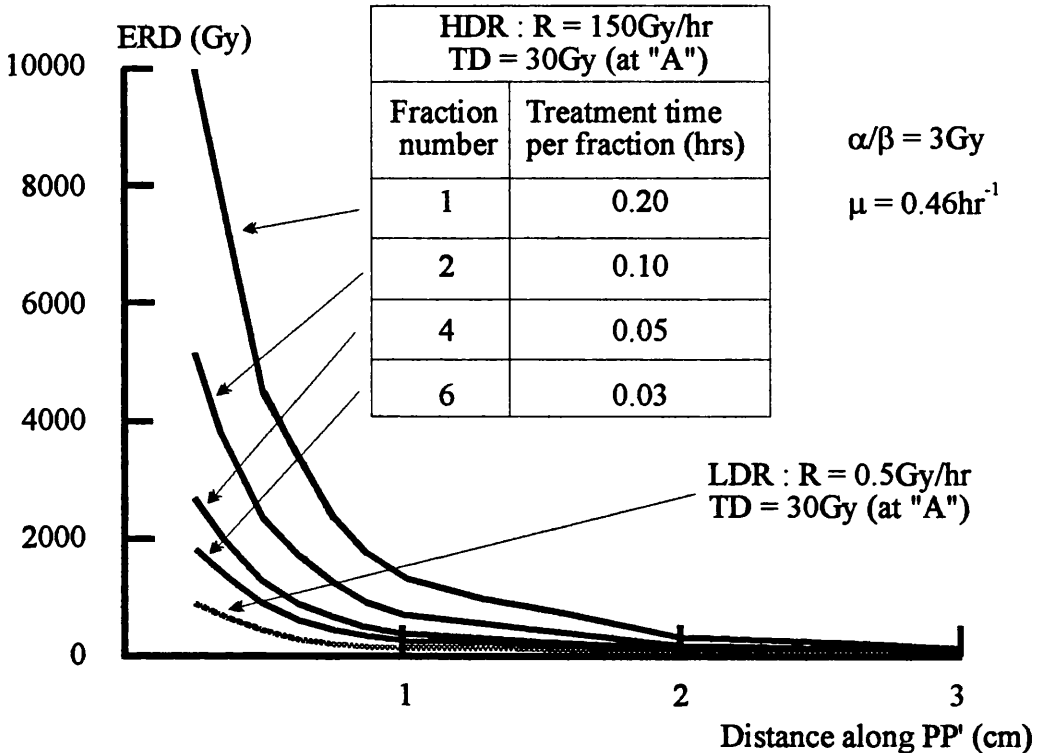


Figure 7.7 Plot of tumour ERDs for an LDR reference schedule and for HDR schedules with a fraction number of 6 and different total doses.

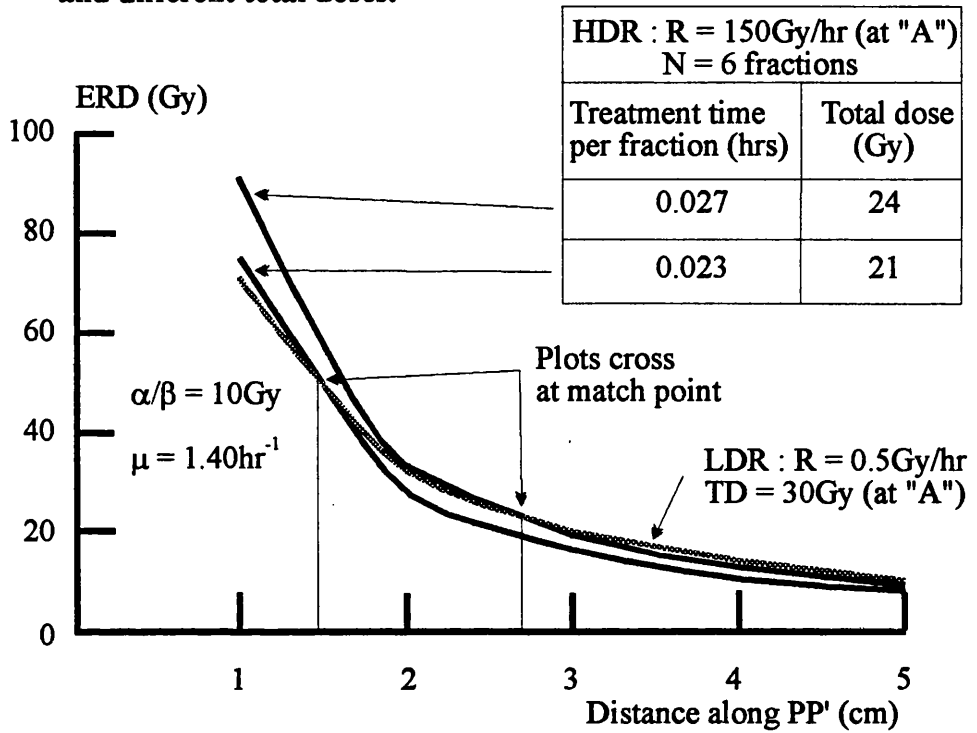


Figure 7.8 Plot of late ERDs for an LDR reference schedule and for an HDR schedule with a fraction number of 6 and a different total dose.

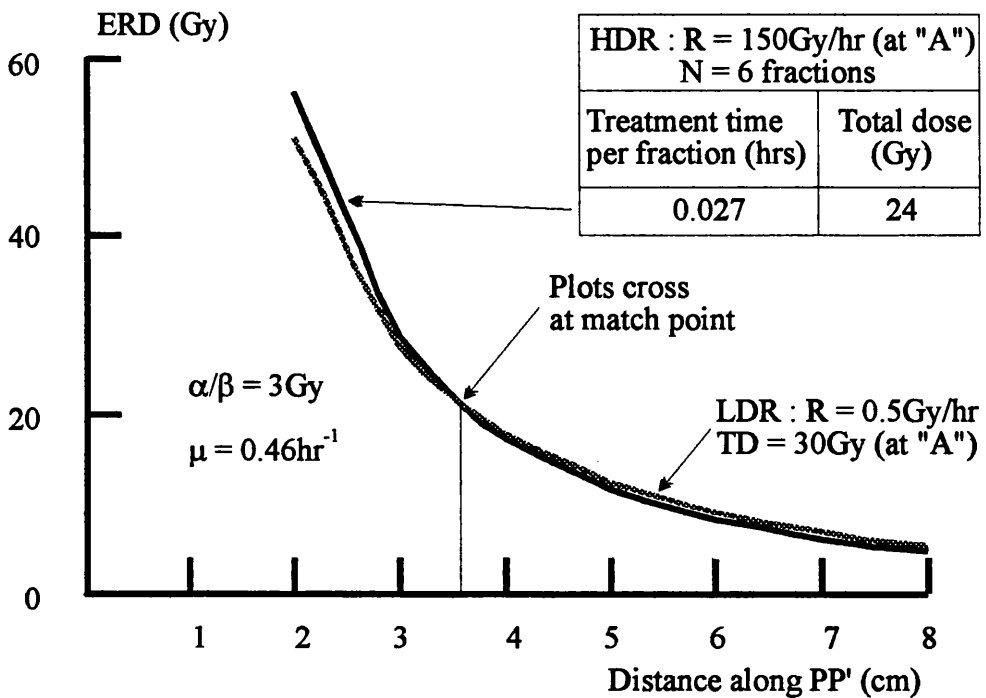


Figure 7.9 Movement of Iso-effect surfaces --- Tumour.

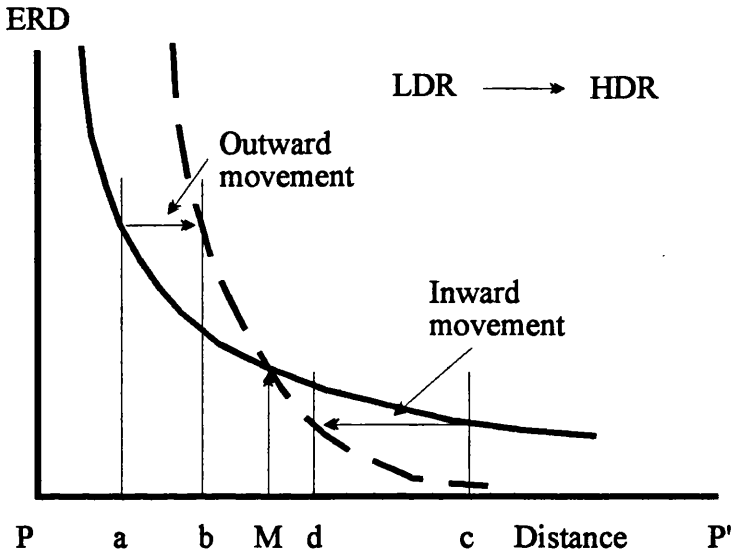


Figure 7.10 Variation of ERD plot with fraction number for HDR.

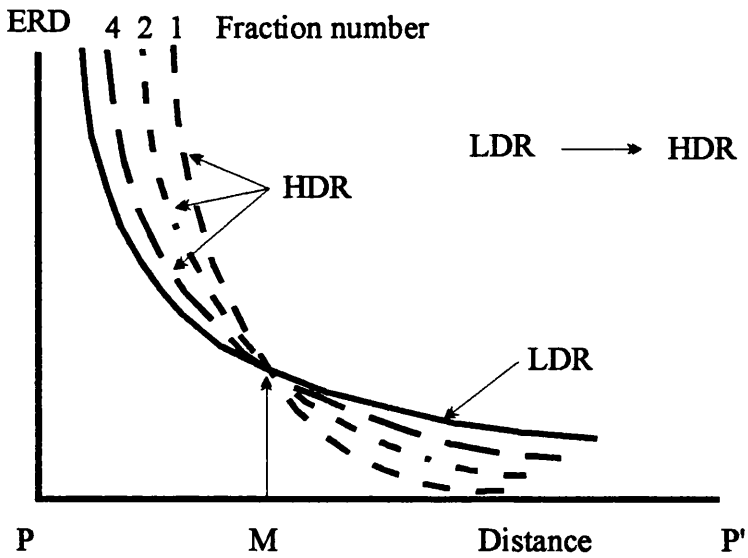


Figure 7.11 Variation of tumour iso-effect surface movement at HDR with fraction number. For all fraction numbers LDR and HDR schedules are matched for tumour effects at the Manchester A point (ie 2cm lateral to P).

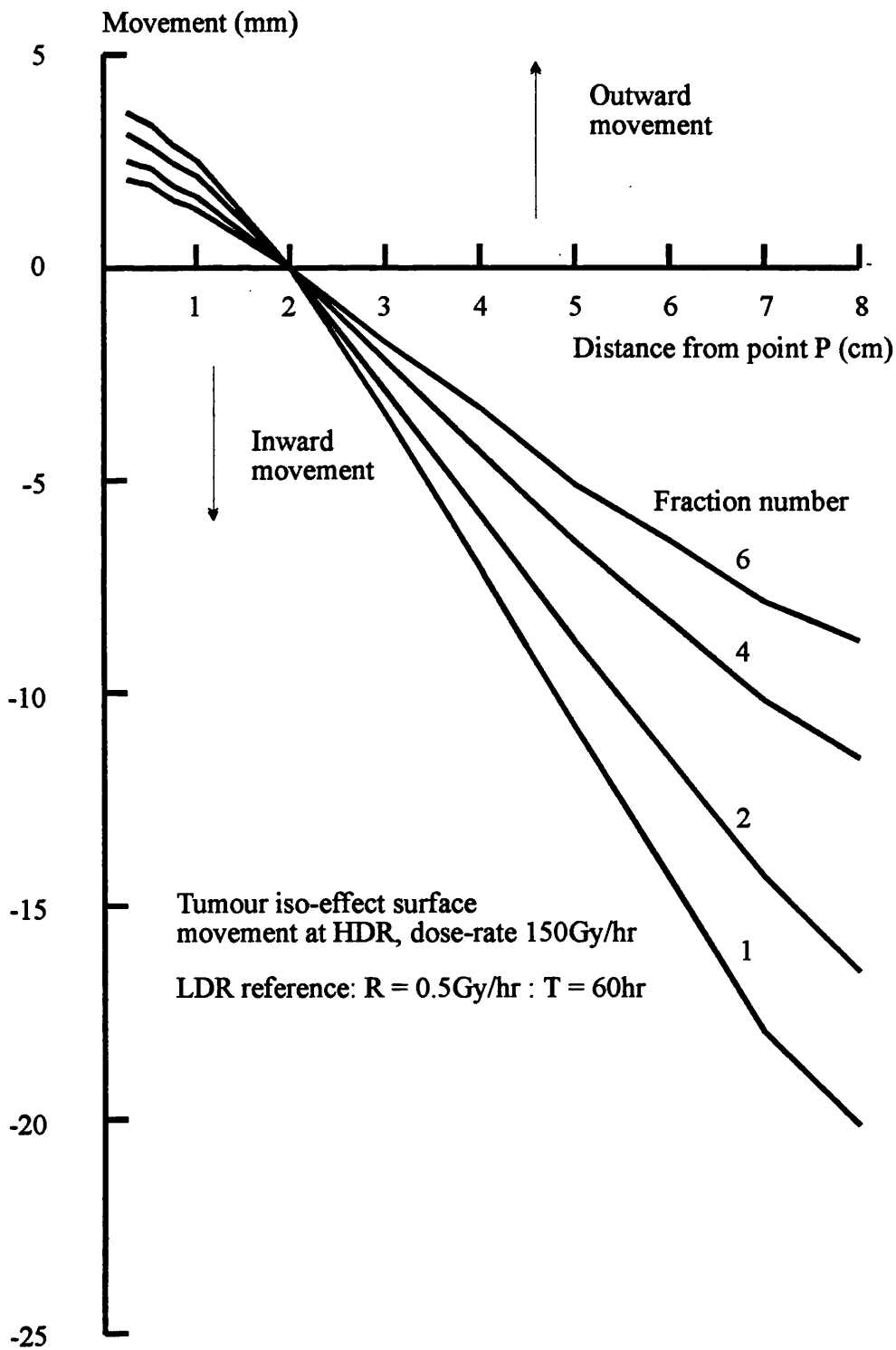
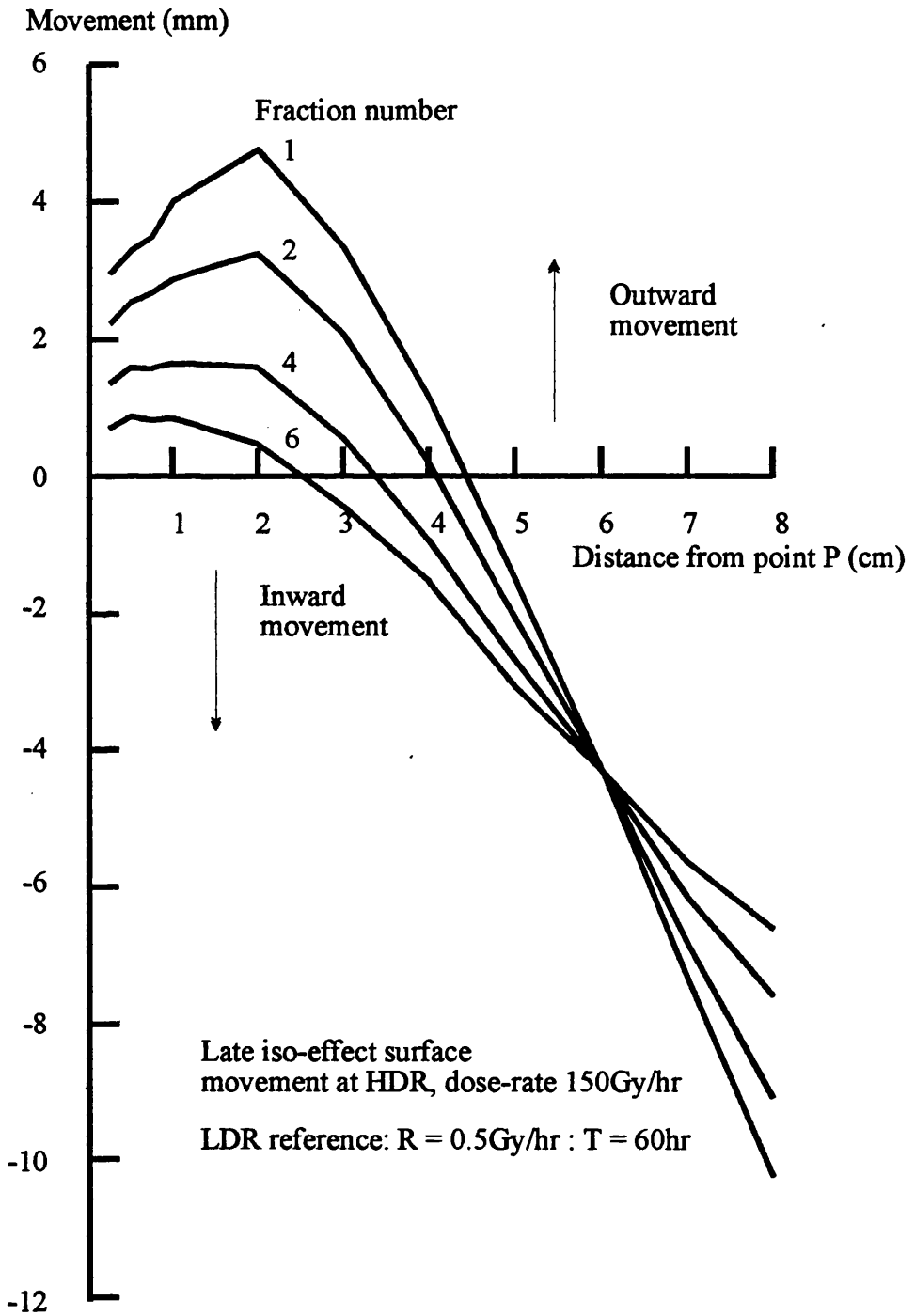
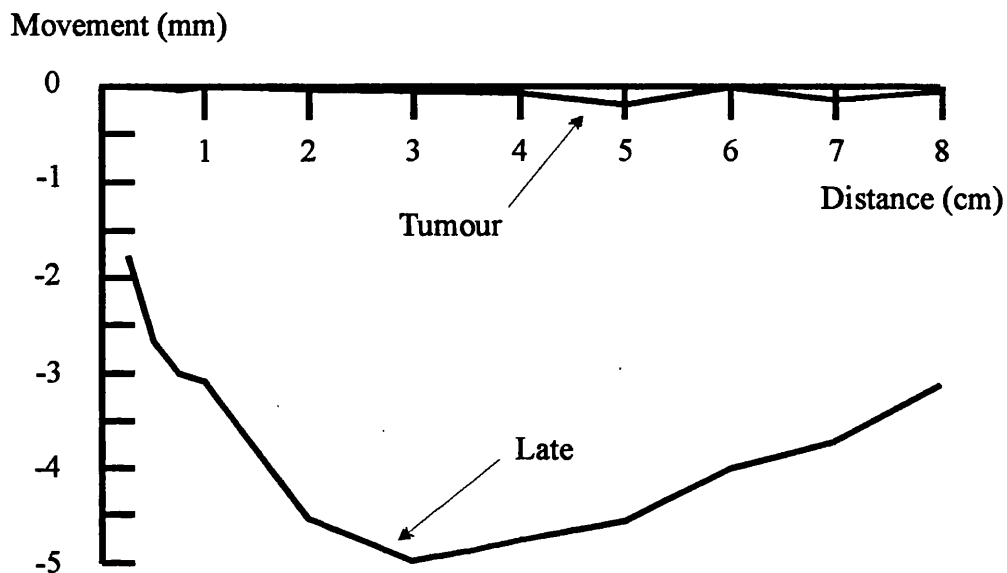


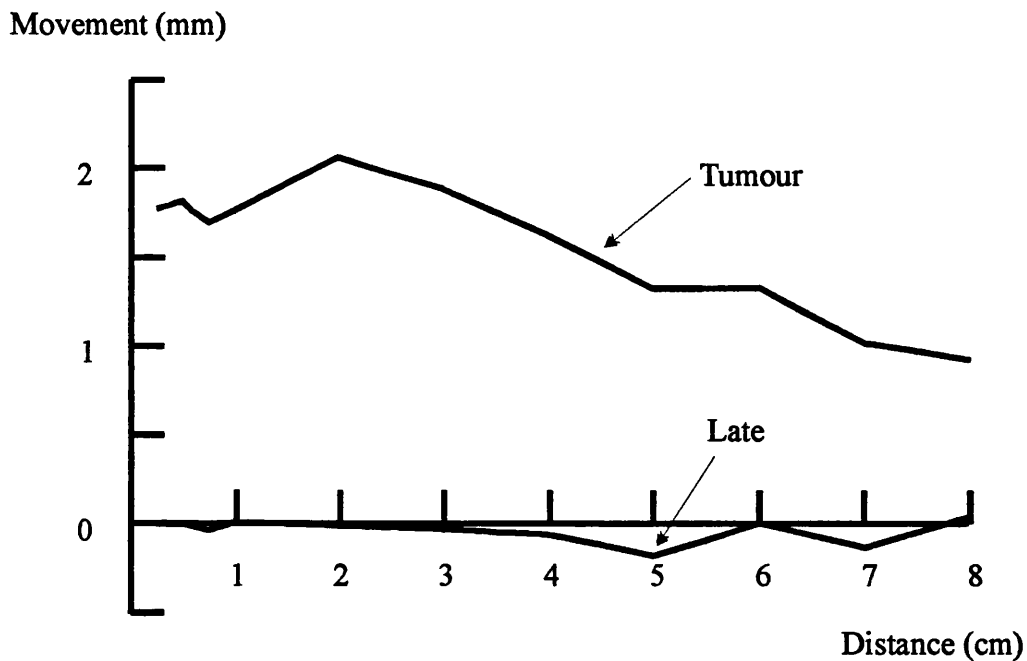
Figure 7.12 Variation of late iso-effect surface movement at HDR with fraction number. For all fraction numbers LDR and HDR schedules are matched for tumour effects at the Manchester A point (ie 2cm lateral to P see figure 7.8).



**Figure 7.13 Iso-effect surface movement for the transition between
 LDR : N = 1 : R = 0.5Gy/hr : T = 60hr and
 HDR : N = 42.5 : R = 150 Gy/hr : 0.00473hr
 Matching for tumour effects.**



**Figure 7.14 Iso-effect surface movement for the transition between
 LDR : N = 1 : R = 0.5Gy/hr : T = 60hr and
 HDR : N = 14.3 : R = 150 Gy/hr : 0.0139hr
 Matching for late effects.**



Chapter 8

The movement of iso-effect surfaces in fractionated external beam radiotherapy and changes in enclosed volume in intracavitary brachytherapy treatments.

8.1. Introduction.

It has already been shown in chapter 7 for gynaecological insertions that the consideration of iso-effect surfaces can reveal changes in the biological effect distribution. Iso-effect surfaces also show such changes in a way that point representation cannot. This chapter extends the concept to fractionated external beam treatments and examines the predictions of the general equivalence approach using iso-effect surfaces to show that the equivalence conditions derived hold not just at a point but all around the treatment volume. Changes in volume caused by the movement of iso-effect surfaces are also discussed using a standard intracavitary insertion as an example.

8.2. Total dose and effect profiles in fractionated external beam radiotherapy.

In radiotherapy, iso-dose lines can be used to display the dose distribution in a plane of interest. This is normally in the transverse plane although sagittal, coronal and even oblique displays are possible with current planning computers. Many sites are treated with external beam radiotherapy but here a simple pelvis treatment is considered using four beams which produces a high dose volume with a shape similar to a building brick. Figure 8.1 shows a transverse slice through the centre of the treatment volume. In this plan iso-dose values are normalised to the iso-centre, point "O", and the overall distribution shows the desired result with a relatively flat, high dose plateau (hot spot

2% higher than the iso-centre) and the fairly rapid drop off in dose outwards from the 95% iso-dose line.

In addition to dose distributions, effect distributions may also be derived from these plots and this has been described by Kirk et al (1973). This thesis goes on from that point to examine for the first time the changes that take place in the effects distributions when treatment schedules are altered. As a first step in this process it is useful to produce effect profiles along a line in the same way as for intracavitary insertions in chapter 7. The line chosen is in this case is "OP" which runs from the iso-centre in figure 8.1 to the posterior edge of the contour. Dose and effect levels are important along this line because it passes through the tumour volume and the position of the rectum which is known to be a radiosensitive structure. The percentage depth dose profile normalised to the iso-centre is shown in figure 8.2 and it will be assumed that a standard reference schedule of 30 fractions of 2 Gy per fraction (ie. a typical 6 week course) is to be given with this treatment. From the normalised depth dose profile the total dose (TD) profile can easily be plotted along "OP" since the reference dose of 60Gy is given to the iso-centre in this case. The total dose profile is also shown in figure 8.2. Using the total dose data from figure 8.2 and the linear quadratic (LQ) model it is possible to obtain ERD plots along the line "OP" for both tumour and late responding normal tissue effects. This was done using equation 2.18:

$$ERD = Nd(1 + d/(\alpha/\beta)) \text{ ----- } 2.18$$

where N is the number of fractions and d the dose per fraction at each point obtained from figure 8.2. A value of α/β of 10Gy was used for tumour effects and 3Gy

for late responding tissues. The ERD plots are shown in figures 8.3 (a) and (b). When tumour or late responding tissues are considered individually, different regions of the effect plots will be of interest. For example in the case of tumour the region from the iso-centre out to about 6cm will probably be the region of interest. This is because 6cm roughly coincides with the 95% of TD which is nominally regarded as the outer treatment border. Late responding tissues, on the other hand, could lie along all parts of "OP" not just in the treatment volume (ie less than 6cm) but also at greater distances especially where sensitive structures such as the rectum are located (ie perhaps between 7 and 9cm from O in this case).

If, instead of the standard reference schedule, another is used it can be shown that the ERD profiles change and from these changes it is possible to plot the associated movement of iso-effect surfaces. This movement is discussed here in a manner similar to that used for intracavitary treatments in chapter 7, although in this case a graphical method is used to determine the actual movement of iso-effect surfaces. This is because the dose profiles for fractionated treatments are not as easy to model mathematically as those of the intracavitary insertion.

If the reference schedule $N_r:d_r$ (30f:2Gy) is replaced by one with 15 fractions, then the new dose per fraction can be calculated for a specific α/β ratio using equation 3.3

$$d_1 = \frac{-N_1 + \left(\frac{N_1^2 + 4N_1ERD_r}{\alpha/\beta} \right)^{1/2}}{\left(\frac{2N_1}{\alpha/\beta} \right)} \quad \text{----- 3.3}$$

where ERD_r is the reference schedule ERD and N_1 the new fraction number (15f).

For an α/β ratio of 10Gy (tumour), d_1 is 3.54 Gy per fraction. This is of course the dose per fraction delivered to the iso-centre in figure 8.1 but for other points along OP the new dose per fraction can be determined from the percentage depth dose plot in figure 8.2. At every point therefore, a new ERD can be calculated for this schedule for both tumour and late effect. Table 8.1 shows the data obtained using this method. From this table, ERD plots can be obtained to show the new shape of the ERD profile along OP. These are shown in figure 8.4 (a) and (b) for tumour and late responding tissues respectively, where they are compared with the corresponding plots from the reference schedule. The two plots in figure 8.4 (a) show that for tumour effects both the reference schedule and the alternative schedule appear well matched, especially in the region around the treatment volume and only at distances of about 6 to 7cm do the plots begin to separate noticeably. Even so the match is much better than that obtained for late responding tissues shown in figure 8.4 (b). Indeed for late responding tissues the whole pattern has changed, most noticeably in the region less than 4cm distant from the iso-centre, which is now some 15% more damaging for late responding tissues; comparison of the remaining plot shows that at every point along OP the expected damage to these tissues would be higher.

8.3. Iso-effect surfaces.

If we now look at these results with iso-effect surfaces in mind then the above example leads to a general outward movement of iso-effect surfaces for late effects. This can be seen clearly in figure 8.4 (b) where a level of effect (ERD) seen at a specific point

on the reference schedule plot occurs at a greater distance on the plot for the alternative schedule. For example a level of effect seen at a distance of 4.25cm on the reference plot (figure 8.4(b)) would now be expected at 6.25cm if the alternative schedule was used. Where the tumour effect plots diverge the movement is in the inward direction using the same reasoning (figure 8.4(a)).

Movement of iso-effect surfaces is shown in figure 8.5 for both types of effect and these plots were obtained by measurement from figure 8.4(a) and (b). It can be seen that the movement involved does not produce a smooth curve of the type observed in the case of intracavitary insertions described in chapter 7. Here with late responding tissues the displacement calculated at around 4cm from the iso-centre along OP is about 2cm in the outward direction, this decreases to about 0.25cm at around 7cm only to rise again afterwards to reach a peak value at 9cm before dropping off with increasing distance. The magnitude of the movement is dependent on the gradient of the ERD plot which is in turn related to the original plot of dose distribution. The flatter the dose distribution and hence the ERD plot the greater the displacements seen in the iso-effect surfaces.

Because the variation in position of surfaces for late effects is in the outward direction this would lead to an increase in late damage, which is what radiobiology theory would predict when altering the reference treatment schedule to one with fewer, but larger fractions, while at the same time matching for tumour effects. It is reasonable to assume that the degree to which late damage manifests itself depends on the magnitude of the movement. At distances of between 6 and 7.25cm therefore and greater than perhaps 10.5cm the change in effect on late tissues would be least. However at less than 6cm and at between 7.25cm and 10.5cm movements of 2cm are indicated so that greater variations in effects would be more probable. Therefore rectum

which in this case would lie between 7 and 9cm from point O, occupies a region where the surfaces have moved by a considerable amount. Tumour iso-effect surfaces behave in a different way. It will be obvious that unless tumour has infiltrated tissues far from the high dose boundary then interest in the region beyond the 95% TD border drops off sharply with distance as far as tumour effects are concerned. Tumour effects are matched to about 4.5cm from O and beyond this point iso-effect surfaces move inwards. Movement is only about 0.5cm in this direction to a distance of about 7cm along OP and this would lead to slightly less effective treatment around the boundary region of the treatment volume. Beyond 7cm, the movement of the iso-effect surfaces continues in the inward direction with a maximum displacement of 1.3 cm at a distance of 10 cm from O. In this example, therefore, late tissues are likely to receive greater damage and tumour effects, though matched over most of the treatment volume, are not as good at the edge of the treatment volume as those of the reference schedule.

In the above example, tumour effects were matched between the reference and the alternative schedule. It is also possible to look at the result when matching is achieved for late effects. Using the same alternative fraction number of 15 and also equation 3.3 with an α/β ratio of 3Gy gives a new dose per fraction d_1 of 3.22Gy per fraction. Table 8.2 shows the corresponding dose per fraction along the line OP as well as the associated ERDs for tumour and late responses. Figure 8.6 displays the plots of ERD at various distances along OP with (a) comparing the plots for tumour effects and (b) those for late effects. In figure 8.6(a) the two plots are separate along the full distance of OP and over the major part of the tumour volume the ERD is about 12.5% less with the new schedule than for the reference schedule. Thereafter the tumour ERD plot for the

alternative schedule also runs below that of the reference schedule. Late effects are matched over most of the treatment volume with the alternative schedule plot running below that of the reference beyond 6.25cm. Figure 8.7 shows the movement of iso-effect surfaces obtained from figure 8.6 and the movement for both tumour and late effects is inwards. As expected, matching for late effects should produce less late damage beyond 6cm but this would lead to a reduction in tumour control.

From the examples above it is apparent that use of iso-effect surfaces can be most effective when comparing two schedules. Also, by considering iso-effect movement, a much clearer view is obtained of the changes that take place when fractionated schedules are altered than would ever be possible if single points were considered alone. This is in keeping with the finding described in chapter 7 for intracavitary insertions. Finally, movement is not necessarily uniform along a line of interest but is influenced by the gradient of the dose and ERD distributions, with shallow gradients leading to the greatest movements.

8.4. General equivalence and iso-effect surface movement.

In chapter 4 (section 4.3.2) the principle of general equivalence was defined and conditions derived which were necessary for fractionated schedules and regimes to be generally equivalent. This derivation was based on a point calculation and the question is now asked: do the conditions for general equivalence hold in three dimensions? If we recall the conditions for general equivalence between a reference schedule $N_r:d_r$ and a regime $N_1:d_1, N_2:d_2, \dots, N_k:d_k$ these are (see chapter 4 section 4.3.2):

$$N_r d_r = \sum_{i=1}^{i=k} N_i d_i \text{ ----- 4.4}$$

$$N_r d_r^2 = \sum_{i=1}^{i=k} N_i d_i^2 \text{ ----- 4.5}$$

These led to the relationships:

$$N_r = \frac{\left(\sum_{i=1}^{i=k} N_i d_i \right)^2}{\sum_{i=1}^{i=k} N_i d_i^2} \text{ ----- 4.6}$$

$$d_r = \frac{\sum_{i=1}^{i=k} N_i d_i^2}{\sum_{i=1}^{i=k} N_i d_i} \text{ ----- 4.7}$$

If we consider the diagram shown in figure 8.8 and assume that conditions for general equivalence hold at "A", do they also hold for point "B" at all other points on space? It is assumed that both the reference schedule $N_r:d_r$ and the regime $N_i:d_i$ produce the same overall depth dose profiles ie the same treatment plan is used in both cases.

So that:

The dose per fraction at point B

= The dose per fraction at A x the percentage depth dose at B

i.e. $d_r(b) = d_r(a) \times (X\%)$

and similarly:

$$d_i(b) = d_i(a) \times (X\%).$$

The schedule fraction numbers, N_r and N_i , of course apply to both points A and B.

If a dose per fraction d_r is required at point A for general equivalence then does this result in general equivalence at B?

For general equivalence at B:

$$d_r(b) = \frac{\sum_{i=1}^{i=k} N_i d_i^2(b)}{\sum_{i=1}^{i=k} N_i d_i(b)} = \frac{\sum_{i=1}^{i=k} N_i ((d_i(a) \times (X\%))^2)}{\sum_{i=1}^{i=k} N_i (d_i(a) \times (X\%))}$$

$$= (X\%) \left(\frac{\sum_{i=1}^{i=k} N_i d_i^2(a)}{\sum_{i=1}^{i=k} N_i d_i(a)} \right) = (X\%) \times d_r(a)$$

Therefore: $d_r(b) = (X\%) \times d_r(a)$ which is the result that is expected from the depth dose profile so that in terms of the dose per fraction the conditions for general equivalence are satisfied at all points.

Also:

$$N_r(b) = \frac{\left(\sum_{i=1}^{i=k} N_i d_i(b) \right)^2}{\sum_{i=1}^{i=k} N_i d_i^2(b)} = \frac{(X\%)^2 \left(\sum_{i=1}^{i=k} N_i d_i(a) \right)^2}{(X\%)^2 \sum_{i=1}^{i=k} N_i d_i^2(a)}$$

Therefore $N_r(b) = N_r(a)$ for general equivalence. This shows that once the conditions for general equivalence are satisfied between a schedule and a regime at one point they hold at every point around the treatment volume, provided the overall dose distribution is the same (ie the same treatment plan is used). In this discussion any daily variation in set up which leads to slight differences in the dose distribution has been ignored.

For an example of this consider the regime of 10 fractions of 1.52Gy followed by 5 fractions of 4Gy which is generally equivalent to a schedule of 12.02 fractions of 2.93Gy. If we assume the same treatment plan is used as in figure 8.1 then along the line OP the ERDs for these schedules can be calculated and the results are shown in table 8.3 for both tumour and late effects. It can be seen that at any point (ignoring slight rounding errors) the sum of the ERDs of the regime equals that of the reference

schedule. Figure 8.9 shows the plot of the late ERDs for the two schedules of the regime and the equivalent single schedule which further confirms these results.

8.5. Volume effects.

Until now the iso-effect movement has been discussed in terms of one dimensional displacement but it will be clear that the movement of these surfaces is three dimensional (Deehan & O'Donoghue, 1991, 1994). A true picture of the changes in volume can only be obtained with a three dimensional display but this is not possible to demonstrate in this thesis. It is possible, however, to calculate changes in the enclosed volume of iso-effect surfaces and this will now be illustrated using a standard intracavitary insertion. The volume changes to be calculated will be those associated with the transition between the low dose rate (LDR) reference schedule $N_T:R_T:T_T$ (1:0.83Gy/hr:48hr) and the high dose rate (HDR) schedule $N_1:R_1:T_1$ (6:150Gy/hr:0.03hr). In order to calculate these volume changes, it is necessary to determine the volume enclosed by a surface associated with a specific dose-rate (or total dose). To perform this calculation an existing computer programme was used which had been written by Mrs O Smith, Principal Physicist, Dept. Clinical Physics and Bio-Eng, Glasgow. Figure 8.10 illustrates the method used. The area enclosed by the intersection of plane 1 and the surface was calculated by the addition of grid squares enclosed by the intersection. Squares which lie partially outside of intersection have to be dealt with by an approximation method. If the grid is small enough however these errors are not significant. If another plane is chosen parallel to the first and the process repeated then the volume enclosed by these can be found if the plane separation (s) is known and, if this is small, errors will be negligible.

The programme was checked using a point source which gave spherical volumes which were easy to calculate by hand.

As in chapter 7 (section 7.3), it must be remembered that a standard source geometry is assumed when comparing different intracavitary treatments so that the geometry does not alter when the dose-rate changes. This constraint allows iso-effect surface changes associated with the radiobiological factors to be isolated clearly.

Using the programme described above and the reference LDR schedule $N_r \cdot R_r \cdot T_r$, a plot of dose-rate versus volume can be drawn (see figure 8.11). Assuming constant geometry and only a variation in dose-rate the dose-rate axis in figure 8.11 can be scaled to suit the new treatment schedule by multiplying by a factor of (R_1/R_r) where R_1 is the new dose-rate. This means that the same dose-rate/volume plot can be used (with an appropriate scaling factor applied to the dose-rate axis) with insertions with different source activities provided the dose-rate at a specific point is known for both treatments. At LDR a specific dose-rate value will be associated with a specific enclosed volume and this in turn will be the volume enclosed by the associated iso-effect surface (ie specific value of α/β ratio and μ). The ERD of this surface can be calculated and used to determine the new dose-rate to which this corresponds at HDR (Deehan and O'Donoghue 1991,1994). Using the appropriate scaled axis, the new enclosed volume can be found from figure 8.11. This is illustrated in the following example where, just as in chapter 7, the movement of iso-effect surfaces is considered along the line PP' (a line running out from point P through the Manchester "A" point). As will be seen, relatively small movement of surfaces can result in considerable changes in enclosed volume. The movement of iso-effect surfaces can be calculated in going from the LDR to the HDR

schedule using the method described in chapter 7 (section 7.3.4). This depends on a knowledge of the dose-rate profile along the line PP'. Once the ERD for a specific effect is known at a point for LDR then equation 7.3 can be solved to find the dose-rate at HDR that corresponds to this ERD. The position at which this dose-rate occurs on PP' is the new position of the iso-effect surface and from this any movement can be calculated. Figure 8.12 shows these movements for tumour and late responding tissues when the two treatments are compared. Movement of the iso-effect surfaces in an outward direction is shown as a positive displacement on the graph. The plot of movement for tumour shows that surfaces move outwards at distances of less than about 2cm from the insertion. At 2cm the movement then changes to an inward direction which increases with distance. The movement plot for late responding tissues appears to be in an inward direction along the entire length of PP' and follows the trend seen with tumour surfaces (ie increasing with distance) and also that described in chapter 7, figures 7.8 and 7.9. Notice also that the plots are much smoother than those shown earlier in this chapter for fractionated treatments.

Next, volume changes can be calculated. The programme referred to earlier in this chapter allows the volume enclosed by a given dose-rate surface to be calculated. Knowing the ERD associated with this dose-rate at LDR it is possible to determine the corresponding dose-rate at HDR and this will in general correspond to the new volume, which can be found as described earlier using figure 8.11 and the appropriate scaling factor (in this case $150/83$). Figure 8.13 shows the volume changes expressed as a percentage of their value at LDR for tumour and late responding tissues along the line PP'. It can be seen that at short distances (tumour plot) small displacements seen in figure 8.12 correspond to large changes in the volume enclosed by iso-effect surfaces. In

this example tumour surfaces show a large increase in volume at short ranges (less than 2cm) and late responding surfaces show a progressive reduction along all of the line PP'.

8.6. Conclusions.

It has been seen in this chapter that iso-effect surfaces move when fractionated treatments are altered. The movement appears to be more erratic than that seen with intracavitary treatments and this seems to be related to the changing dose gradients and hence effect gradients involved. Iso-effect surfaces give a better overall picture of the changes in effect distribution than point calculations could ever do and produce results that are in keeping with the trends expected in classical radiobiology theory. Volume effects can also be determined and these show that large changes in volume are possible even when the movement of individual surfaces is only of the order of millimetres. This is not surprising since the original volume has to be taken into account and if this is small then small surface movements can result in large percentage changes in volume. When these results are compared with published clinical findings they could suggest why changing from LDR to HDR does not necessarily produce more late responding tissue damage for the same tumour control. This aspect is discussed in chapter 9.

Figure 8.1 Depth dose distribution through the central transverse axis of a typical pelvis plan.
The line OP is shown running from the iso-centre to the posterior edge of the contour.

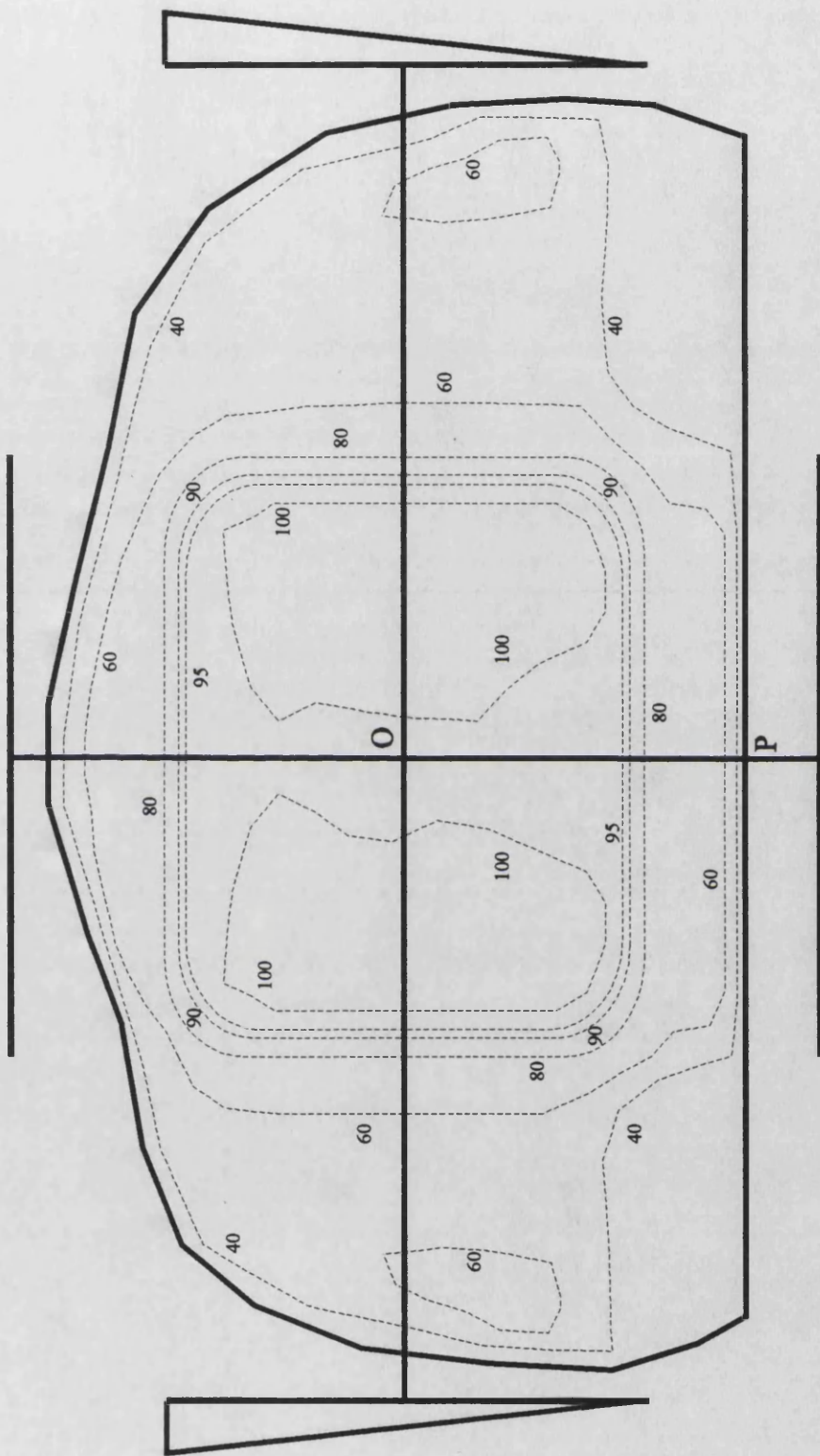


Figure 8.2 Total dose, (a) and percentage depth dose, (b) plots along the line OP in figure 8.1 For the schedule (N_r:d_r) (30:2Gy).

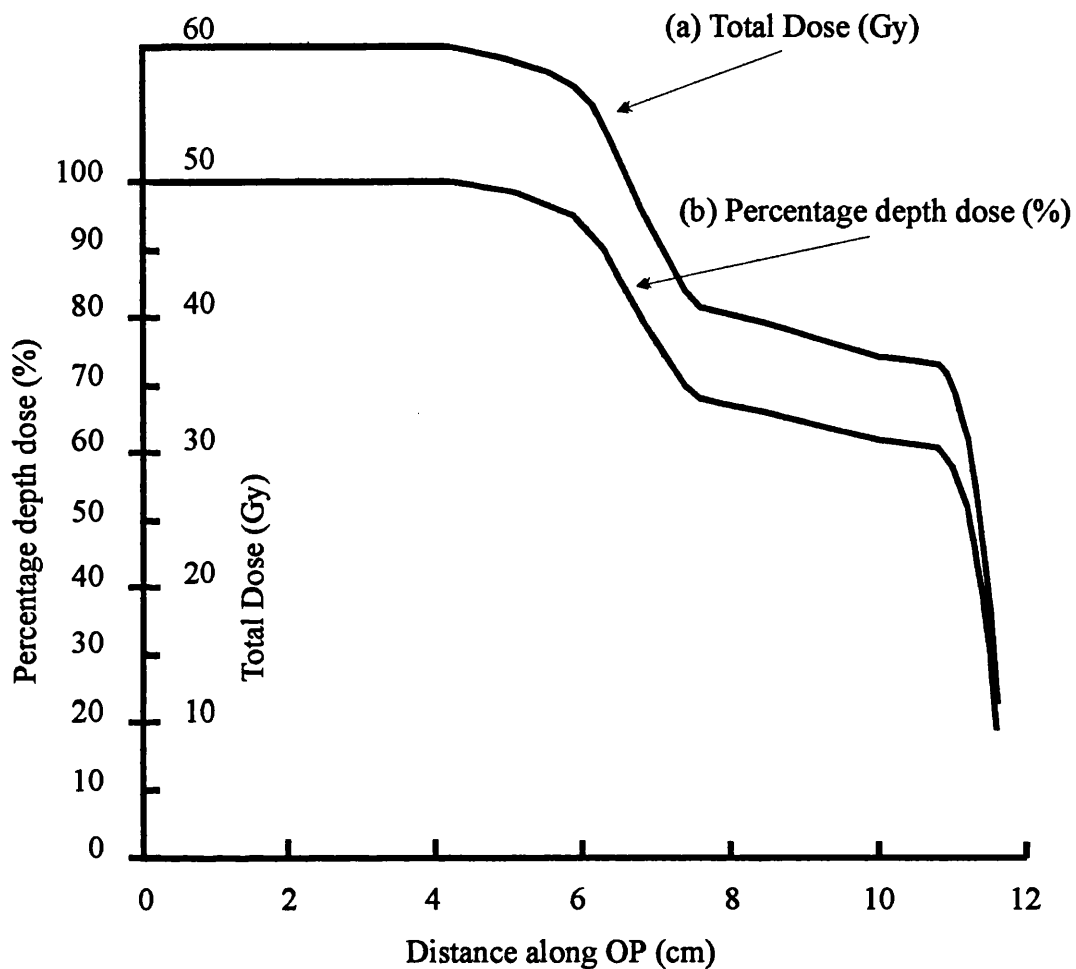


Figure 8.3 (a) ERD plot along the line OP calculated by the linear quadratic (LQ) model for tumour effects.

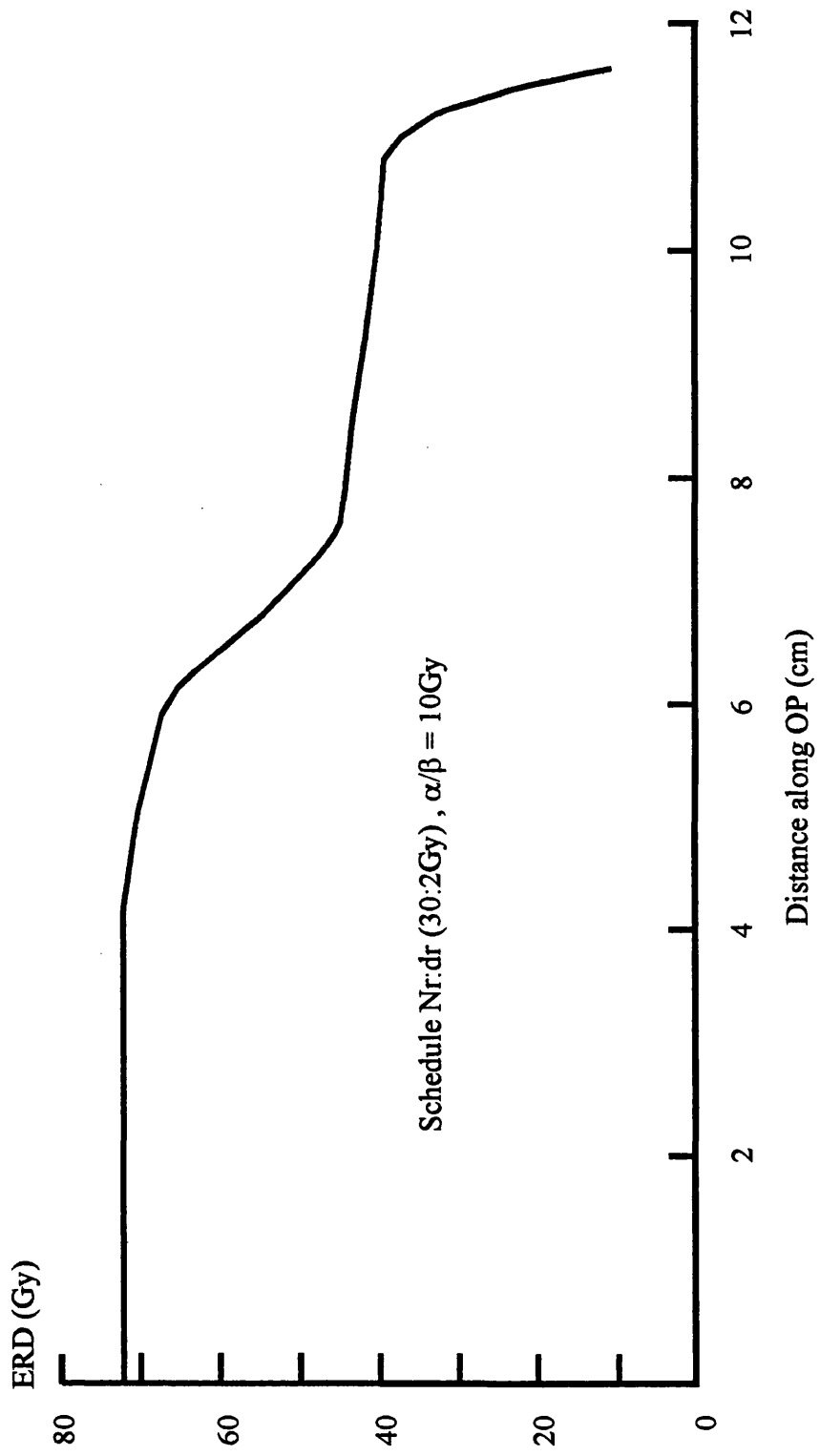


Figure 8.3 (b) ERD plot along the line OP calculated by the linear quadratic (LQ) model for late effects.

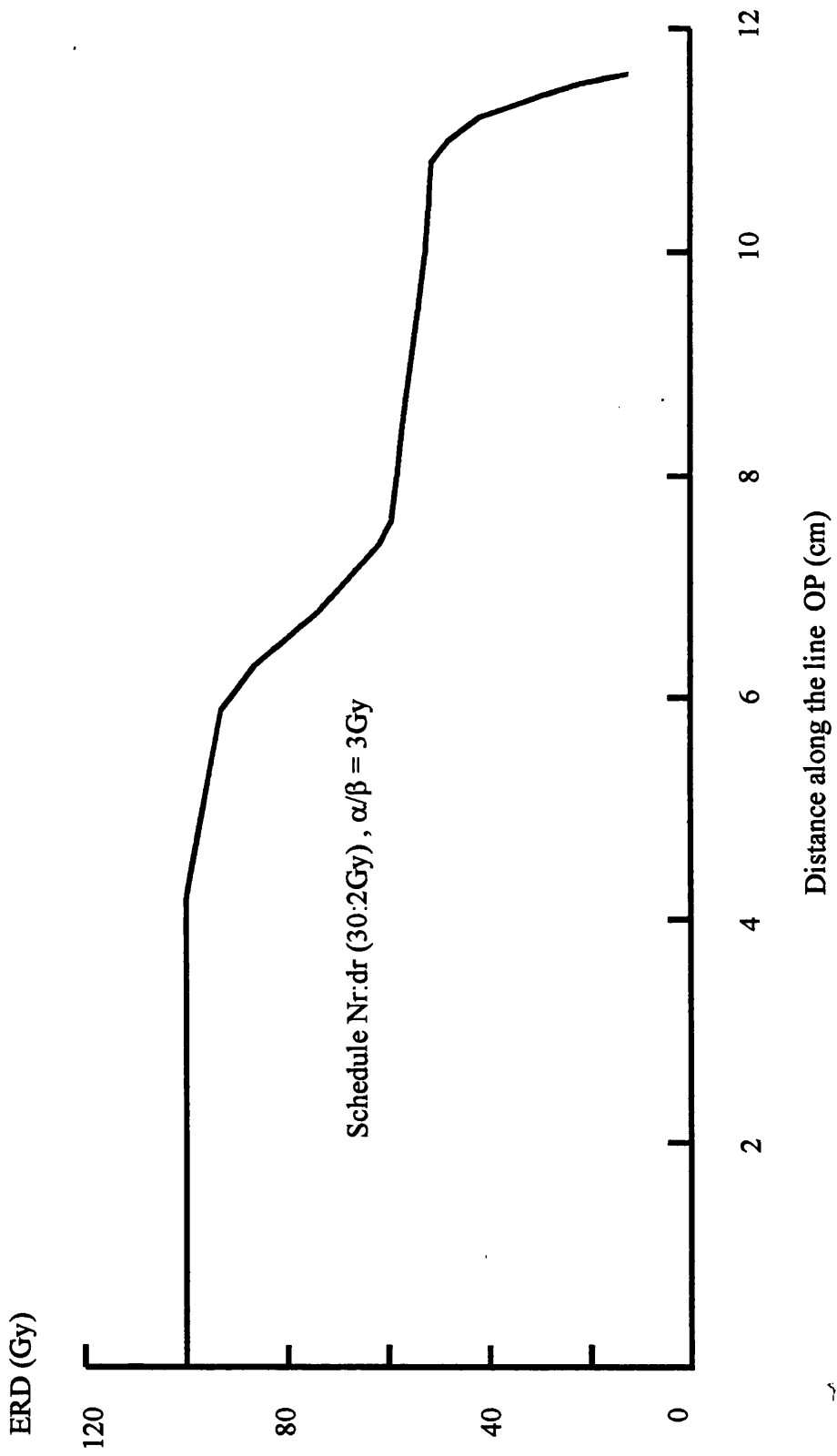


Figure 8.4(a) ERD plot for Tumour effects. Comparison between $(N_r:d_r)$ (30:2Gy) and $(N_1:d_1)$ (15:3.54Gy)

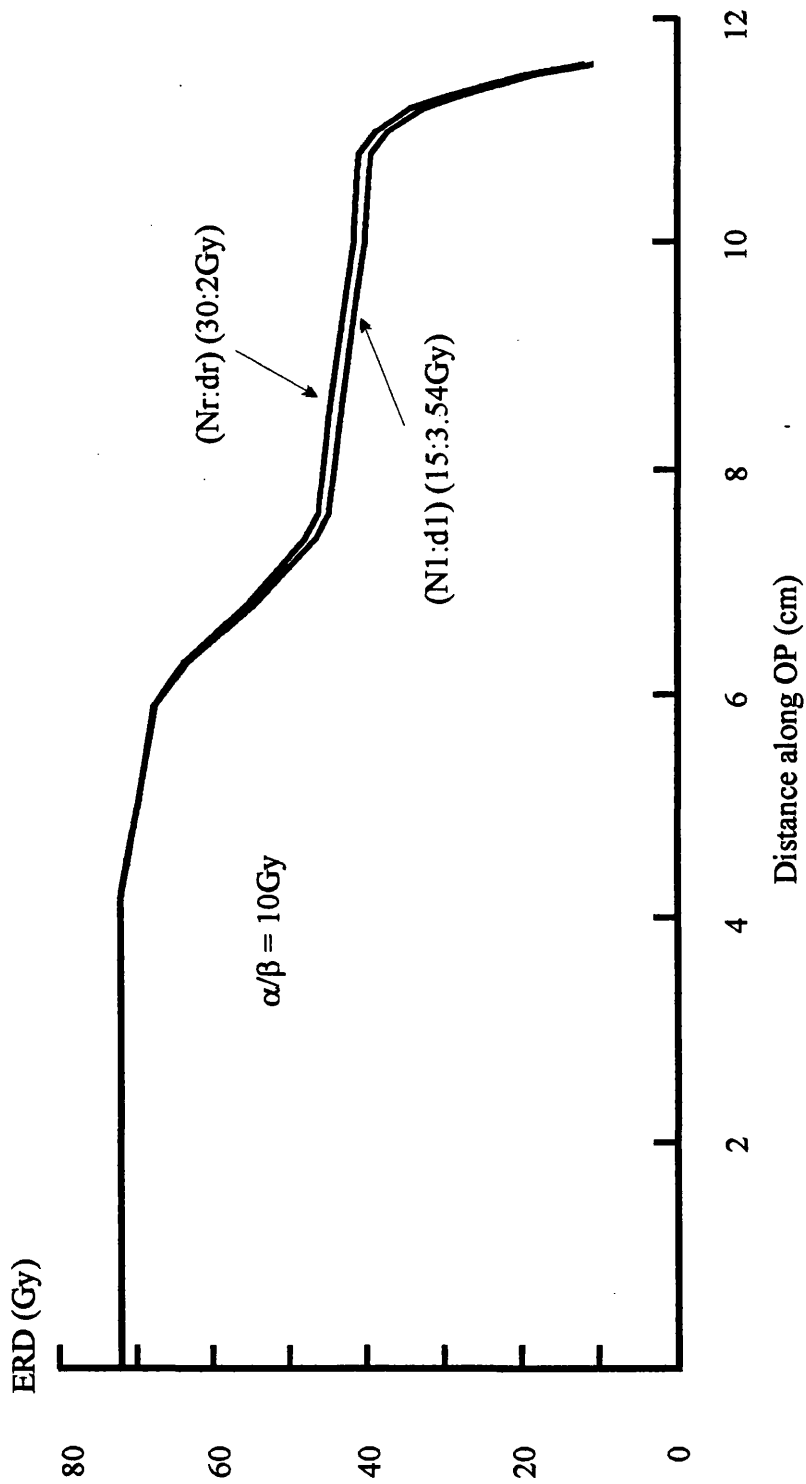


Figure 8.4 (b) ERD plot for Late effects. Comparison between $(N_r:d_r)$ (30:2Gy) and $(N_i:d_i)$ (15:3.54Gy).

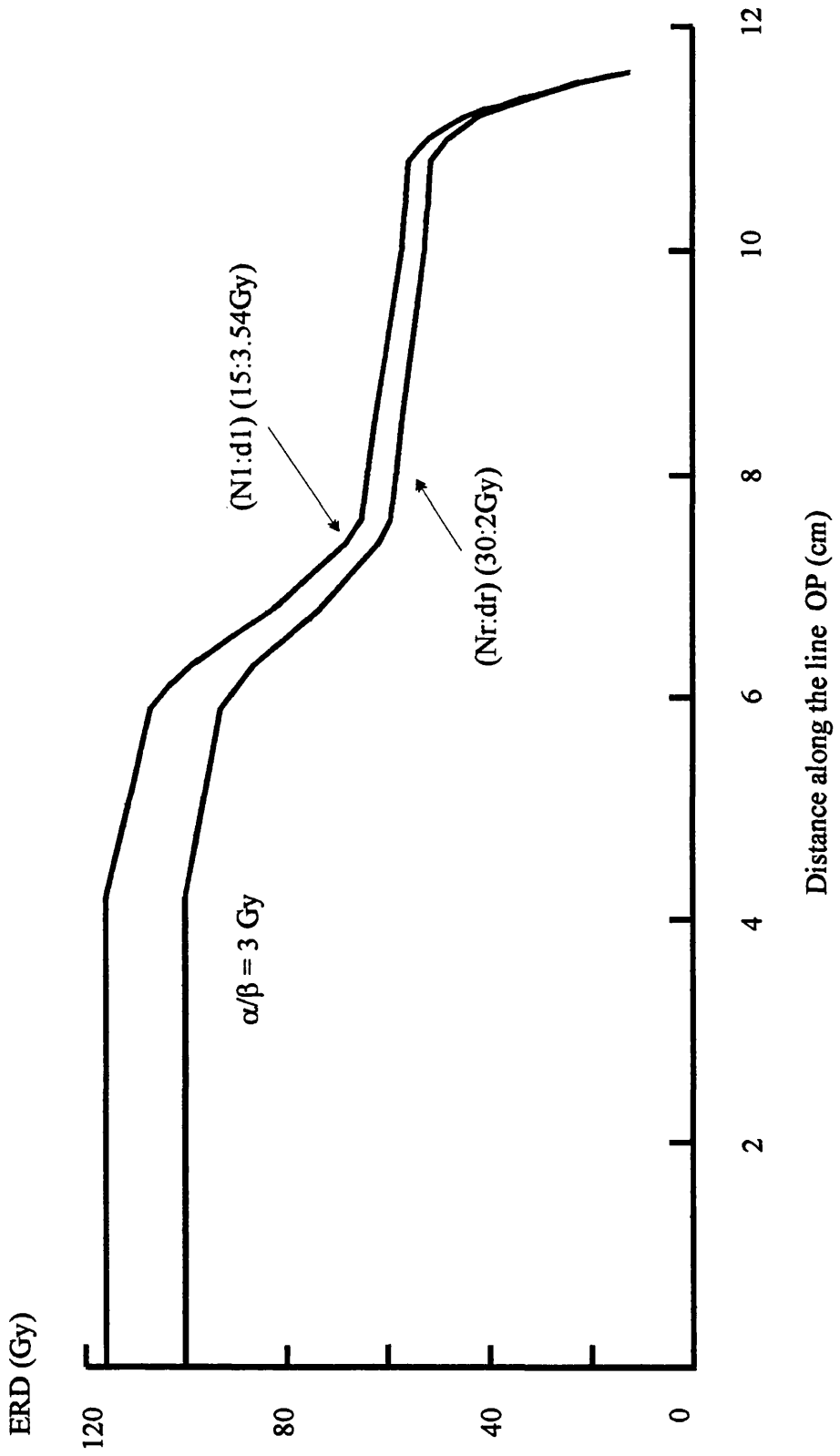


Figure 8.5 Iso-effect surface movement for tumour and late responding tissues along the line OP as a result of changing from $(N_r:d_r)$ (30:2Gy) to $(N_1:d_1)$ (15:3.54Gy).

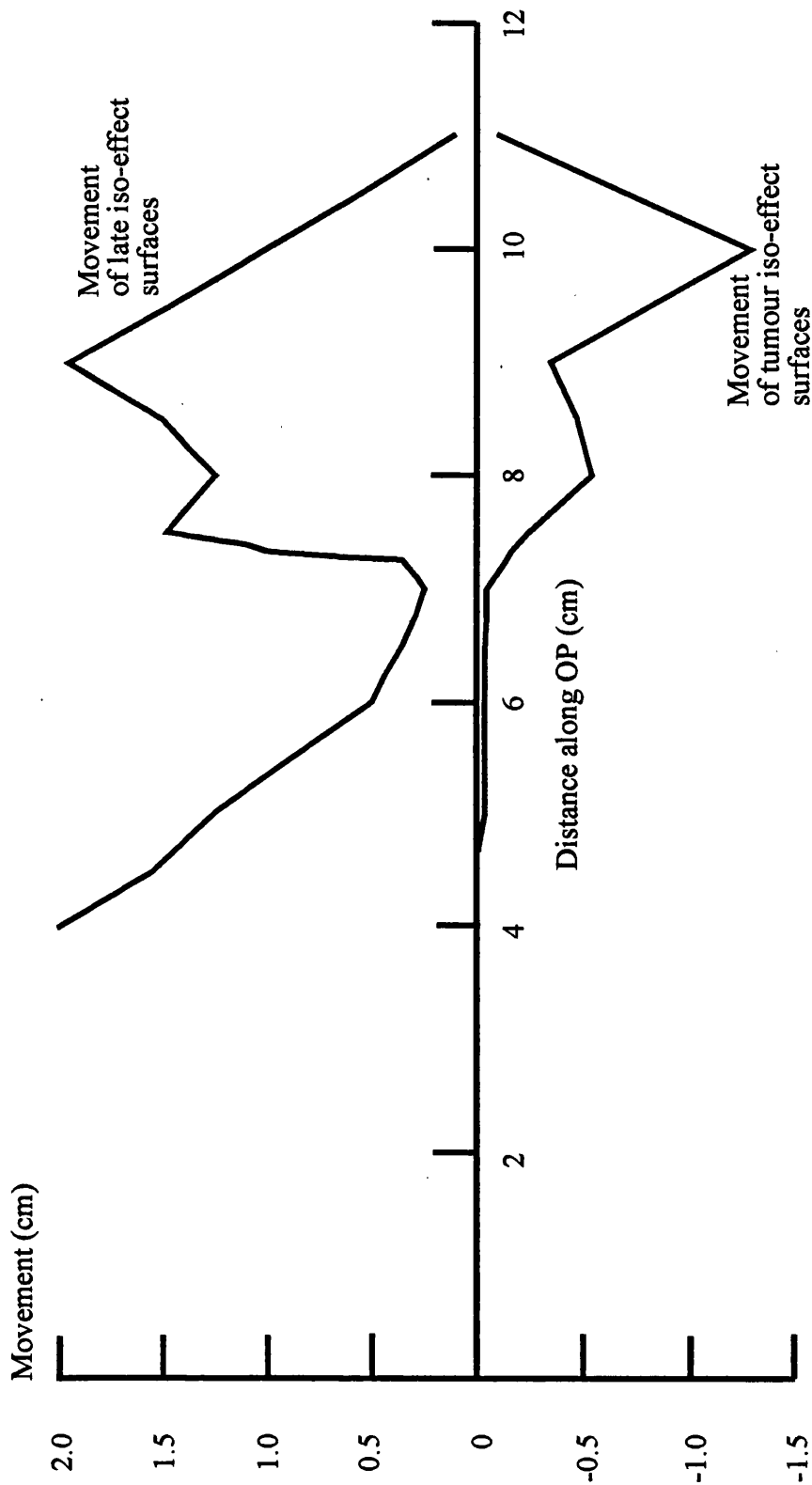


Figure 8.6(a) ERD plots compared for tumour effects in the transition between the schedule $(N_1:d_1)$ (30:2Gy) and $(N_1:d_1)$ (15:3.22Gy)

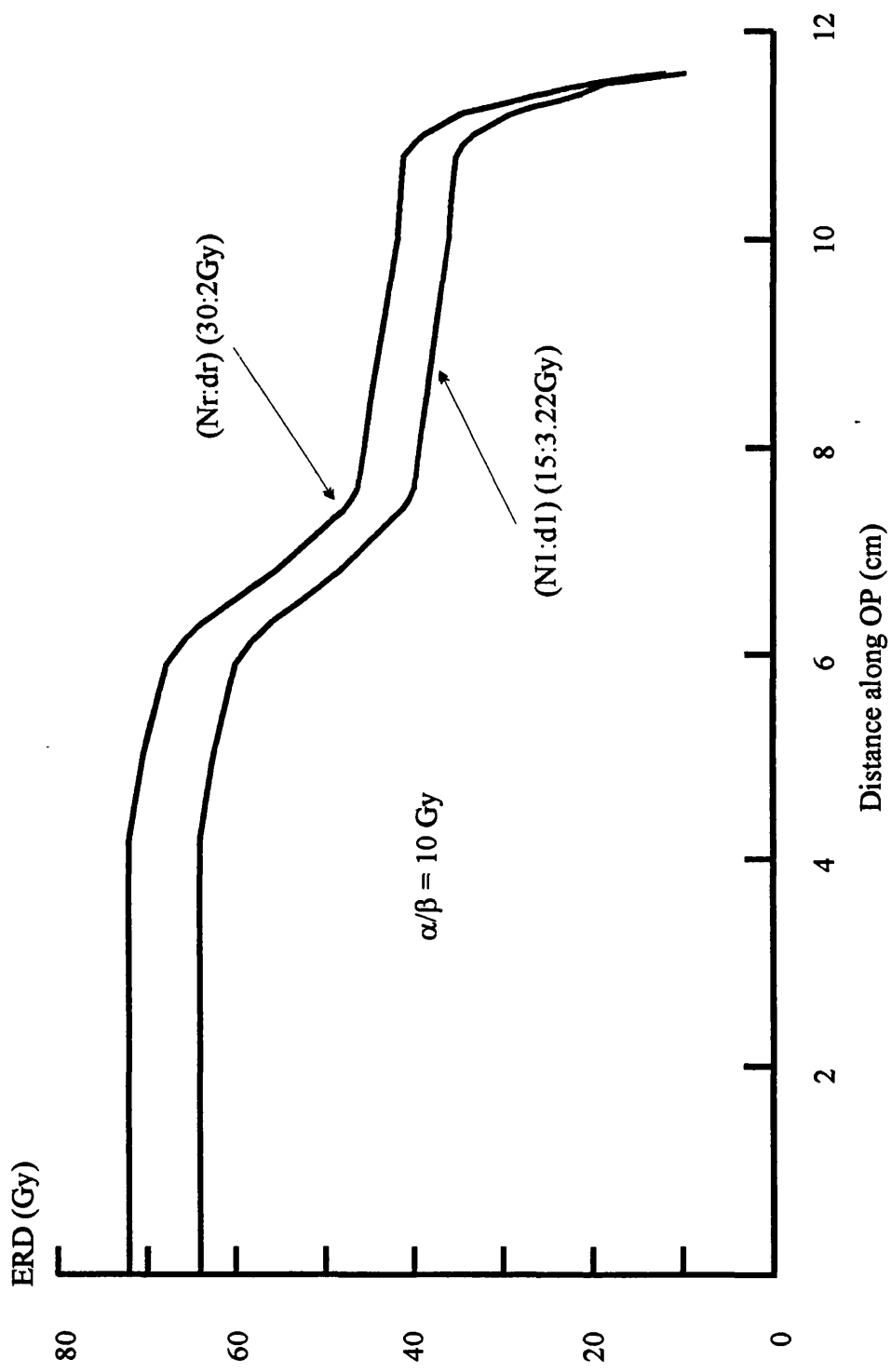


Figure 8.6(b) ERD plots compared for late effects in the transition between the schedule (N_r:d_r) (30:2Gy) and (N₁:d₁) (15:3.22Gy)

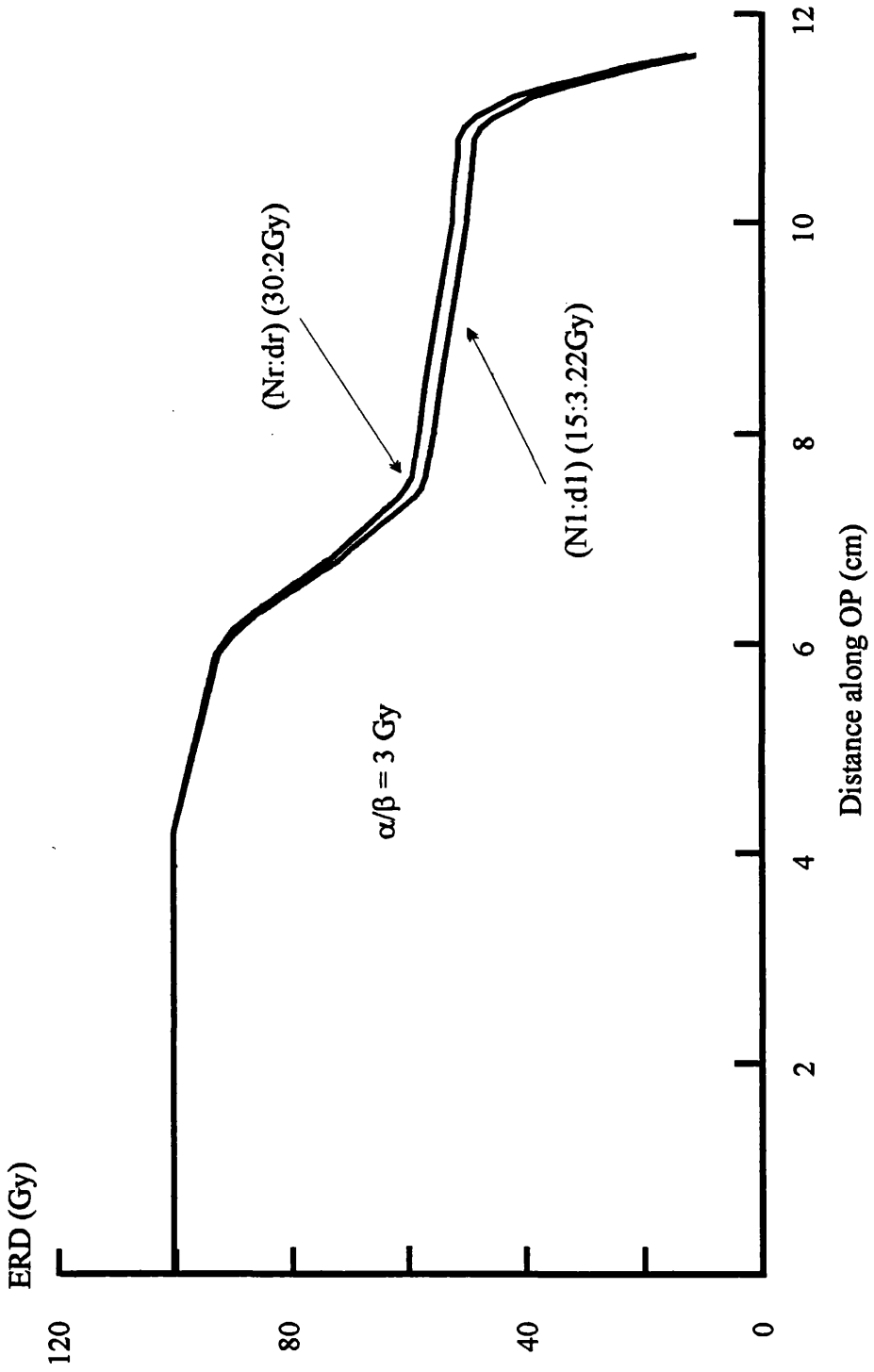


Figure 8.7 Iso-effect surface movement for tumour and late responding tissues along the line OP as a result of changing from $(N_i;d_i)$ (30:2Gy) to $(N_i;d_i)$ (15:3.22Gy).

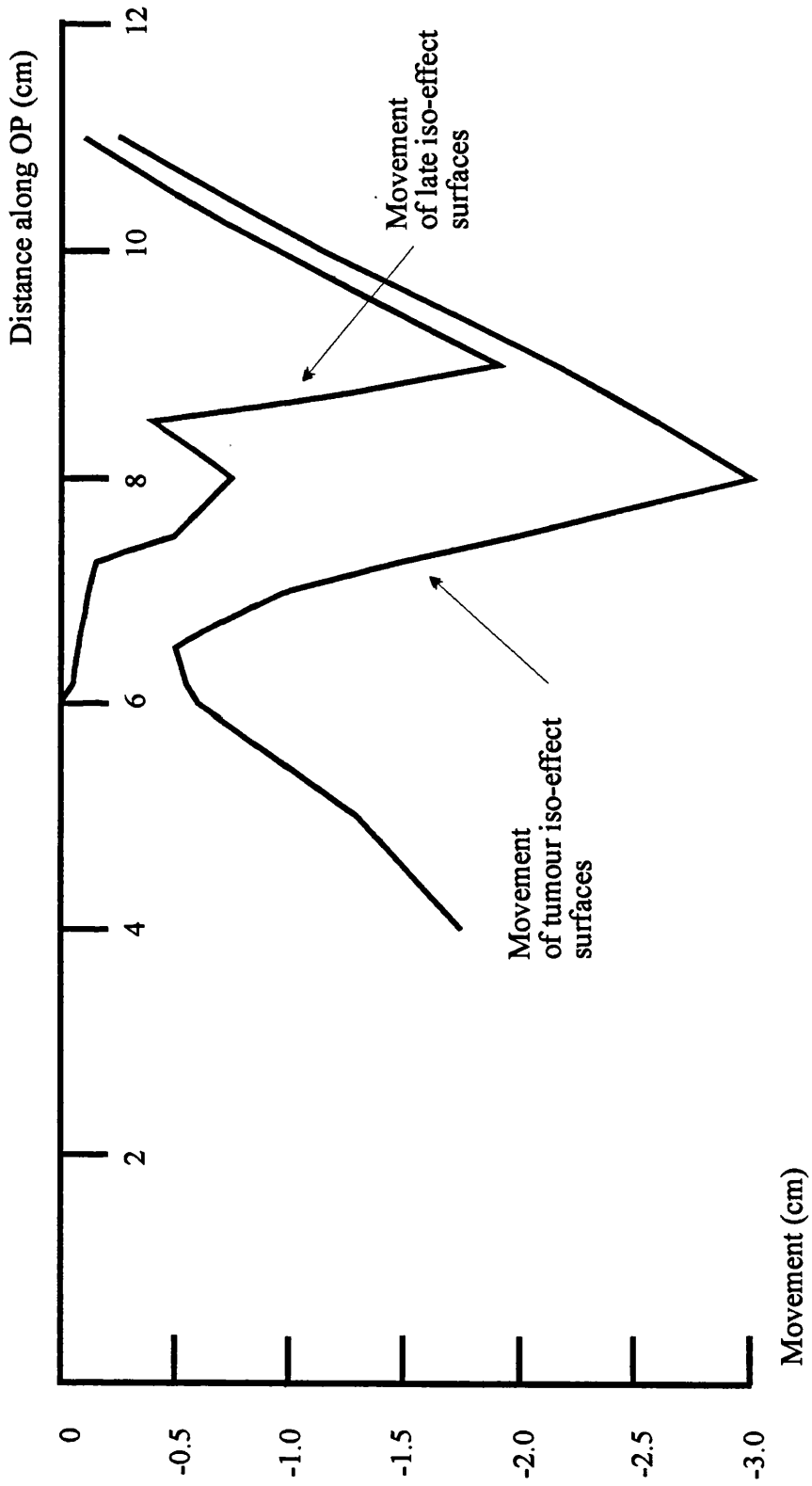


Figure 8.8 Total dose plot for a reference schedule $N_r:d_r$ along the line OP.

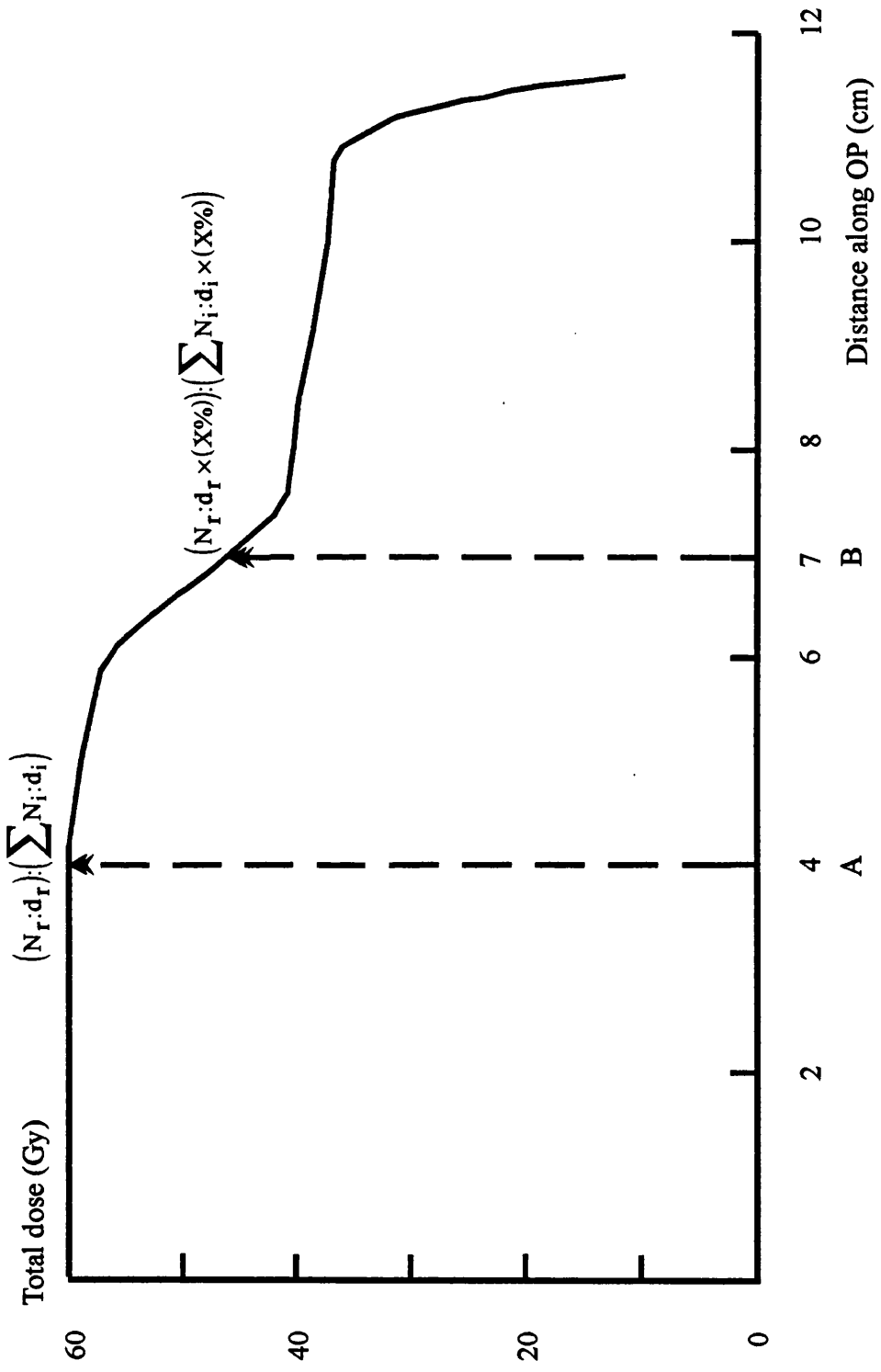


Figure 8.9 ERD plots for late effects for general equivalence between the schedule $(N_1;d_1):(12.02:2\text{Gy})$ and the regime $(N_1;d_1):(10:1.52\text{Gy}) + (N_2;d_2):(5:4\text{Gy})$

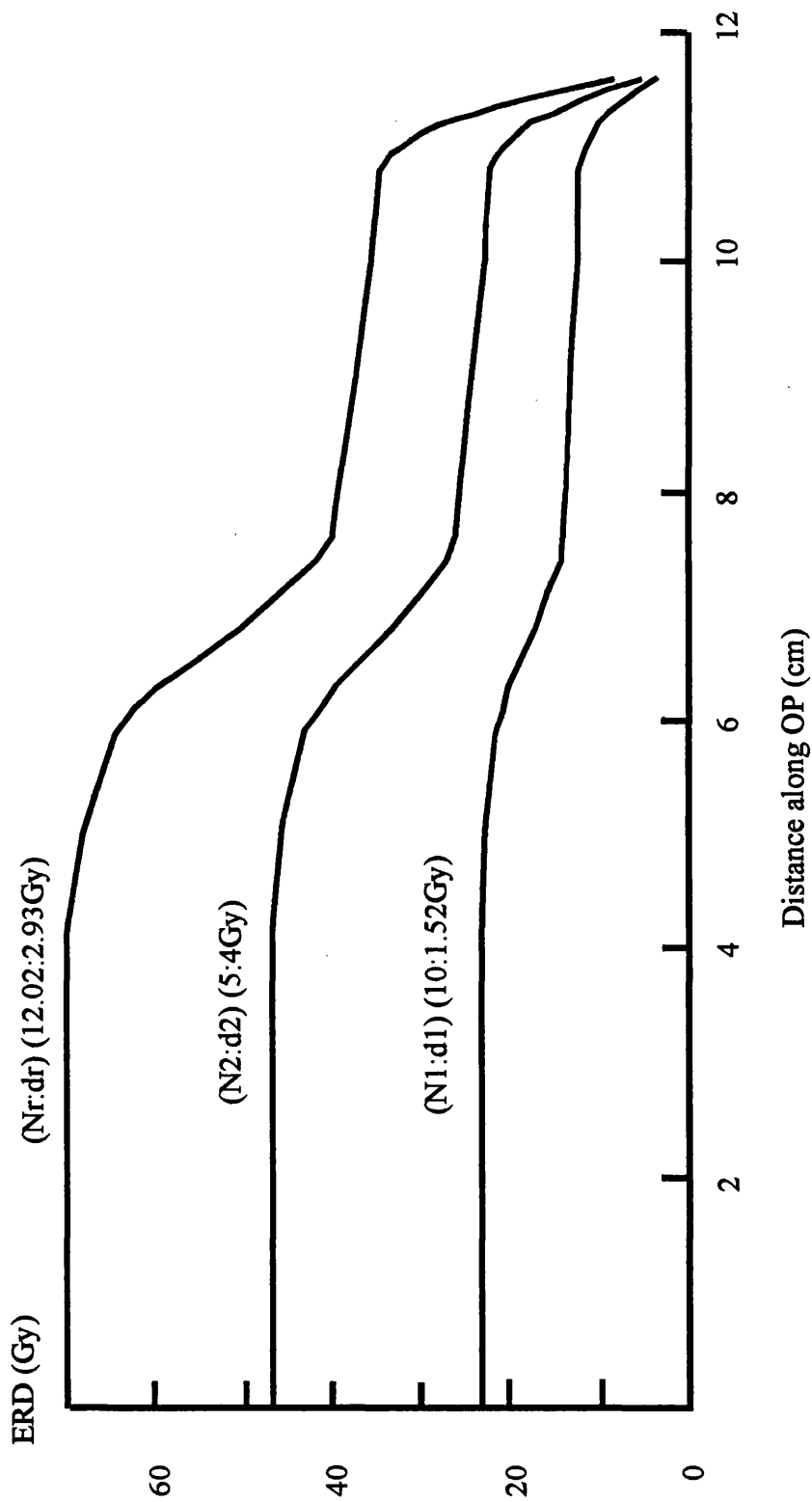


Figure 8.10 Calculating the volume enclosed by a surface surrounding a distribution of radioactive sources.

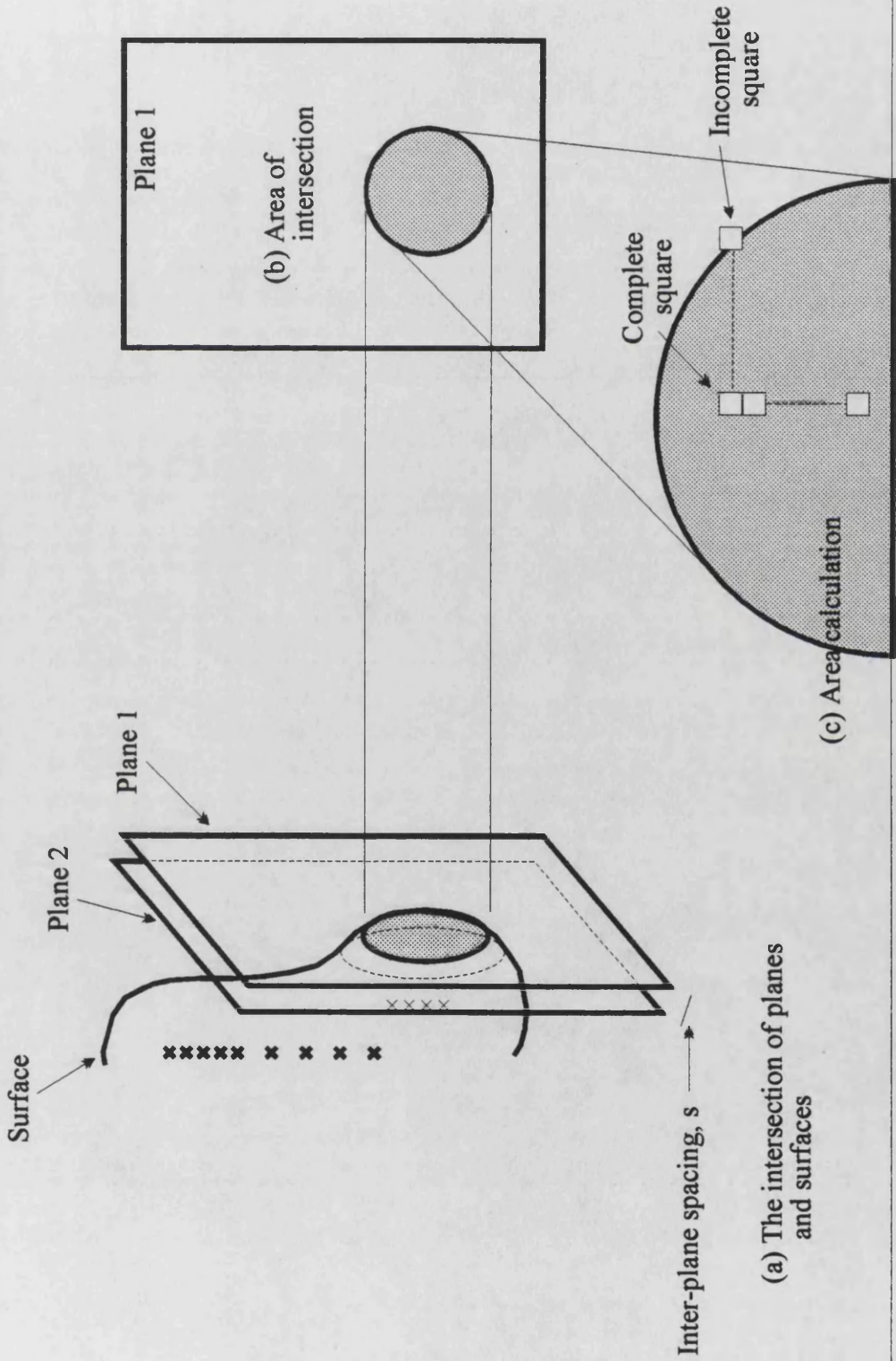


Figure 8.11 Dose-rate versus enclosed volume relationship for a standard low dose-rate insertion.

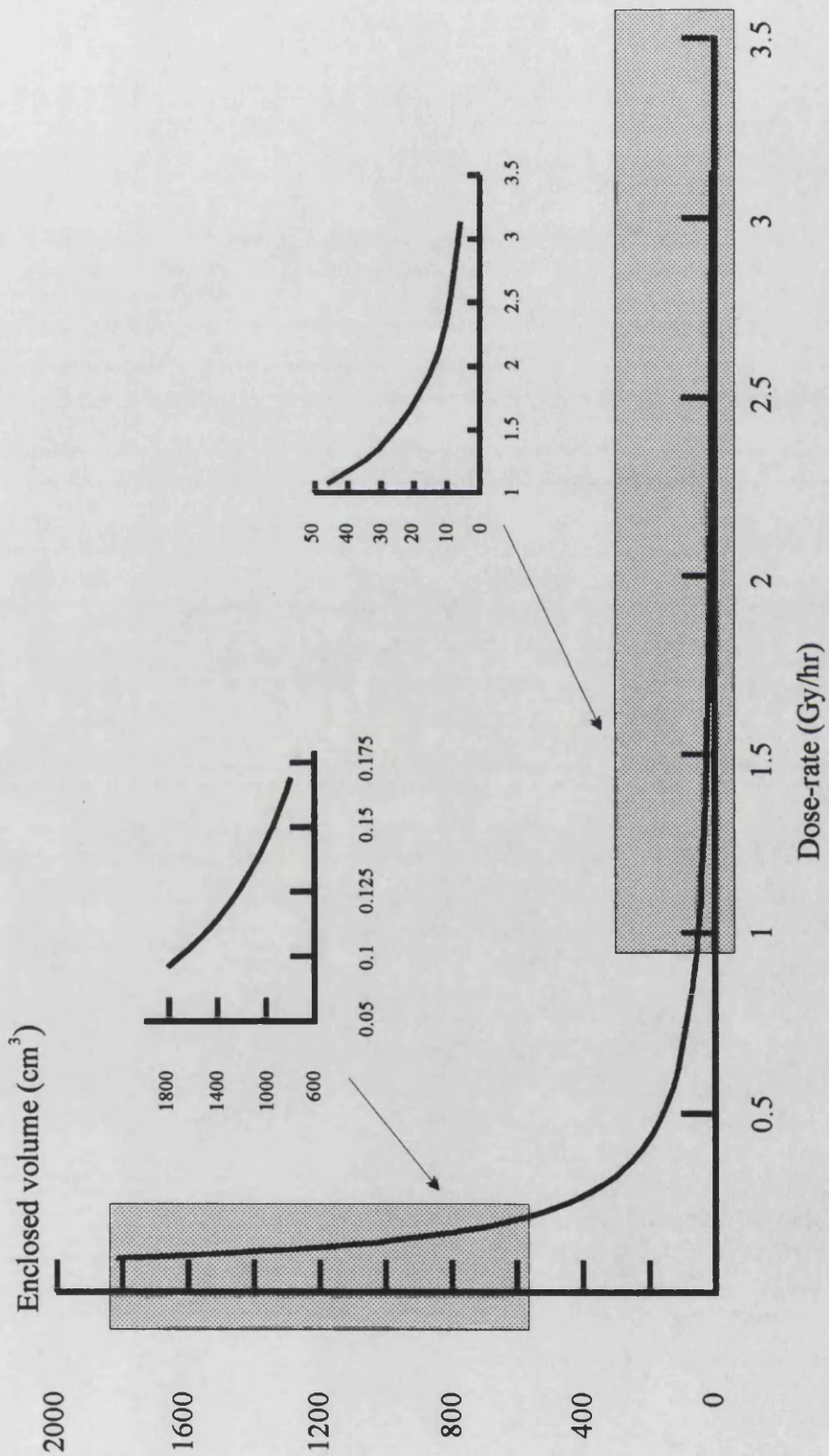


Figure 8.12 Movement of tumour and late iso-effect surfaces along the line PP' in the transition from $(N_1:R_1:T_1)$ (1:0.83Gy/hr:48hr) to $(N_1:R_1:T_1)$ (6:150Gy/hr:0.03hr)

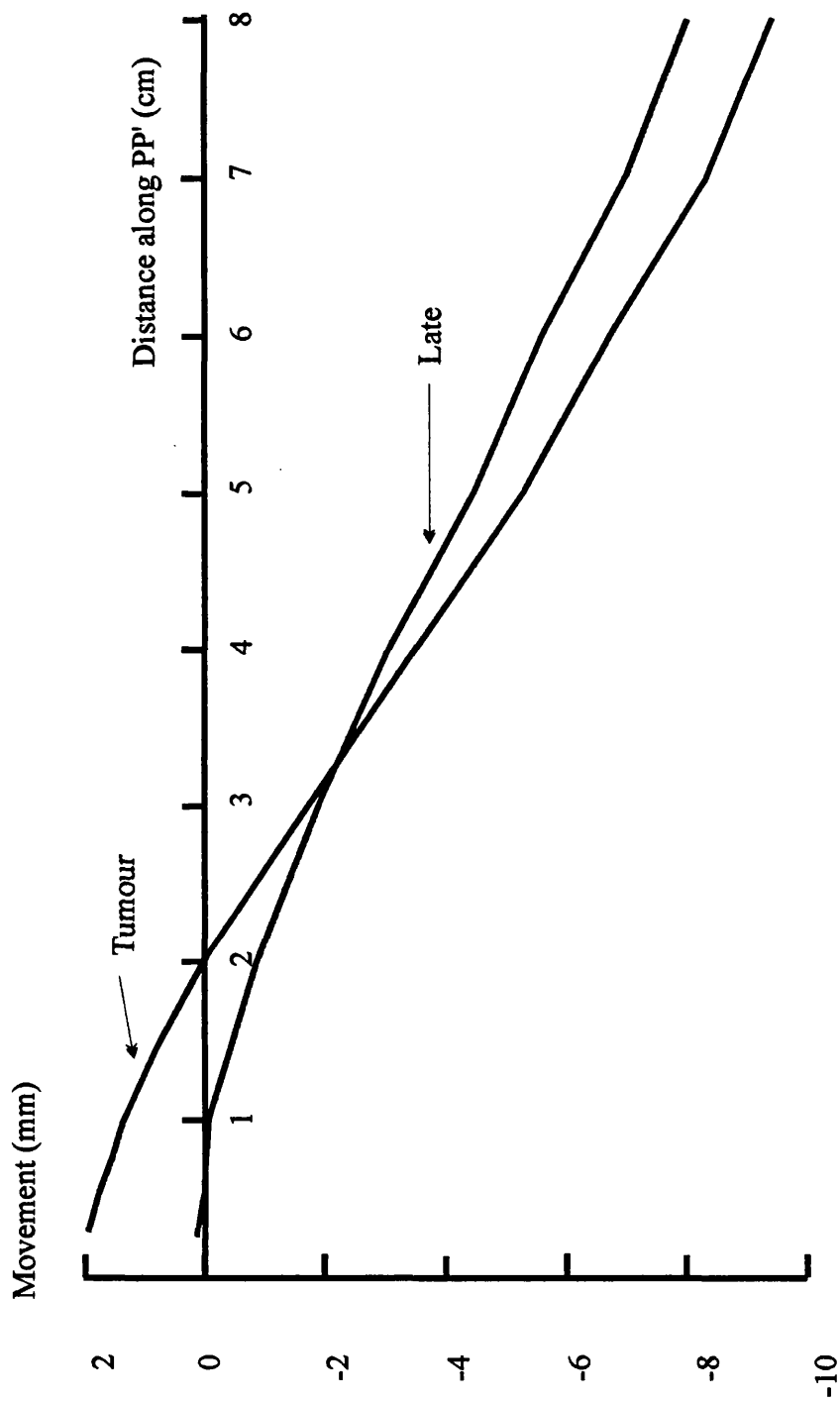


Figure 8.13 Percentage change in the enclosed volume of iso-effect surfaces in the transition from $(N_1:R_1:T_1)$ (1:0.83Gy/hr:48hr) to $(N_1:R_1:T_1)$ (6:150Gy/hr:0.03hr)

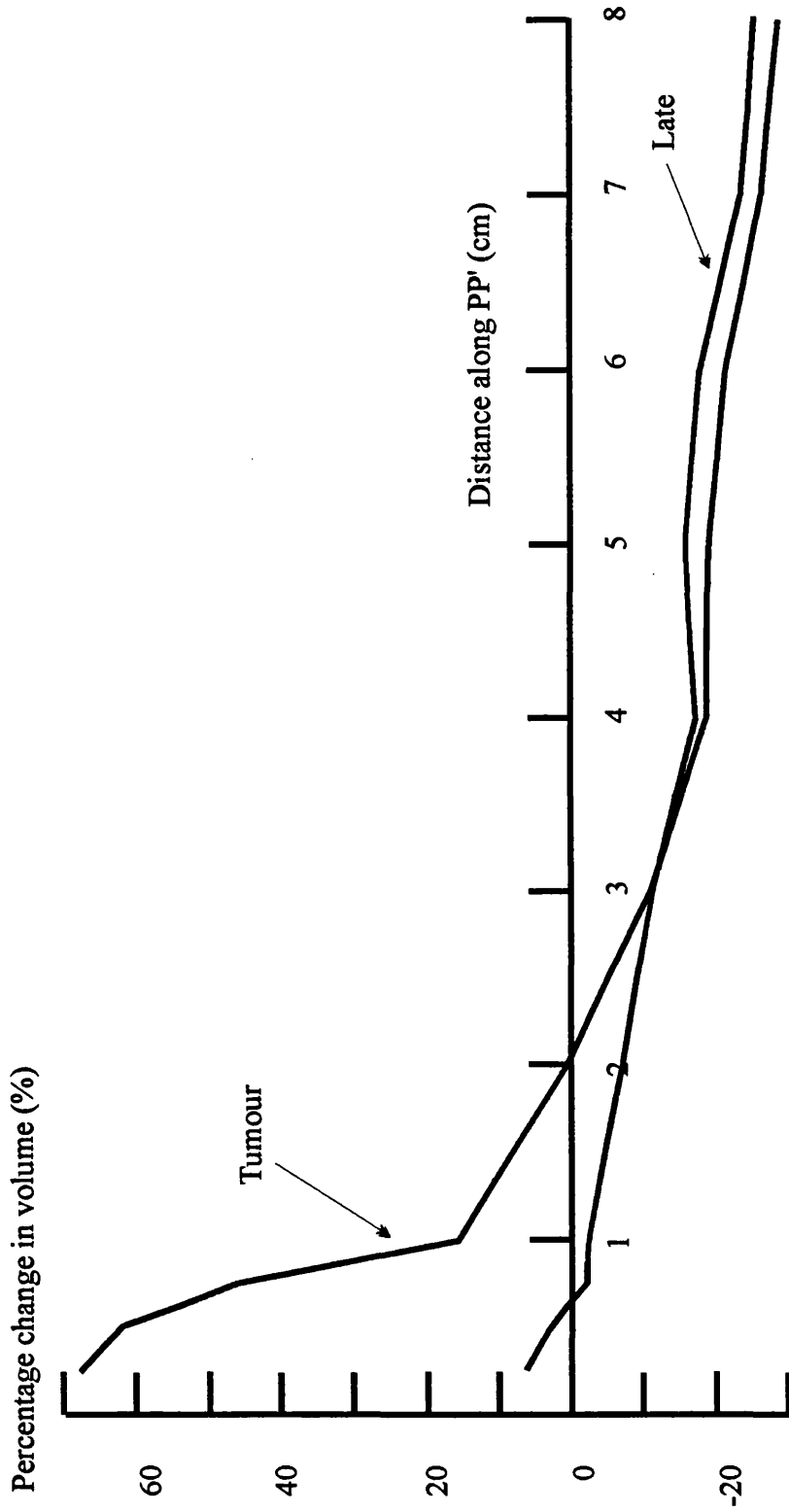


Table 8.1 ERD and depth dose data for points along the line OP in figure 8.1 for the transition between the reference schedule (a), ($N_r:d_r$) (30:2Gy) and an alternative schedule (b), ($N_1:d_1$) (15:3.54Gy) which matches for Tumour effects.									
Distance OP	%Depth Dose (DD)	d_r (Gy) ($2 \times \%DD$) (a)	ERD _r (Gy) Tumour ref (a)	ERD _r (Gy) Late ref (a)	d_1 (Gy) $3.54 \times \%DD$ (b)	ERD ₁ Tumour Alt. (b)	ERD ₁ Late Alt. (b)		
4.2	100	2.00	72.00	100	3.54	72.00	115.96		
5.9	95	1.90	67.83	93.10	3.37	67.51	107.19		
6.3	90	1.80	63.72	86.40	3.19	63.11	98.73		
6.8	80	1.60	55.68	73.60	2.83	54.58	82.71		
7.4	70	1.40	47.88	61.60	2.48	46.45	67.99		
7.6	68	1.36	46.35	59.30	2.41	44.86	65/19		
8.5	66	1.32	44.83	57.00	2.34	43.29	62.44		
10.0	62	1.24	41.81	52.58	2.20	40.19	57.09		
10.8	61	1.22	41.06	51.48	2.16	39.44	55.80		
11.0	58	1.16	38.84	48.26	2.05	37.16	51.94		
11.2	52	1.04	34.44	42.02	1.84	32.74	44.63		
11.3	46	0.92	30.14	36.06	1.63	28.43	37.73		
11.4	39	0.78	25.22	29.48	1.38	23.59	30.28		
11.5	31	0.62	19.75	22.44	1.10	18.30	22.52		
11.6	19	0.38	11.83	12.84	0.67	10.77	12.36		

Table 8.2 ERD and depth dose data for points along the line OP in figure 8.1 for the transition between the reference schedule (a), ($N_r:d_r$) (30:2Gy) and an alternative schedule (b), ($N_1:d_1$) (15:3.22Gy) which matches for Late effects.									
Distance OP	%Depth Dose (DD)	d_r (Gy) ($2 \times \%DD$) (a)	ERD _r (Gy) Tumour ref (a)	ERD _r (Gy) Late ref (a)	d_1 (Gy) $3.22 \times \%DD$ (b)	ERD ₁ Tumour Alt. (b)	ERD ₁ Late Alt. (b)		
4.2	100	2.00	72.00	100	3.22	63.85	100.00		
5.9	95	1.90	67.83	93.10	3.06	59.94	92.70		
6.3	90	1.80	63.72	86.40	2.90	56.11	85.50		
6.8	80	1.60	55.68	73.60	2.58	48.68	71.98		
7.4	70	1.40	47.88	61.60	2.25	41.34	59.06		
7.6	68	1.36	46.35	59.30	2.19	40.04	56.83		
8.5	66	1.32	44.83	57.00	2.12	38.54	54.27		
10.0	62	1.24	41.81	52.58	2.00	36.00	50.00		
10.8	61	1.22	41.06	51.48	1.96	35.16	48.61		
11.0	58	1.16	38.84	48.26	1.87	33.29	45.53		
11.2	52	1.04	34.44	42.02	1.67	29.23	38.99		
11.3	46	0.92	30.14	36.06	1.48	25.48	33.15		
11.4	39	0.78	25.22	29.48	1.25	21.09	26.56		
11.5	31	0.62	19.75	22.44	1.00	16.50	20.00		
11.6	19	0.38	11.83	12.84	0.61	9.71	11.01		

Table 8.3 ERD and depth dose data for points along the line OP in figure 8.1 for general equivalence between the reference schedule (a), (N _r :d _r) (12.05:2.93Gy) and the regime consisting of (b), (N ₁ :d ₁) (10:1.52Gy) and (c), (N ₂ :d ₂) (5:4Gy)										
Distance OP	%Depth Dose (DD)	d _r (Gy) 2.93× %DD (a)	ERD _r (Gy) Tumour ref (a)	ERD _r (Gy) Late ref (a)	d ₁ (Gy) 1.52× %DD (b)	ERD ₁ Tumour Alt. (b)	ERD ₁ Late Alt. (b)	d ₂ (Gy) 4.00× %DD (c)	ERD ₂ Tumour Alt. (c)	ERD ₂ Late Alt. (c)
4.2	100	2.93	45.65	69.79	1.52	17.51	22.90	4.00	28.00	46.67
5.9	95	2.78	42.81	64.54	1.44	16.47	21.31	3.8	26.22	43.07
6.3	90	2.64	40.21	59.81	1.37	15.58	19.96	3.60	24.48	39.60
6.8	80	2.34	34.79	50.19	1.21	13.56	16.98	3.20	21.12	33.06
7.4	70	2.05	29.77	41.58	1.06	11.72	14.34	2.80	17.92	27.07
8.5	66	1.93	27.74	38.22	1.00	11.00	13.33	2.60	16.68	24.82
10.0	62	1.82	25.92	35.23	0.94	10.28	12.34	2.50	15.47	22.65
10.8	61	1.79	25.43	34.44	0.93	10.16	12.18	2.44	15.18	22.12
11.0	58	1.70	23.97	32.09	0.88	9.57	11.38	2.32	14.29	20.57
11.2	52	1.52	21.10	27.60	0.79	8.52	9.98	2.08	12.56	17.61
11.3	46	1.35	18.46	23.59	0.70	7.49	8.63	1.84	10.89	14.84
11.4	39	1.14	15.30	18.96	0.59	6.25	7.06	1.56	9.02	11.86
11.5	31	0.91	11.96	14.29	0.47	4.92	5.44	1.24	6.97	8.76
11.6	19	0.56	7.12	8.01	0.29	2.98	3.18	0.76	4.01	4.76

Chapter 9

Analysis of clinical treatments

9.1. Introduction.

Chapters 4, 5 and 6 discussed the use of the linear quadratic model to investigate general equivalence conditions between combinations of fractionated and continuous treatments using single point calculations. In chapters 7 and 8, it was shown that the concept of iso-effect surfaces allowed a 3 dimensional assessment of the changes in effect distributions to be obtained which was useful when comparing different treatment schedules. This chapter sets the findings of this thesis in the context of clinical results which have emerged in recent years.

9.1.1. Clinical results.

Clinical results will be drawn from the area of intracavitary brachytherapy (rather than external fractionated radiotherapy) because there have been some detailed studies recently published in this field. In addition, the types of absorbed dose profiles encountered with these treatments can be more easily modelled using mathematical functions and consequently produce a clearer picture of the changes in effect distributions (chapter 7).

9.1.2. Brachytherapy.

Developments in intracavitary brachytherapy over the last 15 years have made it possible to alter the treatment dose rate. However as dose-rate increases, damage to

tumour and normal tissues increases (for a fixed total dose), and does so with a gradient which depends on the radiobiological properties of that tissue (eg the α/β ratio). Therefore, any adjustment of total dose to maintain the same level of effect on a particular tissue when dose-rate changes, will necessarily have a different effect on any other tissue having different radiobiological properties. This has implications when treatment dose-rates increase in gynaecological brachytherapy. Because of this, it would appear from radiobiology theory that if a dose is chosen to maintain tumour (usually high α/β ratio) effect, this should lead to an increase in late effects (low α/β ratio) and maintaining the level of late effects should produce in turn an effective underdosing of tumour. This prediction implicitly assumes that the tumour experiences the same dose-rate as critical normal tissues. In practice, this is often not the case, especially in gynaecological brachytherapy because tumour and critical organs (bladder, rectum etc.) are separated in space. These spatial aspects have been insufficiently considered in discussion of dose-rate effects in gynaecological brachytherapy. The iso-effect analysis presented in this thesis has been designed to facilitate in-depth consideration of these effects.

Generally speaking, late responding tissues are more sensitive to changes in dose-rate than tumours and it was apparent by the mid 1980s that these differences in response could be, to some extent, offset by delivering the treatment as a series of fractions instead of a single fraction (Fowler 1990). Consequently, there has been much debate surrounding the introduction of new brachytherapy treatment schedules in order to determine the optimum number of fractions and dose per fraction (or total dose) which should be given at higher dose-rates (Fowler 1990, Dale 1991) in order to reproduce the effects observed at lower dose-rate.

Ultimately, only careful analysis of clinical data will determine these treatment parameters. Although definitive clinical trials are still not available, there have been reports in the literature which give some indication of the trends involved. From these it is clear that increasing the treatment dose-rate from LDR to MDR (Jones et al, 1990) or HDR (Orton, 1991; Patel et al, 1994) does not necessarily lead to an unacceptable increase in late effects even if the level of tumour control remains the same as with LDR.

Iso-effect calculations predict that single treatments of continuous radiotherapy which are matched for tumour effects at some point, will in general be mismatched for effects on late responding tissues at the same point and vice versa. This is apparently a dilemma which lies at the heart of any attempt to substitute one treatment with another and appears to contradict the clinical findings which show that similar results on both tumour control and morbidity can be obtained in spite of the predicted mismatching of effects. It has been shown in this thesis for the first time that a study of iso-effect surface movements can produce a better understanding of how the effect distribution changes with treatment parameters, and how the spatial relationships of the tumour and critical normal organs enter into the problem. The use of iso-effect surfaces sometimes shows that, when going from low to higher treatment dose-rates, the predicted clinical outcome may differ from that reached on the basis of a calculation at any single point. For all biological effect calculations in this chapter tissue parameters used are as stated in Table 9.3(a), columns 3 and 5.

In this chapter four clinical studies are considered which cover two different dose-rate transitions:

1) Transitions from LDR to MDR.

a) In the Glasgow study (Jones et al 1990), a traditional (Manchester type) low dose-rate schedule was compared with a higher dose-rate treatment. Additional fractionated external beam treatment was given which was the same, regardless of the brachytherapy dose-rate.

b) In the Manchester study, conducted by the Christie Hospital Group (Hunter et al 1991), a traditional (Manchester type) LDR schedule was replaced by a series of MDR schedules each with different total doses. This study did not involve the use of external beam radiotherapy and compares the effects of intracavitary treatments alone.

2) Transitions from LDR to HDR.

a) The Orton report (Orton et al 1991) represents a survey of some 56 centres where various LDR treatments had been replaced by HDR treatments. As in the case above, LDR and HDR intracavitary treatment was supplemented with identical external beam therapy, irrespective of the dose-rate at which brachytherapy was given.

b) In the Patel report (Patel et al 1993) the outcome of 246 LDR and 236 HDR treatments with identical external beam treatment were compared.

In all the above studies intracavitary treatment dose-rates were quoted with reference to the Manchester "A" point and possible differences in the insertion geometry at different dose-rates were generally ignored. In the discussion that follows, however, changes in geometry as reported in the literature will be included where appropriate.

The above clinical reports will be examined separately and in each case details of the changes in treatment parameters (i.e. dose-rates, treatment times and fraction number) will be stated along with the clinical findings. Following this the reasoning developed in previous chapters of this thesis will be applied to determine the expected radiobiological implications of the changes in treatment.

Analysis will be mainly concerned with the movement of iso-effect surfaces which resulted from schedule changes since these should reflect the observed clinical changes. General equivalence theory is also mentioned in the cases of the Glasgow and Orton studies to show the treatment parameters that would be necessary for absolute matching for one type of effect based on radiobiology theory.

The implications of these schedule changes derived from iso-effect movements will then be compared with the reported clinical findings.

9.2. Geometrical Effects

This refers to differences in geometry of the intracavitary insertions in different situations, aspects which have not been included in any biological effect analysis before this thesis. These clearly cannot be ignored since alterations in the treatment dose-rate are often accompanied by changes in applicator geometry. In the reports that follow it is assumed that there are no significant differences in either the dose-fractionation, or dose distribution pattern of any external beam components used and that geometrical changes are confined to the intracavitary insertion.

Two different categories of transition can be identified when considering insertions.

These are:

a) Transitions from using flexible applicators to using rigid applicators. The final orientation of flexible rubber intrauterine applicators and ovoids is often determined by patient anatomy and may show marked differences from the ideal geometry shown in figure 7.1 (chapter 7). On the other hand, afterloading carrier systems, (for example those used in Selectron equipment) are rigid, so flexing of individual applicators is not possible. In addition these carriers are fixed together and so do not move relative to each other. Although efforts may be made to devise a source loading at higher dose-rate which reproduces exactly that of the lower dose-rate treatment, it is clear that changes in geometry cannot be accounted for easily. In such cases movement of iso-effect surfaces between treatments of different dose-rates would arise from a combination of geometrical and radiobiological considerations.

b) Transitions where the carrier system is rigid at each treatment dose-rate and has the same or very similar geometry. Changes in the effect distribution in this case would arise mainly from radiobiological considerations. It must be mentioned however that HDR treatments make the retraction of sensitive tissues during treatment a feasible proposition and so this will introduce an additional geometrical effect.

When the concept of afterloading was first introduced, transitions of the type described in a) were the most common and this is the situation which applies in the first two reports discussed in this chapter i.e. Glasgow (Symonds et al, 1989; Jones et al, 1990) and Manchester (Hunter et al, 1991). However since afterloading is now widely

used, transitions of type b) are perhaps the most common and is this is the case in the Patel report (Patel et al, 1993). The Orton study (Orton et al 1991) is assumed to be a combination of both since it does not give details of changes in geometry.

It is often assumed that when changing from LDR to HDR for example, it is the geometry that has the dominant influence on the outcome rather than radiobiological factors (Orton, 1993). This assumption is examined more closely in this chapter by determining movement caused by changes in the schedule parameters, using the method described earlier in chapter 7 (section 7.3.4.) and then comparing this with movement caused by changes in geometry.

Geometrical changes in transitions of type a) (flexible to rigid applicators) above have been reported in the literature (Jones et al, 1987) when the traditional radium applicators were replaced by Selectron afterloading applicators. The main features of this movement in the lateral view are summarised in figure 9.1. for patients where both insertions matched in terms of applicator size. The Selectron insertion was displaced with respect to the traditional radium applicators as follows:

- i) The tip of the uterine tube was more anterior in the pelvis (median difference 11 mm).
- ii) The cervix was more caudal in the pelvis (median difference 10 mm).
- iii) The cervix was more anterior in the pelvis (median difference 18 mm).
- iv) The ovoids were more anterior in the pelvis (median difference 10 mm).
- v) The separation between the ovoids was increased (median difference 9 mm).

9.2.1. Position of sensitive organs

In moving forward in the pelvis (i.e. in the Selectron treatment) the applicators move towards the bladder, ureters and the urethra but away from the anterior rectal wall but it cannot be assumed that these organs move with the applicators. Factors such as the connections between the organ structures as well as previous surgery or disease infiltration together with the difficulties of identifying identical soft tissue points between different radiographs make it impossible to say exactly how they move (Jones et al, 1987). Direct comparison of absorbed radiation dose to organs in these circumstances and therefore detailed biological effect analysis requires better methods of imaging, such as CT scanning, with applicators in place.

A study conducted by Lukka et al (1987) used CT scans to determine the distance from the central tube to the posterior wall of the bladder in 59 patients undergoing intracavitary radiotherapy treatment. This distance ranged from 15 mm to 42 mm and these authors stress that the position of the bladder is variable and recommend that it must be defined in each case and cannot be assumed to occupy a standard position. These results will be used later in this chapter.

9.2.2. Geometry versus radiobiology

From the above results it is possible to conclude that where geometrical changes occur in different insertion treatments these can have a dominant influence on the biological effect distributions especially at short ranges. This can be seen by recalling the movement of iso-effect surfaces shown in chapters 7 and 8. If 4 to 6 fractions of HDR treatment replaces an LDR treatment then the maximum displacement of the iso-effect surfaces is around 4 or 5 mm, at a distance of 5 cm out from point P (see figures 7.11,

7.12 and 8.12), due to radiobiological considerations alone. Displacement due to alterations in geometry may be up to 4 times this value (see figure 9.1. and iii) above) at the same point if results reported above are typical (Jones et al, 1987). Increasing the fraction number beyond 6 may not result in any significant difference in overall matching of effects, where treatment dose-rates are altered. This perhaps indicates one reason why a successful transition from LDR to HDR can be achieved with only a few HDR fractions and that it is unnecessary and inappropriate to use fraction numbers as large as those predicted by the Liversage relationship (see chapter 7, section 7.4).

It should be stressed however that the above comments only apply to transitions of type a) where geometrical factors are significant and even then the movement of iso-effect surfaces are caused by changes in both geometry and treatment parameters. Changes in iso-effect surfaces due to alterations in treatment parameters alone can produce large changes in the volume enclosed by these surfaces especially at short distances (see chapter 8, section 8.5). Clearly the contribution of both factors has to be considered carefully when changes are being assessed and these are included in the following clinical reports.

9.3. Glasgow study (Symonds et al 1989; Jones et al 1990)

This study reports comparative results with some 240 carcinoma of cervix patients treated at two different dose-rates. Of these, 100 patients were treated using a reference LDR technique based on the traditional (Manchester) method (assumed in this case to be 0.55Gy/hr) and 140 were treated with an afterloading device (Selectron) at a higher dose-rate (in the range 0.8Gy/hr to 1.4Gy/hr at point A). Patients were staged using FIGO criteria following examination under anaesthetic, cystoscopy, chest x-ray and IVP.

A summary of treatment for different stages of disease is shown in table 9.1 and the relative numbers of patients treated in each dose-rate band are shown in table 9.2.

Stages I and II were treated with two insertions one week apart. If manually inserted (traditional Manchester) caesium was used then the total dose to the A point was 60Gy (for a dose-rate of 0.55Gy/hr). Following this, external beam treatment was given over a 3 week period using parallel opposed square fields arranged such that the diagonal of the square aligned along the patients mid-line ("Cervix diamond" configuration (Cowell & Laurie, 1967)). The external beams were intended to treat the pelvic wall and a specially shaped shielding block was used to reduce the dose to the region already treated by the insertion (see figure 9.3). A further dose of 16.5Gy was given to the A points in this way (i.e. 15 fractions of 1.1Gy per fraction).

More advanced lesions (bulky stage IIb, stage III and stage IVa) were treated with a four field box treatment giving 42.5Gy to the whole pelvis in 20 fractions (i.e. 2.125Gy per fraction). This was followed by a single intracavitary insertion giving 33.5Gy to the A point (for a dose-rate of 0.55Gy/hr).

Where manually inserted caesium was replaced by Selectron afterloading treatments the treatment time and hence the total dose was reduced in accordance with the predictions of the CRE formula described in chapter 2, (section 2.3) and later in chapter 4 (appendix 4.1). This can be expressed for continuous treatments in the form:

$$T_2 = T_1 \left(\frac{R_1}{R_2} \right)^{\frac{1}{0.17}} \quad \text{----- 9.1}$$

Where T_1 and T_2 are the treatment times at dose-rates R_1 (reference dose-rate) and R_2 (Selectron dose-rate) respectively.

In Glasgow therefore two continuous reference schedules were used (see table 9.1):

a) Total dose of 60Gy, given in two fractions of $T_1 = 54.54$ hr per fraction and dose-rate of $R_1 = 0.55$ Gy/hr for stages I and II.

b) Total dose of 33.5Gy, given in one fraction of 60.91hr and a dose-rate of 0.55Gy/hr for stages IIb, III and IVa. (stage IIb tumours which were greater than 5cm in diameter were treated as stage III.)

The reference schedule for a) above is shown as the top row in table 9.3(a) and Selectron dose-rates are shown in column 1 with treatment times calculated using equation 9.1 shown in column 2. The corresponding figure for reference b) above is shown in columns 1 and 2 of table 9.3(b). In this study, the position of the Selectron (higher dose-rates) sources was chosen to produce iso-dose patterns as similar as possible to that of the standard Manchester reference (lower dose-rates) and external beam therapy was not altered as the intracavitary dose-rate increased.

The authors reported that patients treated using traditional Manchester dose-rates seemed to fare better than those at higher dose-rates in terms of local recurrence-free survival, a finding which appeared to be most marked in stage II. This apparent difference, however, proved not to be statistically significant. Selectron patients tended to have bigger tumours and this can account for most of the difference in recurrence rate. These authors conclude that both intracavitary techniques yield similar results,

though there remains a non-significant trend towards higher recurrence rates (especially in association with distant metastases) with Selectron therapy.

Late effects seen in patients treated in this trial were scored as follows:

Grade 1: Mild complications requiring only outpatient treatment.

Grade 2: Moderate complications requiring in patient treatment or investigation.

Grade 3: Severe complications involving major structural abnormalities usually requiring operative correction. The incidence of complications in this trial was very similar for both intracavitary techniques but when assessed in terms of severity the Selectron seemed to produce the more severe complications.

9.4. Iso-effect analysis for the Glasgow data.

9.4.1. ERD calculations: single point.

Before applying the theory derived in this thesis to the study above, it is possible to gain an impression of the resulting effects of the schedule alterations by performing single point ERD calculations at point A for the various schedules involved. These have been calculated in this chapter using equation 2.17 and the results are shown in columns 3 and 5 of tables 9.3(a) and 9.3(b). Percentage differences in tumour ERD values between reference and Selectron schedules are shown in columns 4 and 6 of the same tables. It can be seen that for tumour effects in stages I and II (table 9.3(a)), the Selectron (higher dose-rate) treatments produce a reduced value of ERD which ranged from -11.49% to -24.58%, at the A point. This would suggest that the higher dose-rate treatment is less effective for tumour at the reference point. Values of the ERD corresponding to late responding tissues show a slight increase in their ERD value at A: percentage differences between ERDs ranges from +1.14% to +5.50%. This is

consistent with the fact that the CRE correction to total dose when dose-rate changes leads to schedules which are roughly iso-effective for late responding tissues (O'Donoghue, 1986). The same trend is seen for stages IIb, III and IVa in table 9.3(b) as for the previous stages, i.e. roughly matched late effects and apparent reduced tumour effects when ERDs are compared.

The implications of the changes in treatment parameters of this report will now be examined using the theory derived in chapters 4 to 6 for single point calculations and in chapters 7 and 8 for iso-effect surfaces.

9.4.2. General equivalence.

It is possible to calculate alternative treatment parameters at higher dose-rates (using the relationships derived in chapter 6, table 6.1), which would result in equivalence for tumour or late responding tissues.

Using the relationships shown in chapter 6, table 6.1:

$$\frac{\sum_{p=1}^{p=a} 2R_p^2 T_p S_p (1/(\mu))}{\sum_{p=1}^{p=a} R_p T_p} = \frac{2}{\mu} R_R S_R \text{ ----- } 9.2$$

$$\frac{\left(\sum_{p=1}^{p=a} R_p T_p \right)^2}{\sum_{p=1}^{p=a} 2R_p^2 T_p S_p (1 / (\mu))} = \frac{\mu T_R}{2S_R} \text{----- 9.3}$$

Where R_R and R_p correspond to the reference and higher dose-rate values respectively and T_R and T_p the treatment times for these two alternatives respectively.

Here $S = (1 - (1/\mu T)(1 - \text{EXP}(-\mu T)))$ and $p = N$ the number of fraction at the new, higher dose-rate.

If we consider only one fraction of the reference schedule equation 9.2 reduces to:

$$R_N S_N = R_R S_R \text{----- 9.4}$$

and equation 9.3 reduces to:

$$(N_N T_N) / S_N = T_R / S_R \text{----- 9.5}$$

Rearranging 9.4 gives:

$$S_N = R_R S_R / R_N \text{----- 9.6}$$

For the purposes of these calculations, a value of $R_N = 1.26 \text{ Gy/hr}$ was used (see the last row of tables 9.3(a) and (b)). This represents the mean dose-rate weighted in accordance with the patient numbers in each Selectron dose-rate band (tables 9.2, 9.3).

Values of $R_R = 0.55 \text{ Gy/hr}$, $T_R = 54.54 \text{ hr}$ (i.e. stage I and II reference) and $R_N = 1.26 \text{ Gy/hr}$ were then substituted into equation 9.6 which was solved iteratively to give T_N for different values of μ . These values were then substituted into equation 9.5 to give the corresponding fraction number, N_N . Each value results in two distinctly different treatment schedules, one for each value of μ :

General equivalence results for stages I and II

a) Matching for tumour effects requires $N_N = 25.515$ fractions each with a treatment time of $T_N = 0.898$ hrs.

b) Matching for late effects requires $N_N = 9.079$ fractions each with a treatment time of $T_N = 2.622$ hrs.

Both schedules lead to the same total dose of 30 Gy to the A point. The most obvious feature of these results is the large fraction number, especially for matching of tumour effects. It must be stressed that these results represent the alternative treatment schedule for only one fraction of the reference schedule and to produce the same effect as both fractions of the reference then it would be necessary to deliver a) or b) twice depending on which type of matching was required. It is of course impossible to give such large fraction numbers because of practical limitations including patient compliance. Indeed in the case of this report only one higher dose-rate treatment is used

in place of each reference and yet acceptable clinical results were obtained, a finding which seems at variance with the general equivalence predictions and to a lesser extent those of the simple ERD calculations of section 9.4.1. The factors associated with this apparent disagreement will be discussed later.

9.4.3. Movement of iso-effect surfaces for the Glasgow study.

Stages I and II.

The method outlined in chapters 7 and 8 is now used to compare the different schedules of the Glasgow report for stage I and II treatments. In doing so the assumption is made that the contribution to biological effects from the external beam treatment at LDR (about 0.55 Gy/hr) and higher dose-rate (from 0.8 Gy/hr to 1.4 Gy/hr) is identical so that any changes in tumour or late effects arise from the change in continuous treatment. This assumption is reasonable since, at any point along PP', the ERD value for any tissue from the external beam treatment is the same for both of the treatment regimes.

Initially any differences in geometry of insertions are ignored, which means that the overall intracavitary dose distribution is taken to be the same for both low and higher dose-rate and a single scaling factor can be used to convert dose-rates at specific points (see chapter 7, section 7.3.4 and chapter 8, section 8.5). Geometrical differences in the insertions are however considered later. The movement of iso-effect surfaces is calculated along the line PP'(i.e. a line from the Manchester P point running out through the A point, see section 7.3.4.) and the same relationship between dose-rate and distance along this line is assumed as in chapter 7 (equation 7.5). The computer programme used to calculate movement is listed in appendix 9.1.

A reference schedule of 0.55Gy/hr and 54.54hrs per fraction was used with an alternative schedule of 1.26Gy/hr and 16.97hr per fraction to represent the transition that took place for stages I and II. The latter time was calculated using the CRE relationship in equation 9.1. and using the reference schedule parameters. Movement of iso-effect surfaces is plotted in figure 9.4.

Using the method described in chapter 8, section 8.5, changes in the enclosed volume arising from this movement were also calculated. This was done by referring to a plot of enclosed volume as a function of dose-rate for a standard insertion with a dose-rate of 0.55Gy/hr at the A point. A standard (Manchester type) radium insertion was assumed to be loaded as follows: one intra-uterine applicator tube, loaded superior to inferior with 15, 10 and 10 mg Radium (or Radium equivalent), plus two medium ovoids each loaded with 20 mg of Radium. The length of the tube was assumed to be 6.2cm with an ovoids spacing of 3cm, between mid points (including spacers). Dose-rate values corresponding to the new positions of the iso-effect surfaces are scaled by a factor of $0.55/R$, where in this case $R=1.26\text{Gy/hr}$ is the dose-rate at the A point for the alternative schedule. Using the scaled data the volume corresponding to specific dose-rate values can be obtained from the graph. In order to read the graphs more accurately they have been divided into three different regions, shown in figures 9.5(a) to 9.5(c) which when combined correspond to figure 8.11 in chapter 8. Data obtained in this way are plotted in figure 9.6.

In figure 9.4. positive values of iso-effect surface displacement correspond to outward movement (i.e. lateral displacement along the line PP') relative to their position using the reference schedule, and negative values inward displacement (i.e. medial displacement). Surfaces associated with late effects show an outward movement at

distances less than 2.55 cm on PP' and an inward movement at greater distances. Over the range of values plotted, movements associated with tumour iso-effect surfaces are all inward; this would suggest a less effective treatment compared with the reference low dose-rate schedule. The Glasgow group felt that there was a trend, though not statistically significant, towards reduced local control in the higher dose-rate case.

As can be seen the plot for late effects crosses the distance axis (zero displacement) near point A. For exact agreement with the CRE model this crossing point would be at A and the difference is due to a slight disagreement between the effective tissue parameters of the CRE and LQ models. Figure 9.4 shows that late effects are matched at a single point. In three dimensions this would correspond to a ring lying around the insertion in the same plane as the A points. *The LQ model with the parameters used here predicts the ring diameter would be 5.1 cm (i.e. $2 \times 2.55\text{cm}$). The therapeutic advantage or disadvantage depends on where sensitive organs are situated in relation to this ring.*

Inwards from this ring, late iso-effect surfaces would move outwards, so that the treatment should have a slightly higher probability of late damage whereas outside the ring the movements are in the opposite direction, reducing the probability of late damage. Tumour iso-effect surfaces all move inward suggesting a probability of less effective treatment.

Effects caused by changes in enclosed volume are being given increased emphasis (Hilaris, 1994). Percentage changes in enclosed volume caused by the movement of iso-effect are shown in figure 9.6 and reveal that the pattern of movement of iso-effect surfaces described in figure 9.4 can lead to considerable changes in the enclosed iso-effect surface. Once again matching is seen at a distance of 2.55 cm (i.e. zero volume

change) for late effects; trends suggested in figure 9.4 are also apparent. Linear displacements of the order of a millimetre can lead to enclosed volume changes of 30%. This is especially true at short ranges where enclosed volumes are small. Comparing figure 9.4 and 9.6 it can be seen that for late effects movement of between +0.1 cm (short range) and -0.7 cm (longer range) in the lateral direction produces a $\pm 30\%$ change in enclosed volume. Beyond the match point the late iso-effect surfaces show a volume reduction and go through a minimum at around 7 cm. As indicated by the medial movement of all tumour iso-effect surfaces in figure 9.4, enclosed tumour volumes are all reduced.

The iso-effect movements predict a clear therapeutic loss especially at distances less than 2.55cm from P along PP'. In this region there is a higher probability of late effects and a lower probability for effective treatment of the tumour than at the reference schedule. At distances greater than 2cm, although the probability of late effects falls off steadily so does that for effects on tumour; if the late effect incidence had already been clinically acceptable this will result in a net therapeutic loss.

9.4.4. Movement of iso-effect surfaces for complete matching of either tumour or late effects.

Earlier in the chapter (section 9.4.2., general equivalence) alternative schedules with a dose-rate of 1.26Gy/hr were devised for the reference schedule (stages I and II) which gave complete matching for tumour and late effects. These schedules are now analysed in the same way as above to produce iso-effect movement plots and percentage changes in volume with respect to the reference for stages I and II. The results are

summarised for the matching of tumour effects in figures 9.7 (movement) and 9.8 (percentage volume change), and for the matching of late effects in figures 9.9 and 9.10 respectively. Although mainly of academic interest, these results provide a useful check on the methodology since in these cases tumour or late effects surface displacements should be zero depending on which effect is matched. In actual fact displacements are not exactly zero and this is due to small truncation and rounding errors in the calculation, but these can be regarded as negligible.

Matching for tumour effects produces a tumour iso-effect displacement plot which lies along the distance PP' axis figure 9.7. Late iso-effects are all displaced in a medial direction. Over the major part of the range of interest this displacement varies from 2.5 to 4.5 mm. This would indicate that if complete matching for tumour effects was achieved then it would result in less late damage over the entire range of interest. These results translate to no change in tumour iso-effect volume and a decrease in all late iso-effect volumes, see figure 9.8. Such conditions would represent a therapeutic gain.

Matching for late effects produces a plot of tumour effect displacements which are all in the lateral direction along PP' , see figure 9.9. Displacement of tumour surfaces is always less than 1 mm and this produces volume changes which are greatest at short range and rapidly drop off with distance along PP' . In this case there are no changes in late iso-effect volumes. In theory this treatment should produce identical late effects and perhaps a slight increase in tumour effects. This also represents a therapeutic gain.

It must be remembered that the results in this section are really included as a check of the methodology used to calculate the movement of iso-effect surfaces and that the number of fractions would be too large to be used in practice (see section 9.4.2.). It is obvious from figures 9.7. to 9.10. that these equivalence conditions do not lead to a ring

of matched points for either tumour or late effects as was the case for the actual transition described in the Glasgow study (see section 9.4.3.). This is because the plots of movement do not cross the distance axis in figures 9.7 (for late effects in figure 9.8 as they do in figure 9.4.).

9.4.5. Iso-effect analysis for stages IIb, III and IVa of the Glasgow study.

These stages from the Glasgow report were treated with a single reference or alternative schedule, see tables 9.1 and 9.3(b). The same alternative dose-rates were used as in the previous staging. Table 9.3(b) shows the results of ERD calculations for the different dose-rates and the percentage differences compared with the reference schedule. These produce similar results to those displayed in table 9.3(a). Once more an average dose-rate of 1.26Gy/hr was chosen to represent the alternative higher dose-rate schedule and using the CRE formula this led to a treatment time of 18.95hr.

General equivalence analysis was used to predict the treatment parameters at the higher dose-rate which would produce exactly the same tumour or late effects as the reference LDR schedule using the procedure outlined in section 9.4.2. These results are:

a) Matching for tumour effects requires 29.550 fractions each with a treatment time of 0.900 hrs.

b) Matching for late effects requires 10.074 fractions each with a treatment time of 2.639 hrs.

These in turn were analysed using the method above to determine the movement of the iso-effect surfaces. It was found that the displacement results were identical which

is due to the fact that the dose-rate transition (0.55Gy/hr to 1.26Gy/hr) is the same in both cases. Only the new general equivalence treatment parameters have changed and all comments arising from the discussion of figures 9.4 and 9.7 to 9.10 are applicable to these results.

The foregoing radiobiology analysis would suggest for both arms of the Glasgow study (stages I and II and stages IIb, III and IVb) that late effects at higher dose-rate should match the reference schedule at least near the A point but that tumour effects should be less, in other words a therapeutic loss compared to the reference schedule.

9.4.6. Iso-effect surface movement with geometrical changes included

Bladder complications

In a recent and more detailed Glasgow analysis, soon to be published, severe morbidity trends for specific tissues have been determined and these are shown in table 9.4. In this table three different Selectron treatments are shown numbered 1, 2 and 3, these refer to three treatment dose-rate ranges indicated. The first two ranges were reported in Jones et al (1990) and the third was derived from an analysis of more recent results.

An increase in severe complications is clearly shown in table 9.4. and this trend is most marked for bladder. Because of this, and the fact that data exist which allow the position of the bladder relative to the central tube to be estimated (Lukka et al, 1987), it is worthwhile to see if the movement of late iso-effect surfaces can explain increased bladder complications.

It will be assumed that geometrical changes in these insertions are similar to those shown in figure 9.1. (see section 9.2). This is because the arrangement of flexible and

rigid applicators used in Glasgow are similar to those used by Jones, Notley and Hunter (1987) in Manchester. Until now the movements of iso-effect surfaces have been plotted along the line from point P, in a lateral direction through point A to some arbitrary point P', which gave the lateral or medial movement of surfaces. In this case it is necessary to calculate movement in the anterior or medial direction along the lines B_{Man} to B' and B_{Sel} to B' running out from the insertion to the posterior wall of the bladder as shown in figure 9.2.

The degree to which the applicators are flexed in figure 9.2. is clearly different and therefore it will no longer be possible to use one function to represent the relationship between dose-rate and distance (see equations 7.4 and 7.5). Two relationships were used to model the dose-rate profile, one corresponding to the direction B_{Man} to B' (Manchester radium) and another to the direction B_{Sel} to B' (Selectron). These were obtained in the same way as equation 7.4 by using an IGE Data General planning computer using standard source strengths for both arrangements as shown by Jones et al (1987) and are (see figure 9.2):

Along B_{Man} to B', distance (X) as a function of dose-rate (R):

$$R = 2.1 \times \text{Exp}(-1.48X) + 1.12 \times \text{Exp}(-0.3X) \text{ ----- } 9.7$$

Along B_{Sel} to B', dose-rate (R) as a function of distance (X):

$$X = 7.85 \times \text{Exp}(-4.1R) + 5.87 \times \text{Exp}(-0.647R) + .63 \times \text{Exp}(-0.0032R) \text{ ----- } 9.8$$

The total movement of late iso-effect surfaces can be calculated in two parts. Firstly that due to a combination of treatment parameter and orientation changes and secondly

that due to translational displacement of the insertion in a general anterior direction. These can be seen by considering figure 9.1.

The contribution of treatment parameters and orientation can be plotted by using equations 9.7 and 9.8 above. At any point along $B_{Man} - B'$, the dose-rate can be determined from 9.7 and hence the late effects ERD calculated. The dose rate corresponding to this ERD at the new higher dose-rate, for the Selectron insertion, can be determined using equation 7.3. Finally the position at which this dose-rate occurs along $B_{Sel} - B'$ can be found from equation 9.8 and this can be compared with the original position along the line $B_{Man} - B'$. The difference between these represents the movement of iso-effect surfaces due to changes in treatment parameters and orientation, in other words that which would result if the point B_{Sel} coincided with the point B_{Man} . A computer program which will perform the above calculation is listed in appendix 9.2.

Next the effects of the general anterior movement must be superimposed onto these values. In the region of the cervix the insertion has moved a distance of about 18 mm in the anterior direction. This means that if B_{Man} is considered to be the origin then 18 mm must be added to each late iso-effect surface movement at this point. The results for stages I and II of this report are shown in figure 9.11.

The lower curve shows the movement corresponding to the first stage, that is due to changes in treatment parameters and changes in orientation. The match point is now just less than 1.0 cm out from B_{Man} and not at 2.55 cm as would be expected when there was no change in geometry. This is perhaps to be expected since the Selectron insertion is straighter than the Manchester radium insertion and this will pull the match point inwards towards the Selectron insertion along this line. Since it is reasonable to

assume that the dose-rate profile has not changed along the line PP' (ie running from P in a lateral direction) for either insertion, in this direction the match point would still be at 2.55 cm as in the case for identical geometry. Flexing of the applicators therefore would appear to change the matching "ring", mentioned earlier, to an "ellipse".

Next the effect of the anterior translation of the insertion is accounted for by adding 18 mm to the movement at each point. This produces the upper curve in figure 9.11 and represents the overall movement of late iso-effect surfaces when B_{Sel} occupies a position 18 mm from B_{Man} along the line B_{Man} to B'. It can be seen that indeed the effects of geometrical changes can produce large changes in the overall effect distribution as would be expected. It can also be seen that at close range geometrical factors dominate (ie at between 4 to 6 cm) and at longer ranges radiobiological effects are comparable. The end result can only be seen by combining both.

The results reported by Lukka et al (1987) can now be included and the range of posterior bladder wall positions relative to B_{Sel} for all patients studied is shown in the hatched area in figure 9.11. The posterior bladder wall occupies a region where the late iso-effect surfaces have moved in an outward direction relative to their position when the Manchester radium insertion was used. This would indicate an increase in late bladder effects and if the geometry in this clinical report is similar to that reported by Jones et al (1987), this could indeed account for the increase in observed bladder complications shown in table 9.4.

Clearly a more detailed study would be required to show exactly how the effect distribution is changing in any individual case. These results show that if changes in scheduling are contemplated then the relative position of all sensitive tissues would have

to be determined using some means such as CT scanning in order to predict the outcome.

9.5. Manchester study.

The Christie Hospital (Manchester) group have now reported the results of a study involving 531 cancer of cervix patients (stage I and IIa) treated from 1980 to 1985 with intracavitary insertions alone (Stout, 1989; Hunter, 1994). Patients were randomised to receive either two manual radium insertions (nominal dose-rate of 0.53 Gy/hr at point "A") or two insertions using a Selectron afterloading system (average dose-rate of 1.6 Gy/hr at point "A"). In the case of Selectron treatments, a number of correction factors were applied to the total dose in an attempt to determine the optimal correction factor appropriate for the dose-rate transition. These reduction factors, ranging from no reduction to 19% reduction, are shown in column 1 of table 9.5 which also shows the parameters of the various schedules involved.

Between 1980 and 1982 the 0% and 6% factors were in use but these were discontinued at the end of this period because of a marked increase in late morbidity. The observed morbidity levels were 57% and 35.7%, respectively compared to a level of 11% with manual radium treatments at that time.

Between 1982 and 1985 correction factors of 12.5% and 19% were applied and a recent analysis of a group of 232 of these patients (stages Ib and IIa) was reported by Hunter et al (1994). This revealed no true difference in overall result compared to

manual radium insertions which led to the conclusion in this case that the optimal correction factor for late equivalence lay between 12.5% and 19%.

9.6 Iso-effect analysis of Manchester data.

9.6.1. ERD calculations: single point.

ERD calculations at point "A" for the various schedules in this report are shown in table 9.5, along with the percentage difference in ERD with respect to the manual insertion at this position (columns 5 and 7). For tumour these range from -9.21% (19% correction) to 13.65% (0% correction) and for late responding tissues 39.88% to 77.92% respectively. In the case of late effects, reducing the total dose by 19% reduces the increase in ERD value, caused by the higher dose-rate treatment, by about 50% (relative to that arising from 0% correction). The initial high level of ERD value for late effects and the magnitude of the reduction broadly agree with the clinical findings but these values are only calculated at one point and may not reflect the consequences of schedule changes at other points.

9.6.2. Movement of iso-effect surfaces for the Manchester study.

The movement and changes in enclosed volume of iso-effect surface for the higher dose-rate schedules in this study were calculated along the line PP' using the method in section 9.4.3. assuming no changes in geometry. These are shown for tumour and late effects in figures 9.12 to 9.15. The movement of tumour iso-effect surfaces for different levels of reduction in total dose are shown in figure 9.12 The plot for 0% correction is

relatively flat with movement in the outward direction along PP' of between 1mm to 2mm. As the total dose is reduced the curves become steeper and cross the horizontal axis at progressively shorter distances. As this happens the inward movement increases and the maximum is about 9mm at 8cm along PP' (19% correction).

Late iso-effect movement is almost all in the outward direction. This is most marked for the 0% correction plot. All curves go through a relative peak at between 2cm to 4cm along PP'. The shape of these late effect movement curves is quite different from that seen in the Glasgow study (figure 9.4) and also those associated with the transition between LDR and HDR that follow. Outward movement of the late effect curves in this case is consistent with increased levels of morbidity especially where the dose reduction factor is low. The lower the dose correction factor the flatter the peak and the further it occurs along PP'.

Figure 9.14 shows the corresponding percentage change in enclosed volume resulting from the movement of tumour iso-effect surfaces. The familiar pattern is seen where the greatest percentage volume changes are seen at short distances along PP', these range from about 14% (19% dose correction) to about 57% (0% dose correction). Between 2cm and 4cm along PP' the extremes of change are between $\pm 20\%$.

Percentage changes in volume for late effects are shown in figure 9.15. Here large changes in volume can be seen especially for small dose reductions. These typically lie between 71% (19% dose correction) and 112% (0% dose correction). At distances between 2cm and 4cm along PP' volume changes vary between 72% and 8.5%.

The effects of geometrical differences in the insertions can be estimated using the same technique as in section 9.4.3. and by referring to figures 9.1. and 9.2. The total movements of late iso-effect surfaces are plotted in figure 9.16. As in the case of the

previous report these surfaces show an outward movement over the range of positions occupied by the posterior wall of the bladder as determined by Lukka et al (1987). This is true for all values of the correction factor and would suggest that an increase in bladder complications would be expected in the transition described in this report.

9.7. The Orton survey.

A survey of centres which had used both low dose-rate (LDR) and high dose-rate (HDR) was conducted by Orton et al (1991). Over 17,000 treatments were included in the study which compared recurrence and morbidity rates for LDR and HDR treatments. The scoring of morbidity levels was similar to that in the Glasgow study (section 9.3.), above, as were the survival criteria. Since the data were drawn from 56 institutions, treatment dose-rates varied both at HDR and LDR. The average values of number of fractions and dose per fraction at HDR, as well as treatment time and dose-rate at LDR are shown in table 9.6(a) and (b) for each stage. The grand average taken over all stages is also shown in the last row (all) of these tables. In this study the reduction in total dose in going from LDR to HDR ranged from 38.6% to 50.3%.

The effect of supplementary external beam treatments which were used was not taken into account and details of these are not reported. It was assumed by the authors that since no significant change was involved in external beam treatments between the two arms of the study then only intracavitary components needed to be considered.

As with the previous work, the Manchester A point was used to plan the treatment at both dose-rates.

For stage III disease there seemed to be a significant improvement in survival at HDR compared with LDR. Other stages showed no detectable difference. Complications were not broken down into stages and were merely grouped under the headings of severe and moderate-plus-severe. In all stages, complication rates were significantly less for HDR than for LDR.

The authors noted that the HDR treatments exhibited some geometrical advantage. This could be seen when the ratio of rectal or bladder dose to A point dose was compared for HDR and LDR. It was found that this ratio was lower for HDR; this is shown in table 9.7 along with the corresponding dose-rate ratios.

These authors concluded that HDR intracavitary therapy of the cervix is at least as good as LDR as far as survival data is concerned and perhaps a little better. Also normal late responding tissue toxicity is significantly better at HDR than with LDR.

9.8. Iso-effect analysis for Orton survey.

The results of the iso-effect analysis will be presented in the same order as that for the previous report.

9.8.1. ERD calculations: single point.

ERD calculations for tumour and late responding tissues for both LDR and HDR are shown in table 9.6(a) (columns 4 and 5) and (b) (columns 4 to 7). These show for both tumour and late response the ERD values at the A point are less for HDR than for LDR.

Theory derived from chapters 4 to 8 is applied here and the implications compared with the observations made in this clinical report.

9.8.2. General equivalence for the Orton survey.

Starting with grand average LDR schedule in table 9.6(a) (last row (all)) and assuming an HDR treatment dose-rate of 150 Gy/hr the following relationship from table 6.1, chapter 6, may be used to derive HDR schedules which are matched for tumour and late effects.

$$N_N = \frac{\left(\sum_{p=1}^{p=a} R_p T_p \right)^2}{\sum_{p=1}^{p=a} 2R_p^2 T_p S_p (1 / (\mu))} \quad \text{-----} \quad 9.9$$

where N_N is the number of fractions at HDR and R_p , T_p and S_p are the parameters of the LDR schedule. As before:

$$S = (1 - (1/\mu T)(1 - \text{EXP}(-\mu T)))$$

Since $p=1$ equation 9.8 reduces to the Liversage equation:

$$N_N = \frac{\mu T_R}{2S_R} \quad \text{-----} \quad 9.10$$

and since use of this relationship means that the total dose must remain constant when going from HDR to LDR for this level of equivalence:

$$N_N R_N T_N = R_R T_R$$

where R_R , T_R and S_R above now refer to the LDR schedule.

or

$$T_N = \frac{R_R T_R}{N_N R_N} \text{ ----- 9.11}$$

where R_N and T_N are the HDR parameters. Equations 9.10 can be solved for N_N , which in turn can be substituted into 9.11 to give the new times of the matched HDR treatments for tumour and late effects. The results in this case are:

a) Matching for tumour effects requires 55.175 fractions each with a treatment time of 0.00802 hrs.

b) Matching for late effects requires 18.477 fractions each with a treatment time of 0.02395 hrs.

As can be seen the above schedules have fraction numbers which are far outside the range of practical interest. These results are used in the next section on iso-effect surfaces.

9.8.3. Movement of iso-effect surfaces for the Orton survey.

Movement and enclosed volume changes of iso-effect surfaces were calculated by the same method as in section 9.4.3. Dose-rate versus volume plots in figures 9.5(a) to 9.5(c) were used and the dose-rate scaling factor in this case was $0.55/R$ where

$R=150\text{Gy/hr}$. The displacement of iso-effect surfaces and the associated changes in enclosed volume for the transition between the grand averaged LDR and HDR schedules in table 9.6(a) and (b) are shown in figure 9.17 (movement) and 9.18 (percentage change in volume). Tumour effect surfaces move outwards at distances shorter than 1.2 cm and inwards thereafter. Late effect surfaces are mainly inward moving, and move outward only very slightly at extremely short range. Volume changes in figure 9.18 show considerable expansion of tumour iso-effect surfaces at distances of less than 1.2 cm. Beyond this point, late iso-effect changes are all negative both for tumour and late effects.

From section 9.8.2. data for matched tumour effects are plotted in figures 9.19 (movement) and 9.20 (volume) while corresponding data for matched late effects are shown in figures 9.21 and 9.22. When tumour effects are matched, late iso-effect surfaces all move inwards. This is the same direction as those in figure 9.7 for the Glasgow data, but this time the movement is in general slightly greater. This leads to a greater change in enclosed volume comparing figures 9.20 and 9.8. This trend is continued in figures 9.21 and 9.22 where late effects are matched. There is a generally greater movement of the tumour iso-effect surfaces in the outward direction than was seen in the Glasgow report. The number of fractions which would require to be used is even farther outside of the practical range than those in the Glasgow report.

The trends noticed in the Orton study should be seen from the data in figures 9.17 and 9.18. Volume changes shown in figure 9.18 suggest that tumour lying less than 1 cm from the axis of the insertion should be treated more effectively at HDR, but that lying at greater distances should be treated less effectively than at LDR. This implies that small tumours would be treated more effectively and large tumours less effectively, at

HDR. Late effects on the other hand should usually be less at HDR than LDR since the volume changes are mostly negative. Orton reports that in terms of effectiveness the HDR treatment is as good as the LDR and possibly a little better. However significant improvements are found for late effects in Orton's study. As mentioned earlier the authors claim that there was some geometrical advantage of HDR over LDR in terms of reduced doses to sensitive structures (table 9.7). Without actual geometrical details it is not possible to include the influence of this here but it is clear that, even without this factor, movement of late iso-effect surfaces is almost all in the inward direction. This means that the iso-effect analysis alone would suggest a reduction in late effect morbidity.

9.9. The Patel study.

Patel et. al. (1994) conducted a randomised clinical trial to compare low dose-rate versus high dose-rate intracavitary treatments of carcinoma of the uterine cervix. This trial ran from 1986 to 1989 and involved 482 patients analysed for local control, 5 year survival and morbidity. Patients were divided into two groups both of which were given a mixture of intracavitary and external beam therapy:

Group I: Stage I and II patients where the main part of the treatment was given as intracavitary radiotherapy.

Group II: Stages III patients where the main part of the treatment was given as external beam radiotherapy.

Details of the treatment parameters which refer to point "A" are given in table 9.8. In this study the 5 year disease free survival rates showed no statistical difference but the retrosigmoid morbidity was less with HDR than with LDR.

9.10. Iso-effect analysis for the Patel data.

9.10.1. ERD calculations: single point.

ERD calculations were performed at point “A” for the treatment schedules in this group and these are shown in table 9.9. It can be seen that results are very similar between both groups with HDR schedules having a slightly lower tumour ERD and a slightly higher late effects ERD than corresponding LDR schedules results which do not readily explain the trends reported. As will be seen in the next section, this is because a single point calculation may not convey an overall picture of the effect distribution.

9.10.2. Movement of iso-effect surfaces for the Patel study.

Movement of iso-effect surfaces and resulting changes in enclosed volume for HDR schedules are plotted in figures 9.23 to 9.26. If corresponding plots are compared between groups it can be seen that they are very similar. This is not surprising since the average dose-rates and dose per fraction for LDR and HDR for both groups is almost the same with only the total dose approximately halved in each case. The pattern of change seen is similar to that shown earlier in the Glasgow and Orton reports. Also obvious is the fact that late effects do appear to be less at HDR than at LDR at distances greater than 3cm along PP' which was not obvious from the single point ERD calculations. Geometrical factors arising from changes in the shape of applicators can be ignored in this case since the Patel group used identical insertion geometry when going from LDR to HDR. However this group did retract sensitive organs during treatment at HDR and this will have introduced a geometrical factor, but since no details are available it is not possible to assess its effect.

9.11. Conclusions.

Continuous treatment schedules from four clinical reports have been examined in this chapter by performing ERD calculations at single points and by considering the movement of iso-effect surfaces and the resulting changes in enclosed volume.

The first conclusion possible is that consideration of iso-effect surfaces gives a far more complete picture of the changes that take place when the treatment dose-rates are increased than single point ERD calculations. This can be seen in Patel's report (section 9.10) where ERD calculations performed at point "A" seem to suggest a conclusion opposite to that of the clinical findings with respect to late effects. This stresses the fact that if only point calculations are to be performed their position must be chosen carefully, and that point A is not necessarily the most relevant single point to choose.

The direction of movement of iso-effect surfaces also suggests that increasing the treatment dose-rate need not always be accompanied by increases in morbidity levels in late responding normal tissues. This fact has begun to emerge from clinical reports but has always seemed at odds with conventional thinking in radiobiology, which may be a result of depending on single point calculations. Even more controversial is that the movement of surfaces with increased dose-rate can point to a reduction in morbidity levels for certain values of treatment parameters without loss of tumour effect, a finding which is emerging from clinical trials

Detailed agreement between clinical findings and surface movement does not always exist, particularly when the dose-rate transition is over a relatively short range (Glasgow and Manchester studies). This arises from a number of reasons. For example, tissue parameter values are not by any means firmly established and the effects of geometrical changes had to be ignored for this comparison. Agreement seems best in the

area of late responses and this is particularly true when going from LDR to HDR. However results have to be considered carefully since reduction in morbidity particularly at HDR could result from an ability to retract sensitive tissues away from sources more reliably than at LDR or MDR because of short treatment times (Patel et. al. 1993).

The movement of iso-effect surfaces can be used to look at trends which appear when treatment dose-rates are changed. The characteristic shape of the plots may be useful in assessing the effects of new scheduling. This can be seen in the previous clinical reports where successful transitions in dose-rate produced profiles which had a similar appearance (Glasgow, Orton and Patel studies), while a transition which resulted in a high level of morbidity (Manchester study) produced profiles which were manifestly different in appearance.

Accurate predictions based on mathematical models must await developments in the form of the models themselves and knowledge of tissue parameters. Even so this chapter has shown that iso-effect surfaces can be useful even if only to identify possible trends caused by changes in scheduling. This method can be used in conjunction with any radiobiological model and can continue to be used as more sophisticated models emerge.

9.12. Appendix 9.1: Program for calculating the movement of iso-effect surfaces along the line PP'.

```

10 REM ISMCH9 CALCULATES ISOSURFACES DATA VERSION 06 (CH9
    THESIS)--- 26/11/93 CD
20 LPRINT CHR$(12):CLS:PRINT"THIS PROGRAMME CALCULATES THE
    POSITION OF ISO-EFFECT SURFACES FOR NEW DOSE RATES RELATED TO
    SOME REFERENCE SCHEDULE":PRINT:PRINT
30 REM -----TISSUE PARAMETERS-----
40 INPUT"TISSUE PARAMETERS: ACUTE MU (1/hr) = ";UA:INPUT"LATE MU
    (1/hr) = ";UL:INPUT"ACUTE A/B (Gy) = ";AA:INPUT"LATE A/B (Gy) =
    ";AL:LPRINT"UA/UL AA/AL";UA;UL;AA;AL:LPRINT
50 REM -----REFERENCE SCHEDULE-----
60 INPUT"REFERENCE SCHEDULE: DOSE RATE AT REF. POINT (Gy/hr) =
    ";RF:INPUT"TREATMENT TIME PER FRACTION (hrs) =
    ";TRF:INPUT"NUMBER OF FRACTIONS =";NRF:PRINT
65 LPRINT"RTP DSRT/TRT T/FR N";RF;TRF;NRF:LPRINT
70 PRINT"NEW TREATMENT PARAMETERS"
80 INPUT"NEW TREATMENT TIME PER FRACTION (hrs) = ";TN:
    INPUT"NUMBER OF TREATMENTS = ";NN:INPUT"NEW DOSE RATE AT REF
    POINT";RN:PRINT
85 LPRINT"NTP TRT T/FR N/DSRT";TN;NN;RN:LPRINT
86 LPRINT"POSITION RRF DXACUTE DXLATE NDRA RNW
    NDRL":LPRINT
90 INPUT "DISTANCE FROM AXIS OF INSERTION =";XI:GOTO 320
100 SARF=(2/(AA*UA))*(1-(1/(UA*TRF))*(1-EXP(-
    UA*TRF))):ERCA=NRF*RRF*TRF*(1+RRF*SARF):PRINT"ERD ACUTE REF =
    ";ERCA
110 SLRF=(2/(AL*UL))*(1-(1/(UL*TRF))*(1-EXP(-
    UL*TRF))):ERCL=NRF*RRF*TRF*(1+RRF*SLRF):PRINT"ERD LATE REF =
    ";ERCL:PRINT
120 ERAT=ERCA:ERLT=ERCL
130 ENFA=0:ENFL=0
140 SANT=(2/(AA*UA))*(1-(1/(UA*TN))*(1-EXP(-UA*TN)))
150 SLNT=(2/(AL*UL))*(1-(1/(UL*TN))*(1-EXP(-UL*TN)))
160 LET RNIA = ((TN^2+4*TN*SANT*((ERAT-ENFA)/NN))^5-
    TN)/(2*TN*SANT):PRINT"OLD ACUTE ISOSURFACE IS NOW AT POSITION
    OF DOSERATE (Gy/hr) = ";RNIA
170 LET RNIL = ((TN^2+4*TN*SLNT*((ERLT-ENFL)/NN))^5-
    TN)/(2*TN*SLNT):PRINT"OLD LATE ISOSURFACE IS NOW AT POSITION OF
    DOSERATE (Gy/hr) = ";RNIL:PRINT
180 RA=(.56*(RNIA/RN)):XA=8.5*EXP(-17!*RA)+6.3*EXP(-4.2*RA)+2!*EXP(-
    .64*RA)
190 RL=(.56*(RNIL/RN)):XL=8.5*EXP(-17!*RL)+6.3*EXP(-4.2*RL)+2!*EXP(-
    .64*RL)
200 PRINT"MOVEMENT: OUTWARDS +VE"
210 DXA=XA-XI:PRINT"ACUTE MOVEMENT (CM) =";DXA

```

```

220 DXL=XL-XI:PRINT"LATE MOVEMENT (CM) =";DXL:LPRINT USING
"###.### ";XI;RRF;DXA;DXL;RNIA;RNW;RNIL:PRINT:PRINT
230 PRINT"SEPARATION: WRT ACUTE SURF. OUTWARDS +VE"
240 SEPN=DXL-DXA:PRINT"SEPN. =";SEPN
250 INPUT"ANOTHER YES(Y) OR NO(N)";A$
260 IF A$="Y" THEN GOTO 90
270 IF A$="N" THEN GOTO 280
280 INPUT"NEW PARAMETERS (P) OR EXIT (E)";B$
290 IF B$="P" THEN GOTO 10
300 IF B$="E" THEN GOTO 310
310 STOP
320 IF XI>=.2 AND XI<=.5 THEN LET RRF=2:LET RINC=.01:LET
TST=.001:GOTO 390
330 IF XI>.5 AND XI<=1 THEN LET RRF=1:LET RINC=.01:LET TST=.001:GOTO
390
340 IF XI>1 AND XI<=2 THEN LET RRF=.5:LET RINC=.001:LET
TST=.0001:GOTO 390
350 IF XI>2 AND XI<=3 THEN LET RRF=.3:LET RINC=.001:LET
TST=.0001:GOTO 390
360 IF XI>3 AND XI<=5 THEN LET RRF=.1:LET RINC=.001:LET
TST=.0001:GOTO 390
370 IF XI>5 AND XI<=8 THEN LET RRF=9.000001E-02:LET RINC=.001:LET
TST=.00001:GOTO 390
380 LET RRF=RRF+RINC
390 LET DIFF=8.5*EXP(-17!*RRF)+6.3*EXP(-4.2*RRF)+2!*EXP(-.64*RRF)-XI
400 IF DIFF>TST THEN GOTO 380
410 PRINT "RRF=";RRF:RNW=RRF*(RN/.56):RRF=RRF*(RF/.56):PRINT
"RRF=";RRF:GOTO

```

100

9.13. Appendix 9.2: Program for calculating the movement of iso-effect surfaces along the line B_{Man} to B' .

```

10 REM ISMCH9 CALCULATES ISOSURFACES DATA VERSION 06 (CH9
THESES)--- CD
20 PRINT CHR$(12): CLS : PRINT "THIS PROGRAMME CALCULATES THE
POSITION OF ISO-EFFECT SURFACES FOR NEW DOSE RATES RELATED TO
SOME REFERENCE SCHEDULE": PRINT : PRINT
30 REM -----TISSUE PARAMETERS-----
40 INPUT "TISSUE PARAMETERS: ACUTE MU (1/hr) = "; UA: INPUT "LATE
MU (1/hr) = "; UL: INPUT "ACUTE A/B (Gy) = "; AA: INPUT "LATE A/B (Gy) = ";
AL: LPRINT "UA/UL AA/AL"; UA; UL; AA; AL: LPRINT
50 REM -----REFERENCE SCHEDULE-----
60 INPUT "REFERENCE SCHEDULE: DOSE RATE AT REF. POINT (Gy/hr) = ";
RF: INPUT "TREATMENT TIME PER FRACTION (hrs) = "; TRF: INPUT
"NUMBER OF FRACTIONS ="; NRF: PRINT
65 LPRINT "RTP DSRT/TRT T/FR N"; RF; TRF; NRF: LPRINT
70 PRINT "NEW TREATMENT PARAMETERS"
80 INPUT "NEW TREATMENT TIME PER FRACTION (hrs) = "; TN: INPUT
"NUMBER OF TREATMENTS = "; NN: INPUT "NEW DOSE RATE AT REF
POINT"; RN: PRINT
85 LPRINT "NTP TRT T/FR N/DSRT"; TN; NN; RN: LPRINT
86 LPRINT "POSITION RRF DXACUTE DXLATE NDRA RNW
NDRL": LPRINT
90 INPUT "DISTANCE FROM AXIS OF INSERTION ="; XI
95 RR1 = 2.1 * (EXP(-1.48 * XI)) + 1.12 * (EXP(-.3 * XI)): RRF = (RF * RR1 / .55)
100 SARF = (2 / (AA * UA)) * (1 - (1 / (UA * TRF)) * (1 - EXP(-UA * TRF))): ERCA
= NRF * RRF * TRF * (1 + RRF * SARF): PRINT "ERD ACUTE REF = "; ERCA
110 SLRF = (2 / (AL * UL)) * (1 - (1 / (UL * TRF)) * (1 - EXP(-UL * TRF))): ERCL
= NRF * RRF * TRF * (1 + RRF * SLRF): PRINT "ERD LATE REF = "; ERCL:
PRINT
120 ERAT = ERCA: ERLT = ERCL
130 ENFA = 0: ENFL = 0
140 SANT = (2 / (AA * UA)) * (1 - (1 / (UA * TN)) * (1 - EXP(-UA * TN)))
150 SLNT = (2 / (AL * UL)) * (1 - (1 / (UL * TN)) * (1 - EXP(-UL * TN)))
160 LET RNIA = ((TN ^ 2 + 4 * TN * SANT * ((ERAT - ENFA) / NN)) ^ .5 - TN) /
(2 * TN * SANT): PRINT "OLD ACUTE ISOSURFACE IS NOW AT POSITION OF
DOSERATE (Gy/hr) = "; RNIA
165 LET RA = (2.1 * RNIA / RN): XAA = 7.85 * EXP(-4.1 * RA) + 5.87 * EXP(-.647
* RA) + .63 * EXP(-.0032 * RA): PRINT "NEW POSITION OF TUMOUR
SURFACE WRT. NEW INS. = "; XAA
170 LET RNIL = ((TN ^ 2 + 4 * TN * SLNT * ((ERLT - ENFL) / NN)) ^ .5 - TN) / (2
* TN * SLNT): PRINT "OLD LATE ISOSURFACE IS NOW AT POSITION OF
DOSERATE (Gy/hr) = "; RNIL
175 LET RL = (2.1 * RNIL / RN): XAL = 7.85 * EXP(-4.1 * RL) + 5.87 * EXP(-.647
* RL) + .63 * EXP(-.0032 * RL): PRINT "NEW POSITION OF LATE SURFACE
WRT. NEW INS. = "; XAL

```

```
200 PRINT "MOVEMENT: OUTWARDS +VE"  
210 DXA = XAA - XI: PRINT "ACUTE MOVEMENT (CM) ="; DXA  
220 DXL = XAL - XI: PRINT "LATE MOVEMENT (CM) ="; DXL: LPRINT USING  
"###.###  "; XI; RRF; DXA; DXL; RNIA; RNW; RNIL: PRINT : PRINT  
230 PRINT "SEPARATION: WRT ACUTE SURF. OUTWARDS +VE"  
240 SEPN = DXL - DXA: PRINT "SEPN. ="; SEPN  
250 INPUT "ANOTHER YES(Y) OR NO(N)"; A$  
260 IF A$ = "Y" THEN GOTO 90  
270 IF A$ = "N" THEN GOTO 280  
280 INPUT "NEW PARAMETERS (P) OR EXIT (E)"; B$  
290 IF B$ = "P" THEN GOTO 10  
300 IF B$ = "E" THEN GOTO 310  
310 STOP
```

Stages	Continuous schedules N:R(at "A" Gy/hr):T(hr)	Fractionated schedules N:d(Gy)
I and II	LDR -- 2 : 0.55 : 54.54	15 : 1.1
	Selectron (see table 9.2*)	15 : 1.1
IIb and III	LDR -- 1 : 0.55 : 60.91	20 : 2.15
	Selectron (see table 9.2*)	20 : 2.15

Dose-rate at point "A" (Gy/hr) (1)	Patient number (2)
LDR	
0.55	100
Selectron*	
0.8 - 0.9	12
1.2 - 1.4	128

	Treatment parameters		ERD (Gy)			
	Dose-rate at point "A" (Gy/hr) (1)	Treatment time per fraction (hr) (2)	Tumour $\alpha/\beta=10\text{Gy}$ $\mu=1.4\text{hr}^{-1}$ (3)	% Diff (4)	Late $\alpha/\beta=3\text{Gy}$ $\mu=0.46\text{hr}^{-1}$ (5)	% Diff (6)
Reference schedule	0.55	54.54	64.65		105.91	
Selectron treatment	0.8	32.17	57.22	-11.49	107.12	1.14
	0.9	27.26	55.21	-14.60	107.96	1.93
	1.2	18.18	50.82	-22.33	110.44	4.28
	1.4	14.63	48.76	-24.58	111.74	5.50
Weighted mean Selectron	1.26	16.97	50.14	-22.44	110.86	4.67

Table 9.3 (b) ERD values for different schedules at higher dose-rate compared with a reference schedule of dose-rate 0.55Gy/hr. For the Glasgow study, stages IIb, III and IVa.

	Treatment parameters		ERD (Gy)			
	Dose-rate at point "A" (Gy/hr) (1)	Treatment time per fraction (hr) (2)	Tumour (3)	% Diff (4)	Late (5)	% Diff (6)
Reference schedule	0.55	60.91	36.10		59.25	
Selectron treatment	0.8	35.93	31.96	-11.47	60.05	1.35
	0.9	30.44	30.83	-14.60	60.58	2.24
	1.2	20.30	28.39	-21.36	62.19	4.96
	1.4	16.34	27.25	-24.51	63.13	6.35
Weighted mean Selectron	1.26	18.95	28.01	-22.41	62.48	5.45

Table 9.4. Site distribution of 36 cases of severe radiation morbidity in 26 patients by intracavitary treatment method from the Glasgow study.

Site	Treatment method				
	Selectron				Caesium
	1*	2*	3*	Total	
Vagina	0	2	2	4	0
Bladder	1	3	4	8	0
Rectum	1	4	1	6	1
Colon	1	4	0	5	2
Small Bowel	1	4	2	7	2
Bone	0	0	1	1	0
Other	0	0	0	0	0
A point dose-rate Gy/r	0.8 - 0.9	1.2 - 1.4	1.8 - 2.1		0.55

Table 9.5 ERD values for different schedules at higher dose-rate compared with a reference schedule of dose-rate 0.53Gy/hr. For the Manchester study.

Two Fractions given with LDR and Selectron	Treatment parameters			ERD (Gy)			
	Dose-rate at point "A" (Gy/hr)	Corr. to total dose (%)	Treatment time per fraction (hr)	Tumour	% Diff	Late	% Diff
	(1)	(2)	(3)	(4)	(5)	(6)	(7)
Reference schedule	0.53		70.75	80.61		130.83	
Selectron treatment	1.6	0	23.44	91.61	13.65	232.78	77.92
		-6	21.87	85.48	6.03	216.19	65.24
		-12.5	20.31	79.33	-1.59	199.59	52.56
		-19	18.75	73.19	-9.21	183.00	39.88

Table 9.6 (a) Mean dose-rates, treatment times and corresponding ERD values for LDR schedules in the Orton survey (from Orton et al 1991)

Stage	Treatment parameters		ERD (Gy)	
	Dose-rate point "A" (Gy/hr)	Treatment time per fraction (hr)	Tumour	Late
(1)	(2)	(3)	(4)	(5)
I	0.87	75.4	73.67	145.92
II	0.80	80.2	71.43	136.92
III	0.87	77.3	75.53	149.66
IV	0.89	79.6	79.77	159.73
All	0.85	78.1	74.37	145.89

Table 9.6 (b) Mean number of fractions, dose per fraction and corresponding ERD values for HDR schedules from the Orton survey (from Orton et al 1991)						
Stage	Treatment parameters		ERD (Gy)			
	Fraction number	Dose per fraction (Gy)	Tumour	% Diff	Late	% Diff
(1)	(2)	(3)	(4)	(5)	(6)	(7)
I	5.3	7.6	70.18	-4.74	141.53	-3.01
II	4.7	7.4	59.93	-16.45	119.92	-12.16
III	4.6	7.4	58.66	-22.33	117.37	-21.57
IV	4.7	7.5	61.05	-23.47	122.70	-23.18
All	4.8	7.4	62.05	-16.56	124.41	-14.72

Percentage differences between ERD values for LDR (Table 9.5 (a)) and HDR (above) are shown in columns 5 and 7.

Table 9.7 Mean values of the ratios of the "hot-spot" rectal and bladder doses (D) and dose-rates (R). From the Orton survey (Orton et al 1991)				
Modality	Parameter	Value	P-value	ratio HDR/LDR
(1)	(2)	(3)	(4)	(5)
HDR	Dr/Da	0.65 ± 0.02	} < 0.001	0.85 ± 0.03
LDR	Rr/Ra	0.76 ± 0.02		
HDR	Db/Da	0.60 ± 0.002	} 0.042	0.90 ± 0.05
LDR	Rb/Ra	0.67 ± 0.03		
HDR	D(r,b)/Da	0.63 ± 0.02	} < 0.001	0.87 ± 0.04
LDR	R(r,b)/Ra	0.72 ± 0.02		

The letters r and b are for rectal and bladder tissues respectively, (r,b) refers to the average of the rectal and bladder "hot-spot" doses, and the ± are standard errors of the mean.

Table 9.8. Treatment details of the Patel study.

Stages	Continuous schedules N:R(at "A" Gy/hr):T(hr)	Fractionated schedules Total dose (Gy)
I and II	LDR -- 2 : 0.6 : 62.5	35
	HDR -- 4 : 88 : 0.1079	35
III	LDR -- 1 : 0.6 : 58.33	45
	HDR -- 2 : 88 : 0.1023	45

Table 9.9 ERD values for different schedules at higher dose-rate compared with two reference schedules of dose-rate 0.6Gy/hr for the Patel study.

	Treatment Parameters			ERD (Gy)			
	Dose-rate at point "A" (Gy/hr) (1)	Fract No. (2)	Treatment time per fraction (hr) (3)	Tumour (4)	% Diff (5)	Late (6)	% Diff (7)
Reference schedule	0.6	2	62.5	81.35		137.95	
Selectron treatment	88	4	0.1079	72.29	-11.14	156.23	13.25
Reference schedule	0.6	1	58.33	37.96		64.30	
Selectron treatment	88	2	0.1023	33.47	-11.84	71.19	10.73

Figure 9.1 Movement of intracavitary insertion when changing from Manchester radium to Selectron applicators

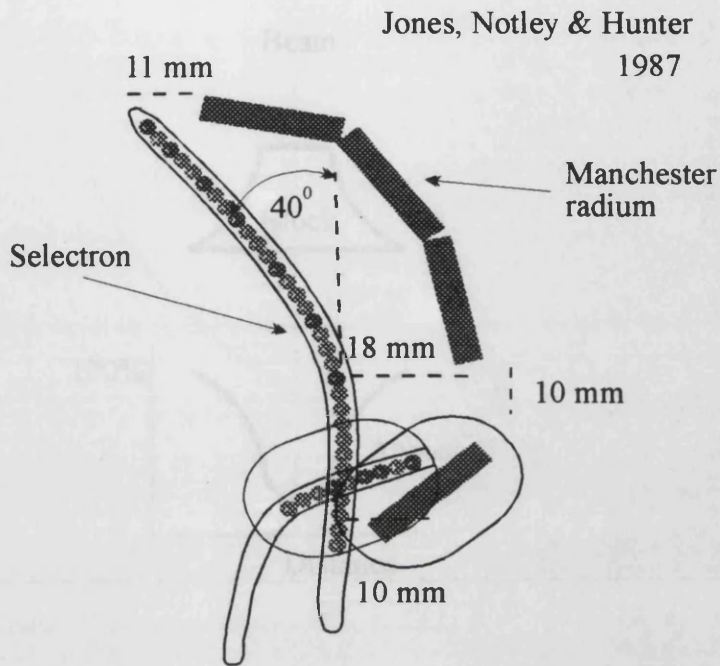


Figure 9.2 Dose-rate profiles in the direction of the bladder for Manchester radium and Selectron applicators

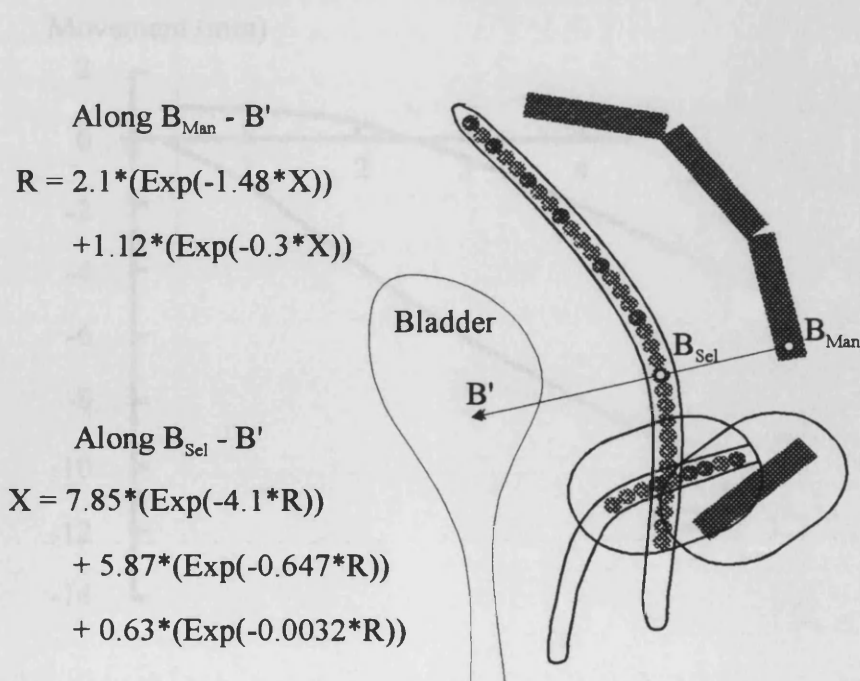


Figure 9.3 Specially shaped shielding block used in the Glasgow report.

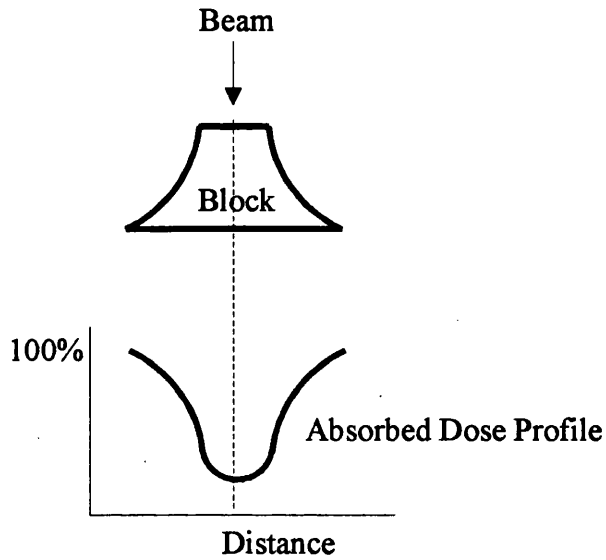


Figure 9.4 Movement of Tumour and Late iso-effect surfaces for the Glasgow report. Stages I and II.

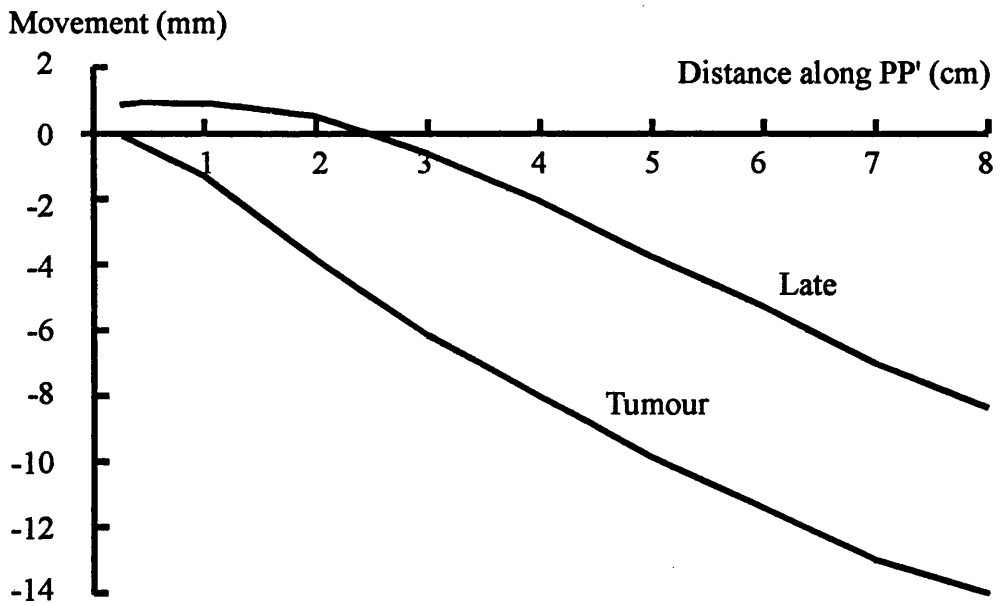


Figure 9.5 (a) and (b) Plot of enclosed volume versus dose-rate for a standard insertion with an A point dose-rate of 0.55Gy/hr (see following page for figure 9.3 (c)).

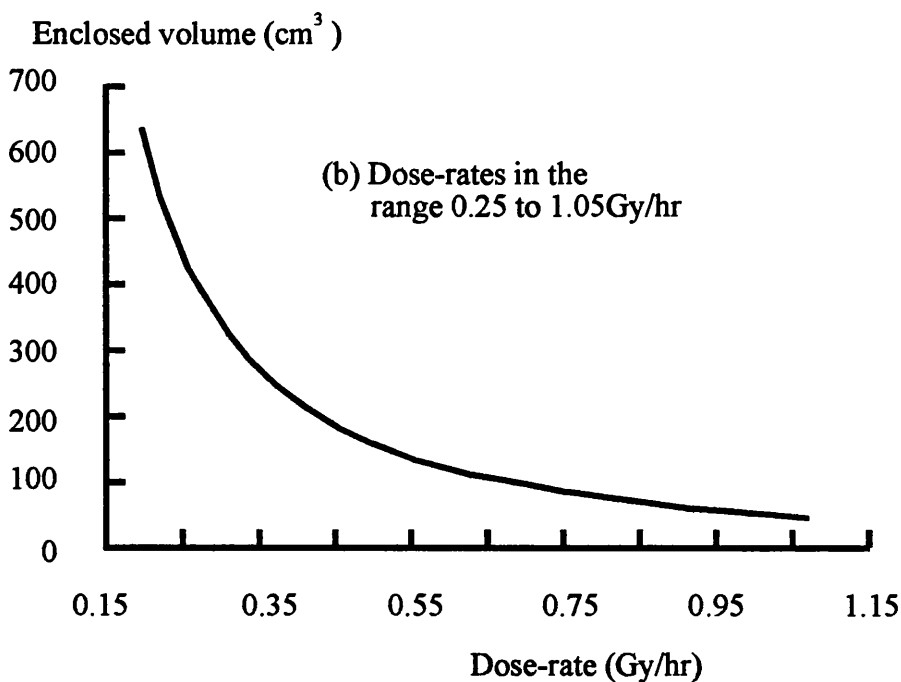
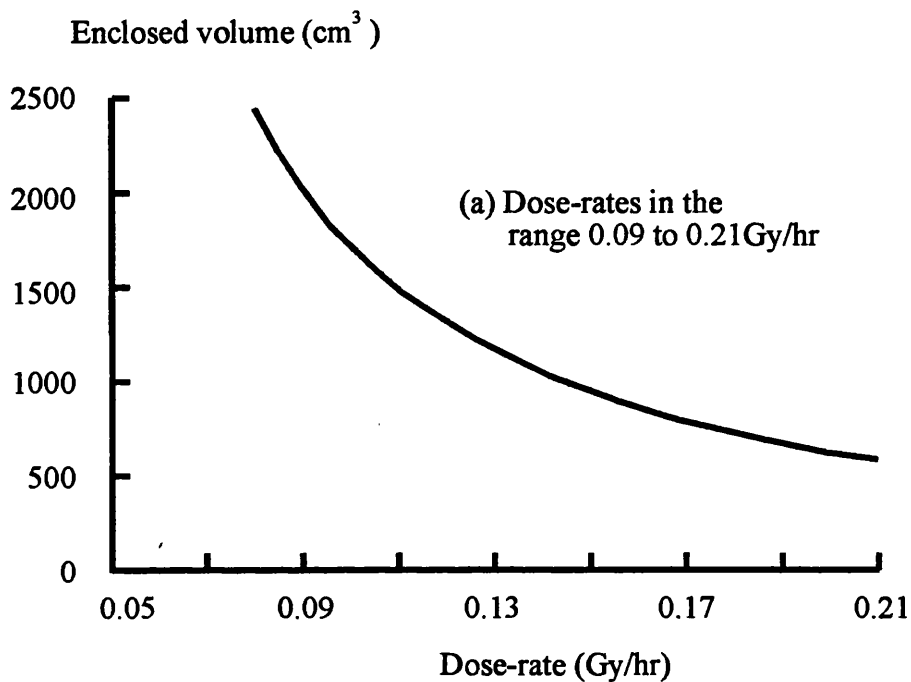


Figure 9.5 (c) Plot of enclosed volume versus dose-rate for a standard insertion with an A point dose-rate of 0.55Gy/hr.

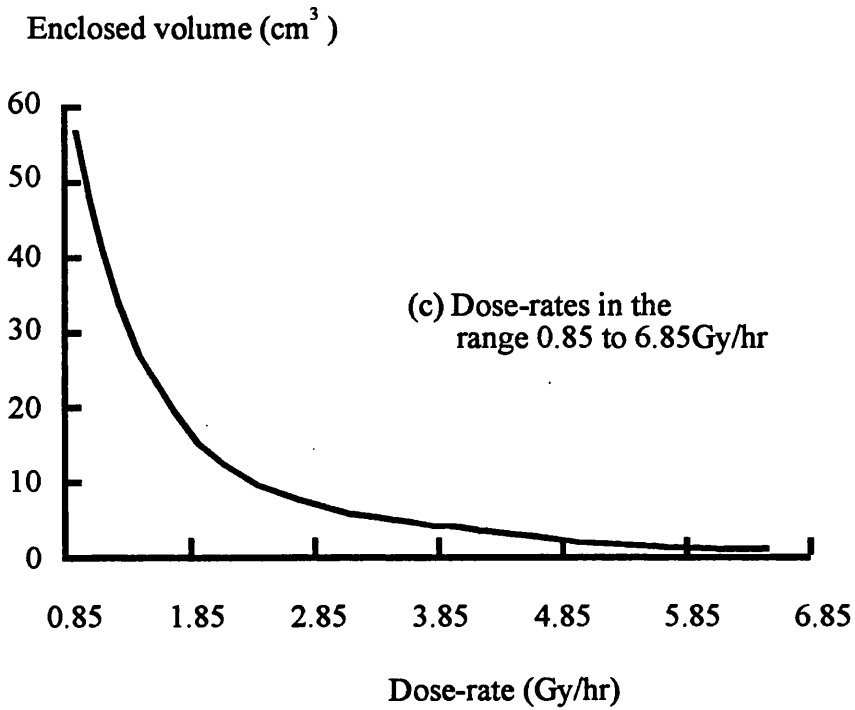


Figure 9.6 Percentage change in volume corresponding to the movement of iso-effect surfaces in figure 9.4. For stages I and II of the Glasgowreport 1.

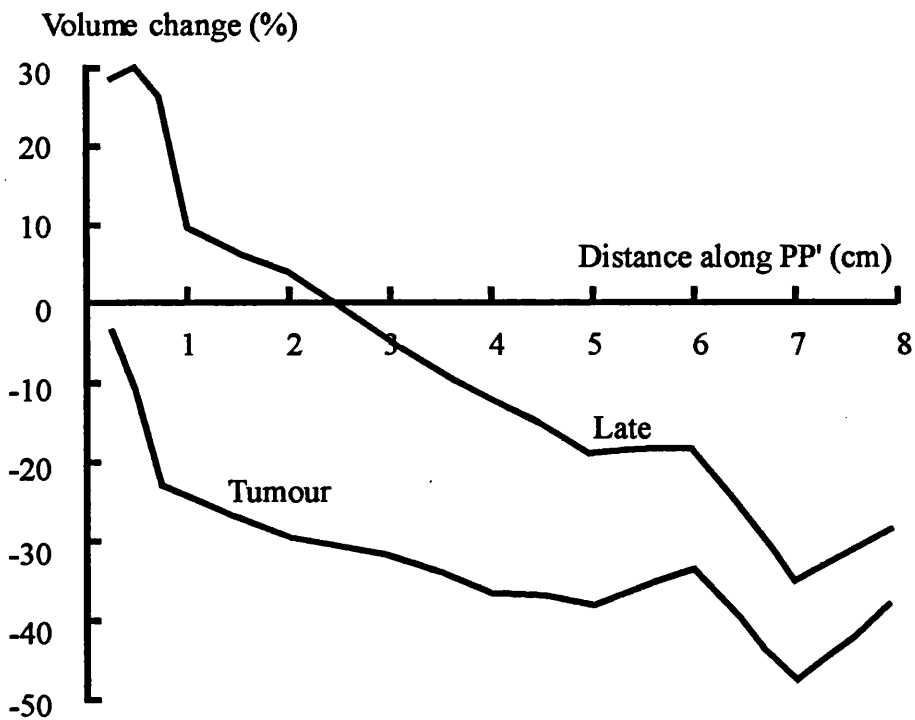


Figure 9.7 Movement of iso-effect surfaces for stage I and II of the Glasgow report assuming a complete match for tumour effects.

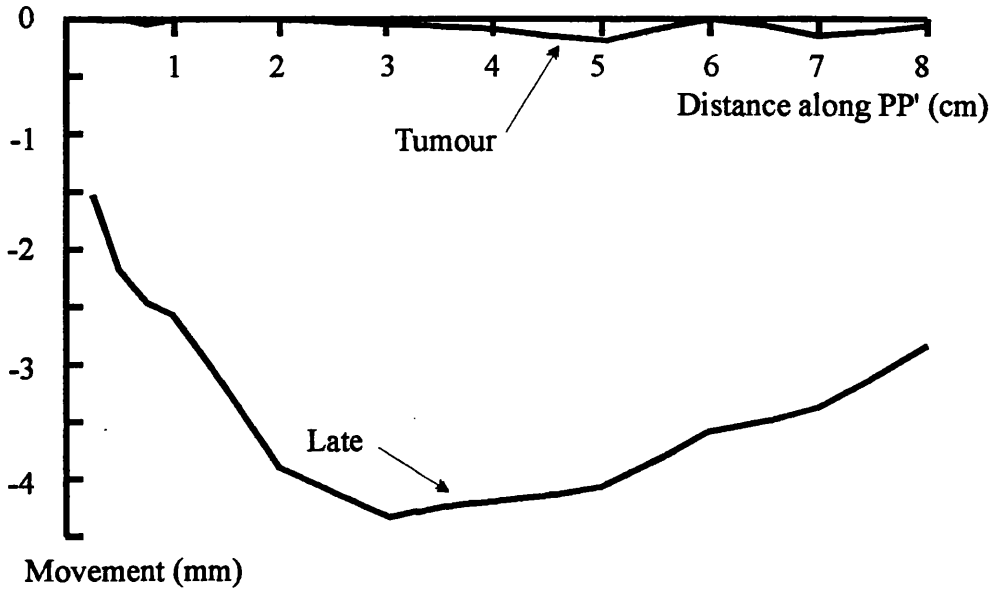


Figure 9.8 Percentage change in volume enclosed by iso-effect surfaces for stage I and II of the Glasgow report assuming a complete match for tumour effects.

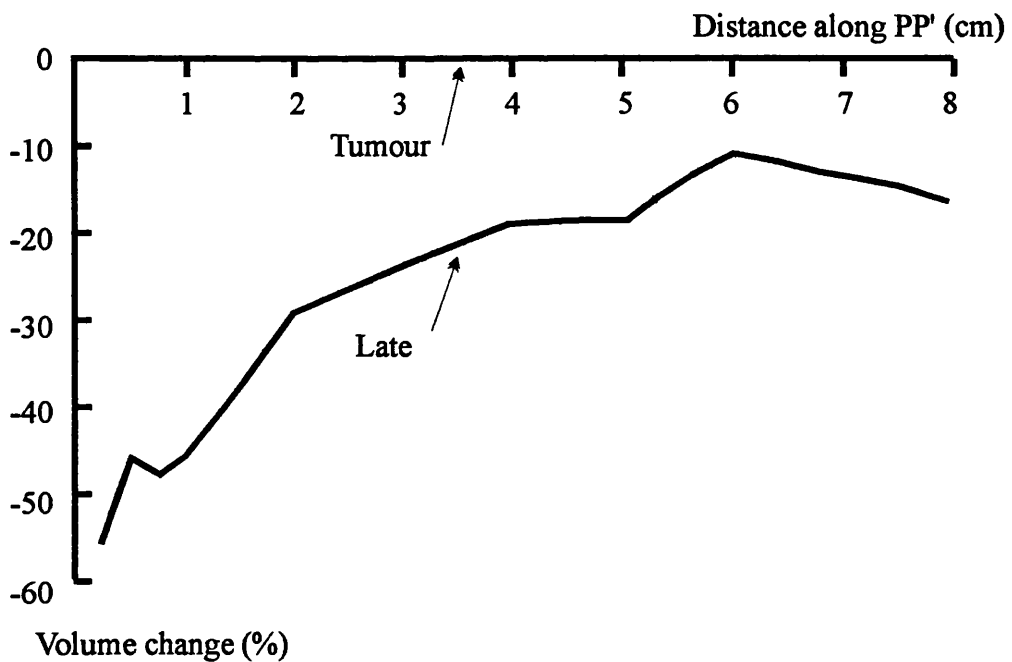


Figure 9.9 Movement of iso-effect surfaces for stage I and II of the Glasgow report assuming a complete match for late effects.

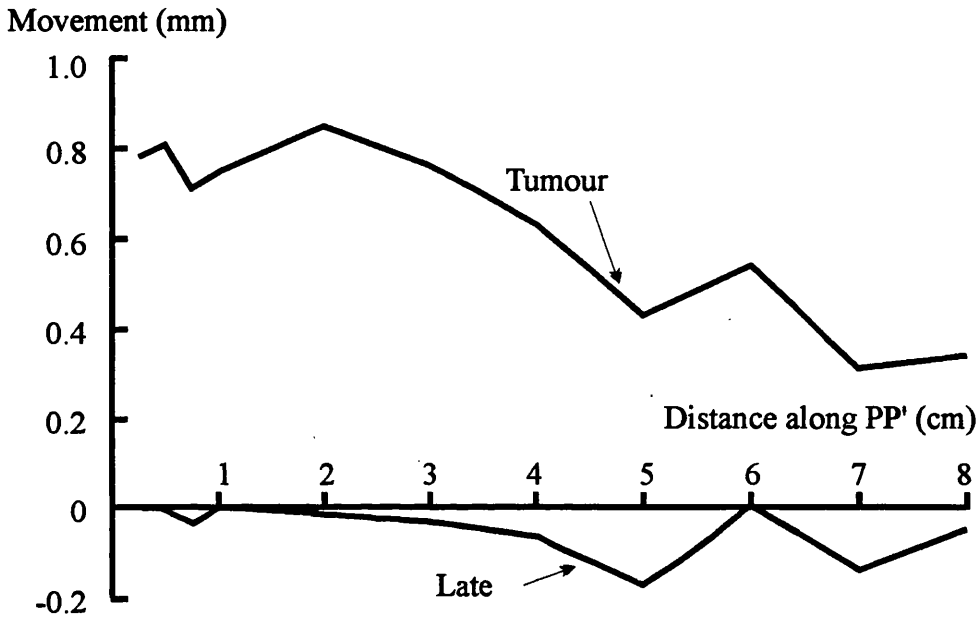


Figure 9.10 Percentage change in volume enclosed by iso-effect surfaces for stage I and II of the Glasgow report assuming a complete match for late effects.

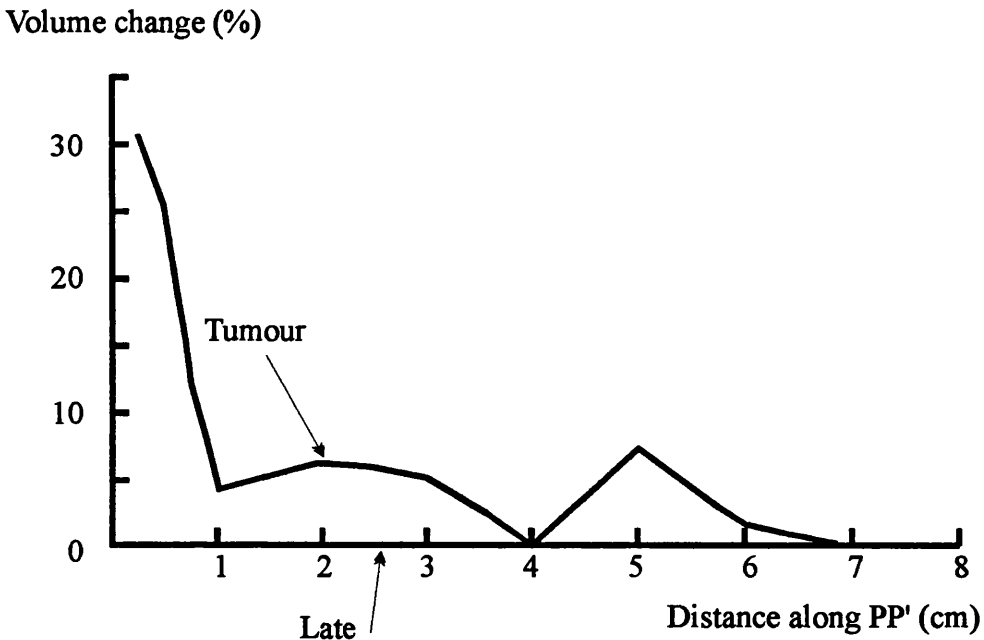


Figure 9.11 Movement of late iso-effect surfaces including the contribution of both geometry and radiobiology for the Glasgow report, Stages I and II.

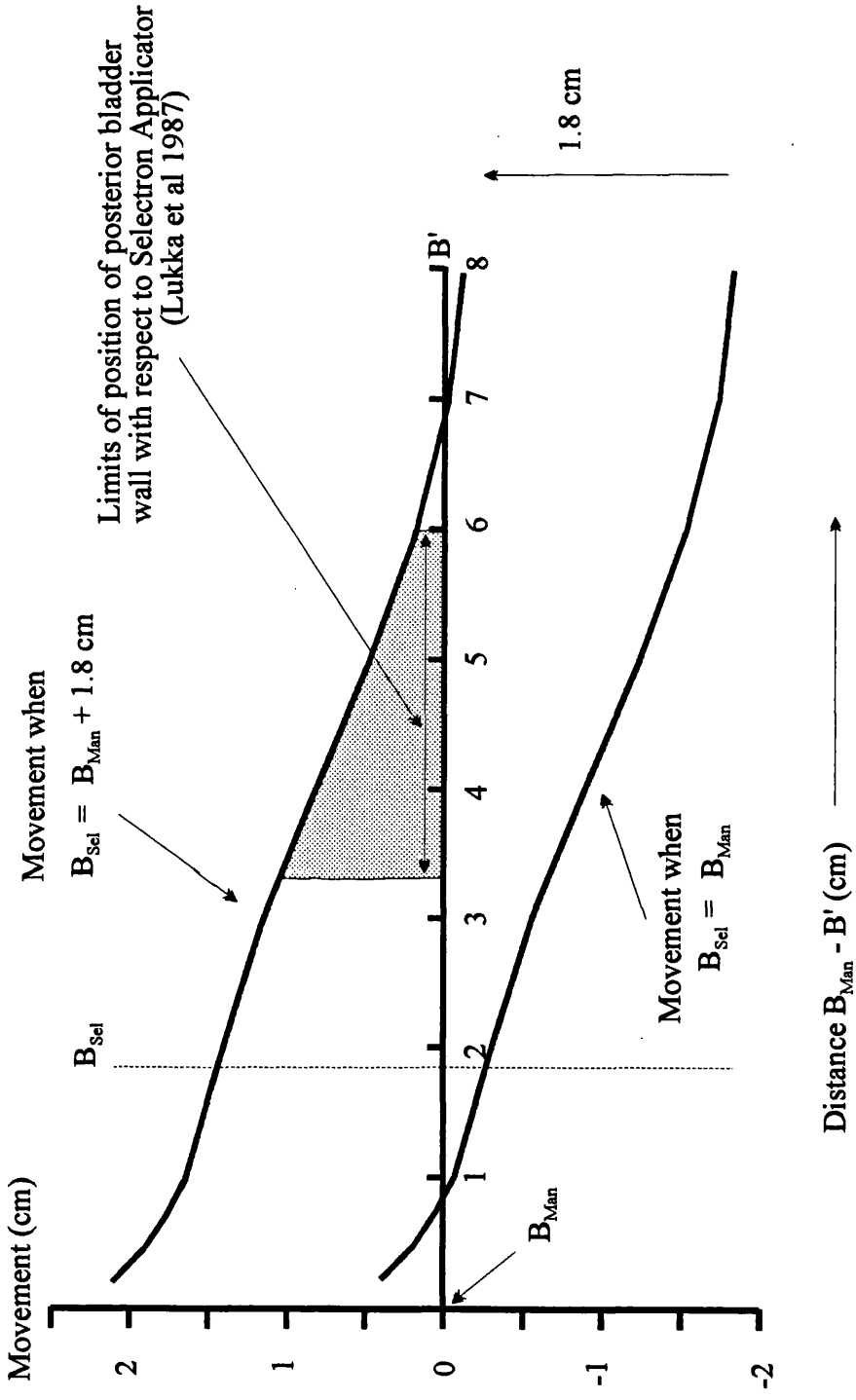


Figure 9.12 Movement of tumour iso-effect surfaces for Manchester report, showing the effect of four different values of total dose.

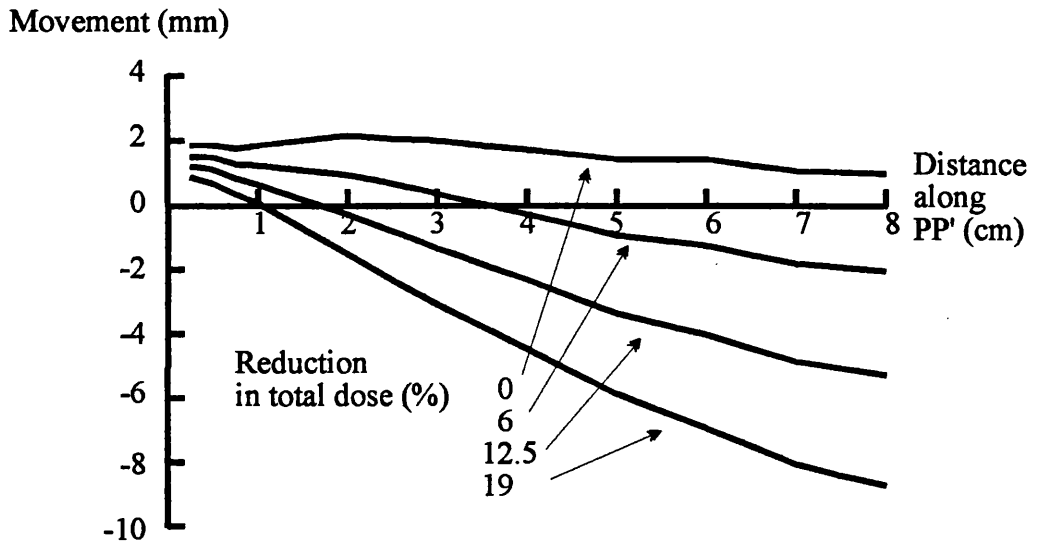


Figure 9.13 Movement of late iso-effect surfaces for the Manchester report, showing the effect of four different values of total dose.

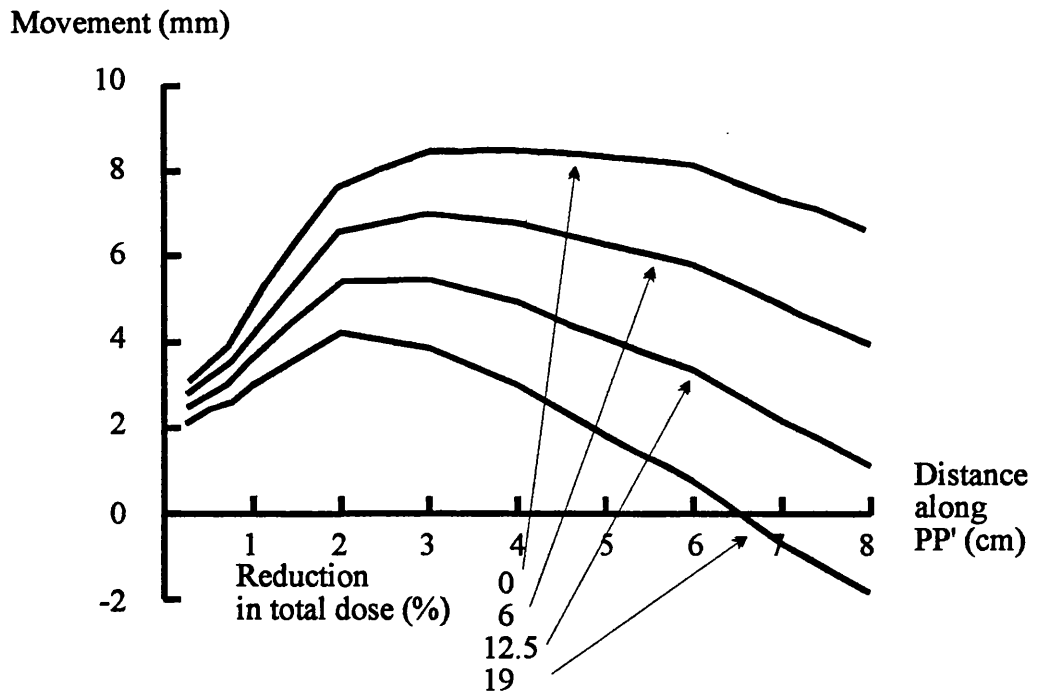


Figure 9.14 Percentage change in enclosed volume of tumour iso-effect surfaces for the Manchester report, showing the effect of four different values of total dose.

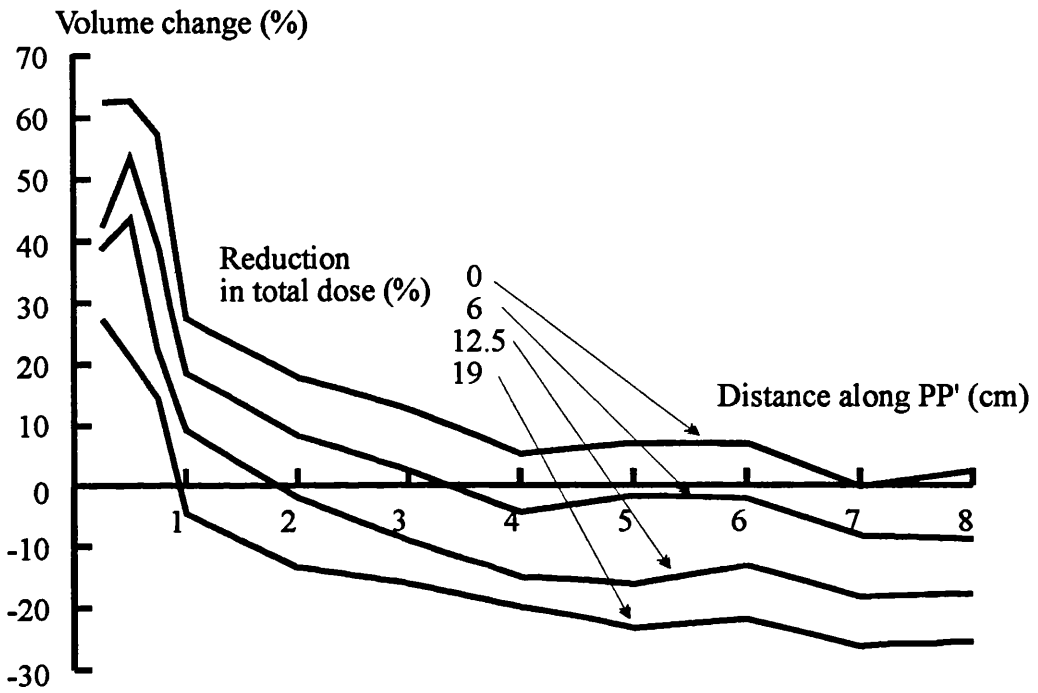


Figure 9.15 Percentage change in enclosed volume of late iso-effect surfaces for Manchester report, showing the effect of four different values of total dose.

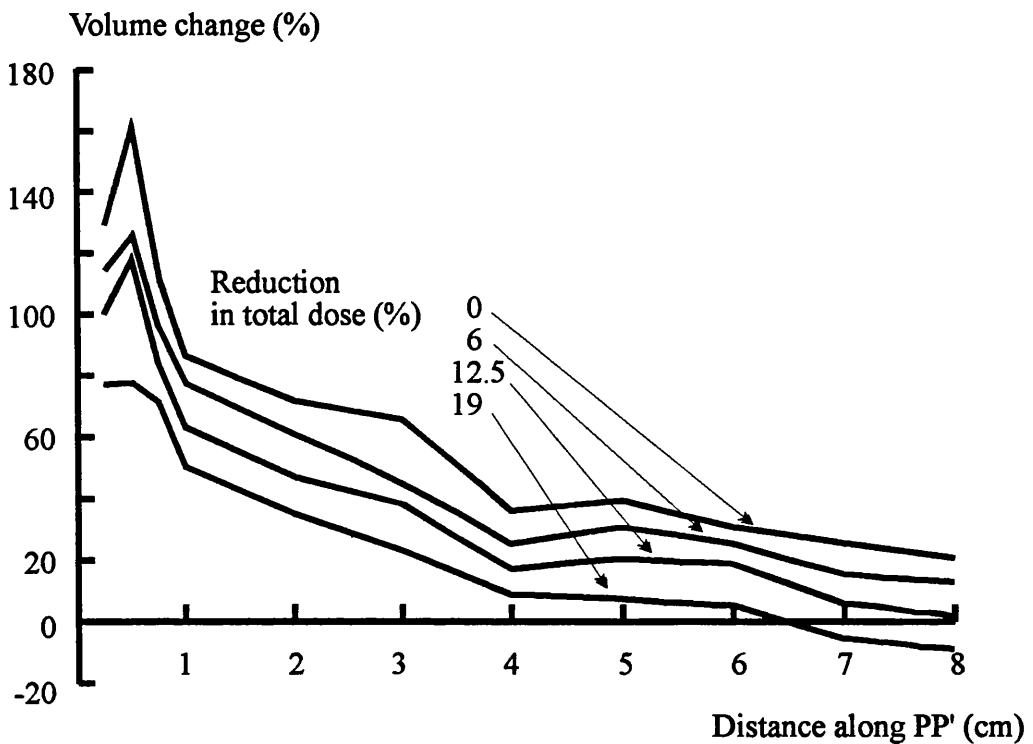


Figure 9.16 Movement of late iso-effect surfaces including the contribution of both geometry and radiobiology for the Manchester report.

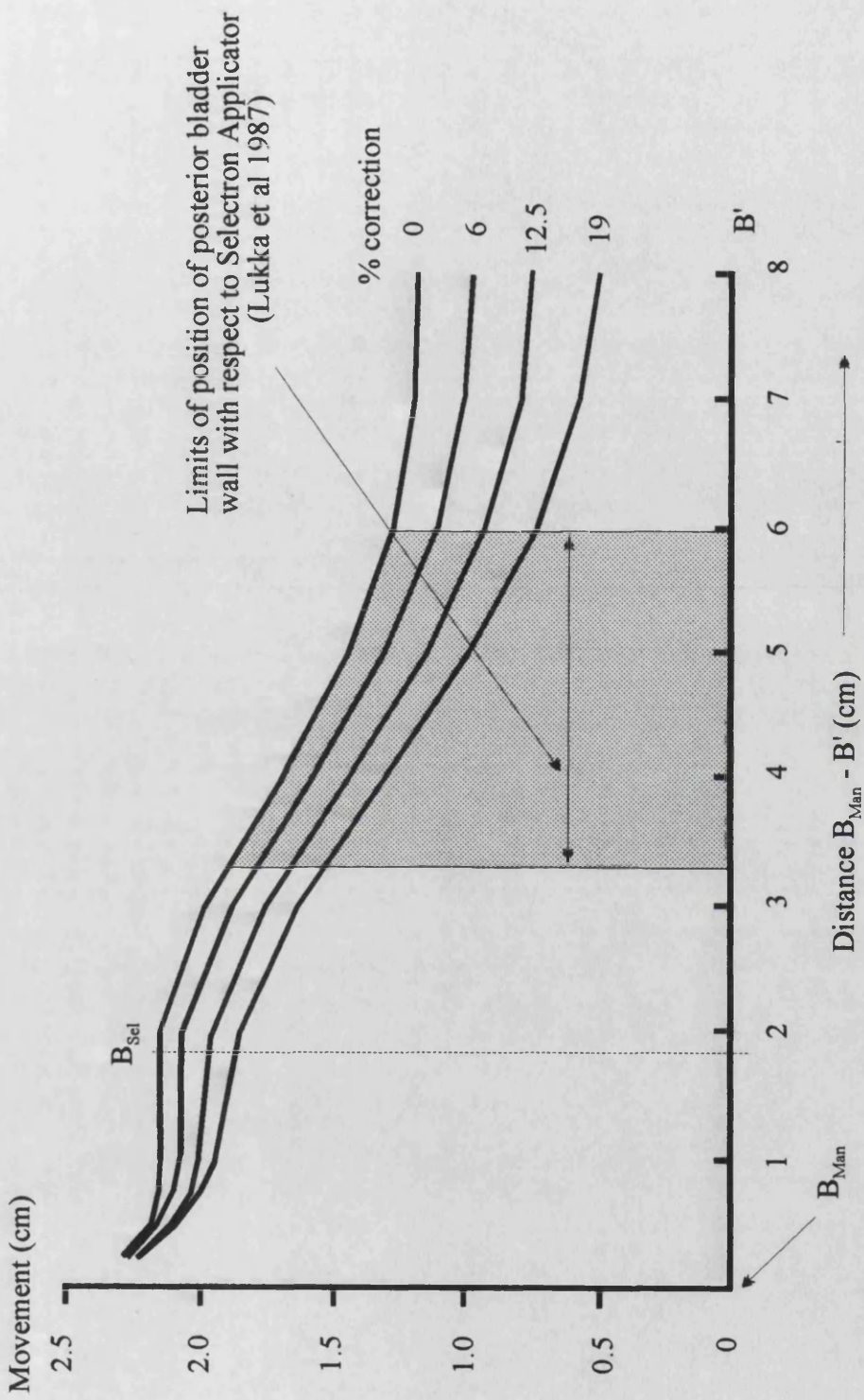


Figure 9.17 Movement of iso-effect surfaces for the Orton survey.

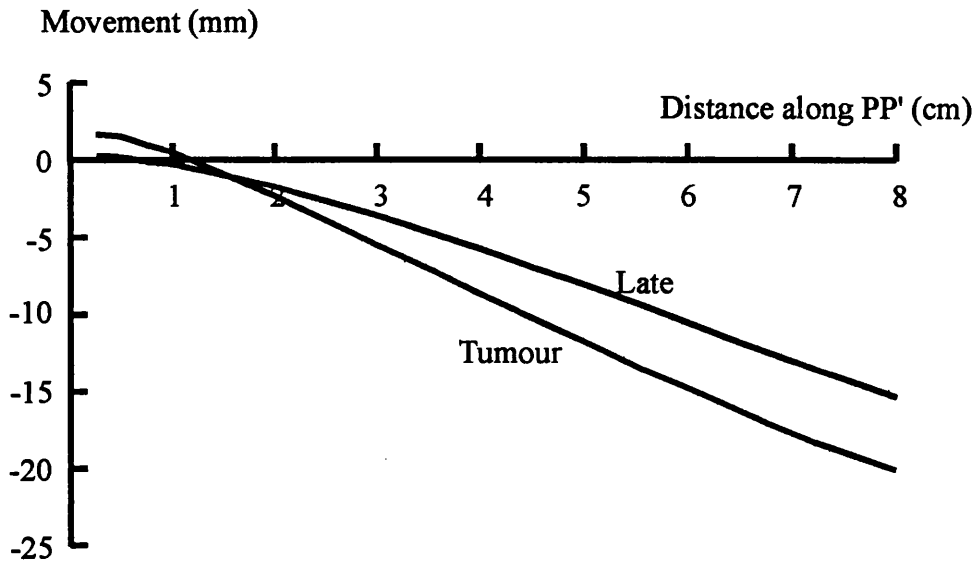


Figure 9.18 Percentage change in enclosed volume of iso-effect surfaces for the Orton survey.

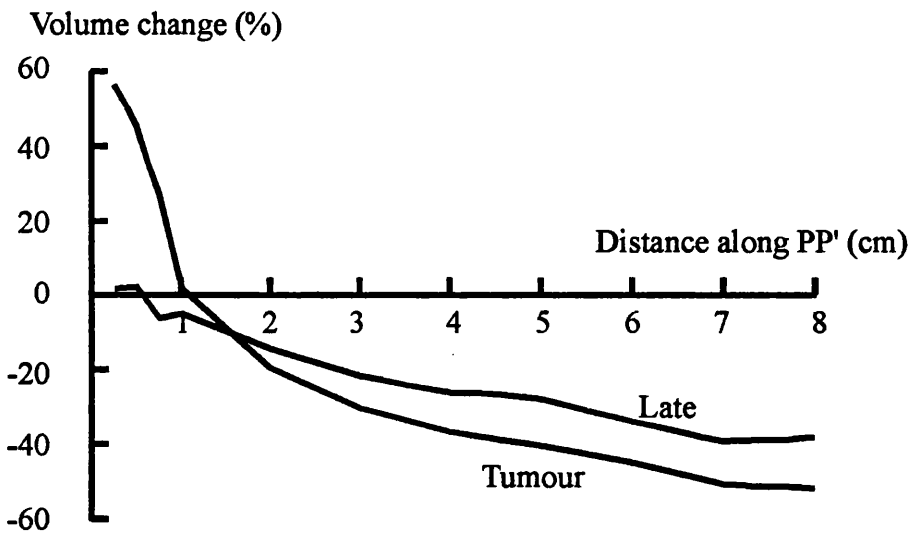


Figure 9.19 Movement of iso-effect surfaces for the Orton survey assuming a complete match for Tumour effects.

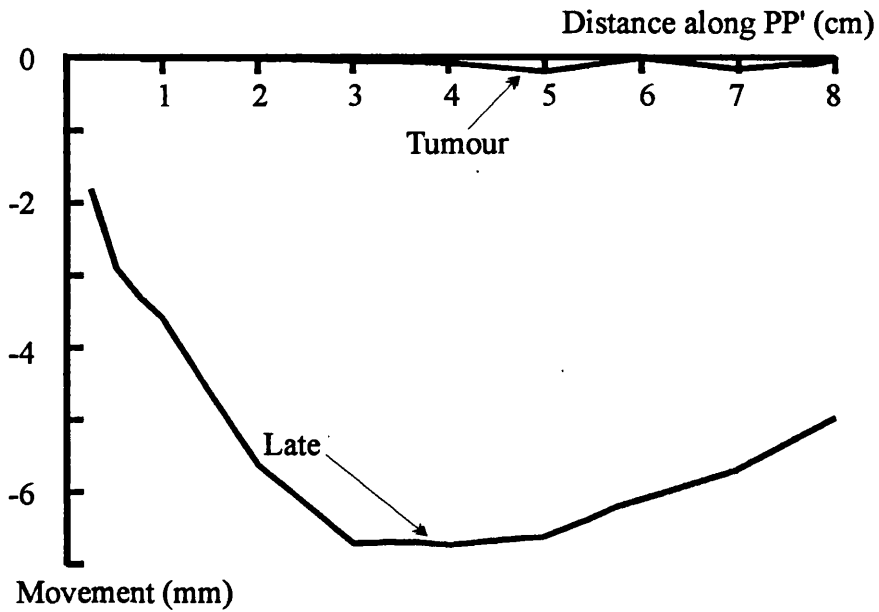


Figure 9.20 Percentage change in enclosed volume of iso-effect surfaces for the Orton survey assuming a complete match for Tumour effects.

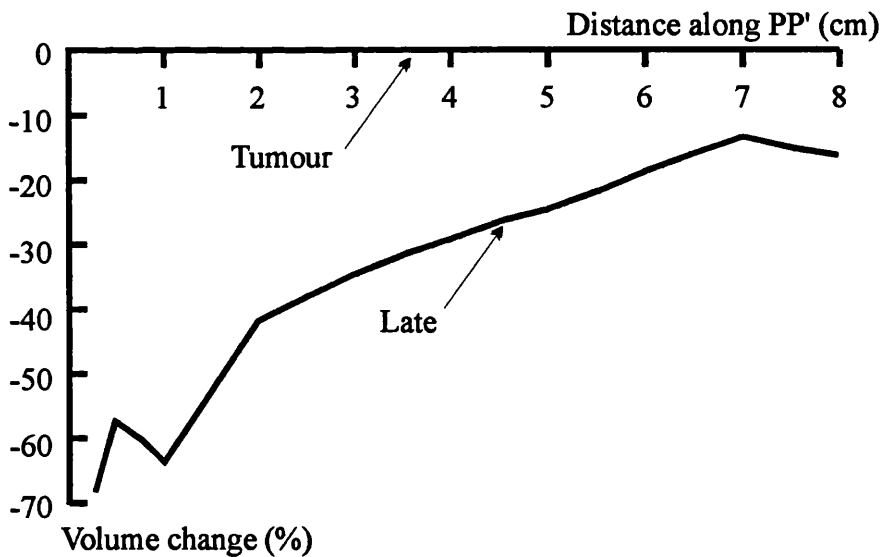


Figure 9.21 Movement of iso-effect surfaces for the Orton survey assuming a complete match for Late effects.

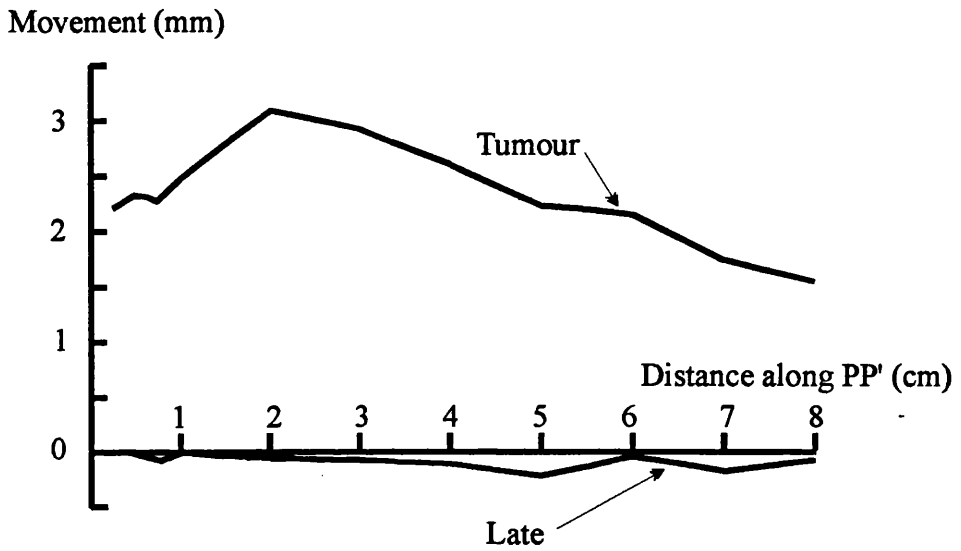


Figure 9.22 Percentage change in enclosed volume of iso-effect surfaces for the Orton survey assuming a complete match for Late effects.

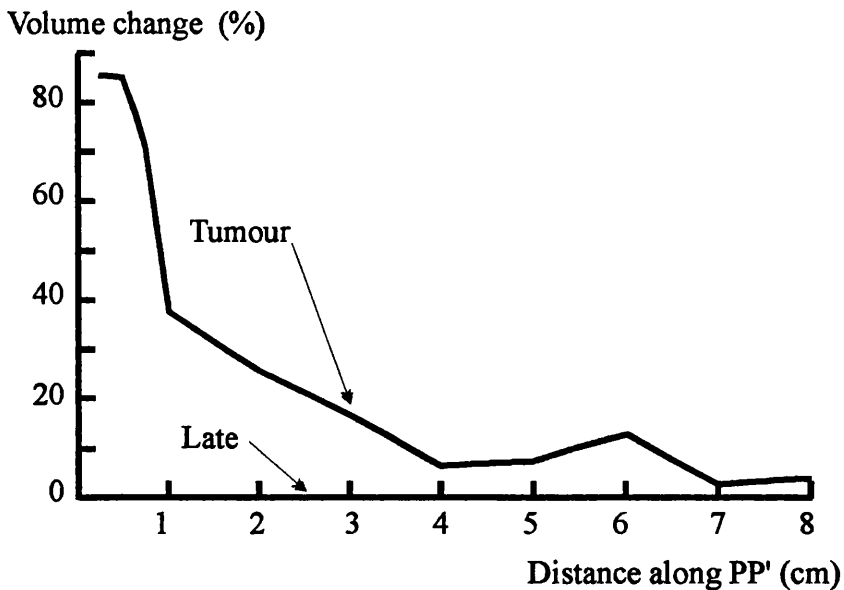


Figure 9.23 Movement of iso-effect surfaces for group 1 of the Patel report.

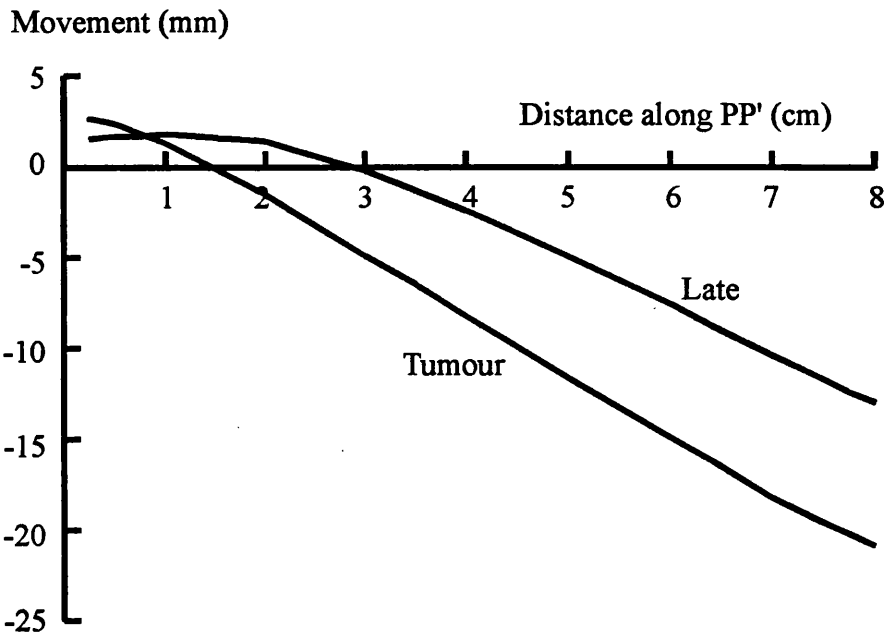


Figure 9.24 Percentage change in enclosed volume of iso-effect surfaces for group 1 of the Patel report.

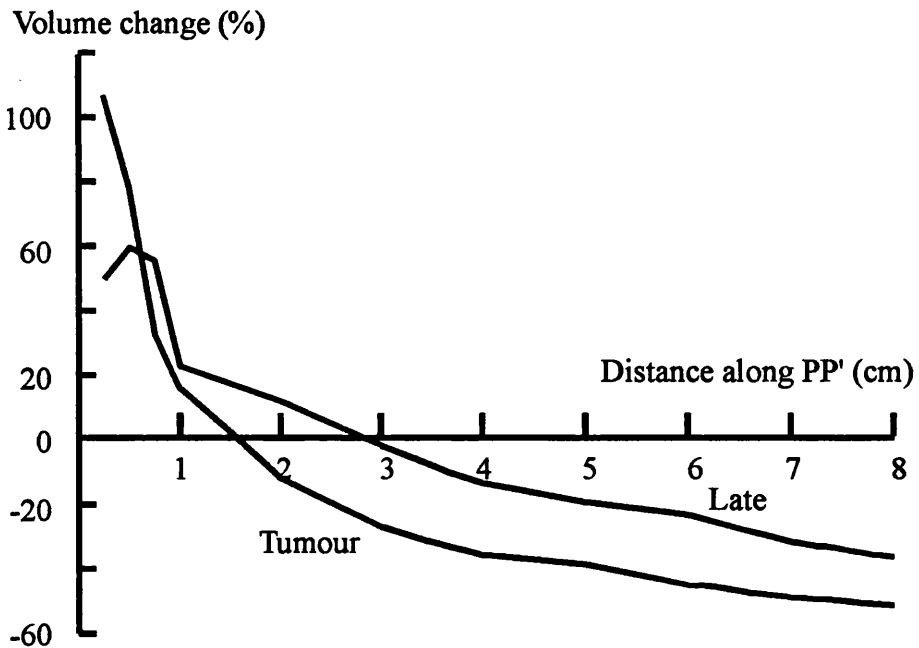


Figure 9.25 Movement of iso-effect surfaces for group II of the Patel report.

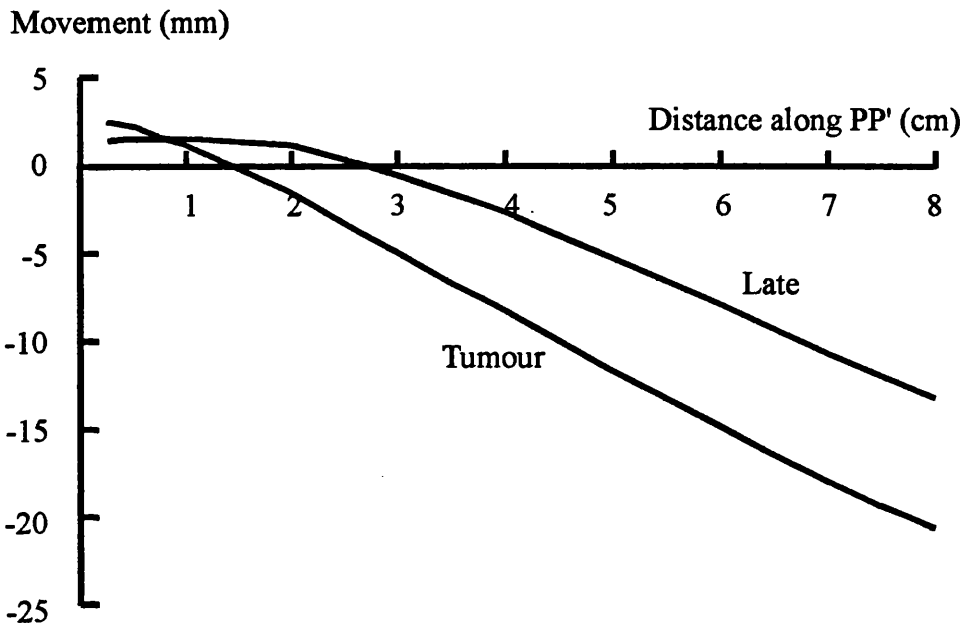
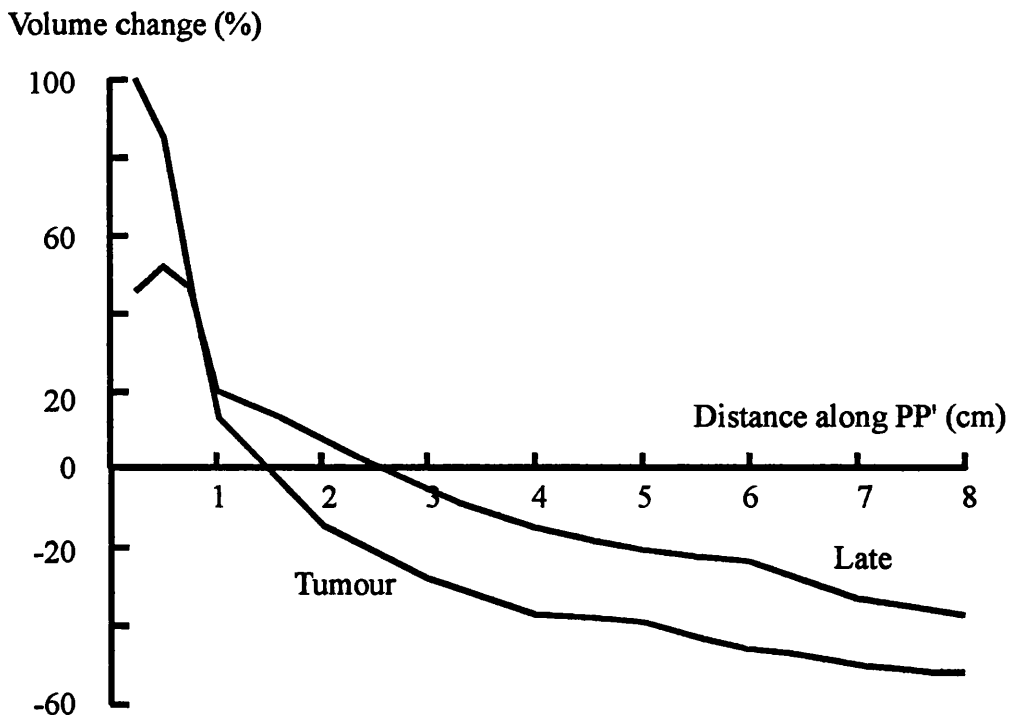


Figure 9.26 Percentage change in enclosed volume of iso-effect surfaces for group II of the Patel report.



Chapter 10.

Conclusions

10.1. Advantages and limitations of general equivalence.

It has been shown in this thesis that conditions can be derived for equivalence between different radiotherapy schedules which are independent of both the α/β ratio and, when treatment times are short, μ , the sublethal damage repair time constant. This finding makes general equivalence more applicable in fractionated high dose-rate therapy than with continuous treatments. The method of obtaining equivalence condition, by equating coefficients, is an extremely simple one (Deehan & O'Donoghue, 1988) which has been explored fully in this thesis. Although the LQ model is used here, this method is model independent and can be adapted for use with early power relationships as shown in chapter 4, appendix 4A. This means that general equivalence is not a unique feature of the LQ model. Furthermore if other terms are added to the LQ formalism (e.g. a time factor to account for proliferation) the equivalence argument can be re-examined using the same method, although this is likely to lead to more constraints than those shown here.

One obvious limitation of the general equivalence approach was that it appeared to be inappropriate where μ could not be eliminated from the equations (chapters 5 and 6). Variations in the value of this parameter for different tissues are not clearly defined nor is the exact form of the mathematical expression which governs repair of sublethal damage, (for example whether it is a single or multiple exponential). This fact does not weaken the argument for general equivalence but does mean that the conditions may

have to be re-defined as knowledge grows, especially where continuous treatments are concerned. The smaller the variation in the value of μ for different tissues (or the expression for repair containing μ), the more important the concept of general equivalence becomes, since variations in the α/β ratio can be ignored completely. In connection with the worked examples it has to be pointed out that treatment dose-rates can be more accurately defined in external beam therapy than in brachytherapy. This is because the latter dose-rates are often dependent to a large extent on the geometry of the sources which can cause shifts in the overall dose-rate distribution. With commonly used after-loading systems and the older manually loaded insertions, this fact makes it difficult to fine-tune the dose-rate at any specific point to the exact value required to satisfy the general equivalence conditions. However the new generation of afterloading systems, which uses a single source that occupies a pre-determined position within the insertion for specified dwell time, makes this fine-tuning possible. Dwell times can be altered to give an average optimal dose-rate at any specific point and may allow general equivalence to be satisfied.

Another limitation of general equivalence is that the conditions were derived using calculations referred to specific points of interest around a dose distribution. An overall view of equivalence cannot be easily obtained by such a method and it is difficult to see if the equivalence conditions hold at other points in space. This deficiency also applies to the iso-effect calculations which appeared in the literature before this thesis. General equivalence is also of limited use in analysing retrospective clinical studies where comparisons have to be made between treatments already given. Schedule and regimes compared are often chosen with little or no radiobiological basis. In such cases another

method of comparison has to be adopted and the use of iso-effect surfaces is developed in chapters 7 and 8 for this purpose.

10.2. Iso-effect surfaces.

Dose distributions can be converted easily into effect distributions (Joslin et al, 1972; Kirk et al, 1976). However it is shown in chapters 7 and 8 that using the concept of iso-effect surfaces can reveal how the effect distribution changes with treatment parameters. In going from one treatment to another, surfaces move resulting in changes in enclosed volume. The degree to which the three dimensional changes in iso-effect surfaces can be demonstrated in this thesis is limited, and movement of effect distributions is plotted along lines. Nevertheless this is sufficient to demonstrate some important features of these changes.

Chapter 7 shows how movement of iso-effect surfaces can be calculated when the treatment dose-rate changes (from lower to a higher dose-rate) in intracavitary brachytherapy, if the dose-rate profile is known along a line. This example assumes that the two treatments are matched at some point around the insertion for either tumour or late effects. If this is the case then the higher dose-rate iso-effect surfaces move outwards relative to their position at lower dose-rate at distances shorter than the match point and inwards at greater distances. Depending on the position of the match point (this is determined by the treatment parameters) this pattern of movement can point to a lower probability of late responding normal tissue damage. This at first seems surprising since it is generally assumed that changing from low to high dose-rate treatments is always accompanied by higher levels of late responding tissue damage. The latter assumption is indeed true if the total dose is kept constant when the treatment dose-rate

changes as shown in figures 7.5 and 7.6 (see section 7.3.2). However the assumption is not necessarily true if the HDR treatment is given as a series of fractions with a reduced total dose as shown in figures 7.7 and 7.8. Furthermore if the correct choice of total dose and fraction number is made at HDR it could lead to a reduction in late responses at certain points around the insertion compared with the LDR situation. This result is in broad agreement with recently published clinical results of brachytherapy trials (chapter 9) which have shown that increasing the treatment dose-rate need not necessarily produce more late responding normal tissue morbidity and may in fact produce less, even for similar levels of tumour effect.

It should be noted that calculation of the ERD at single points will lead to the same conclusions as those obtained from iso-effect plots, if enough points are calculated. Therefore the results of iso-effect analysis are not at odds with any existing radiobiology theory. Examining the changes in surfaces merely shows the changes in effect distribution more clearly than single point ERD calculations, just as iso-dose plots can be more useful in displaying changes in dose distributions than doses calculated at single points.

Considering both the predictions of general equivalence and iso-effect analysis together, it can be seen that for general equivalence to hold it would often be necessary to give extremely large numbers of fractions. In the case of brachytherapy this leads to no movement of iso-effect surfaces for the specific type of effect involved (i.e. tumour or late effects), whereas moving to fewer fractions leads to more and more movement away from the ideal. Yet it appears that acceptable clinical results can be obtained with modest numbers of fractions. Absolute matching of effects is obviously not always necessary and a process of diminishing returns appears to apply where, after some point

the fraction number has to be increased more and more to produce any significant further movement. The question that still needs to be addressed is how much movement of iso-effect surfaces is necessary to give rise to clinically evident changes in effect. This knowledge will only become available as more clinical data emerges along with more detailed data on the values of the tissue parameters used in the LQ model. If movement of iso-effect surfaces is large, they could help the understanding of trends seen in treatment, because, if tumour effect surfaces move outwards (i.e. are more effective), at short range and late effect surfaces move inwards (i.e. less damaging) at longer range when going to HDR, this would suggest that some HDR treatments have advantages over earlier LDR treatment. If the movement is small, then this may indicate why satisfactory clinical results can be obtained with modest numbers of fraction at HDR when other indications, for example the Liversage equation, predict that many more fractions should be necessary for an exact biological match (Joslin 1990, Orton 1991). More work is required to determine the relationship between movement of iso-effect surfaces (i.e. changes in the overall biological effect distribution) and effects on tumour and normal tissues.

10.3. Future developments.

This thesis has shown that in order to fully appreciate the effects of altering treatment schedules in radiotherapy it is necessary to consider three dimensional changes in the effect distribution. This can be done by studying the movement of iso-effect surfaces which must be viewed along with patient anatomy for this method to be useful. To do this effectively an imaging technique will have to be used, such as CT scanning,

which is capable of determining the position of all sensitive tissue structures and combining this information with iso-effect surface plots.

10.3.1. External beam treatments.

Treatment planning from CT images is now common for many sites where absorbed dose calculations are performed and displayed in the form of iso-dose plots along with anatomical details. To study changes in the effect distribution it will be only be necessary to convert the iso-dose plots into iso-effect plots. This transition is simple and would require little effort; indeed some existing treatment planning computers are already able to perform ERD calculations.

Three dimensional iso-effect calculations are important, as was shown in chapter 8 (section 8.3). By studying the movement of iso-effect surfaces it will be possible to assess more fully the effects of different scheduling strategies such as CHART (section 4.3.3.) and hyperfractionation (section 1.5.4.). It will also be possible to make intercomparisons between existing conventional schedules from different centres in a more detailed way than has previously been possible.

10.3.2. Brachytherapy treatments.

The preceding analysis illustrates the dangers of predicting the effects of changing practice in brachytherapy on the basis of single point analysis. Formerly, one dimensional analysis had led to the following, seemingly robust, conclusion: *that a change from low to high dose-rate, with the total dose chosen to give equivalent late effects, would lead to reduced tumour effects and a probable increase in tumour recurrence.*

Iso-effect analysis shows that this conclusion is not necessarily true in all circumstances. Combinations of tumour size and location, position of critical organ and dose rate distribution can exist in which, contrary to former expectations, increased dose-rate (with modified total dose) may result in a therapeutic advantage rather than a disadvantage.

We need to know whether such configurations are rare, occur in a minority of patients or are typical of the majority. To answer this question will require a compilation of anatomical, geometrical and dosimetric parameters in a series of brachytherapy patients. Iso-effect surface analysis could then provide a simulation of spatially distributed radiobiological effects in each patient in turn, for alternative treatment strategies (dose rate, fraction number etc.) of brachytherapy, and should enable identification of strategies most likely to benefit the majority.

In addition, these considerations suggest that *individualised* strategies may be necessary for optimal therapeutic benefit. The work described in this thesis has mostly been concerned with formal analysis of the concept of equivalence and its ramifications. Hopefully, it will have provided the analytical tools which might allow further improvement in cancer treatment by radiation.

This is particularly true when dealing with treatments which produce inhomogeneous dose distributions similar to those mentioned in the Glasgow report in chapter 9. In this case a special shielding block was used with the external beam component of the treatment; the resulting dose distributions being shown in figure 10.1.(a) and (b). The intention in this case was to use the external beam treatment to boost the dose to the pelvis at the same time shielding the region already treated by the intracavitary insertion (Jones et al, 1990). The resulting dose distribution (and in turn the

biological effect distribution) is a complex one and it can be seen here (figure 10.1.) that only a truly three dimensional view of the effect distribution would reveal the consequences of alterations in either the scheduling or the physical shape of the shielding.

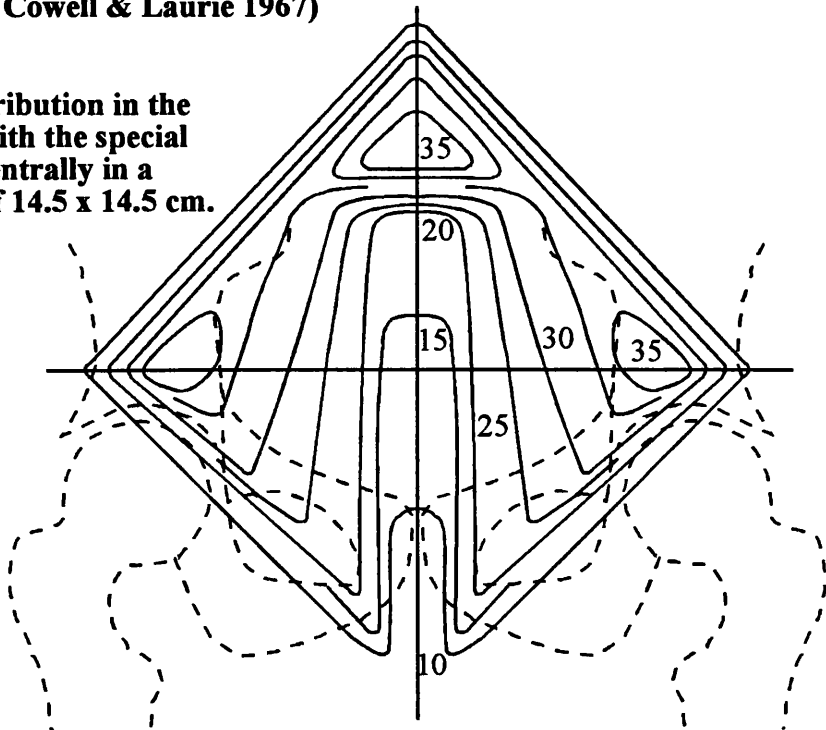
10.3.3. Application in new areas and in the study of volume effects.

Development of this work will be greatly enhanced by the improvements in three dimensional imaging which allow interactive display of iso-effect surfaces. This would provide a much clearer view of iso-dose surfaces and hence iso-effect surfaces around insertions. New afterloading systems using variable source dwell times allow far greater flexibility when producing iso-dose surfaces of specified shapes. Such devices used in conjunction with a three dimensional treatment planning system would allow iso-effect surfaces to be constructed which account for changes in both dose-rate and geometry between different insertions. Planning systems with the ability to calculate the volume of intersection between surfaces and sensitive structures (a feature which is currently under development in a number of systems) could make use of the iso-effect concept as a basis for the study of volume effects in brachytherapy. In fractionated radiotherapy the means already exist to display three dimensional iso-dose information. This technique could easily be adapted to produce iso-effect distributions and volume effects could be also be studied in the same way as with brachytherapy. Volume effects are now of increasing interest as has been mentioned earlier (chapter 1). The volume of intersection of an effect envelope and a sensitive organ could be calculated as easily as the intersection of dose envelopes and organs which are at present being calculated routinely in some centres (Hilaris, 1994). If the topic of volume effects is not developed it doubtful if the

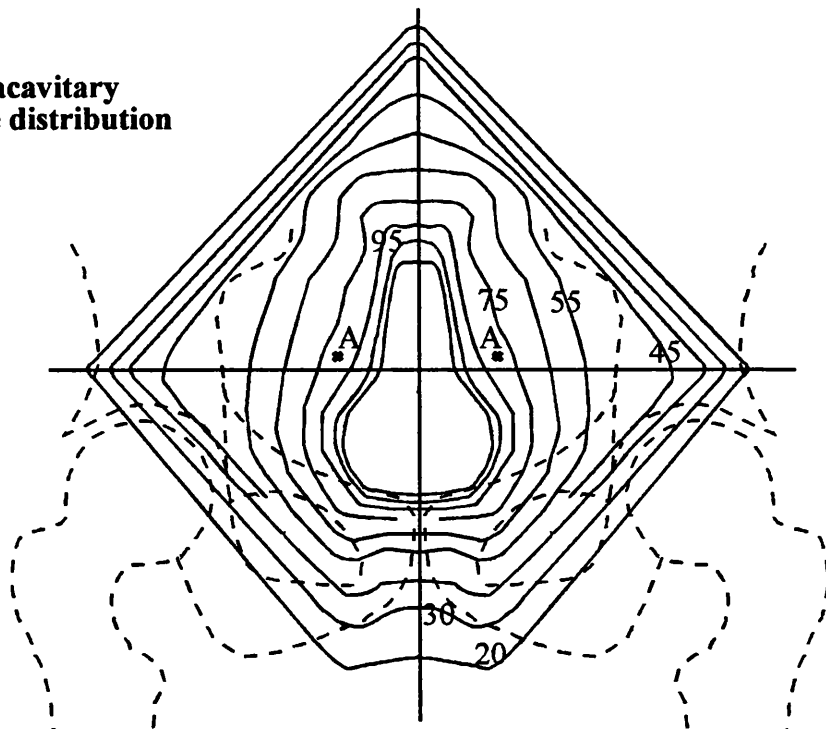
relationship of normal tissue damage to dose, dose-rate and fractionation will ever be properly understood.

**Figure 10.1. Dose distributions used in the Glasgow report, chapter 9
(from Cowell & Laurie 1967)**

a) X-ray dose distribution in the coronal plane with the special wedge placed centrally in a diagonal field of 14.5 x 14.5 cm. (doses in Gy)



b) Combined intracavitary and X-ray dose distribution (doses in Gy)



References

- Baclesse, F. (1958) Clinical experience with ultra-fractionated radiotherapy. In *Progress in Radiation Therapy*, New York: Grune & Stratton.
- Bahari, I., Berdford, J.S., Giaccia, A.J. & Stamato, T.D. (1990) Measurement of the relative proportion of symmetrical and asymmetrical chromosome-type interchanges induced by gamma radiation in human-hamster hybrid cells. *Radiation Research*, **76**, 573-586.
- Barendsen, G.W. (1982) Dose fractionation, dose-rate and iso-effect relationships for normal tissue responses. *International Journal of Radiology Oncology Biology and Physics*, **8**, 1981-1997.
- Bedford, J.S. (1991) Sublethal damage, potentially lethal damage, and chromosomal aberrations in mammalian cells exposed to ionising radiations. *International Journal of Radiology Oncology Biology and Physics*, **21**, 1457-1469.
- Belli, J. & Shelton, M. (1969) Potentially lethal radiation damage: repair of mammalian cells in culture. *Science*, **1654**, 490-492.
- Brenner, D.J. & Hall, E.J. (1991) Fractionated high dose-rate versus low dose-rate regimes for intracavitary brachytherapy of the cervix. 1 General considerations based on radiobiology, *British Journal of Radiology*, **64**, 133-144.

Brenner, D.J. & Hall, E.J. (1991) Conditions for equivalence of continuous to pulsed low dose-rate in brachytherapy. *International Journal of Oncology, Biology and Physics*, **20**, 181-190.

Brenner, D.J. (1992) Corrections between α/β and $T_{1/2}$: implications for clinical biological modelling. *British Journal of Radiology*, **65**, 1051-1054.

Chadwick, K.H. & Leenhouts, H.P. (1973) A Molecular theory of cell survival. *Physics in Medicine and Biology*, **78**, 78-87.

Chaney, E.L. & Pizer, S.M. (1992) Defining anatomical structures from medical images. *Seminars in Radiation Oncology*. **2**, 215-225.

Corbett, P.J. (1990) Brachytherapy in carcinoma of the cervix: The state of the art. In *Brachytherapy LDR and HDR*, ed. Martinez, A.A., Orton, C.G. & Mould, R.F. Ch. 10
The Netherlands: Nucletron International B.V.

Cornforth, M.N. & Bedford, J.S. (1987) A quantitative comparison of potentially lethal damage repair and the rejoining of interphase chromosome breaks on low passage normal human fibroblast. *Radiation Research*, **111**, 385-405.

Coutard, H. (1932) Roentgentherapy of epitheliomas of the tonsillar region, hypopharynx, and larynx from 1920 to 1926. *American Journal of Roentgenology*, **28**, 313-331.

Cowell, M.A.C. & Laurie, J. (1967) The treatment of carcinoma of cervix uteri Stage 1 and 2 with radium and supplementary X-rays. A preliminary communication. *British Journal of Radiology*, **40**, 43-47.

Coutard, H. (1932) The conception of periodicity as a possible directing factor in roentgentherapy of cancer. *Proceedings of the Medical Institute of Chicago*, **10**, 1-14.

Dale, R.G. (1985) The application of the linear-quadratic dose effect equation to fractionated radiotherapy. *British Journal of Radiology*, **58**, 515-528.

Dale, R.G. (1986) A Graphical method to simplify the application of the linear quadratic dose-effect equation to fractionated radiotherapy. *British Journal of Radiology*, **59**, 1111-1115.

Dale, R.G. (1989) Time-dependent tumour repopulation factors in linear-quadratic equations - implications for treatment strategies. *Radiotherapy and Oncology*, **15**, 371-382.

Dale, R.G. (1990) The potential for radiobiological modelling in radiotherapy treatment design. *Radiotherapy and Oncology*, **19**, 245-255.

Dale, R.G. (1990) The use of small fraction numbers in high dose-rate gynaecological afterloading: some radiobiological considerations. *British Journal of Radiology*, **63**, 290-294.

Deacon, J.M., Peckman, M.J. & Steel, G.G. (1984) The radioresponsiveness of human tumour and the initial slope of the cell survival curves. *Radiotherapy and Oncology*, **2**, 317-323.

De Blasio, D.S., Hilaris, B.S., Nori, D., Fuks, Z., Whitmore, W. F. & Anderson, L.L. (1988) Permanent interstitial implantation of prostatic cancer in the 1980's. *Endocurietherapy, Hyperthermia and Oncology*, **4**, 193-201.

Deehan, C. & O'Donoghue, J.A. (1988) Biological equivalence between fractionated treatments using the linear-quadratic model. *British Journal of Radiology*, **61**, 1187-1188.

Deehan, C. & O'Donoghue, J.A. (1991) Biological equivalence between treatment schedules containing continuous irradiation. *Activity*, **5**, 131-134.

Deehan, C. & O'Donoghue, J.A. (1994) Biological equivalence of LDR and HDR brachytherapy. In *Brachytherapy from Radium to Optimisation*, ed. Mould, R.F., Batterman, J.J., Martinez, A.A. & Spieser, B.L., Ch. 3 The Netherlands: Nucletron International B.V.

del Regato, J.A., (1968) Historical changes in time-dose-fractionation relationships in therapeutic radiology. In *Frontiers in Radiation Therapy and Oncology*, 3, Basel, New York:Karger.

del Regato, J.A. (1990) Fractionation: a panoramic view. *International Journal of Radiology Oncology Biology and Physics*, 19, 1329-1331.

De Vita, V.T., Goldin, A., & Olivero VT, (1979) The drug development and clinical trials program of the Division of Cancer Treatment, National Cancer Institute., *Cancer Clinical Trials*, 2: 195-216.

Dische, S. & Saunders, M.I. (1990) *The rationale for continuous, hyperfractionated, accelerated radiotherapy, (CHART)*, 19, 1317-1320.

Douglas, B.G. & Fowler, J.F. (1976) The effect of multiple small doses of X rays on skin reactions in the mouse and a basic interpretation. *Radiation Research*, 66, 401-426.

Down, J.D. & Fowler, J.F. (1983) The expression of early and late damage after thoracic irradiations: A comparison between CBA and C57BL mice. *Radiation Research*, 96, 603-610.

Dutreix, J. (1989) Expression of dose-rate effect in clinical curietherapy. *Radiotherapy and Oncology*, **15**, 25-37.

Elkind, M.M. & Sutton, H. (1960) Radiation response of mammalian cells grown in culture. I. Repair of x-ray damage in surviving Chinese hamster cells. *Radiation Research*, **13**, 556-593.

Elkind, M.M. & Whitmore, G.F. (1967) In *The radiobiology of cultured mammalian cells*. New York: Gordon and Breach.

Elkind, M.M. (1976) Fractionated dose radiotherapy and its relationship to survival curve shape. *Cancer Treatment Reviews*, **3**, 1-15.

Ellis, F.E. (1967) Fractionation in radiotherapy. In *Modern trends in radiotherapy*, ed. Deeley, T.J. & Wood, R. Vol. 1. London: Butterworth.

Ellis, F.E. (1969) Dose, time and fractionation. A clinical hypothesis. *Clinical Radiology*, **20**, 1-7.

Ellis, F.E. (1985) Is NDS-TDF useful to radiotherapy ? *International Journal of Radiology Oncology Biology and Physics*, **11**, 1685-1697.

Fertil, B. & Malaise, E.P. (1981) Inherent cellular radiosensitivity as a basic concept for human tumour radiotherapy. *International Journal of Radiology Oncology Biology and Physics*, **7**, 621-629.

Fleishman, A.B. (1983) Cost benefit analysis of radiological protection: a case study of remote after-loading in gynaecological radiotherapy. *British Journal of Radiotherapy*, **56**, 737-744.

Fowler, J.F. (1965) The estimation of total dose for different numbers of fractions in radiotherapy. *British Journal of Radiotherapy*, **38**, 365-368.

Fowler, J.F. (1984) What next in fractionated radiotherapy? *British Journal of Cancer*, *suppl. VI*, **49**, 285-300.

Fowler, J.F. (1989) The radiobiology of brachytherapy. In *Brachytherapy LDR and HDR*, ed Martinez, A.A., Orton, C.G. & Mould, R.F. Ch. 12 The Netherlands: Nucletron International B.V.

Fowler, J.F. (1989) The linear-quadratic model and progress in fractionated radiotherapy. *British Journal of Radiology*, **62**, 679-694.

Fowler, J.F. (1990) Dose-rate effects in normal tissues. In *Brachytherapy 2*, ed. Mould, R.F. Ch. 4 The Netherlands: Nucletron International B.V.

Freund, L. (1930) Die gegenwärtigen methoden und erfolge der kerbsbestrahlung mit verteilten doses. *Strahlentherapie*, **37**, 795-797.

Gilbert, C.W., Hendry, J.H. & Major, D. (1980) The approximation in the formulation for survival $S = \exp(-\alpha D + \beta D^2)$. *International Journal of Radiology Oncology Biology and Physics*, **37**, 469-471.

Godden, T.J. (1988) *Physical aspects of brachytherapy*. Medical physics handbooks **19**, ed. Lenihan, J.M.A. Bristol & Philadelphia: Adam Hilgar.

Greening, J.R. (1985) *Fundamentals of radiation dosimetry*. Medical Physics Handbooks **15**. ed. Lenihan, J.M.A. Bristol & Boston: Adam Hilger.

Hall, E.J. (1972) Radiation dose-rate: a factor of importance in radiobiology and radiotherapy. *British Journal of Radiology*, **45**, 81-97.

Hall, E.J. (1988) *Radiobiology for the radiologist*, London: Harper and Row.

Hall, E.J. (1991) Weiss Lecture. The dose-rate factor in radiation biology. *International Journal of Radiation Biology*, **59**, 595-610.

Hall, E.J. & Brenner, D.J. (1991) The dose-rate effect revisited: Radiobiological considerations of importance in radiotherapy, *International Journal of Radiology Oncology Biology and Physics*, **21**, 1043-1414.

Hahn, G. (1975) Radiation and chemical induced potentially lethal lesions in noncycling mammalian cells: Recovery analysis in terms of X-ray and ultraviolet-like systems. *Radiation Research*, **64**, 553-545.

Hendry, J.H. & Moore, J.V. (1985) Derived absolute values for α and β for dose fractionation, using dose-incidence data. *British Journal of Radiology*, **58**, 885-890.

Hethcote, H.W., McLarty, J.W. & Thames, H.D. (1976) Comparison of mathematical models for radiation fractionation. *Radiation Research*, **67**, 387-407.

Hilaris, B.S., Tenner, M., Moorthy, C., High, M., Shih, L., Silvern, D., Mastoras, D. & Stabile, L. (1994) Three-dimensional brachytherapy treatment planning at New York Medical College. In *Brachytherapy from Radium to Optimisation*, ed. Mould, R.F., Batterman, J.J., Martinez, A.A. & Spieser, B.L., Ch. 32 The Netherlands: Nucletron International B.V.

Holznecht, G. (1923) Review of the present state of deep roentgentherapy. *American Journal of Roentgenology*, **10**, 476-479.

Hopewell, J.W. & van der Aardweg, G.J.M.J. (1991) Studies of dose-fractionation on early and late responses in pig skin: a reappraisal of the importance of the overall treatment time and its effects on radiosensitization and incomplete repair. *International Journal of Radiation Oncology, Biology and Physics*. **21**, 1441-1450.

Horiot, J.C., Lefur, R., Nguyen, T., Schraub, S., Chenal, C., DePaw, M. & Van Glabbeke, M. (1988) Two fractions per day versus a single fraction per day in the radiotherapy of oropharynx trial. *International Journal of Radiation Oncology, Biology and Physics*. **15 (Suppl. 1)**, 178.

Horiot, J.C., (1991) What has radiation biology contributed to the evolution of radiotherapy? *European Journal of Cancer*, **27**, 399-402.

Hunter, R.D. (1994) Dose rate correction in LDR intracavitary therapy. In *Brachytherapy from Radium to Optimisation*, ed. Mould, R.F., Batterman, J.J., Martinez, A.A. & Spieser, B.L., Ch. 7 The Netherlands: Nucletron International B.V.

Joiner, M.C. (1994) Models for radiation cell killing. In *The ESTRO Course Book on Basic Clinical Radiobiology for radiation Oncologists*. ed. Steel, G.G., Ch 6, Kent, Surrey: Edward Arnold.

Jones, D.A., Notley, H.M. & Hunter, R.D. (1987) Geometry adopted by Manchester radium applicators and Selectron afterloading applicators in intracavitary treatment for carcinoma cervix uteri. *British Journal of Radiology*, **60**, 481-485.

Jones, R.D., Symonds, R.P., Habeshaw, T., Watson, E.R., Laurie, J. & Lamont, D.W. (1990) A comparison of remote afterloading and manually inserted caesium in the treatment of carcinoma of the cervix. *Clinical Oncology*, **2**, 193-198.

Joslin, C.A.F., Smith, C.W. & Mallik, A. (1972) The treatment of cervix cancer using high activity cobalt-60 sources. *British Journal of Radiology*, **45**, 257-270.

Joslin, C.A.F. (1990) Brachytherapy: A clinical dilemma, *International Journal of Radiation Oncology Biology and Physics*, **19**, 801-802.

Joslin, C.A.F. (1994) The future of brachytherapy. In *Brachytherapy from Radium to Optimisation*, ed. Mould, R.F., Batterman, J.J., Martinez, A.A. & Spieser, B.L., Ch. 14 The Netherlands: Nucletron International B.V.

Kingary, L.B. (1920) Saturation in roentgentherapy; its estimation and maintenance. *Arch. Derm. Syph.*, **1**, 423.

Kirk, J., Gray, W.M. & Watson, E.R. (1971) Cumulative radiation effect. Part 1: Fractionated treatment regimes. *Clinical Radiology*, **22**, 145-155.

Kirk, J., Gray, W.M. & Watson, E.R. (1972) Cumulative radiation effect. Part II: Continuous radiation therapy - long lived sources. *Clinical Radiology*, **23**, 93-105.

Kirk, J., Gwen, W.H. Wingate, & Watson, E.R. (1976) High-dose effects in the treatment of carcinoma of the bladder under air and hyperbaric oxygen conditions. *Clinical Radiology*, **27**, 137-144.

van der Kogel, A. (1993) Radiobiology of normal tissues. In *The ESTRO Course Book on Basic Clinical Radiobiology for radiation Oncologists*. ed. Steel, G.G., Ch 13, Kent, Surrey: Edward Arnold.

van der Kogel, A. (1993) Cell proliferation in normal tissues. In *The ESTRO Course Book on Basic Clinical Radiobiology for radiation Oncologists*. ed. Steel, G.G., Ch 4, Kent, Surrey: Edward Arnold.

Lea, D.E. (1947) *Actions of Radiations on Living Cells*. Cambridge: University Press.

Laurie, J.M.A., Orr, J.F. & Foster, C.J. (1972) Repair processes and cell survival. *British Journal of Radiology*, **45**, 362-368.

Lichter, A.S., Sandler, H.M. & Robertson, J.M. (1992) Clinical experience with three dimensional treatment planning. *Seminars in Radiation Oncology*, **2**, 257-266.

Little, J.B. (1969) Repair of sub-lethal and potentially lethal radiation damage in plateau phase cultures of human cells. *Nature*, **224**, 804-806.

Liversage, W.E. (1969a) A general formula for equating protracted and acute regimes of radiation. *British Journal of Radiology*, **42**, 432-440.

Lukka, H.R., Moore, C.J. & Hunter, R.D. (1987) The relationship between the bladder and the cervix in patients undergoing intracavitary therapy. . *British Journal of Radiology*, **60**, 355-358.

Millar, W.T. & Canney, P.A. (1993) Derivation and application of equations describing the effects of fractionated protracted irradiations, based on multiple and incomplete repair processes. Part I. Derivation of equations. *International Journal of Radiation Biology*, **12**, 1-17.

Michalowski, A. (1981) Effects of radiation on normal tissues: hypothetical mechanisms and limitations of in situ assays of clonogenicity. *Radiation and Environmental Biophysics*, **19**, 157-172.

Mould, R.F. (1992) From Marie Curie and radium to the state of the art brachytherapy, In *Brachytherapy in the Peoples Republic of China*, ed. Mould, R.F. The Netherlands:Nucletron International B.V.

Liversage, W.E. (1971) A critical look at the ret. *British Journal of Radiology*, **44**, 91-100.

O'Donoghue, J.A. (1986) Agreement of the quadratic and CRE models in predicting the late effects of continuous low dose-rate radiotherapy. *British Journal of Radiology*, **59**, 193-194.

Oliver, M.A. (1962) IV. Theoretical implications of cell survival data in relation to fractionated radiotherapy treatments. *British Journal of Radiology*, **36**, 178-182.

Orton, C.G. (1973) A simplification in the use of the NSD concept in practical radiotherapy. *British Journal of Radiology*, **46**, 529-537.

Orton, C.G. (1988) What minimum number of fractions is required with high dose-rate afterloading, *British Journal of Radiology*, **60**, 300-302,.

Orton, C.G. (1990) Biological treatment planning. In *Brachytherapy LDR and HDR*, ed. Martinez, A.A., Orton, C.G. & Mould, R.F. Ch. 18 The Netherlands: Nucletron International B.V.

Orton, C.G., Seyedsadr, M. & Somnay, A. (1991) Comparison of high and low dose-rate remote afterloading for cervix cancer and the importance of fractionation. *International Journal of Radiation Oncology Biology and Physics*, **21**, 1425-1434.

Orton, C.G. (1991) Application of the linear quadratic model to radiotherapy for gynaecological cancers. *Activity*, **2**, 15-18.

Orton, C.G. (1993) High dose-rate versus low dose-rate brachytherapy for gynecological cancer. In *Seminars in Radiation Oncology*, ed Tepper, J.E., Harrison, L.B., **3**, 232-239.

Overgaard, J. (1993) Time-dose relationships: the origins. In *The ESTRO Course Book on Basic Clinical Radiobiology for radiation Oncologists*. ed. Steel, G.G., Ch 7, Kent, Surrey: Edward Arnold.

Overgaard, J. (1993) Clinical manifestation of normal-tissue damage. In *The ESTRO Course Book on Basic Clinical Radiobiology for radiation Oncologists*. ed. Steel, G.G., Ch 12, Kent, Surrey: Edward Arnold.

Paine, C.H. (1972) Modern after-loading methods for interstitial therapy. *Clinical Radiology*, **23**, 263-272.

Paine, C.H. & Ash, D.V. (1991) Interstitial brachytherapy: Past-present-future. *International Journal of Oncology Biology and Physics*, **21**, 1479-1483.

Patel, F.D., Sharma, S.C., Negi, P.S., Ghoshal, S. & Gupta, B.D. (1994) Low dose-rate vs. high dose-rate brachytherapy in the treatment of carcinoma of the uterine cervix: a clinical trial. *International Journal of Radiation Oncology Biology and Physics*, **28**, 335-341.

Parsons, J.T., Bova, F.J. & Million, R.R. (1980) A re-evaluation of split-course technique for squamous cell carcinomas of the head and neck. *International Journal of Radiation Oncology Biology and Physics*, **6**, 1645-1652.

Parsons, J.T., Mendenhall, W., Cassisi, N., Isaacs, J. & Million, R.R. (1988) Accelerated hyperfractionation for head and neck cancer. *International Journal of Radiation Oncology Biology and Physics*, **14**, 649-658.

Paterson R, (1963) *The Treatment of Malignant Disease by Radiotherapy*. London: Edward Arnold.

Pearlman, A.W. & Friedman ,M. (1968) Radiation therapy of benign giant cell tumours arising in Paget's disease of the bone, iso-effect recovery study. *American Journal of Roengenology*, **102**, 645-651.

Peters, L.J., Ang, K.K. & Thames, H.D. (1988(a)) Accelerated fractionation in the treatment of head and neck cancer: a critical comparison of different strategies. *Acta Oncologica*, **27**, 185-194.

Peters, L.J., Brock, W.A., Chapman, D.J. Wilson, G.D. & Fowler, J.F. (1988(b)) Response predictors in radiotherapy: A review of research onto radiobiological based assays In *Megavoltage Radiotherapy 1937-1987*, *British Journal of Radiology*, **Suppl. 22**, 96-108.

Philips, R.A. & Tolomach, L.J. (1966) Repair of potentially lethal damage in X-irradiated HeLa cells. *Radiation Research*, **29**, 413-432.

Regaud, C., (1922) Influence de la dose, de l'irradiation sur les effets déterminés, dans la testicule par le radium. *Comp. Rend. Sur. Biol. (Paris)*, **86**, 787-790.

Saunders, M.I., Dische, S., Fowler, J.F., Denekamp, J., Dunphy, E., Grosch, E., Fermont, D., Ashford, R., Maher, J. & Des Rocher, C. (1988) Radiotherapy with three fractions per day for twelve consecutive days for tumours of the thorax, head and neck. *Frontiers of Radiation Therapy and Oncology*, **22**, ed. Vaeth, J. & Meyer, J. Basel: Karger.

Saunders, M.I. & Dische, S. (1990) Continuous, hyperfractionated, accelerated radiotherapy (CHART) in non-small cell carcinoma of the bronchus. *International Journal of Radiation Oncology, Biology and Physics*, **19**, 1211-1215.

Sherrah-Davies, E. (1985) Morbidity following low-dose-rate Selectron therapy for cervical cancer. *Clinical Radiology*, **36**, 131-139.

Stapleton, G.E., Bilan, D. & Hollander, A. (1953) Recovery of X-irradiated bacteria at suboptimal temperatures. *Journal of Cell Composition and Physiology*, **41**, 345-357.

Steel, G.G., Julian, D.D., Peacock, J.H. & Stephens, T.C. (1986) Dose-rate effects and the repair of radiation damage. *Radiotherapy and Oncology*, **5**, 321-331.

Steel, G.G., Kelland, L.R. & Peacock, J.H. (1989) The radiobiological basis for low dose-rate radiotherapy. In *Brachytherapy 2*, ed. Mould, R.F. Ch. 3 The Netherlands: Nucletron International B.V.

Steel, G.G. (1993) The significance of Radiobiology for Radiotherapy. In *The ESTRO Course Book on Basic Clinical Radiobiology for radiation Oncologists*. ed. Steel, G.G., Ch 1 Kent, Surrey: Edward Arnold.

Steel, G.G. (1993) Molecular aspects of radiation biology. In *The ESTRO Course Book on Basic Clinical Radiobiology for radiation Oncologists*. ed. Steel, G.G., Ch 25 Kent, Surrey: Edward Arnold.

Steel, G.G. (1993) Clonogenic cells and the concept of cell survival. In *The ESTRO Course Book on Basic Clinical Radiobiology for radiation Oncologists*. ed. Steel, G.G., Ch 5 Kent, Surrey: Edward Arnold.

Seitz, S. & Wintz, H. (1920) *Unsere Method der Roentgen Tiefentherapie und ihre Erfolge*. Berlin: Urban & Schwarzenberg.

Stenström, W. (1926) Study of skin reactions after divided reontgenray dosage. *American Journal of Reontgerol*, 15, 513-519.

Stewart, F.A., Sorenson, J.A., Alpen, E.L., Williams, M.V. & Denekamp, J. (1984) Radiation induced renal damage: effects of hyperfractionation. *Radiation Research*, **98**, 407-420.

Stitt, J.A., Fowler, J.F., Thomadsen, B.R., Buchler, D.A., Paliwal, B.P. & Kinsella, T.J. (1992) High dose-rate intracavitary brachytherapy for carcinoma of the cervix: The Madison system: I Clinical and radiobiological considerations. *International Journal of Radiation Oncology Biology and Physics*, **24**, 335-348.

Stout, R. & Hunter, R.D. (1989) Clinical trials of changing dose-rates in intracavitary low dose-rate radiotherapy. In *Brachytherapy 2*, ed. Mould, R.F. Ch. 31 The Netherlands: Nucletron International B.V.

Strandqvist, M. (1944) Studieren under die cumulative wirkung der roentgenstrahlen bei franktionierung. In *Acta Radiobiology*. Stockholm, **suppl. 55**.

Symonds, R.P., Jones, R.D., Laurie, J.M.R., Habeshaw, T., Watson, E.R. & Lamont, D.A. (1989) Use of the cumulative radiation effect (CRE) formula to correct for the increased dose-rate when carcinoma cervix is treated by Selectron. In *Brachytherapy 2*, ed. Mould, R.F. Ch. 6 The Netherlands: Nucletron International.B.V.

Thames, H.D., Withers, H.R., Peters, L.J. & Fletcher, M.D. (1982) Changes in early and late radiation responses with altered dose fractionation: Implications for dose-survival relationships, *International Journal of Radiation Oncology Biology and Physics*, **8**, 219-226.

Thames, H.D., Peters, L.J., Withers, H.R., & Fletcher, G.H. (1983) Accelerated fractionation versus hyperfractionation: rationales for several treatments per day. *International Journal of Radiation Oncology Biology and Physics*, **9**, 127-138.

Thames, H.D. & Hendry, J.H. (1985) An "incomplete repair" model for survival after fractionation and continuous irradiations. *International Journal of Radiation Biology*, **47**, 319-339.

Thames, H.D. & Hendry, J.H. (1987) *Fractionation in radiotherapy*. London: Taylor and Francis.

Thames, H.D., Bentzen, S.M., Turesson, I., Overgaard, M. & van der Bogaert, W. (1989) Fractionation parameters for human tissues and tumours. *International Journal of Radiation Oncology Biology and Physics*, **56**, 701-710.

Tod, M.C. & Meredith, W.J. (1938) A dosage system for use in the treatment of cancer of the uterine cervix. *British Journal of Radiology*, **11**, 809-824.

Warmelink, C., Ezzell, G. & Orton, C.G. (1989) Use of time-dose-fractionation model to design high dose-rate fractionation schemes. In *Brachytherapy 2*, ed. Mould, R.F. Ch. 5 The Netherlands: Nucletron International B.V.

Wilkinson, J.M. (1982) The precision of dose calculations and the activity distributions of Selectron sources. *British Journal of Radiology*, **55**, 778-779.

Wilkinson, J.M., Moore C.J., Notley, H.M. & Hunter, R.D. (1983) The use of Selectron afterloading equipment to simulate and extend the Manchester System for intracavitary therapy of the cervix uteri. *British Journal of Radiology*, **56**, 409-414.

Williams, M.V., Denekamp, J. & Fowler J.F. (1985) A review of ratios for experimental tumours: Implications for clinical studies of altered fractionation. *International Journal of Radiation Oncology Biology and Physics*, **11**, 87-96.

Withers, H.R., Thames, H.D. & Peters, L.J. (1983) A new iso-effect curve for change in dose per fraction. *Radiotherapy and Oncology*, **1**, 187-191.

Withers, H.R., Thames, H.D. & Peters, L.J. (1982(c)) Differences in fractionation response of acute and late-responding tissues. In *Progress in Radio-Oncology*, vol. 2, ed. Karcher T.F. New York: Raven Press.